The Dissertation Committee for George Miloshevich
certifies that this is the approved version of the following dissertation:

Hamiltonian description of Hall and sub-electron scales in collisionless plasmas with reduced fluid models

Committee:

Philip J. Morrison, Supervisor

Richard Hazeltine

Boris Breizman

Richard Fitzpatrick

Irene M. Gamba

Hamiltonian description of Hall and sub-electron scales in collisionless plasmas with reduced fluid models

by

George Miloshevich,

DISSERTATION

Presented to the Faculty of the Graduate School of

The University of Texas at Austin

in Partial Fulfillment

of the Requirements

for the Degree of

DOCTOR OF PHILOSOPHY

THE UNIVERSITY OF TEXAS AT AUSTIN

August 2018

Dedicated to my father, Dragan Milošević (1947 - 2014), who has inspired me to look to the stars...

Acknowledgments

I will start by expressing many thanks to my family, who through their care and upbringing have shaped me into the person I became.

Perhaps instrumental in directing my interest towards physics was my high school teacher Nikoloz Chkhaidze. With his charismatic teaching and patient training he has prepared me for various difficulties I later faced.

I am thankful to my alma mater, Tbilisi State University for bestowing me with opportunities to excel in research as well as variety of fellowships I have received that provided support in difficult times. This also concerns my mentors Prof. Ramaz Khomeriki and Prof. Nana Shatashvili for their clear guidance. In addition, I must express my thanks to Adelina Chubititze for the quality of my English classes in the TCS school.

But of course my acknowledgments would be incomplete without discussing the university where the current work has been accomplished. I would like to thank the Institute for Fusion Studies for providing me with funding and in particular my supervisor Prof. Philip J. Morrison for his exciting lectures, guidance and expertise, allowing me to pursue different projects and nurturing the capacity for independent thought. I am also thankful to the faculty, including Prof. Richard Fitzpatrick for his well structured course of Electromagnetism, Prof. Boris Breizman, for interesting discussions in Plasma

Physics class and style of teaching as well as Prof. Richard Hazeleltine, for providing me with autonomy when I was a teaching assistant in his classes. And of course, I would like to thank Prof. Irene Gamba for a valuable input as a member of my dissertation committee.

I would love to thank my collaborator, Dr. Manasvi Lingam, who through our discussions had motivated many of the topics that eventually became part of this thesis. The acknowledgments also extend to my other collaborator and friend Santiago Benavides (a former member of our group) for his hospitality and great times in Boston, as well as agreeing to work on simulations that provided evidence on cascade reversal discussed here.

Progress in graduate school can be difficult and sporadic and thus peer comradery of the fellow graduate students is quite welcome. My special thanks go to my roommate Abhranil Das, who has broadened my horizons with his weekly Molotov Seminars (on various topics) and introduced me to UT meditate group. I would also love to thank my friends Georgios Stratis and Sarah Serwe for hosting annual Thanksgiving parties and Tess Bernard for organizing camping to the Big Bend national park. My stay at Austin has been further enriched by the retreats for astronomical observations with Dr. Akarsh Simha, involvement in a book club with Josiah Couch and Stefan Eccles and dance classes I have taken at the Inspired Movement, Longhorn Salsa and Esquina Tango. Finally, I would like to thank Bill and Linda Hallidy for their pleasant hospitality in the house, where I rented a room for so many years.

Hamiltonian description of Hall and sub-electron scales in collisionless plasmas with reduced fluid models

Publication No. _____

George Miloshevich, Ph.D.
The University of Texas at Austin, 2018

Supervisor: Philip J. Morrison

In MHD magnetic helicity has been shown to represent Gauss linking numbers of magnetic field lines by Moffatt and others; thus it is endowed with topological meaning. The noncanonical Hamiltonian formulation of extended MHD models (that take two-fluid effects into account) has been used to arrive at their common mathematical structure, which manifests itself via the existence of two generalized helicities and two Lie-dragged 2-forms. The helicity invariants play an important role in the second part of thesis dedicated to understanding the directionality of turbulent cascades.

Generally speaking, invariants (such as energy) can flow in two directions in a turbulent cascade: forward (towards small scales, leading to dissipation) and inverse (towards large scales), leading to the formation of a condensate. This directionality in extended MHD models is estimated using analytical considerations as well as tests involving 2D numerical simulations. The

cascade reversal (transition) of the square magnetic vector potential is found, viz. when the forcing wavenumber exceeds the inverse electron skin depth the square magnetic vector potential starts to flow towards large wavenumbers, as opposed to the typical MHD behavior. In addition, the numerics suggest a simultaneous transition to the inverse cascade of energy in this inertial MHD regime. This is accompanied by the appearance of large scale structures in the velocity field, as opposed to the magnetic field as in the MHD case.

Final chapters of the thesis are devoted to devising the action principle for the relativistic extended MHD. First the special relativistic version is discussed, where the covariant noncanonical Poisson bracket is found. This is followed by a short recourse towards describing relativistic collisionless reconnection mediated by the electron thermal inertia (purely relativistic effect). Next, 3+1 splitting inside the Poisson bracket is performed, while only nonrelativistic terms are retained. Thus one arrives at nonrelativistic extended MHD bracket with arbitrary ion to electron mass ratio. In conclusion, it is outlined how the Hamiltonian 3+1 formalism can be developed for general relativistic Hall MHD using canonical Clebsch parametrization and some comments are added on possible issues regarding the quasi-neutrality assumption in the model that is used throughout the chapter.

Table of Contents

List of Tables

List of Figures

Chapter 1

Action principles and Hamiltonian dynamics in matter models

The early discovery of action principles (AP)s and associated Hamiltonian structure, undoubtably of groundbreaking importance in the history of physics, has unified existing physical models and provided a means for the development of new models. In physics it is now believed that an empirically derived physical model, devoid of phenomenological constitutive relations, would not be justified unless an underlying AP exists. In addition to mathematical elegance, APs are of practical importance for seeking invariants via symmetries using Noether's theorem [194] (see, e.g., Refs. [203, 64] for plasma examples), obtaining consistent approximations (e.g., Ref. [120]), and developing numerical algorithms (e.g., Refs. [85, 257, 143]).

In most areas of fusion, space and astrophysical plasmas, fluid models have proven to be highly useful in capturing the relevant physics [81, 90]. Since the pioneering works of Hannes Alfvén in the 1930s, ideal magnetohydrodynamics (MHD) has established itself as a cornerstone in fusion and astrophysical plasmas [142, 104, 146]. The ubiquity of ideal MHD stems from its combination of simplicity and (fairly) wide applicability. As MHD is a

fluid theory, it shares deep connections with ideal hydrodynamics, including the concept of helicity conservation. Helicities are of considerable interest as they are topological quantities [177, 36, 156], and share a close kinship with the relaxation and self-organization [256, 245] of plasmas. A third advantage of ideal MHD is that it possesses an elegant action principle [192] and Hamiltonian [185] formulation, each of which has several advantages of its own.

Although MHD has proven to be very successful in predicting many phenomena, it is known to be valid only in certain regimes. There exist a wide class of systems, particularly in astrophysics and space science, which are collisionless with non-ideal MHD effects becoming important. For instance, one such notable contribution is the Hall effect that becomes non-negligible when the characteristic frequencies become comparable to, or greater than, the ion cyclotron frequency ω_{ci} [31]. Another crucial effect worth highlighting is due to electron inertia, which becomes important when one considers characteristic length scales that are smaller than the electron skin depth $d_e = c/\omega_{pe}$ with ω_{pe} denoting the electron plasma frequency.

Thus, it is advantageous to seek fluid models containing the above two effects. Extended MHD, [234, 163] henceforth referred to as XMHD, is a model that is endowed with both the Hall drift and electron inertia [163]. It can be rigorously derived from two-fluid theory through a series of systematic orderings and expansions, as shown in [81, 104, 120]. Although it has long since been known that ideal MHD has both action principle [192] and Hamiltonian [185] formulations, the XMHD equivalents proved to be quite elusive. This

is imporant since we know that XMHD is derived from the two-fluid model, which is Hamiltonian in nature [233]. Yet, several models in the literature have failed to recognize the Hamiltonian nature of extended MHD, thereby giving rise to spurious dissipation; see [130] for a discussion of the same. We note that many of the extended MHD models have been derived via an action principle formulation [120], but a Hamiltonian formulation has proven elusive - it was only very recently that a unified Hamiltonian approach to extended MHD was proposed in [1] - the former was presented in [120, 72] and the latter in [1, 158]. At this stage, it is important and instructive to pose two crucial questions. What general benefits do the Hamiltonian and Action Principle (HAP) formulations accord? Secondly, what are the physical systems and phenomena where extended MHD has been successfully employed?

The first question has already been explored extensively, and we refer the reader to the reviews by [225, 181, 266, 112, 216, 265, 182, 183]. Some of the chief advantages, apart from their inherent mathematical elegance and simplification, include:

- A systematic and rigorous means of constructing equilibria and obtaining sufficient conditions for their stability [112]. This was recently applied to ideal MHD in a series of works by [12, 13]; see also [188].

- A clear derivation of reduced models without the loss of the Hamiltonian nature, and thereby avoiding 'spurious' dissipation. A few such examples include [186, 110, 187, 65].

- An excellent way of building in constraints *a priori* and permit a natural analysis of symmetries and associated invariants via Noether's theorem; we refer the reader to [187, 120, 157, 159, 73]

- The extraction of important invariants such as the magnetic helicity and its generalizations [58, 112, 199, 156]. This is done by means of the particle relabeling symmetry [199] in the action principle approach and via the degeneracy of the noncanonical Poisson bracket in the Hamiltonian formulation [262]. It is also possible to establish and elucidate topological properties of XMHD by means of the HAP approach, as recently shown in [72, 156]. A comprehensive discussion of the Hamiltonian formulation is found in the works of [185, 181, 216, 182, 183, 184, 10, 11, 12].

- A detailed understanding of how magnetic reconnection operates by taking advantage of the underlying Hamiltonian structure, such as the aforementioned invariants [198, 56, 106, 242, 68, 69, 111].

- A natural means of arriving at weak turbulence theories, as described in [265, 264, 191]. This methodology was applied to Hall MHD by [212]. The reader is directed to the analysis by [2] that drew extensively upon the HAP approach (for e.g., to construct nonlinear wave solutions), and thereby arrived at the energy and helicity spectra of XMHD. We also point out the recent beatification procedure of [251] as an elegant alternative, that explicitly relies on the Hamiltonian formulation.

- The knowledge of the HAP structures has proven to be highly useful numerically for constructing structure preserving integrators (variational and symplectic) [61, 205, 85, 83, 246, 143, 173, 174]. These integrators have (definitively) outperformed other conventional choices, as the latter lack the unique conservation laws and geometric properties of the former.

In addition to these (admittedly representative) benefits, we also observe that the HAP approach has been tangentially employed in astrophysical phenomena such as Hall MHD dynamos [175, 152, 153] and jets [155]. Thus, it is quite evident that a thorough understanding of the Hamiltonian and Action Principle (HAP) formalisms for XMHD is quite warranted.

Fortunately, there are several instances where XMHD has proven to be a very useful physical model. From the perspective of fundamental plasma phenomena, both turbulence and reconnection results have been radically altered since the Hall term and electron inertia were taken into account. In the case of the latter in particular, it is not an exaggeration to say that the whole field was revitalized through the inclusion of this one simple term. The reader may consult the excellent texts by [41, 39] on this subject. In turbulence, it has been shown that the introduction of Hall drift (and electron inertia) leads to the steepening of spectra [144, 97, 98, 228, 2]. Each of these theoretical consequences has been confirmed through detailed observations of the Earth's magnetosphere [131, 53], and the solar wind and corona [214, 200, 51, 215, 8, 189]. Lastly, we also wish to note that certain fusion phenomena, such as sawtooth crashes [109], have also been explained well by utilizing XMHD.

Chapter 2

Review of Hamiltonian methods

2.1 Functional calculus

Since we are going to be relying on functional calculus in this thesis it is reasonable to provide a small tutorial. For background see [70, 182]. The variational derivative can be thought of as a continuum limit of a partial derivative in the limit of infinite degrees of freedom. Consider a functional $K = K[u]$ for some $u = u(x)$, then *first variation* is defined as

$$\delta K := \lim_{\epsilon \to 0} \frac{K[u + \epsilon \delta u] - K[u]}{\epsilon} = \int dx \, \delta u \, \frac{\delta K}{\delta u} \tag{2.1}$$

If the Kernel of K is $\mathcal{K}$ we can write using integration by parts and ignoring the surface terms which is the philosophy that will be employed in the rest of the thesis

$$\frac{\delta K}{\delta u} = \frac{\partial \mathcal{K}}{\partial u} - \partial_x \frac{\partial \mathcal{K}}{\partial u_x} + \partial_x^2 \frac{\partial \mathcal{K}}{\partial u_{xx}} + \dots, \tag{2.2}$$

where ∂_x denotes differentiation with respect to the x and $u_x := \partial u / \partial x$. If one performs a coordinate change $u \to v$ one also obtains a functional chain rule

$$\frac{\delta F}{\delta u} = \left(\frac{\delta v}{\delta u} \right)^\dagger \frac{\delta F}{\delta v}, \tag{2.3}$$

where $\dagger$ denotes Hermitian adjoint and if there are multiple fields the multiplication can be treated as matrix times vector multiplication.

2.2 Phase Space Action Principle

As stated in Chapter 1 action principles play a prominent role in physical theories. Conventionally, in particle theories one formulates a Lagrangian $L := L[q, \dot{q}]$ using $\dot{q} := q_t$ and defines the action as

$$S[q, \dot{q}] = \int_{t_0}^{t_1} dt\, L \tag{2.4}$$

One varies the path connecting $x(t_1)$ and $x(t_0)$ keeping the ends fixed. The stationarity of the action corresponds to the physical paths the classical systems takes. This, according to (2.2), naturally leads to Euler-Lagrange equations. Under some constraints on Lagrangian this can be turned into an action principle that generates first order differential equations, Hamilton's equation. This is done using the Legendre transform

$$H = p\,\dot{q} - L. \tag{2.5}$$

One can then introduce the phase space action principle that reads

$$S[q, p] = \int_{t_0}^{t_1} dt\ (p\,\dot{q} - L)\,. \tag{2.6}$$

The resulting Hamilton's equations can be written using $z := (q, p)$ as

$$\dot{z} = J\,\frac{\partial H}{\partial z} =: \{H, z\}, \tag{2.7}$$

where J is the so-called co-symplectic two-form consisting of four distinct blocks

$$J := \begin{pmatrix} 0 & 1 \\ -1 & 0 \end{pmatrix}. \tag{2.8}$$

We have also defined a Poisson bracket

$$\{F, G\} := \frac{\partial F}{\partial z} J \frac{\partial G}{\partial z} \tag{2.9}$$

The coordinates q and p making up z are known as canonical coordinates. In general one may wish to perform transformations to some other coordinate systems that could be noncanonical. In this case J becomes a function of z. However there are still properties that J and thus the underlying Poisson Bracket must satisfy such as

- Antisymmetry: $\forall F, G : \{F, G\} = -\{G, F\}$.
- Jacobi identity: $0 = \{F, \{G, H\}\} + \{G, \{H, F\}\} + \{H, \{F, G\}\}$

If we find a Poisson bracket with these properties then we know from the Lie-Darboux theorem that locally there exists a coordinate transformation such that J takes the form

$$J := \begin{pmatrix} 0 & 1 & 0 \\ -1 & 0 & 0 \\ 0 & 0 & 0 \end{pmatrix}. \tag{2.10}$$

Where the dimensions of the bottom rightmost block coincides with the dimension of the null space of J. A consequence of the degeneracy of the cosymplectic form is that the null-space is spanned by the gradients of the so-called Casimir invariants, which foliate the phase space into Casimir leaves and constrain the dynamics of the system (See Fig 2.1). Indeed if we allow

$$J \frac{\partial C}{\partial z} = 0, \tag{2.11}$$

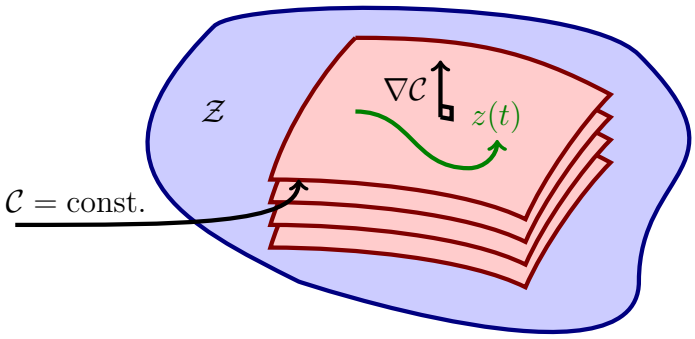

Figure 2.1: Foliation of phase space $\mathcal{Z}$ by Casimirs $\mathcal{C}$ in *finite* dimensions. Observe how dynamical system evolves ($z = z(t)$) on individual Casimir leaves. But field theories like XMHD are uncountably *infinite* dimensional!

it follows that

$$\dot{C} = \frac{\partial C}{\partial z} J \frac{\partial H}{\partial z} = 0. \tag{2.12}$$

Of course one has to be careful when applying the wealth of knowledge about finite-dimensional dynamics to infinite dimensions, which describe fluid/kinetical theories. A rule of thumb is that sums become integrals and matrices - operators. For instance, the antisymmetry of the matrix J becomes skew-symmetry of the operator J.

2.3 Differential Geometry

Geometry has a strong prominence in physics. One of the reasons is the understanding that the physical law must be manifest in the coordinate free language. In addition many theorems can be more easily proved adopting such methods. This section is merely written to set up the definitions and the

reader is advised to consult more in-depth materials on the subject such as an excellent book [88].

We define as is customary p-forms as p-linear cotangent vectors acting on the vectors of the tangent bundle. In this context symbol d will refer to exterior differentiation. A map between two manifolds can be denoted $\phi : M \to N$, which induces pullbacks $\phi_\star$ of forms and pushforwards $\phi^\star$ of vectors. In Chapter 4 an important role is played by the Lie derivative with respect to some vector field u that is defined as

$$\mathcal{L}_u \alpha := \lim_{\epsilon \to 0} \frac{\phi^\star(t+\epsilon)\alpha - \phi^\star(t)\alpha}{\epsilon} \tag{2.13}$$

Here the flow $\phi(t)$ represents the flow generated by the vector field u. An identity that will be useful for us will be

$$\frac{\mathrm{d}}{\mathrm{d}t}\phi^\star(t)\,\alpha = \phi^\star(t)\,(\partial_t \alpha + \mathcal{L}_u \alpha) \tag{2.14}$$

When this quantity is set to zero, we will refer to the phenomenon as Lie-dragging. In the plasma literature this corresponds to flux freezing and will be discussed in the next chapter.

Chapter 3

Hamiltonian properties of extended magnetohydrodynamics

3.1 Introduction

A wide variety of phenomena in astrophysics requires models that operate on scales smaller than ideal MHD. For instance, Hamiltonian reconnection can take place when electron inertia is taken into account. In [130] several reduced 2-fluid models (that can be found in literature) were analyzed to see if they conform to the fundamental law of energy conservation upon removal of viscosity and resistivity. As a result a particular version of the extended MHD was presented based on original Lüst's work [163].

Our goal in this chapter is to demonstrate that most extended MHD models are endowed with a common underlying structure, which originates via the underlying Lagrangian picture of fluid models. We use this commonality to derive Casimir invariants, such as the helicities, through simpler means. After establishing the correspondence(s) between variants of extended MHD in Sec. 3.2 and Chapter 4, we prove the Jacobi identity for Hall MHD in detail in Appendix A. Our work [158] serves as a complement of [1], where the Hamiltonian structure of extended MHD was analyzed in detail.

Material in this chapter is largely lifted from Ref [158] [1]. In the present section, we introduce the equations of the extended MHD model, and discuss its Hamiltonian structure as well as the insights that follow as a natural consequence.

3.1.1 Preliminary model considerations

Although a correct form of the equations of XMHD has been known since the 1950s [81, 163], many different variants exist in the literature. Of these, it is worth remarking that some of them are incorrect and do not conserve energy (for details see Ref. [130]).

The XMHD equations comprise of the continuity equation, the momentum equation and the generalized Ohm's law [104, 39]. They are respectively given by

$$\frac{\partial \rho}{\partial t} + \nabla \cdot (\rho \mathbf{V}) = 0, \tag{3.1}$$

$$\rho \left(\frac{\partial \mathbf{V}}{\partial t} + \mathbf{V} \cdot \nabla \mathbf{V} \right) = -\nabla p + \mathbf{J} \times \mathbf{B} - \frac{m_e}{e^2} \mathbf{J} \cdot \nabla \left(\frac{\mathbf{J}}{n} \right), \tag{3.2}$$

$$\mathbf{E} + \mathbf{V} \times \mathbf{B} - \frac{\mathbf{J} \times \mathbf{B} - \nabla p_e + \mu \nabla p_i}{en} = \tag{3.3}$$

$$\frac{m_e}{ne^2} \left[\frac{\partial \mathbf{J}}{\partial t} + \nabla \cdot \left(\mathbf{V}\mathbf{J} + \mathbf{J}\mathbf{V} - \frac{1}{en} \mathbf{J}\mathbf{J} \right) \right]. \tag{3.4}$$

Here, note that the one-fluid variables ρ, $\mathbf{V}$ and $\mathbf{J} = \mu_0 \nabla \times \mathbf{B}$ are the total mass density, the centre-of-mass velocity and the current, respectively. $\mathbf{E}$ and

[1] M. Lingam, P. J. Morrison, G. Miloshevich, "Remarkable connections between extended magnetohydrodynamics models." Phys. Plasmas, 22(7):072111 July 2015. George Miloshevich is a tertiary author. His contribution was significant (confirming that the model is indeed Hamiltonian) but the bulk of the work was done by the coauthors.

$\mathbf{B}$ denote the electric and magnetic fields, whilst p_s is the pressure of species 's' and $p = p_i + p_e$ is the total pressure. The variables m_e and e are the electron mass and charge, whilst $\mu = m_e/m_i$ is the mass ratio. An inspection of (3.3) reveals that it is far more complex than the ideal MHD Ohm's law that follows by setting all terms except the first two (on the LHS) to zero.

The next step is to render the above equations dimensionless. This is done by normalizing everything in terms of Alfvénic units, and the reader is directed to [1, 156] for further details. We also introduce the dynamical variable

$$\mathbf{B}^* = \mathbf{B} + d_e^2 \, \nabla \times \left[\frac{\nabla \times \mathbf{B}}{\rho} \right], \tag{3.5}$$

which is well known from previous theories that relied upon electron inertia, such as [198, 56]. After some algebraic manipulation (3.2) and (3.3) can be expressed in a simpler manner as follows:

$$\frac{\partial \mathbf{V}}{\partial t} + (\nabla \times \mathbf{V}) \times \mathbf{V} = -\nabla \left(h + \frac{V^2}{2} \right) + \frac{(\nabla \times \mathbf{B}) \times \mathbf{B}^*}{\rho} - d_e^2 \nabla \left[\frac{(\nabla \times \mathbf{B})^2}{2\rho^2} \right], \tag{3.6}$$

$$\frac{\partial \mathbf{B}^*}{\partial t} = \nabla \times (\mathbf{V} \times \mathbf{B}^*) - d_i \nabla \times \left(\frac{(\nabla \times \mathbf{B}) \times \mathbf{B}^*}{\rho} \right) + d_e^2 \nabla \times \left[\frac{(\nabla \times \mathbf{B}) \times (\nabla \times \mathbf{V})}{\rho} \right]. \tag{3.7}$$

In obtaining the above two equations, we observe that a barotropic pressure was implicitly assumed; for a non-barotropic treatment, we refer the reader to [130, 120, 72]. In the above expressions, note that $d_s = c/(\omega_{ps} L)$ is the skin depth of species 's' normalized to the characteristic length scale L, and ω_{ps} is the corresponding plasma frequency. All of these values are in terms of the fiducial units that were adopted for the purpose of normalization.

3.2 On the similarities and equivalences of extended MHD models

In this section, we analyze Hall MHD and demonstrate the equivalence of Poisson brackets with inertial MHD. We exploit this equivalence to determine the helicities, which are Casimir invariants, of these models in a straightforward manner.

3.2.1 Hall MHD: an analysis

Hall MHD represents the most widely used variant of the extended MHD models, and is also one of the simplest. In Hall MHD, it is assumed that the two species drift with different velocities (as opposed to ideal MHD), but it is assumed that the electrons are inertialess (akin to ideal MHD). We commence our analysis with the Hall MHD bracket of [258, 1], expressed as

$$\begin{aligned}\{F,G\}^{HMHD} &= -\int_D d^3x \Bigg\{ [F_\rho \nabla\cdot G_{\mathbf{V}} + F_{\mathbf{V}}\cdot\nabla G_\rho] \\ &- \left[\frac{(\nabla\times\mathbf{V})}{\rho}\cdot(F_{\mathbf{V}}\times G_{\mathbf{V}})\right] - \frac{\mathbf{B}}{\rho}\cdot(F_{\mathbf{V}}\times(\nabla\times G_{\mathbf{B}}) \\ &- G_{\mathbf{V}}\times(\nabla\times F_{\mathbf{B}}) + d_i\,(\nabla\times F_{\mathbf{B}})\times(\nabla\times G_{\mathbf{B}})) \Bigg\},\end{aligned} \tag{3.8}$$

where $d_i = c/(\omega_{pi}L)$ is the normalized ion skin depth and the likes of F_ρ, $F_{\mathbf{V}}$, etc. represent the functional derivatives with respect to the subscripted variables. We can re-express (3.8) as

$$\{F,G\}^{HMHD} = \{F,G\}^{MHD} + \{F,G\}^{Hall}, \tag{3.9}$$

where $\{F,G\}^{MHD}$ is the ideal MHD bracket, first obtained in [185] and $\{F,G\}^{Hall}$ is the term in (3.8) that involves the ion skin depth d_i. As a consequence, we conclude that *any* Casimir of ideal MHD that is independent of $\mathbf{B}$ will automatically serve as a Casimir of Hall MHD. Next, observe that

$$\mathcal{C}_1 = \int_D d^3x\, \mathbf{A}\cdot\mathbf{B}, \tag{3.10}$$

is a Casimir of ideal MHD. Furthermore, it also satisfies $\{F,\mathcal{C}_1\}^{Hall} = 0$ as well. Together, they ensure that (3.10) is a Casimir of Hall MHD. Next, let us suppose that we introduce a new variable

$$\boldsymbol{\mathcal{B}}_i = \mathbf{B} + d_i\nabla\times\mathbf{V}, \tag{3.11}$$

and re-express the bracket in terms of the new set of observables. We find that

$$\{F,G\}^{HMHD} \equiv \{F,G\}^{HMHD}\left[\boldsymbol{\mathcal{B}}_i\right] = \{F,G\}^{MHD}\left[\boldsymbol{\mathcal{B}}_i\right] - \{F,G\}^{Hall}\left[\boldsymbol{\mathcal{B}}_i\right], \tag{3.12}$$

and the notation '$\boldsymbol{\mathcal{B}}_i$' indicates that the respective components of (3.12) are the same as (3.9) except that $\mathbf{B}$ is replaced by $\boldsymbol{\mathcal{B}}_i$. Thus, by following the same line of reasoning, we conclude [158] that

$$\mathcal{C}_2 = \int_D d^3x\, \boldsymbol{\mathcal{A}}_i\cdot\boldsymbol{\mathcal{B}}_i = (\mathbf{A}+d_i\mathbf{V})\cdot(\mathbf{B}+d_i\nabla\times\mathbf{V}), \tag{3.13}$$

is a Casimir of ideal MHD, with $\mathbf{B}\to\boldsymbol{\mathcal{B}}_i$ and it also satisfies $\{F,\mathcal{C}_1\}^{Hall}\left[\boldsymbol{\mathcal{B}}_i\right] = 0$. Hence, we conclude that $\mathcal{C}_2$ is also a Casimir of Hall MHD.

The transformation $\mathbf{B}\to\boldsymbol{\mathcal{B}}_i$ exhibits two very special properties:

- We see that it preserves the form of the Hall MHD bracket, i.e. it is evident that (3.9) and (3.12) are identical to one another upon carrying

out this transformation, apart from the change in sign. The latter can be absorbed simply via $d_i \to -d_i$ as well.

- It allows us to quickly determine the second Casimir of Hall MHD, without going through the conventional procedure of solving a set of constraint equations. In fact, we see that (3.10) and (3.13) possess the same form.

Thus, it is evident that such transformations play a crucial role, both in exposing the symmetries of the system and in determining the Casimirs. In Chapter 4, we shall explore this issue in greater detail.

3.2.2 Hall MHD and inertial MHD

Both ideal MHD and Hall MHD assume that the electrons are inertialess, i.e. this is undertaken by taking the limit $m_e/m_i \to 0$ everywhere. However, there are several regimes where electron inertia effects may be of considerable importance, such as reconnection [198]. To address this issue, a new variant of MHD, dubbed inertial MHD, was studied in [130] and the Hamiltonian and Action Principle (HAP) formulation of two-dimensional inertial MHD were presented in [159].

We shall now turn our attention to inertial MHD, whose non-canonical bracket is given by

$$\{F,G\}^{IMHD} = \{F,G\}^{MHD}[\mathbf{B}^\star] + d_e^2 \int_D d^3x \left[\frac{\nabla\times\mathbf{V}}{\rho}\cdot((\nabla\times F_{\mathbf{B}^\star})\times(\nabla\times G_{\mathbf{B}^\star}))\right], \tag{3.14}$$

and the bracket $\{F,G\}^{MHD}[\mathbf{B}^\star]$ constitutes the ideal MHD bracket with $\mathbf{B} \to \mathbf{B}^\star$. The variable $\mathbf{B}^\star$ is the 'inertial' magnetic field, and was first introduced in [159]. It is given by

$$\mathbf{B}^\star = \mathbf{B} + d_e^2 \nabla \times \left(\frac{\nabla \times \mathbf{B}}{\rho} \right), \tag{3.15}$$

where $d_e = c/(\omega_{pe} L)$ represents the normalized electron skin depth. We shall now apply the transformation

$$\boldsymbol{\mathcal{B}}_e = \mathbf{B}^\star - d_e \nabla \times \mathbf{V}, \tag{3.16}$$

and re-express our bracket in terms of the new set of observables. Upon doing so, we find that

$$\begin{aligned} \{F,G\}^{IMHD} &\equiv \{F,G\}^{IMHD}[\boldsymbol{\mathcal{B}}_e] = \{F,G\}^{MHD}[\boldsymbol{\mathcal{B}}_e] \\ &- 2d_e \int_D d^3x \left[\frac{\boldsymbol{\mathcal{B}}_e}{\rho} \cdot ((\nabla \times F_{\boldsymbol{\mathcal{B}}_e}) \times (\nabla \times G_{\boldsymbol{\mathcal{B}}_e})) \right]. \end{aligned} \tag{3.17}$$

The second term in the above expression can be compared against the last term in (3.8) - we see that the two are identical under $d_i \to 2d_e$ and $\mathbf{B} \to \boldsymbol{\mathcal{B}}_e$. Thus, we arrive [158] at one of our central results:

$$\{F,G\}^{IMHD} \equiv \{F,G\}^{HMHD}[2d_e; \boldsymbol{\mathcal{B}}_e]. \tag{3.18}$$

In other words, the inertial MHD bracket is equivalent to the Hall MHD bracket when the transformations $d_i \to 2d_e$ and $\mathbf{B} \to \boldsymbol{\mathcal{B}}_e$ are applied to the latter. As a result, we are led to a series of remarkable conclusions:

- As the inertial and Hall MHD brackets are identical under a change of variables (and constants), proving the Jacobi identity for one of them constitutes an automatic proof of the other.

- We can obtain the Casimirs of inertial MHD since the equivalent Casimirs were determined for Hall MHD. In particular, two helicities emerge:

$$\mathcal{C}_I = \int_D d^3x \, (\mathbf{A}^\star - d_e \mathbf{V}) \cdot (\mathbf{B}^\star - d_e \nabla \times \mathbf{V}) \,, \tag{3.19}$$

$$\mathcal{C}_{II} = \int_D d^3x \, (\mathbf{A}^\star + d_e \mathbf{V}) \cdot (\mathbf{B}^\star + d_e \nabla \times \mathbf{V}) \,, \tag{3.20}$$

  where $\mathbf{B}^\star = \nabla \times \mathbf{A}^\star$, and the RHS is determined via (3.15).

- By taking the difference of (3.20) and (3.19), we obtain a Casimir:

$$\mathcal{C}_{III} = \int_D d^3x \, \mathbf{V} \cdot \mathbf{B}^\star, \tag{3.21}$$

  which is identical to the cross-helicity invariant of ideal MHD, after performing the transformation $\mathbf{B} \to \mathbf{B}^\star$. The existence of this invariant has also been documented in [159].

We observe that (3.20) and (3.21) were obtained as the Casimirs for inertial MHD in [1], but the authors do not seem to have realized that inertial MHD has not one, but *two* Casimirs (helicities) of the form $\int_D d^3x \, \mathbf{P} \cdot (\nabla \times \mathbf{P})$, as seen from (3.19) and (3.20). As a result, this allow us to emphasize a rather unique feature of inertial MHD:

- One can interpret inertial MHD as consisting of two helicities akin to the magnetic (or fluid) helicity, cementing its similarity to Hall MHD and the 2-fluid models [233].

- Alternatively, we can view inertial MHD as being endowed with one Casimir resembling the magnetic helicity and the other akin to the cross helicity. Such a feature renders it analogous to ideal MHD, which possesses similar features [185].

To summarize thus far, we have shown an unusual correspondence between Hall MHD (inertialess, finite Hall drift) and inertial MHD (finite electron inertia, no Hall drift) by showing that the two brackets are equivalent under a suitable set of transformations. We shall explore their origin in more depth in Chapter 4.

3.2.3 Comments on extended MHD

In the sections above, we have discussed models that incorporate the Hall drift and those that possess a finite electron inertia. Extended MHD merges these effects, giving rise to a more complete model. The non-canonical bracket for this model is

$$\{F, G\}^{XMHD} = \{F, G\}^{IMHD} + \{F, G\}^{Hall}\left[\mathbf{B}^{\star}\right], \tag{3.22}$$

and the second term on the RHS denotes the Hall term with $\mathbf{B} \to \mathbf{B}^{\star}$, and the latter is defined in (3.15).

It is evident that a clear pattern begins to emerge:

1. The Jacobi identity for the Hall bracket can be proven in a simple manner as it represents the sum of two components, one of which already satisfies the Jacobi identity (the ideal MHD component). The details are provided in Appendix A.

2. The Jacobi identity for inertial MHD automatically follows as per the discussion in Section 3.2.2.

3. It is easy to see from (3.22) that the extended MHD bracket will then be composed of a component (inertial MHD) that already satisfies the Jacobi identity, apart from a second component that represents the Hall contribution. As a result, the calculation mirrors the proof of the Jacobi identity for Hall MHD, and the similarities are manifest upon inspecting (3.9) and (3.22).

Finally, let us consider extended MHD (XMHD) in its entirety, i.e., where no terms are dropped from the Ohm's law (3.3). The noncanonical Poisson bracket for this model was derived by [1], and [158] showed that another beautiful equivalence between the Hall and extended MHD brackets existed. In mathematical terms, it amounts to

$$\{F, G\}^{XMHD} \equiv \{F, G\}^{HMHD} \left[d_i - 2\kappa_\pm; \boldsymbol{\mathcal{B}}_\pm\right], \tag{3.23}$$

where the RHS indicates that the substitutions

$$\mathbf{B} \to \boldsymbol{\mathcal{B}}_\pm := \mathbf{B}^* + \kappa_\pm \nabla \times \mathbf{V}, \tag{3.24}$$

and $d_i \to d_i - 2\kappa_\pm$ in (3.8) lead to the XMHD bracket. Again, there are two such transformations since $\kappa_\pm$ follow from determining the two roots of the quadratic equation

$$\kappa^2 - d_i \kappa - d_e^2 = 0. \tag{3.25}$$

Here, observe that setting $d_i = 0$ leads us to the inertial-Hall MHD equivalence discussed above, and also transforms (3.24) to $\boldsymbol{\mathcal{B}}_{\pm}^{(I)}$.

Before proceeding further, a comment on why these connections between the different models are remarkable is in order. In Hall MHD, there is *no* electron inertia but there is a *finite* Hall drift. In inertial MHD, the situation is exactly reversed, i.e. there is no Hall drift but there is electron inertia. Thus, it is not at all intuitively obvious that the two models could share a common Hamiltonian structure, since their effects are mutually exclusive. Yet, the above relations show that there does exist a deep, and non-trivial, equivalence between the two models. This equivalence is also shared by extended MHD, which has *both* Hall drift and electron inertia. Here, it must be understood that the "equivalence" referred to thus far between Hall MHD and inertial MHD is only concerned with their respective Poisson brackets. The corresponding Hamiltonians for these two models are not identical, as they differ by a single term.

Chapter 4

Topological extended magnetohydrodynamics

Material from this chapter is partly based on Ref [158] [1]

4.1 Topological properties of magnetohydrodynamics

In the pioneering work of Moffatt [177], magnetic helicity has acquired a topological property, namely a measure of linking of magnetic field lines. This can be seen easily in the following illustration. Suppose we have two linked flux tubes. Using the fact that $\boldsymbol{B}\, d^3x = \psi\, \boldsymbol{d\ell}$, magnetic helicity in flux tube C_1 (See Figure 4.1) can be evaluated as

$$H_1 = \int d^3x\, \boldsymbol{A}\cdot\boldsymbol{B} = \psi_1 \int_{C_1} \boldsymbol{A}\cdot\boldsymbol{d\ell} = \psi_1\psi_2. \tag{4.1}$$

The total helicity is the sum of the contribution from both flux tubes which evaluates to $2\psi_1\psi_2$. Notice that if there is no linking, there is no helicity, although the converse is not necessarily true. One has to be careful when performing the last step in (4.1). At this point it is tacitly implied that flux tubes have no inner structure, which could contribute to the integral.

[1] M. Lingam, G. Miloshevich, P. J. Morrison "Concomitant Hamiltonian and topological structures of extended magnetohydrodynamics." Phys. Lett. A. 380:2400-2406 July 2016. George Miloshevich is a secondary author but his contribution was significant in demonstrating topological properties of XMHD.

A sufficient, although not necessary, requirement for this to be true is that

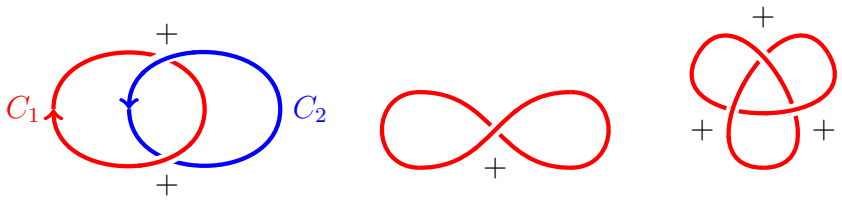

(a) Linked loops (b) Figure 8 (c) Trefoil

Figure 4.1: Schematic of some field configurations. In all of the above crossing numbers are positive as indicated. Subfigure (a) refers to external helicity, while (b) and (c) to self-helicity. (a) Linking number = 1. (b) Writhe = 1 (c) Writhe = 3.

the flux tube is flat and there is no twist (to be defined below) of the field lines. Using the standard $\nabla \cdot \boldsymbol{A} = 0$ gauge one can uncurl $\nabla \times \boldsymbol{A} = \boldsymbol{B}$, which basically means applying Biot-Savart-Laplace equation. This results in the expression for the helicity $H = 2\psi_1\psi_2 L_{12}$, where the Gauss linking number L_{12} [101] is defined as

$$L_{12} := \frac{1}{4\pi} \int_{C_1} ds \int_{C_2} ds' \, \frac{\boldsymbol{X}_1(s) - \boldsymbol{X}_2(s')}{|\boldsymbol{X}_1(s) - \boldsymbol{X}_2(s)|^3} \cdot \hat{\boldsymbol{t}}(s) \times \hat{\boldsymbol{t}}(s'). \tag{4.2}$$

Here $\boldsymbol{X}$'s are curve coordinates, while $\hat{\boldsymbol{t}}$ denotes tangent vectors. Notice that one can substitute velocity for vector potential and get the same result for the fluid velocity. Recent advances in creating fluids with interesting topology can be found in Ref. [219].

Linking number can be defined in the following manner. Flatten the curves so that information about over- and under-crossings remains. The

linking number may be calculated as

$$\text{Link} = \frac{\nu_+ - \nu_-}{2} \tag{4.3}$$

where $\nu_\pm$ stand for positive and negative crossings that are determined using the rule: if the arrow of the over-crossing can be rotated in the positive sense (right hand rule) towards the arrow of the under-crossing then the crossing is positive (see Fig. 4.1). A more rigorous definition of the linking number is found in differential geometry, where given the two curves $\boldsymbol{X}$ and $\boldsymbol{Y}$ both mapping $S^1 \to R^3$, projection on a unit sphere $S^1 \times S^1 \to S^2$ can be defined

$$f_{12} := (s, s') \to \frac{\boldsymbol{X}_1(s) - \boldsymbol{X}_2(s')}{|\boldsymbol{X}_1(s) - \boldsymbol{X}_2(s)|} \tag{4.4}$$

then, denoting pull-back by a star, the Linking number can be represented

$$L_{12} = \frac{1}{4\pi} \int_{S^1 \times S^1} f_{12}^* d^2\,\Sigma \tag{4.5}$$

where $d^2\Sigma$ is the fundamental area 2-form on the sphere. It is not hard to see that this definition is consistent with (4.2) in coordinates if we represent $d^2\Sigma = zdx \wedge dy + xdy \wedge dz + ydz \wedge dx$.

As alluded to earlier, one also has to be concerned with internal helicity. In the subsequent papers [36], [179], [208] it has been shown that linking of field lines inside the flux tube, associated with self-helicity, can be represented as a combination of a twist and writhe of the undrelying flux tube. For more reference see [123], [38], [34], [5], [66], [93], [94], [178], [164], [76]. This fact is based on the Călugareănu theorem [59] and a subsequent multi-dimensional

generalization thereof [254]. To summarize, the theorem considers a closed, possibly knotted ribbon. The ends of the ribbon are two neighboring closed curves. One of the curves ($\mathcal{C}$) is chosen as the axis. It turns out that the linking number of the curves is equal to the sum of the writhe and twist. Twist is defined as the number of right-handed windings that the other curve makes around the axis

$$Tw = \frac{1}{2\pi} \int_{\mathcal{C}} ds \; \hat{\boldsymbol{u}} \times \frac{d\hat{\boldsymbol{u}}}{ds} \cdot \hat{\boldsymbol{t}} \tag{4.6}$$

Here $\hat{\boldsymbol{u}}$ is a unit vector perpendicular to the axis and pointing from the axis to the other curve, while $\hat{\boldsymbol{t}}$ is tangent to the axis.

Writhe is easiest to understand for nearly flat curves like in Figure 4.1. There one only has to sum positive self-crossings and subtract the negative ones. In general writhe can be estimated in the same way but averaged over all possible perspectives (solid angle 4π):

$$Wr = \langle \nu_+ - \nu_- \rangle \tag{4.7}$$

Neither writhe nor twist are isotopic[2] invariants, however their sum is. The technical expression is similar to Gauss linking number, except that integration is taken over the same curve.

$$Wr := \frac{1}{4\pi} \int_{C_1} ds \int_{C_1} ds' \; \frac{\boldsymbol{X}_1(s) - \boldsymbol{X}_2(s')}{|\boldsymbol{X}_1(s) - \boldsymbol{X}_2(s)|^3} \cdot \hat{\boldsymbol{t}}(s) \times \hat{\boldsymbol{t}}(s') \tag{4.8}$$

[2]Isotopy is a continuous set of embeddings from a manifold onto itself. Loosely speaking this allows continuous deformation of a curve without intersections. Isotopy is a form of homotopy.

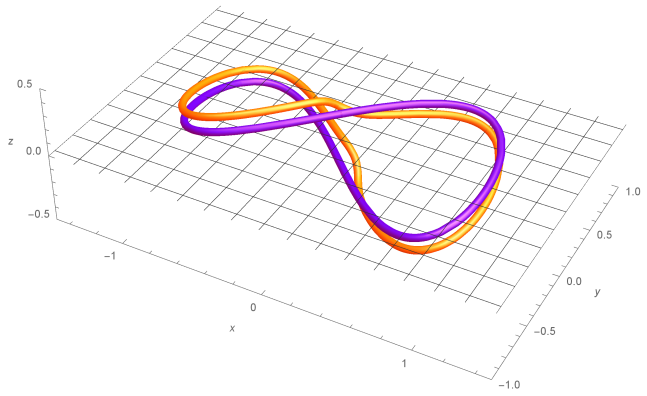

Figure 4.2: Binormal-framed right figure-8. The axis (purple) has $Wr \approx 0.717$ and $Tw \approx -0.717$. Clearly the frame curve (orange) does not link the axis.

The Călugăreanu theorem states

$$\mathrm{Lk} = Wr + Tw \tag{4.9}$$

Since helicity internal to a flux tube has to do with self-linkage of field lines, $H = (Wr + Tw)\Phi^2$, where Φ is the toroidal magnetic flux. Now flux tubes are not ribbons of course, however insight can be gained by considering a ribbon that is spanned from the axis curve by the normal vector pointing towards the field line on the periphery of the tube. Given a flux writhe can ba automatically estimated, however more information is necessary regarding the twist. This is called framing of the ribbon. The simplest framing is the one defined by a Frenet frame consisting of Frenet vectors: tangent, normal and binormal; choosing e.g. the normal as $\hat{\boldsymbol{u}}$ one gets the following pictures

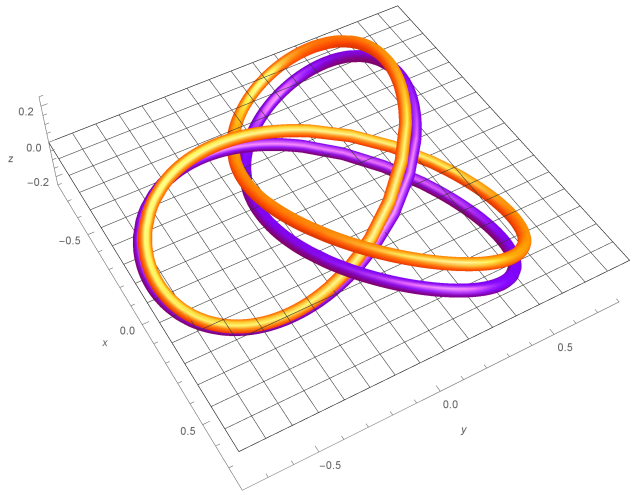

Figure 4.3: Binormal-framed right trefoil. The axis (purple) has $Wr \approx 3.22$ and $Tw \approx -.22$ and, indeed the frame curve (orange) links the axis three times.

(see Figures 4.2 and 4.3). In these curves twist is equal to the total integrated torsion, as expected.

One problem with identifying ribbons with realistic flux tubes at first sight is non-integer rotational transform. Here we define the rotational transform for 3D curves in the same spirit as for Tokamaks. Basically after traversing the tube in the long coordinate, the field line is very unlikely to "bite its own tail". In fact, the set of rational rotational transforms is measure zero of all the possibilities. Fortunately, as can be demonstrated numerically but also by closely inspecting (4.2), helicity can still be decomposed into twist plus writhe.

Until now the discussion has been mostly abstract. To show realiz-

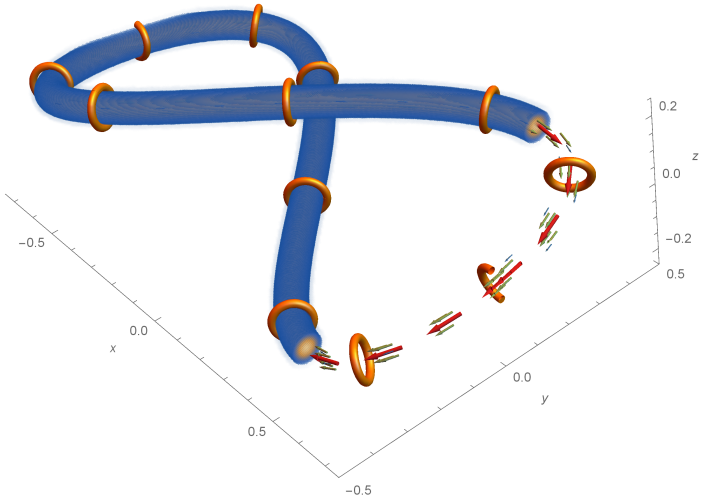

Figure 4.4: Numerically constructed filament-like tube in the form of figure-8. The axis has $Wr \approx .717$ but the tube is framed to have $Tw = 0$, i.e. field vectors are parallel to the axis (displayed by arrows). Magnetic field around the axis has a Gaussian profile. The solid structure (colormap blue to yellow) represents the strength of the field with cutoff at 5% of its maximal value. In addition there is a cut made to reveal the field vectors inside. Finally, orange rings show current density stream lines at chosen locations. Away from the axis the current quickly drops.

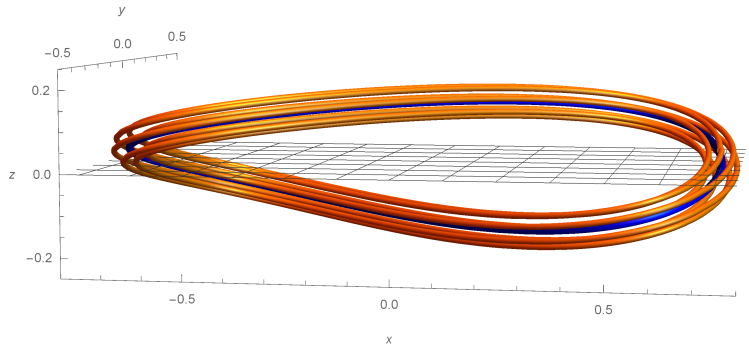

Figure 4.5: Same filament as the above but from a different perspective. In this case we are showing field lines of the magnetic field as apposed to isolated vectors. The blue line represents the axial field, whereas the orange is a single field line on the periphery of the vortex. The field wraps 7 times around the axis before it approximately closes (nearest rationalization).

ability of any of this we would like to construct flux filaments numerically. Furthermore, we have found inconsistencies in the literature, for instance in [31] it is effectively claimed that a flux tube in the form of a helix would have helicity in the amount of $N\Phi^2$ if the field lines are parallel to the center axis. This is at variance with $H = (Wr + Tw)\Phi^2$, since in such configuration $Tw = 0$ and from (4.7) we can estimate that in general helicity should be less. The reason this contradiction occurs is that counter intuitively, field lines in kinked, knotted flux tubes may still link each other even if they don't twist according to the definition above. This will be demonstrated numerically, below. Another way to see this is to choose the appropriate toroidal-poloidal decomposition in zero-framing coordinate system as in [66].

The are two challanges when trying to numerically construct such possibly knotted filament. One has to do with the framing of the tube. It is

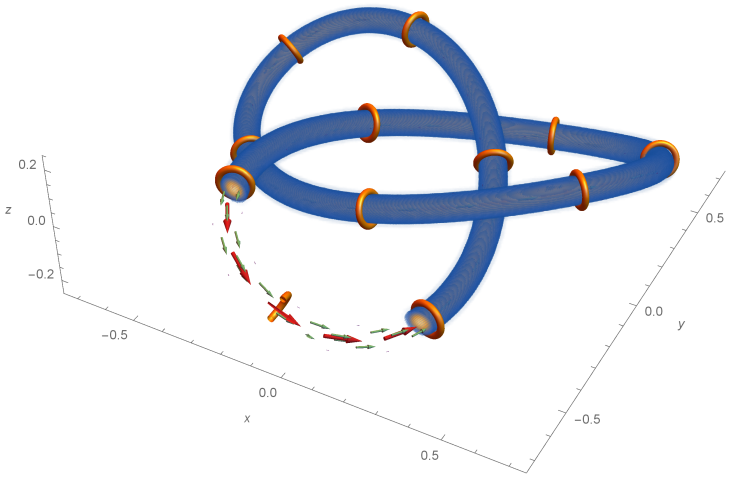

Figure 4.6: Numerically constructed filament tube in the form of trefoil. The axis has $Wr \approx 3.22$ but the tube is framed to have $Tw = 0$.

desirable to have the field lines align parallel to the axis. While we can easily define the axis analytically, the field lines around the axis are not in general copies of it. We need to find the minimal distance to the curve and align the field line with the tangent vector there. Next helicity needs to be estimated, but as can be seen from (4.2) this would require a double volume integral, which in 3 dimensions is very costly. Thus the other problem is instead finding the vector potential for such a flux tube. This can be done by finding the current $\boldsymbol{j} = \nabla \times \boldsymbol{B}$ and solving the Poisson's equation $\Delta \boldsymbol{A} = -\boldsymbol{j}$. We used finite element method by refining the mesh so that it mimics the distribution of the field intensity. The boundary conditions were addressed according to prescription found in [23].

The results can be seen in Figures 4.4 and 4.6. The first case study is the figure-8 like filament with $Wr \approx 0.717$ and $Tw \approx 0$. Notice (Figure 4.5) that even though the twist is zero, because of the torsion (≈ -0.717) the field line doesn't close after going around the figure-8 once. Since $0.717 \approx 5/7$ it approximately links the axis 5 times after going 7 times around. Numerical helicity is estimated at 0.723 which is reasonable given overall convergence as the mesh is subsequently refined. Similarly, in case of a trefoil with $Wr \approx 3.22$ and torsion ≈ -0.22 after a single passage around the knot the fieldline is rotated by 0.22 (even though twist is zero) and it approximately links the axis 2 times after 9 revolutions. The numerical helicity in this case turns out to be ≈ 3.25. There actually is an analytical way of providing twisted, knotted fields with tunable helicity that can be found in Ref. [127].

Natural fields on the other hand can be broken into a tangle of interlinking flux tubes with complex inner structure. When this is done helicity can be decomposed as

$$H = \sum_i (Wr_i + Tw_i)\psi_i^2 + \sum_{ij} L_{ij}\psi_i\psi_j \tag{4.10}$$

Now the problem with identifying topology of the field with helicity is that it is not a one to one map in that helicity does not distinguish between say Borromean rings and the Whitehead link

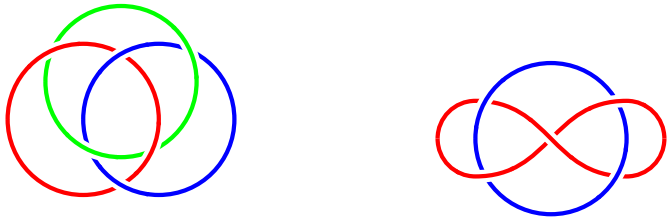

(a) Borromean Rings (b) Whitehead Link

Figure 4.7: Both configurations have the same helicity

4.2 On the topological properties of extended MHD

We have seen earlier that the variable (3.24) lies at the heart of the equivalence between the different models. To understand why, it is instructive to take a step backwards and consider ideal MHD. In any introductory textbook, the frozen-flux property of ideal MHD and the conservation of magnetic helicity $\int_D d^3x\, \mathbf{A} \cdot \mathbf{B}$ are presented. Thus, it is natural to ask if one can seek generalizations of these properties to XMHD, since both of these features are present in two-fluid theory [233, 237] and in Hall MHD [248].

In ideal MHD, the frozen-flux constraint can be expressed as

$$\mathbf{B} \cdot d\mathbf{S} = \mathbf{B}^0 \cdot d\mathbf{S}^0, \tag{4.11}$$

where $d\mathbf{S}$ is the area element, and the superscript '0' denotes the values at $t = 0$ [192]. It is also possible to view the above expression as the statement that the magnetic flux (in ideal MHD) is a Lie-dragged 2-form; for more details, the reader may consult [247].

In XMHD, there are *two* such generalized frozen-flux constraints, given

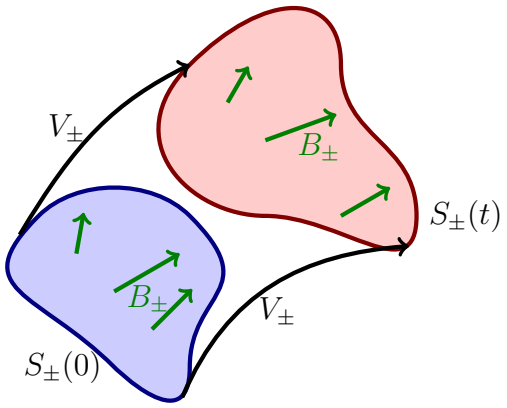

Figure 4.8: Schematics of generalized frozen-flux constraints $\boldsymbol{\mathcal{B}}_\pm \cdot d\mathbf{S}_\pm = \boldsymbol{\mathcal{B}}^0_\pm \cdot d\mathbf{S}^0_\pm$, where $d\mathbf{S}_\pm$ denote the corresponding area elements. It is possible to view the same statement as Lie dragging.

by

$$\boldsymbol{\mathcal{B}}_\pm \cdot d\mathbf{S}_\pm = \boldsymbol{\mathcal{B}}^0_\pm \cdot d\mathbf{S}^0_\pm, \tag{4.12}$$

where $\boldsymbol{\mathcal{B}}_\pm$ was defined in (3.24) and $d\mathbf{S}_\pm$ denotes the corresponding area element. This elegant property was first recognized in [158], later proven in [156] and utilized further in [72].

Next, let us consider the helicity. In ideal MHD, the magnetic helicity is conserved, but it is no ordinary invariant. Instead, it is both a Casimir invariant and a topological invariant. Casimir invariants are special invariants that follow from the degeneracy of the (noncanonical) Poisson bracket, and they are found via $\{F, C\} = 0 \; \forall \, F$, with C denoting the Casimir invariant. They play an important role in regulating the phase space dynamics, as discussed in [182], and have played an important role in reconnection over the

years [198, 56, 106]. Magnetic helicity is also a topological invariant since it is closely connected with the linking and twisting of field lines - more precisely, it shares close connections with the Gauss linking number as discussed in [115, 177, 36].

Thus, one can obtain the generalized counterparts of the magnetic helicity in extended MHD by seeking out the Casimir invariants that resemble it. There are two such invariants

$$\mathcal{K}_{\pm} = \int_D d^3x \, \boldsymbol{\mathcal{A}}_{\pm} \cdot \boldsymbol{\mathcal{B}}_{\pm}, \tag{4.13}$$

where $\boldsymbol{\mathcal{B}}_{\pm} = \nabla \times \boldsymbol{\mathcal{A}}_{\pm}$, and the LHS is given by (3.24). It is clear that these generalized helicities have the same form of the magnetic and fluid helicities (for MHD and HD respectively), and hence one may expect them to share similar topological properties. This conjecture was confirmed in [156], where we have discussed (See Sec. 4.5) some connections with Chern-Simons theory, a ubiquitous (topological) quantum field theory that appears in high-energy and condensed matter physics.

From the preceding discussion, it is clear that the variables $\boldsymbol{\mathcal{B}}_{\pm}$ that facilitate the equivalence between the different extended magnetofluid models is *not* arbitrary. It has close connections with the generalized frozen-fluxes, helicities and Lie-dragged 2-forms all of which have clear mathematical and physical significance. Lastly, it is also possible to manipulate (3.6) and (3.7) directly to arrive at

$$\partial_t \boldsymbol{\mathcal{A}}_{\pm} = \mathbf{V}_{\pm} \times \boldsymbol{\mathcal{B}}_{\pm} + \nabla \psi_{\pm} \quad \text{and} \quad \partial_t \boldsymbol{\mathcal{B}}_{\pm} = \nabla \times (\mathbf{V}_{\pm} \times \boldsymbol{\mathcal{B}}_{\pm}), \tag{4.14}$$

where $\mathbf{V}_\pm := \boldsymbol{V} - \kappa_\mp \nabla \times \boldsymbol{B}$ and

$$\psi_\pm := \kappa_\mp h_e - \Big(\kappa_\pm + \frac{d_e^2}{d_i}\Big) h_i - \phi + \kappa_\mp d_e^2 \frac{J^2}{2\rho} - d_e^2 \frac{\mathbf{J}\cdot\mathbf{V}}{\rho}, \tag{4.15}$$

as shown in [156]. Upon inspection, it is clear that the second set of equations in (4.14) exactly resemble the induction equation in ideal MHD, thereby emphasizing the role of $\boldsymbol{\mathcal{B}}_\pm$ as the generalization of the magnetic field. It is, however, more common to refer to it as the generalized (or canonical) vorticity.

Thus, to summarize our discussion up to this point, we have seen that the Hamiltonian formulation of XMHD has led us to two important conclusions.

- There exists a high degree of mathematical similarity between the different models, even though they have contrasting (and sometimes exclusive) physical effects. This mathematical equivalence between the models is rendered very clear when written in Hamiltonian form. Hence, the latter approach serves as a means of unifying the different extended MHD models.

- The similarities between extended MHD and ideal MHD can be understood further by means of the Hamiltonian Action Principle (HAP) formulations, which lead us to the generalizations of the helicity, flux, and induction equation.

Bearing these advantages in mind, we shall now proceed to study some pertinent features of XMHD turbulence in the subsequent sections.

4.3 Frozen-in fields in electron-ion plasma

Motivated by [212] and [158] it is reasonable to look for the equation describing $\mathbf{A}_\pm := \mathbf{A}^* + \kappa_\pm \mathbf{v}$, where

$$\mathbf{A}^* := \mathbf{A} + d_e^2 \frac{\mathbf{J}}{\rho} = \mathbf{A} + d_e^2 \frac{\nabla \times (\nabla \times \mathbf{A})}{\rho} \tag{4.16}$$

Assuming that both fluids are barotropic, it can be shown that

$$\frac{\partial \mathbf{A}_\pm}{\partial t} = \nabla \mathbf{A}_\pm \cdot \mathbf{w}_\pm - \mathbf{w}_\pm \cdot \nabla \mathbf{A}_\pm + \nabla \psi_\pm, \tag{4.17}$$

where

$$\mathbf{w}_\pm := \mathbf{v} - \kappa_\mp \frac{\mathbf{J}}{\rho} \tag{4.18}$$

and

$$\psi_\pm := \kappa_\mp h_e - \Big(\kappa_\pm + \frac{d_e^2}{d_i}\Big) h_i - \phi + \kappa_\mp d_e^2 \frac{J^2}{2\rho} - d_e^2 \frac{\mathbf{J} \cdot \mathbf{v}}{\rho} \tag{4.19}$$

Here and in what follows we use the convention such that gradients only act on the immediate term to the right. We observe (in parallel with relativistic MHD discussion by Yoshida at al [260]) that one can associate a form $\mathcal{A}_\pm$ with components of $\mathbf{A}_\pm$ and from (4.17) we conclude that the Lie-dragged one-form with corresponding the velocity is exact

$$\frac{\partial \mathcal{A}_\pm}{\partial t} + \mathcal{L}_{w_\pm} \mathcal{A}_\pm = d\psi_\pm, \tag{4.20}$$

where $\mathcal{L}_{w_\pm}$ symbol stands for Lie-derivative with respect to the $w_\pm$ flow. The explicit time derivative appears because of the inherent non-relativistic $3+1$ splitting (Similar discussion that touches only on differential forms can be found in Schutz [222] regarding neutral fluids). Using this geometric language

it is natural to construct other interesting forms that we can have in $3D$, namely a two-form $\mathcal{B}_\pm := d\mathcal{A}_\pm$ and a three-form $\mathcal{K}_\pm := \mathcal{A}_\pm \wedge d\mathcal{A}_\pm$. By taking exterior derivative of (4.20), remembering that $d^2 = 0$ and that Lie derivative commutes with the exterior derivative

$$\frac{\partial \mathcal{B}_\pm}{\partial t} + \mathcal{L}_{w_\pm} \mathcal{B}_\pm = 0 \tag{4.21}$$

Defining

$$\mathbf{B}_\pm := \nabla \times \mathbf{A}_\pm = \mathbf{B}^* + \kappa_\pm \nabla \times \mathbf{v}, \tag{4.22}$$

where (the following symbol does not represent the Hodge dual),

$$\mathbf{B}^* := \mathbf{B} + d_e^2 \nabla \times \frac{\nabla \times \mathbf{B}}{\rho}, \tag{4.23}$$

we see that vector density $\mathbf{B}_\pm$ is dual to the two-form $\mathcal{B}_\pm$, i.e. in coordinates

$$\mathcal{B}_\pm = \big(B_\pm\big)_x \, dy \wedge dz + \big(B_\pm\big)_y \, dz \wedge dx + \big(B_\pm\big)_z \, dx \wedge dy \tag{4.24}$$

For more details on how this works in regular MHD see [252]. Notice, however that their approach to integral invariants is a little different. The consequence of (4.22) is

$$\frac{\partial \mathbf{B}_\pm}{\partial t} = \nabla \times (\mathbf{w}_\pm \times \mathbf{B}_\pm) \tag{4.25}$$

since $\nabla \cdot \mathbf{B}_\pm = 0$. This result was independently obtainedin Ref. [73]. The geometric language not only allows a coordinate free expression of physics but also allows us to more easily prove some theorems like extended circulation-vorticity-helicity conservation and prepares us for a natural relativistic generalization of XMHD.

Conservation of extended circulation can be elegantly expressed as

$$\begin{aligned}\frac{d}{dt}\int_{L_\pm(t)}\mathbf{A}_\pm\cdot d\mathbf{l}\Big|_{t=t_0} &= \frac{d}{dt}\int_{L_\pm(t)}\mathcal{A}_\pm(t)\Big|_{t=t_0} = \frac{d}{dt}\int_{L_\pm(t_0)}\Phi^*_{u_\pm,t}\mathcal{A}_\pm(t)\Big|_{t=t_0} = \\ \frac{d}{dt}\int_{L_\pm(t_0)}\mathcal{A}_\pm(t) &+ (t-t_0)\mathcal{L}_{u_\pm}\mathcal{A}_\pm + \mathcal{O}\big((t-t_0)^2\big)\Big|_{t=t_0} = \\ \int_{L_\pm(t_0)}\frac{\partial\mathcal{A}_\pm}{\partial t} &+ \mathcal{L}_{w_\pm}\mathcal{A}_\pm\Big|_{t=t_0} = \int_{L_\pm(t_0)} d\psi_\pm = 0 \end{aligned} \tag{4.26}$$

$\Phi^*_{u_\pm,t}$ denotes a pullback with vector field $\mathbf{v}_\pm$ parametrized by t. Integration is carried over contour $L_\pm(t)$ indicating that vorticity is frozen-in fluid moving with velocity $\mathbf{v}_\pm$. Likewise vorticity is frozen-in:

$$\frac{d}{dt}\int_{S_\pm(t)}\mathbf{B}_\pm\cdot d\mathbf{S}\Big|_{t=t_0} = \int_{S_\pm(t_0)}\frac{\partial\mathcal{B}_\pm}{\partial t} + \mathcal{L}_{w_\pm}\mathcal{B}_\pm\Big|_{t=t_0} = 0 \tag{4.27}$$

Finally, for helicity

$$\frac{\partial\mathcal{K}_\pm}{\partial t} + \mathcal{L}_{w_\pm}\mathcal{K}_\pm = d\psi_\pm\wedge d\mathcal{A}_\pm = d(\psi_\pm d\mathcal{A}_\pm), \tag{4.28}$$

and one can use Stokes theorem to show

$$\frac{d}{dt}\int_{V_\pm(t)}\mathcal{K}_\pm = \int_{V_\pm(t)} d(\psi_\pm d\mathcal{A}_\pm) = \int_{\partial V_\pm(t)}\psi_\pm d\mathcal{A}_\pm = 0 \tag{4.29}$$

as long as vorticity vanishes on the boundary. Thus we recover the result of [1] and [158] regarding conservation of helicities, except that in (4.13) the integration is carried over the whole domain.

4.4 Epi-2D and arbitary mass ratio XMHD

Here we will draw parallels between the approach taken in Ref. [261] for the discription of a fluid and our case of XMHD. We rewrite the previous

expressions in the geometric language and assert that it holds in general coordinate systems. Another difference is that we will Lie-drag with the exact electron and ion-velocities. For more information on the validity of such model see Sec. 7.6. We assume that ρ is a 3-form, B a 2-form, v - 1-form and write the Hamiltonian for barotropic XMHD

$$H = \int_{\mathcal{M}} \Big(\frac{1}{2}\rho |v|^2 + \rho\, U(\rho) + \frac{1}{2} B_e \wedge \star B \Big), \tag{4.30}$$

where $\rho|v|^2 := \rho\langle v, v\rangle = \star\rho\; v \wedge \star v =: \rho^\star\; v \wedge \star v$. Furthermore, define $\lambda_1 = \lambda_2 = \lambda_+ := m_- c/e$ and $\lambda_3 = \lambda_4 = \lambda_- := -m_+ c/e$ as well as $\check{\eta}_i := \eta_i^\star/\rho^\star$. Then we write the Clebsch parametrization

$$v = d\phi + \sum_{i=1}^{4} \check{\eta}_i d\phi_i \quad \text{and} \quad A_e = \sum_{i=1}^{4} \lambda_i \check{\eta}_i d\phi_i, \tag{4.31}$$

while we have

$$A_e := A - \frac{\lambda_+ \lambda_-}{\rho^\star} d^\star B =: A - \frac{\lambda_+ \lambda_-}{\rho^\star} j. \tag{4.32}$$

The symbol introduced above ($d^\star$) stands for co-differential, which in Riemannian coordinates can be represented as $d^\star \beta^p = (-1)^{n(p+1)+1} \star d \star \beta^p$. We choose 3-forms ρ and η_i to be our canonical coordinates, while 0-forms ϕ and ϕ_i to be conjugate momenta.

It is instructive to show how variational derivatives may be applied to the Hamiltonian (4.30). Using the definition of a global or Hilbert space scalar one writes

$$\int_{\mathcal{M}} \frac{1}{2} \langle B_e, B\rangle \,\mathrm{vol}^3 = \int_{\mathcal{M}} \frac{1}{2} B_e \wedge \star B =: (B_e, B) = (B, B_e). \tag{4.33}$$

Assuming that operational manifold $\mathcal{M}$ is without boundary or that fields decay sufficiently fast so they are zero at the boundary one has

$$(d\alpha^{p-1}, \beta^p) - (\alpha^{p-1}, d^\star \beta^p) = \int_{\partial \mathcal{M}} \alpha^{p-1} \wedge \star \beta^p = 0. \tag{4.34}$$

Thus denoting first variation with respect to the variable η_i as δ_{η_i} (keeping other fields constant)

$$\delta_{\eta_i} \frac{(B_e, B)}{2} = (\delta_{\eta_i} B_e, B) = (\delta \eta_i^\star d\phi_i, \lambda_i \frac{j}{\rho^\star}) = \int_{\mathcal{M}} \delta \eta_i \, \mathcal{L}_{(\lambda_i j^\sharp / \rho^\star)} \phi_i \tag{4.35}$$

Here we have introduced musical notation to denote raising operator $v^\sharp := \langle \ , v \rangle$ and invoked the antiderivation law for the inner product

$$i_{j^\sharp}(\alpha^p \wedge \beta^q) = i_{j^\sharp} \alpha^p \wedge \beta^q + (-1)^p \, \alpha^p \wedge i_{j^\sharp} \beta^q, \tag{4.36}$$

and the Cartan identity

$$\mathcal{L}_{j^\sharp} \alpha = i_{j^\sharp} d\alpha + d i_{j^\sharp} \alpha \tag{4.37}$$

Defining

$$v_i := v + \lambda_i \, j / \rho^\star \tag{4.38}$$

we get

$$\dot{\phi}_i = \{\phi_i, H\} = -\mathcal{L}_{v_i^\sharp} \phi_i \Rightarrow \mathcal{L}_{\tilde{v}_i} \phi_i = 0, \tag{4.39}$$

Notice that we have extended the manifold to $\mathcal{M} \times \mathbb{R}$ by adding time so $\mathcal{L}_{\tilde{v}_i} \phi_i := \dot{\phi}_i + \mathcal{L}_{v_i^\sharp} \phi_i$. Likewise one obtains

$$\mathcal{L}_{\tilde{v}} \rho = \mathcal{L}_{\tilde{v}_i} \eta_i = 0 \quad \text{and} \quad \mathcal{L}_{\tilde{v}} \phi = \frac{|v|^2}{2} - h + \frac{\lambda_+ \lambda_-}{2} \frac{|j|^2}{(\rho^\star)^2} + \frac{\langle A_e, j \rangle}{\rho^\star}, \tag{4.40}$$

where h is the enthalpy. Notice that Eulerian conservation of a scalar ϕ_i as in (4.39) can be re-expressed in the Lagrangian form $f_t^\star \phi_i(t) = \phi_i(0)$, where $f_t^\star$ is a pull-back with $\vec{v}_i$. Thus one can think of Lagrangianized $\phi_i(t)$ as a fluid attribute advected with the fluid, this will be elucidated below in the end of the section. Similarly 3-forms like ρ can also be Lagrangianized and the implicit Jacobian in the Euler-Lagrange map can thus be obtained.

We wish to derive a useful identity. Let $\mathcal{L}_{\tilde{u}+u^\sharp}\check{\eta}_i = 0$. In our case we see that $u = \lambda_i d^\star B/\rho^\star$. It is not hard to show that

$$\mathcal{L}_{\tilde{v}+u^\sharp}\check{\eta}_i = \mathcal{L}_{\tilde{v}+u^\sharp}\frac{\eta_i^\star}{\rho^\star} = -\frac{\eta_i^\star}{(\rho^\star)^2} \star \mathcal{L}_{u^\sharp}\rho. \tag{4.41}$$

Now if we specify $u = d^\star B/\rho^\star$ the term on the r.h.s. vanishes since using (4.37)

$$\mathcal{L}_{u^\sharp}\rho = \lambda_i \, d \, i_{(j^\sharp/\rho^\star)}(\rho^\star \mathrm{vol}^n) = \lambda_i \, d \, i_{\nabla\times\vec{B}} \, \mathrm{vol}^n = \lambda_i \, d^2 \star B = 0. \tag{4.42}$$

Here we have introduced a pseudo-vector $\vec{B}$ dual to a form B. In fact (4.41) can be summed up as $\mathcal{L}_{\tilde{v}}\check{\eta}_i = -\mathcal{L}_{(\lambda_i j^\sharp/\rho^\star)}\check{\eta}_i$. This allows natural passage to physical coordinates:

$$\mathcal{L}_{\tilde{v}}A_e = -\sum_{i=1}^{4}\lambda_i\Big(d\phi_i\mathcal{L}_{(\lambda_i j^\sharp/\rho^\star)}(\check{\eta}_i) + \check{\eta}_i d\mathcal{L}_{\tilde{v}}\phi_i\Big) = -\sum_{i=1}^{4}\lambda_i^2\mathcal{L}_{(j^\sharp/\rho^\star)}(\check{\eta}_i d\phi_i). \tag{4.43}$$

Therefore

$$\mathcal{L}_{\tilde{v}}A_e = \mathcal{L}_{(j^\sharp/\rho^\star)}(A_f) - d(\lambda_+\lambda_-\mathcal{L}_{(j^\sharp/\rho^\star)}\phi), \tag{4.44}$$

where $A_f := -(\lambda_+ + \lambda_-)A_e + \lambda_+\lambda_- v$. It looks like some pressure terms are missing. It is not clear exactly why that is the case, although in the barotropic

case it is not a problem since they can be absorbed inside the potential ϕ without changing physics. Similarly

$$\mathcal{L}_{\tilde{v}} v = d\Big(\frac{|v|^2}{2} - h + \frac{\lambda_+\lambda_-}{2}\frac{|j|^2}{(\rho^\star)^2} + \frac{\langle A_e, j\rangle}{\rho^\star}\Big) - \mathcal{L}_{(j^\sharp/\rho^\star)} A_e \tag{4.45}$$

and thus

$$\mathcal{L}_{\tilde{v}} v = -\frac{i_{j^\sharp} B_e}{\rho^\star} + d\Big(\frac{|v|^2}{2} + \frac{\lambda_+\lambda_-}{2}\frac{|j|^2}{(\rho^\star)^2} - h\Big). \tag{4.46}$$

Equations (4.44) and (4.46) are equivalent to electron-ion XMHD version where one only keeps the lowest order contribution of the electron inertia. Then after rescaling $\lambda_+ \to d_i \approx (d_i + \sqrt{d_i^2 + 4d_e^2})/2$ and $\lambda_- \to -d_e^2/d_i \approx (d_i - \sqrt{d_i^2 + 4d_e^2})/2$. Thus we see that either ordering can be cast as a Hamiltonian theory.

Combining (4.44) and (4.46) one confirms that

$$\mathcal{L}_{\tilde{v}_\pm} B_\pm = 0, \quad B_\pm := B_e - \lambda_\mp dv, \quad v_\pm := v + \lambda_\pm \frac{d^\star B}{\rho^\star} \tag{4.47}$$

Where v_+ corresponds to the velocity of ions. Notice that here we are working with the two-form $B_\pm$. It is possible to work instead with dual vector density or dual pseudo-vector $\vec{B}$ that differs by a $\sqrt{g}$ term and both are Lie-dragged, although the expressions for the Lie-dragging differs by a term in those cases. Alternatively one obtains the same result by re-labeling $\eta_1 =: \eta_+^{(+)}$, $\eta_2 =: \eta_+^{(-)}$,$\eta_3 =: \eta_-^{(+)}$,$\eta_4 =: \eta_-^{(-)}$ and re-writing

$$A_\pm = (\lambda_\pm - \lambda_\mp)(\check{\eta}_\pm^{(+)} d\phi_\pm^{(+)} + \check{\eta}_\pm^{(-)} d\phi_\pm^{(-)}) - \lambda_\mp d\phi \tag{4.48}$$

and using expressions derived earlier $\mathcal{L}_{\tilde{v}_\pm}\check{\eta}_\pm = 0 = \mathcal{L}_{\tilde{v}_\pm}\phi_\pm$. From the above it follows that

$$\mathcal{L}_{\tilde{v}_\pm}A_\pm = -\lambda_\mp d\Big(\frac{|v|^2}{2} + \lambda_+\lambda_-\frac{|j|^2}{2(\rho^\star)^2} + \frac{i_{j^\sharp}(A_e + d\phi)}{\rho^\star} - h\Big) =: d\psi_\pm \tag{4.49}$$

and so

$$\frac{d}{dt}\int_{\mathcal{M}} A_\pm \wedge dA_\pm = \int_{\mathcal{M}} \mathcal{L}_{\tilde{v}_\pm}(A_\pm \wedge dA_\pm) = \int_{\mathcal{M}} d(\psi_\pm A_\pm) = 0. \tag{4.50}$$

Clearly, if we consider a case where double-primed quantities are zero the total integrated helicities would evaluate to zero since the integrand is exact. Alternatively, if $\mathcal{M}$ has boundary it can be assumed that the fields vanish at the boundary. Now we are in a position to exploit an idea introduced in Ref. [261] in the relation to the epi-2D flow. Since XMHD is a generalization one expects four charges instead of two.

$$Q_\pm^{(+)} = \int_{\Omega_\pm^{(+)}(t)} \rho f\Big(\frac{\omega_\pm^{(+)} \wedge d\phi_\pm^{(-)}}{\rho^\star}\Big) \quad \text{and} \quad Q_\pm^{(-)} = \int_{\Omega_\pm^{(-)}(t)} \rho f\Big(\frac{\omega_\pm^{(-)} \wedge d\phi_\pm^{(+)}}{\rho^\star}\Big), \tag{4.51}$$

where $\omega_\pm = d\check{\eta}_\pm \wedge d\phi_\pm$. Since $\check{\eta}$ is dragged by v, every infinitesimal element $\Omega(t)$ is viewed as a quasi-particle - epi-2D particle. In this case the symbol for the charge is actually prime and unprimed, since plus and minus are reserved for the two different species.

4.5 Topological aspects of the generalized helicities of extended MHD

Now, we shall take a greater look at the topological ramifications of $K_\pm$ and (4.50), viz. the generalized helicities and their conservation properties

respectively.

Let us begin by recalling that A_+ and A_- serve as 1-forms, appropriately constructed from $\boldsymbol{\mathcal{A}}_\pm$. If one lets $d_e \to 0$ and $d_i \to 0$, we have already indicated that the vector potential $\mathbf{A}$ follows from $\boldsymbol{\mathcal{A}}_\pm$. Yet, it is important to recognize that all other versions of extended MHD have, not one, but *two* such 1-forms. It is well known that the general expression for a helicity-type quantity is given by $H = \int_{\mathcal{M}} P \wedge dP$, where $\mathcal{A}$ is a compact 3-manifold and P is a 1-form. We have dropped the inner product operator (Tr) as noted earlier. Hence, one can duly construct two helicity-like quantities by setting $P = \mathsf{A}_\pm$ and the corresponding (generalized) helicities are given by $K_\pm$.

We have reiterated the above steps because the crucial aspect of our work is that these generalized 1-forms, 2-forms and helicities can be seen as the exact analogues of the vector potential/velocity, magnetic field/vorticity, and magnetic/fluid helicity respectively. As a result, we are in the remarkable position of exploiting every known topological property of ideal HD or MHD by generalizing it to extended MHD via the variable transformations introduced here, and in [158].

For instance, consider the description of the fluid helicity in terms of thin vortex filaments, which are represented collectively by an oriented knot (or link) in $\mathcal{M}$. The expression for the fluid helicity is given by

$$H = \sum_i \nu_i^2 Lk_i + 2 \sum_{i\,j} \nu_i \nu_j Lk_{ij}, \tag{4.52}$$

where ν_i denotes the vortex circulation, whilst Lk_i and Lk_{ij} are the self-linking

and Gauss linking numbers respectively [179, 208]. Moreover, we observe that $Lk_i = Wr_i + Tw_i$, implying that the self-linking number can be decomposed into its writhing and twisting numbers; the latter duo are topologically relevant in their own right [179, 62, 37, 210]. The decomposition of helicity into its various components has also been verified empirically through a series of ingenious experiments [132, 219, 133], and numerical simulations in dynamos [20]. If we replace the vortex filaments, circulation, etc. by the generalized counterparts (corresponding to $\boldsymbol{\mathcal{B}}_{\pm}$), we find that the generalized helicities can be decomposed in a manner exactly identical to (4.52).

For all its elegance and utility, the linking number is beset by a number of limitations. The foremost amongst them is that it cannot distinguish between certain topological configurations, such as the Whitehead link (See Fig. 4.7b) and the Borromean rings (See Fig. 4.7a) [123]. The conventional means of distinguishing between such configurations is via the Massey product [33] and its generalizations [113], or other higher-order invariants [209, 249, 4]. As per the correspondence between ideal MHD (or HD) and the different variants of extended MHD established earlier, we may be able to construct the equivalent (higher-order) topological invariants for the latter class of models. It is at this juncture that we introduce the remarkable insight provided by Witten [255] between topological quantum field theory (TQFT) and knot theory. In particular, Witten demonstrated that the Jones polynomial, a staple of knot theory, could be naturally interpreted in terms of the Chern-Simons action of $(2+1)$ Yang-Mills theory. The Chern-Simons action for a non-Abelian

field theory is given by

$$S = \int_{\mathcal{M}} \left(P \wedge dP + \frac{2}{3} P \wedge P \wedge P \right), \tag{4.53}$$

up to constant factors. Now, suppose that the underlying gauge group is Abelian, and this choice eliminates the second term on the RHS of the above expression. Consequently, we are led to the striking result that the helicity is an Abelian Chern-Simons action [116, 25]. As a result, one can employ the versatile mathematical formulations of Chern-Simons theory (a 3-dimensional TQFT) [22, 24, 82] in the realm of plasma and fluid models, thereby opening up a potentially rich and diverse line of future research, as these methods are more sophisticated than standard paradigm of computing the linking number(s); for instance, the Jones polynomial is capable of distinguishing between the Whitehead link and the Borromean rings (which have an identical linking number of zero, as previously mentioned). Despite the inherent mathematical richness of the helicity/Chern-Simons correspondence, it hasn't been sufficiently exploited from a knot-theoretic perspective – the mathematical works by [15, 160, 161] on the Jones and HOMFLYPT polynomials in HD and MHD constitute the only such examples of this *specific* line of enquiry. Although [160, 161] utilized the formal equivalence between the fluid (or magnetic) helicity and Abelian Chern-Simons theory, there have been prior studies in high energy physics and topological hydrodynamics that were cognizant of this concept (see e.g. [15, 116]). It is also straightforward to apply this framework to non-Abelian magnetofluid models, as briefly stated in [25].

Thus, we are free to import the results of [15, 160, 161] in the context of the generalized helicities. In particular, following the mathematical reasoning delineated in [160], we are free to compute the Jones polynomial for a given configuration of the generalized helicity (of which there are two in all). The proof relies on the construction of the skein relations by means of the Kauffman bracket polynomial, and then introducing orientation to obtain the skein relations of the corresponding Jones polynomial. Let us interpret the results from the preceding discussion for the (simpler) case of Hall MHD. One of the Jones polynomials would arise from the magnetic helicity, whilst the other arises from the canonical helicity. The difference of these two helicities is the sum of the cross and fluid helicities. Hence, the associated Jones polynomial, arising from this remainder, would encapsulate the topological properties of the fluid and cross helicities.

Quite intriguingly, the Chern-Simons forms are *odd-dimensional* differential forms [88], implying that the Chern-Simons action (4.53) is meaningful only for odd dimensions, given that it is proportional to the integral of the Chern-Simons form. In turn, owing to its identification with the generalized helicities, the latter acquire this distinct mathematical structure only in *odd* dimensions. *Ipso facto*, this may imply that helicities (magnetic, fluid or generalized) of this form will naturally emerge in non-relativistic (3D) theories, but not, perforce, in the case of relativistic theories, as they are intrinsically four-dimensional in nature. In particular, we note that relativistic MHD possesses a cross helicity akin to its 3D counterpart, but the 4D version of the

conventional (3D) magnetic helicity has proven to be elusive from a Hamiltonian perspective [73], although it has been derived through other avenues [165, 260, 201].

Apart from the topological properties of helicity, as seen in isolation, one can also probe its relationship with energy. For instance, a classic result by Moffatt [178] established a relation between the minimum magnetic energy E_{min}, the flux Φ and the volume V of a magnetic flux tube as follows:

$$E_{min} = m\Phi^2 V^{-1/3}, \tag{4.54}$$

where m depends on the specific properties of the knot, and it is a topological invariant; see also [89, 35, 207] for similar results. When dealing with extended MHD, the magnetic component of the energy density must be transformed from B^2 to $\mathbf{B}\cdot\mathbf{B}^\star$. As a result, it is natural to ask whether one generalize the result (4.54) to extended MHD, and we intend to pursue this line of enquiry in our subsequent works.

The applications we have outlined thus far barely scratch the surface. There are many other results from HD and MHD that can be imported to extended MHD involving helicity. For instance, one such example is helicity injection. This phenomenon has been widely studied in the solar context [193, 117] as it has important ramifications, but there have been no studies dealing with generalized helicity injection. We shall leave such subjects for later investigations – it is our present goal to highlight the correspondence with HD/MHD, thereby paving the way for conducting in-depth research in

these areas.

4.6 Discussion and Conclusion

In this chapter, we have emphasized and exploited the inherent mathematical power of the unified Hamiltonian structure of several extended MHD models. This enterprise was rendered possible owing to the work of [1], and the unified Hamiltonian (and its underlying action principle) structure was established in [158, 72].

Quite evidently, a host of avenues open up for future analyses. The first, and possibly, the most significant is the derivation of reduced extended MHD models that retain the Hamiltonian properties of the parent model. Such models are likely to be of considerable relevance in reconnection studies, thereby furthering the basic approach adopted in [198, 57, 242, 111]. For this reason, it was equally important to conduct a detailed examination of their stability via Hamiltonian methods [121], analogous to the extensive study of ideal MHD by [12]. We also note the possibility of using extended MHD models to study dynamos and jets [154], as well as helicity injection [86], the last of which appears to be a completely unexplored arena. Although these models are endowed with the ion and electron skin depths, the absence of the corresponding Larmor radii is evident. To rectify this limitation, it is feasible to use the gyromap [187, 157] in the extended MHD context, to develop a gyroviscous theory analogous to the one formulated by Braginskii. In addition, in Sec. 5.3 we will work with the 2D model that takes ion sound Larmor radius

into account.

From the unified Hamiltonian structure of these models, we demonstrated that they possess a common class of Casimir invariants - the generalized helicities. Motivated by these helicities, we sought the generalizations of the vorticity (or magnetic field), and thereby established the existence of two Lie-dragged 2-forms. Thus, the whole enterprise demonstrated that the topological properties of these models are a *natural* consequence of their Hamiltonian structure. We believe that this is a vital, but rather unrecognized, fact that merits further attention. By constructing these helicities and 2-forms, we derived properties such as the generalization of Kelvin's circulation theorem in a geometric setting. Moreover, we also showed that these helicities can be viewed as Abelian Chern-Simons theories, and that the methodology introduced by Witten, for gaining insights into topological quantum field theory, could be employed here. Consequently, we concluded that the Jones polynomials may be used to characterize different (generalized vorticity) configurations, serving as a more powerful tool than the standard Gauss linking number used to characterize fluid or magnetic helicity. By introducing such topological methods for characterizing helicity, their relevance in the domains of astrophysics and fusion is self-evident. One such application, of paramount importance, is to deploy these topological methods in gaining a better understanding of solar magnetic fields [162].

In summary, we have used the noncanonical Hamiltonian formulation of extended MHD models to arrive at their common mathematical structure,

which manifests itself via the existence of generalized helicities and Lie-dragged 2-forms. These helicities, which are topological invariants, can be further studied through a host of techniques, including the Jones polynomial [15, 160]. From a conceptual point-of-view, our results are elegant, as they exemplify the spirit of unification common to most physical theories. On the other hand, we also believe that the results presented herein possess manifold concrete applications, especially since the helicities serve both as important topological invariants, and crucial mediators of relaxation and self-organization, reconnection, turbulence, and magnetic field generation (dynamos) in fusion and astrophysical plasmas.

Chapter 5

Turbulent cascades in plasma models

5.1 Introduction

In various astrophysical and laboratory settings, plasma is known to be in a turbulent state. This claim is bolstered by the estimates of Reynolds numbers for astrophysical flows which turn out to be extremely large. Progress in the understanding of turbulence is thus crucial for explaining the associated phenomena. On sufficiently large scales, magnetohydrodynamics (MHD) is a valid model for describing plasma turbulence and is indeed the basis for theoretical descriptions of several plasma phenomena. Among these, for instance, is the magnetic dynamo action (see, e.g. Ref. [41]), which has been established as a mechanism for conversion of kinetic energy into magnetic energy. Such conversion is relevant for the Earth's magnetosphere as well as the solar wind. The dynamo action has also been linked to the inverse cascade in MHD turbulence [92, 96, 95, 180, 48]. Theoretical predictions for MHD turbulence have been confirmed in numerical simulations [118, 95] and similar works have been successfully undertaken in three-dimensional (3D) Hall MHD.[226] The magnetic relaxation process characterizing magnetically confined plasmas in Reversed Field Pinches [197] is another example of phenomenon whose understanding is based on the MHD description of a turbulent plasma. Further

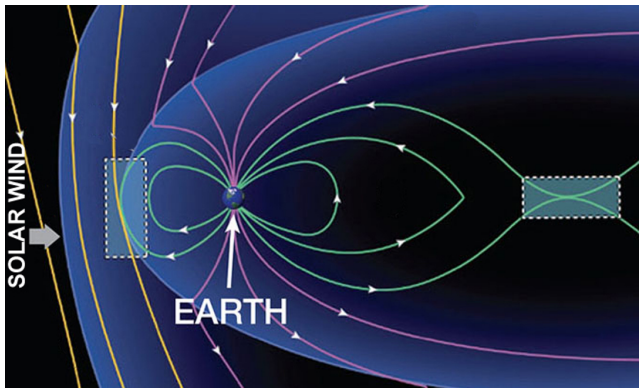

Figure 5.1: MMS will use a two-phase orbit strategy to explore two different regions where magnetic reconnection often occurs, one on the day side and the other on the night side of Earth. One of the stated purposes of the mission is understanding the role of turbulence in the reconnection process.
Credits: NASA

applications of MHD turbulence can be found, for instance, in Ref. [42].

While MHD has been a cornerstone for the description of large scale plasma phenomena, it fails at short scales, such as the electron skin depth $\hat{d}_e = c/\omega_{pe}$, where c is the speed of light and ω_{pe} is the electron plasma frequency. The model of extended MHD (XMHD) generalizes MHD (as well as Hall MHD) by including terms that are relevant at scales of the order of $\hat{d}_e$. The investigation of turbulence at such scales is of relevance for instance for the recently launched Magnetospheric Multiscale Mission (see Fig. 5.1),[54] which is known to be capable of probing such scales (observational results in these regimes have been recently published in Ref. [190]). The probing of such scales may also become feasible in the laboratory, with facilities such as WiPAL.[87]

The emphasis in this chapter will predominantly rely on understanding the direction in which the turbulent cascades flow. In particular, this refers to the *process whereby the energy (or helicity) injected at a certain scale by some force (typically stirring) has a tendency to flow towards higher or lower wavenumbers* in a turbulent state. In order to predict the direction of turbulent cascades of invariants of the model, we resort to the well-known technique of absolute equilibrium states (AES). This technique (see Sec. 5.2.3 and Sec. 5.3.3) has been used in various past works: it was applied to hydrodynamical turbulence in Ref. [138], MHD in Refs. [92, 96, 95], Hall MHD in Refs. [226, 171], two-fluid theory in Ref. [269], 3D XMHD in Ref. [171], gyrokinetics in Ref. [268], and drift wave turbulence in Refs. [99, 137]. AES are derived from the Gibbs ensemble probability density and represent states towards which actual turbulence tends to relax; thereby, they are of value for predicting the direction and structure of the exchange of various invariants among the modes.[141] It is important to mention that these modes are not eigenstates of the various models considered, but Fourier amplitudes allow analyses of how components of the invariants flow through different scales.

One of the earliest suggestions for ascertaining the inverse cascade based on AES in MHD turbulence[42] can be found in Ref. [92], followed by the two-dimensional studies of Ref. [96], inspired by works of Kraichnan in hydrodynamics.[138, 141] Numerical simulations [95] support the predicted relaxed spectra. Although later it was found that deviation from Gaussian statistics occurs as well as breaking of ergodicity in MHD.[229] Good agree-

ment between AES in Hall MHD and numerics was found in Ref. [226]. Later mostly analytical calculations for AES were performed in two-fluid theory [269] and gyrokinetics,[268] where the former alludes to the possibility that the "poles" of AES can appear in the high-k regime and a pole implies condensation of a spectral quantity to that wavenumber (see Sec. VI). More detailed analyses were performed in Ref. [171], predicting the phenomenon of cascade reversal of the magnetic helicity in 3D extended MHD at the electron skin depth scale. An in-depth overview can be found in Refs. [230, 171].

The identification of cascade reversal is a subject that has attracted considerable interest. However, mostly cascade reversals (usually referred to as cascade transitions in the literature) have only been identified in highly idealized systems. For instance, there are many examples of cascade reversal when the interactions of the real physical system have been artificially modified. For example, in Ref. [211] it is demonstrated that 3D hydrodynamics (HD) displays a change in the direction of the energy cascade when varying the value of a free parameter that controls the relative weights of the triadic interactions between different helical Fourier modes. Another useful study was performed in a model of thin layer turbulence, [32] where 2D motions were coupled to a single Fourier mode along the vertical direction. As the height of the layer is varied the authors find critical transitions from forward to backward cascade of energy.

The literature on cascade reversal in real physical systems, ones without artificial modification, is scarcer. Some examples include rotating three

dimensional stirred HD system,[232, 77] where the transition to inverse cascade of energy occurs below certain values of Rossby number. In addition, in Ref. [204] 3D direct numerical simulations of rotating Boussinesq turbulence also demonstrate such transitions. Moreover, there is theoretical and experimental evidence for the inverse energy cascade in the second sound acoustic turbulence in superfluid Helium.[100] In 3D MHD, various simulations have been performed [6, 239] that demonstrate cascade reversal when the system is forced only mechanically. Since the stirring lacks a magnetic component with stronger guide fields the flow becomes two-dimensional, leading to the inverse cascade of energy like in 2D HD. The transition appears to have some interesting features [227] as the magnetic forcing is turned on, viz. there exists a critical value for which the energy flux towards the large scales vanishes. Nevertheless, in the MHD examples above the parameter that is varied is still somewhat ad hoc and idealized, viz. the form of the amplitude of magnetic forcing. In contrast, in this chapter the control parameters will be d_e, d_i and ρ_s (to be defined in Sec. 5.3) and forcing has both mechanical and magnetic components.

The chapter is organized as follows. The first part (Sec. 5.2) is devoted to 3D XMHD and is heavilty based on the material from Ref. [171][1]. We calculate the mean helicity flux transfer rates and the associated dissipation in

[1]G. Miloshevich, M. Lingam, P. J. Morrison , "On the structure and statistical theory of turbulence of extended magnetohydrodynamics" New J. Phys., 19(1):015007 January 2017. George Miloshevich is the first author. He performed most of the analytical calculations and made predictions regarding the directions of cascades under supervision of the co-authors.

Sec. 5.2.1, which leads us to question the direction of the fluxes. To be able to answer this question we first prove Liouville theorem in Sec 5.2.2. and subsequently calculate absolute equilibrium states 5.2.3. The second part based on material form Ref. [172][2] (Sec. 5.3) is devoted to 2D version of XMHD model, where electron temperature is not ignored. We review the reduced fluid model and its Hamiltonian structure in Sec. 5.3.1, while a discussion of its spectral decomposition properties follows in Sec. 5.3.2. In Sec. 5.3.3 we present our calculations of AES, whereas in Sec. 5.3.4 we discuss the different regimes that characterize the AES depending on the values of the parameters. Finally, in Sec. 5.4 we discuss comparisons with other related models and summarize.

5.2 XMHD Turbulence

In the recent work by [27], expressions for the dissipation rates for Hall MHD were computed. Their analysis assumed that the Hall MHD turbulence was homogeneous, but did not rely on the further assumption of isotropy. As noted above, an important limitation of Hall MHD is that it becomes invalid when electron inertia effects start to dominate, i.e. when one considers length scales comparable to the electron skin depth. In such an instance, it makes sense to use extended MHD instead, on account of the fact that it is endowed with electron inertia effects.

[2]G. Miloshevich, M. Lingam, P. J. Morrison , "Direction of cascades in a magnetofluid model with electron skin depth and ion sound Larmor radius scales" Phys. Plasmas, 25(7):072303 July 2018. George Miloshevich is the first author. He performed most of the analytical calculations under supervision of the co-authors.

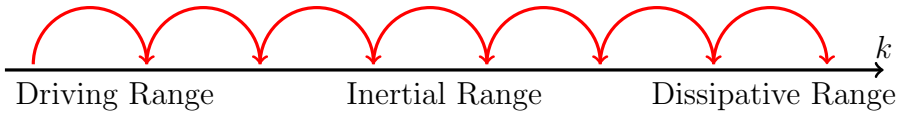

Figure 5.2: Schematic demonstrating the standard Richardson-Kolmogorov direct cascade. Energy injected at low k, e.g., via large scale stirring, cascades through the inertial range and dissipates at small scales (large k). Upon reversal of the arrows along with the driving and dissipative ranges, a depiction of the inverse cascade is obtained.

In recent times, there has also been a great deal of interest focused on the solar wind at sub-electron scales, mostly because of the fact that observations have now become possible in this regime [214, 9, 213, 51, 215]. Hence, in the present section, we shall generalize the results of [27] by including electron inertia.

5.2.1 Mean helicity flux rates

In 3D fluid turbulence, it has been known since the famous works by [136], and subsequent numerical and experimental tests [91, 236, 42], that the energy input at large scales flows to small dissipative scales. This phenomenon is often referred to as a direct Kolmogorov-Richardson cascade [91] - a pictorial description of this phenomenon has been provided in Fig. 5.2. In MHD, the direct (forward) cascade of energy and the inverse cascade of magnetic helicity [92] have been widely explored, and are thus well established [42]. In the inertial range, it must be borne in mind that the dissipation does not play a role. Hence, it is expected that, in the stationary regime, the same flux (of the energy or helicity, for example) flows through each wave number k. This

principle was recently employed to conduct a complementary study of XMHD turbulence in [2].

In our analysis, we are interested in the flux rate of the generalized helicities (4.13) within the framework of XMHD that are injected at some length scale. By following the steps outlined in [27], we first introduce the symmetric two-point correlation function

$$R_{\mathcal{K}_\pm} = R'_{\mathcal{K}_\pm} = \left\langle \frac{\boldsymbol{\mathcal{A}}'_\pm \cdot \boldsymbol{\mathcal{B}}_\pm + \boldsymbol{\mathcal{A}}_\pm \cdot \boldsymbol{\mathcal{B}}'_\pm}{2} \right\rangle, \tag{5.1}$$

where primed quantities are functions of $\mathbf{x}' = \mathbf{x} + \mathbf{r}$, unprimed quantities depend on $\mathbf{x}$, and the brackets $\langle\ \rangle$ are a shorthand notation for ensemble averaging. When the turbulence is homogeneous this can be equivalent to the spatial average. Upon manipulation we find

$$\begin{aligned} \partial_t \big\langle \boldsymbol{\mathcal{A}}'_\pm \cdot \boldsymbol{\mathcal{B}}_\pm + \boldsymbol{\mathcal{A}}_\pm \cdot \boldsymbol{\mathcal{B}}'_\pm \big\rangle = \big\langle \nabla \cdot [(\mathbf{V}_\pm \times \boldsymbol{\mathcal{B}}_\pm) \times \boldsymbol{\mathcal{A}}'_\pm] + \nabla' \cdot [(\mathbf{V}'_\pm \times \boldsymbol{\mathcal{B}}'_\pm) \times \boldsymbol{\mathcal{A}}_\pm] \\ + \mathbf{V}'_\pm \times \boldsymbol{\mathcal{B}}'_\pm \cdot \boldsymbol{\mathcal{B}}_\pm + \mathbf{V}_\pm \times \boldsymbol{\mathcal{B}}_\pm \cdot \boldsymbol{\mathcal{B}}'_\pm + \nabla \psi_\pm \cdot \boldsymbol{\mathcal{B}}'_\pm + \nabla' \psi'_\pm \cdot \boldsymbol{\mathcal{B}}_\pm \big\rangle \end{aligned} \tag{5.2}$$

At this stage, we shall digress a little to explain how the principle of statistical homogeneity can be gainfully employed. Our discussion mirrors the one presented in [102]. We introduce the change-of-variables $\boldsymbol{\xi} = \mathbf{x}' + \mathbf{x}$ and $\mathbf{r} = \mathbf{x}' - \mathbf{x}$, which implies that $\partial/\partial\mathbf{x} = \partial/\partial\boldsymbol{\xi} - \partial/\partial\boldsymbol{r}$ and $\partial/\partial\mathbf{x}' = \partial/\partial\boldsymbol{\xi} + \partial/\partial\mathbf{r}$. For a given vector field $\mathbf{u}$, this implies that

$$\begin{aligned} \left\langle u_j(\mathbf{x}', t) \frac{\partial u_i(\mathbf{x}, t)}{\partial x_i} \right\rangle &= \frac{\partial}{\partial x_i} \langle u_j(\mathbf{x}', t)\, u_i(\mathbf{x}, t) \rangle = -\frac{\partial}{\partial r_i} \langle u_j(\mathbf{x}', t)\, u_i(\mathbf{x}, t) \rangle = \\ &- \frac{\partial}{\partial x'_i} \langle u_j(\mathbf{x}', t)\, u_i(\mathbf{x}, t) \rangle = -\left\langle \frac{\partial u_j(\mathbf{x}', t)}{\partial x'_i} u_i(\mathbf{x}, t) \right\rangle \end{aligned} \tag{5.3}$$

Upon using the above identity in (5.2), we obtain

$$\begin{aligned}
&\left\langle \nabla \cdot [(\mathbf{V}_\pm \times \boldsymbol{\mathcal{B}}_\pm) \times \boldsymbol{\mathcal{A}}'_\pm] + \nabla' \cdot [(\mathbf{V}'_\pm \times \boldsymbol{\mathcal{B}}'_\pm) \times \boldsymbol{\mathcal{A}}_\pm] \right\rangle \\
&\quad = -\left\langle \nabla' \cdot [(\mathbf{V}_\pm \times \boldsymbol{\mathcal{B}}_\pm) \times \boldsymbol{\mathcal{A}}'_\pm] + \nabla \cdot [(\mathbf{V}'_\pm \times \boldsymbol{\mathcal{B}}'_\pm) \times \boldsymbol{\mathcal{A}}_\pm] \right\rangle \\
&\quad = \left\langle \mathbf{V}_\pm \times \boldsymbol{\mathcal{B}}_\pm \cdot \boldsymbol{\mathcal{B}}'_\pm + \mathbf{V}'_\pm \times \boldsymbol{\mathcal{B}}'_\pm \cdot \boldsymbol{\mathcal{B}}_\pm \right\rangle = -\langle \delta(\mathbf{V}_\pm \times \boldsymbol{\mathcal{B}}_\pm) \cdot \delta \boldsymbol{\mathcal{B}}_\pm \rangle \quad (5.4)
\end{aligned}$$

where $\delta f := f' - f$. Likewise, it is possible to show that

$$\left\langle \nabla' \psi'_\pm \cdot \boldsymbol{\mathcal{B}}_\pm + \nabla \psi_\pm \cdot \boldsymbol{\mathcal{B}}'_\pm \right\rangle = -\left\langle \psi'_\pm \nabla \cdot \boldsymbol{\mathcal{B}}_\pm + \psi_\pm \nabla' \cdot \boldsymbol{\mathcal{B}}'_\pm \right\rangle = 0. \quad (5.5)$$

Thus, upon combining everything together, we get

$$\frac{\partial}{\partial t} \left[\frac{1}{2} \left\langle \boldsymbol{\mathcal{A}}'_\pm \cdot \boldsymbol{\mathcal{B}}_\pm + \boldsymbol{\mathcal{A}}_\pm \cdot \boldsymbol{\mathcal{B}}'_\pm \right\rangle \right] = -\left\langle \delta(\mathbf{V}_\pm \times \boldsymbol{\mathcal{B}}_\pm) \cdot \delta \boldsymbol{\mathcal{B}}_\pm \right\rangle + D \,, \quad (5.6)$$

where we have introduced the phenomenological damping D that occurs at the sink scale, following the approach of [27]. In the limit of infinite kinetic and magnetic Reynolds numbers, under the assumption of stationarity, the LHS of the above expression vanishes due to the ruggedness of the helicity invariants [167]. Hence, we obtain our result from Ref [171]: the large scale dissipation equals the mean generalized helicity flux rate

$$\eta_\pm = \left\langle \delta(\mathbf{V}_\pm \times \boldsymbol{\mathcal{B}}_\pm) \cdot \delta \boldsymbol{\mathcal{B}}_\pm \right\rangle , \quad (5.7)$$

which closely resembles the expression of [27]. However, it must be noted that our expression is more general as it duly encompasses electron inertial contributions as well via the definition of $\boldsymbol{\mathcal{B}}_\pm$. In the Hall MHD limit with $d_e \to 0$, we have verified that our result is in exact agreement with the expression of [27].

Although (5.7) is quite compact, a great deal of information can be extracted from it. For instance, it follows that the dissipation rates vanish when the Beltrami condition $\boldsymbol{\mathcal{B}}_{\pm} \parallel \mathbf{V}_{\pm}$ is attained. These (multi) Beltrami states are non-trivial, as they are also equilibria of XMHD [2]. This is easy to verify by inspecting the second set of equations in (4.14), and substituting the above condition. Thus, this result serves as a consistency check indicating that the dissipation vanishes when the system has settled into this equilibrium (in the limit of infinite Reynolds numbers).

In [27] a phenomenological argument for the direction of the cascades was presented. First, let us recall that the generalized helicities become the magnetic and ion canonical helicities in Hall MHD [248]. The first is essentially a copy of the MHD magnetic helicity, while the other is a superposition of MHD cross helicity and fluid helicity after some rearrangement. In the former, it is argued that the inverse cascade is expected just as in ideal MHD. In contrast, the direction of the cascade for the ion canonical helicity (of Hall MHD) can go either way, as it is dependent on the energy budget of the system. It is assumed to exhibit an inverse cascade if the magnetic energy is dominant over the kinetic (and thermal) energy.

Therefore, we see that there is an ambiguity regarding the directionality of the cascade for one of the helicities. The problem becomes far more acute when we include electron inertia effects via XMHD. In that case, the magnetic helicity is not conserved as there is also a (smaller) fluid helicity contribution. If we apply the above line of reasoning, we would expect to witness the direct

and inverse cascades of both helicities in XMHD. This is because of the fact that the two helicities are not fundamentally different, other than the fact that they are associated with different species [158, 156]. Thus, this raises an interesting question: how is it possible to get the Hall MHD limit from XMHD? In other words, why is the direct cascade of one helicity, that corresponds to the magnetic helicity in the HMHD limit, lost? One possible resolution of this paradox is by suggesting that the existence of direct or inverse cascades depends on the length scale we are considering. This question is addressed in more detail in Sec. 5.2.2 that follows.

5.2.2 Liouville's theorem for XMHD

The direction of a cascade can be determined by inspecting the general equilibrium states that the turbulence would tend to relax to, if not for the continual input of energy [42]. Although turbulence as a phenomenon is far from equilibrium, absolute equilibria have been used to predict the direction of the spectral flux [42]. Such equilibria can be obtained from the ideal invariants described in Sec. 4.2. The approach delineated in the present section is a generalization of the pioneering studies in hydrodynamic [149, 139, 138] and MHD [149, 92] turbulence.

However, before applying equilibrium statistical mechanics to the Fourier modes of XMHD, it is necessary to show that their governing equations satisfy Liouville's theorem, as was first done in hydrodynamics by [55]. This is because the variables $\mathbf{B}^\star$ and $\mathbf{V}$ are noncanonical and one must identify an

invariant measure. The Darboux theorem assures that the usual phase space volume measure is preserved in some local canonical coordinate system;[182] however, in the truncated noncanonical coordinates, the finite number of retained Fourier amplitudes, equations (5.68) need to be verified. We emphasize this point because sometimes this step is missing in analyses. It is then possible to apply the conventional assumption of equal *a priori* probabilities in phase space $(z_1, z_2, \ldots, z_n)$ [148], which in turn enables one to express an equilibrium phase space probability density $\mathscr{P} = \mathscr{P}(z_1, z_2, \ldots, z_n)$ as a function of constants of motion; for XMHD, they are further discussed in Sec. 5.2.3. Liouville's theorem was reproven and used for 2D fluids by [141], quasi-geostrophy by [218], incompressible MHD by [149], and more recently similar statistical approaches have been employed in plasma models [145], such as gyrokinetics [268].

For an N-dimensional dynamical system $\dot{z}_i = V_i(z)$, for some vector field V, with $i = 1, 2, \ldots N$, Liouville's theorem (e.g. [129]) states that any phase space volume is preserved provided $\sum_i \partial \dot{z}_i / \partial z_i = \sum_i \partial V_i / \partial z_i = 0$, which is true for any canonical Hamiltonian system. However, incompressible XMHD is a noncanonical Hamiltonian system, which can be shown [3] through the use of Dirac brackets [79]. We emphasise again that because Liouville's theorem is

[3] We shall defer a detailed exposition of subtleties regarding the noncanonical Hamiltonian origin of the present measure and comparison to an actual canonical measure to a future publication. On a related note, we also wish to correct an erroneous statement in [141] - it was stated therein that 2D fluid flow is not Hamiltonian, but the authors were unaware that it actually is a Hamiltonian dynamical system, albeit in terms of noncanonical variables [182].

variable dependent and the natural (Eulerian) variables are noncanonical, one must check its validity directly. The idea of Burgers and Lee was to do this in terms of Fourier amplitudes, which play the role of the particle degrees of freedom of statistical mechanics. Thus, for XMHD we write the system (3.6) and (3.7), after assuming incompressibility, in terms of the coefficients of a Fourier series; i.e. the velocity and magnetic fields are expanded as $\boldsymbol{F}(\boldsymbol{x}) = \sum_{\boldsymbol{k}} \boldsymbol{f}_k(t)\, e^{i\boldsymbol{k}\cdot\boldsymbol{x}}$. Then the equations of motion for the Fourier amplitudes are given by

$$\dot{\boldsymbol{v}}_{\boldsymbol{k}} = i\left(\boldsymbol{I} - \frac{\boldsymbol{k}\,\boldsymbol{k}}{k^2}\right)\cdot \sum_{\boldsymbol{k}'}\left(\boldsymbol{v}_{\boldsymbol{k}-\boldsymbol{k}'}\times[\boldsymbol{k}'\times\boldsymbol{v}_{\boldsymbol{k}'}] - \frac{\boldsymbol{b}^*_{\boldsymbol{k}-\boldsymbol{k}'}\times[\boldsymbol{k}'\times\boldsymbol{b}^*_{\boldsymbol{k}'}]}{1+k'^2 d_e^2}\right), \tag{5.8}$$

where $k^2 = \boldsymbol{k}\cdot\boldsymbol{k}$ and the gradient terms were eliminated via $\nabla\cdot\mathbf{V} = \mathbf{0}$, and

$$\begin{aligned}\dot{\boldsymbol{b}}^*_{\mathbf{k}} \;=\; \sum_{\boldsymbol{k}'}\Bigg(& i\,\boldsymbol{k}\times[\boldsymbol{v}_{\mathbf{k}'}\times\boldsymbol{b}^*_{\boldsymbol{k}-\boldsymbol{k}'}] - \frac{d_i\,\boldsymbol{k}\times\left[\mathrm{b}^*_{\boldsymbol{k}-\boldsymbol{k}'}\times[\boldsymbol{k}'\times\boldsymbol{b}^*_{\boldsymbol{k}'}]\right]}{1+k'^2 d_e^2} \\ &+ \frac{i\,d_e^2}{1+k'^2 d_e^2}\left[\boldsymbol{k}\times\boldsymbol{k}'\;\boldsymbol{v}_{\boldsymbol{k}-\boldsymbol{k}'}\cdot\boldsymbol{k}'\times\boldsymbol{b}^*_{\boldsymbol{k}'} + \boldsymbol{k}\times\boldsymbol{v}_{\boldsymbol{k}-\boldsymbol{k}'}\;\boldsymbol{b}^*_{\boldsymbol{k}'}\cdot\boldsymbol{k}\times\boldsymbol{k}'\right]\Bigg).\end{aligned} \tag{5.9}$$

Notice that $\boldsymbol{k}\cdot\boldsymbol{v}_{\boldsymbol{k}} = 0 = \boldsymbol{k}\cdot\boldsymbol{b}^*_{\boldsymbol{k}}$. Technically, our phase space consists of real and complex parts of the vectors $\boldsymbol{v}_{\boldsymbol{k}} = \overline{\boldsymbol{v}}_{-\boldsymbol{k}}$ and $\boldsymbol{b}^*_{\boldsymbol{k}} = \overline{\boldsymbol{b}^*}_{-\boldsymbol{k}}$, where the overbar denotes complex conjugation. However, it is more straightforward to work with their linear combinations $(\boldsymbol{v}_{\boldsymbol{k}}, \overline{\boldsymbol{v}_{\boldsymbol{k}}}, \boldsymbol{b}^*_{\boldsymbol{k}}, \overline{\boldsymbol{b}^*_{\boldsymbol{k}}})$, and the same results are obtained. After some algebra one arrives at

$$\sum_{l,\boldsymbol{k}}\frac{\partial \dot{v}_{l\boldsymbol{k}}}{\partial v_{l\boldsymbol{k}}} = -2i\sum_{\boldsymbol{k}}\boldsymbol{k}\cdot\boldsymbol{v}_{\mathbf{0}} = 0, \tag{5.10}$$

where l indexes the components of $\boldsymbol{v}_{\boldsymbol{k}}$ and $\boldsymbol{v}_{\mathbf{0}}$ denotes the $k = 0$ Fourier component. Even if this component is present, the sum is still zero since it is

odd in $\boldsymbol{k}$. Similarly, we get

$$\sum_{l,\boldsymbol{k}} \frac{\partial \dot{b^*}_{l\boldsymbol{k}}}{\partial b^*_{l\boldsymbol{k}}} = -2 \sum_{\boldsymbol{k}} \left(i\, \boldsymbol{k} \cdot \boldsymbol{v_0} + \frac{d_i\, \boldsymbol{b_0^*} - i\, d_e^2\, \boldsymbol{k} \times \boldsymbol{v_0}}{1 + k^2 d_e^2} \cdot \boldsymbol{k} \times \boldsymbol{k} \right) = 0. \tag{5.11}$$

Thus, clearly the sum of (5.10) and (5.11) vanishes so we have shown that Liouville's theorem holds true in XMHD. Taking the appropriate limits, it is easy to verify that it also holds true for Hall MHD, electron MHD, and inertial MHD as well. It must be recognized that several past studies of Hall and electron MHD turbulence implicitly relied upon the assumption that Liouville's theorem was valid, without having verified it explicitly. To the best of our knowledge, we have verified it for the first time for XMHD and its simpler variants.

5.2.3 Absolute Equilibrium States

We now turn to our study of turbulent cascades using the statistical mechanics of AES, even though turbulence is an out-of-equilibrium phenomenon. This might be seen as counterintuitive; however, it important to stress here that the AES hypothesis is a tool used to predict the direction of cascades [91, 42]and does not in general describe the distribution of actual invariants in fully developed turbulence in a driven dissipative system. The operative intuitive idea is that the AES captures the relevant properties of the nonlinear dynamics active in the inertial range. It is noteworthy to mention, however, that in 2D HD turbulence AES actually can be used to describe the large structures that are formed due to the inverse cascade. This is in part because of the presence of the inverse energy cascade that dumps energy to large scales

away from the small scales where the dissipation normally occurs. As a consequence, the flow dynamics is dominated by large scale coherent structures, such as vortices or jets.[47] In the 3D fluid case there is the well-established cascade[136] (see Fig. 5.2) from large scales, where stirring occurs, to the short scales, where energy is dissipated, a picture that has been confirmed in experiments.[91, 235, 42]

The idea[149, 55] is to assume that Fourier modes play a role analogous to that of the particle degrees of freedom in statistical mechanics. One calculates spectra in the canonical ensemble, and then makes predictions regarding the direction of the cascades based on where the spectra peak. It is understood that in reality dissipation acts to remove the ultraviolet catastrophe (high k divergence) that typically occurs in Galerkin systems.[141]

There is a problem that may arise in a case when one has non-additive constants of motion that may lead to non-Boltzmann statistics. For more on this see the discussion in Ref. [114]. On the other hand, in the case of the 2D Euler equation, we find that according to Ref. [60], even though the canonical distribution has to be used with caution for long-range interacting systems, the statistical tendency of vortices of the same sign of circulation to cluster in the so-called negative temperature regime can be indeed predicted using the same canonical distribution by observing that spectra peak at low k.

In principle, one can proceed to calculate a partition function for absolute equilibria by using the Hamiltonian and the two invariants of XMHD, given by (4.13). However, because we wish to compare our results with those

in the literature by taking the MHD limit, viz. $d_i \to 0$ and $d_e \to 0$, and because the generalized helicities of (4.13) become degenerate in this limit, reducing to the magnetic helicity in both instances with a loss of the cross helicity, it is convenient to use linear combinations of the helicities (4.13). Thus we consider the following two Casimirs:

$$H_M := \frac{1}{2}\frac{\kappa_+\mathcal{K}_- - \kappa_-\mathcal{K}_+}{\kappa_+ - \kappa_-} = \frac{1}{2}\int d^3x\,(\boldsymbol{A}^*\cdot\boldsymbol{B}^* + d_e^2\,\boldsymbol{V}\cdot\nabla\times\boldsymbol{V}), \quad (5.12)$$

$$H_C := \frac{1}{2}\frac{\mathcal{K}_+ - \mathcal{K}_-}{\kappa_+ - \kappa_-} = \int d^3x\,(\boldsymbol{V}\cdot\boldsymbol{B}^* + \frac{d_i}{2}\,\boldsymbol{V}\cdot\nabla\times\boldsymbol{V}), \quad (5.13)$$

where (5.12) was also presented in [1, 2]. The helicities (5.12) and (5.13) are natural generalizations of the cross and magnetic helicities of ideal MHD where the second terms in each of these relations can be seen as "corrections" that vanish in the MHD limit. Here, we have used incompressibility - also a common assumption in most Hall MHD studies [144, 97] - ensuring that the two dynamical fields are solenoidal in nature. In Fourier series representation the three invariants become

$$H = \frac{1}{2}\sum_{l,\boldsymbol{k}}\Big(v_{l\boldsymbol{k}}\overline{v}_{l\boldsymbol{k}} + \frac{b^*_{l\boldsymbol{k}}\overline{b^*}_{l\boldsymbol{k}}}{1+k^2d_e^2}\Big), \quad (5.14)$$

$$H_M = \frac{i}{2}\sum_{l,m,n,\boldsymbol{k}}\epsilon_{lmn}k_l\Big(d_e^2\,v_{m\boldsymbol{k}}\overline{v}_{n\boldsymbol{k}} + \frac{b^*_{m\boldsymbol{k}}\overline{b^*}_{n\boldsymbol{k})}}{k^2}\Big), \quad (5.15)$$

$$H_C = \frac{1}{2}\sum_{l,\boldsymbol{k}}\Big(v_{l\boldsymbol{k}}\overline{b^*}_{l\boldsymbol{k}} + b^*_{l\boldsymbol{k}}\overline{v}_{l\boldsymbol{k}} + i\sum_{m,n}d_i\,\epsilon_{lmn}k_lv_{m\boldsymbol{k}}\overline{v}_{n\boldsymbol{k}}\Big). \quad (5.16)$$

Notice that the energy as well as the helicities are quadratic in $\mathbf{v}$ and $\mathbf{b}^*$. The absolute equilibrium distribution function is constructed as follows:

$$\mathscr{P} = Z^{-1}\exp[-\alpha H - \beta H_M - \gamma H_C] =: Z^{-1}\exp[-A_{i,j}u^iu^j/2], \quad (5.17)$$

with Z being the partition function. Note in the second equality the vector $\mathbf{u}$ is chosen to consist of 8 entries corresponding to 4 components (two real, two complex) of $\boldsymbol{v_k}$ and $\boldsymbol{b}^*_{\boldsymbol{k}}$. We shall comment on the parameters α, β and γ at a later stage in our discussion. The reduction in the total number degrees of freedom is due to solenoidal property of both fields: $\boldsymbol{k}\cdot\boldsymbol{b}^*_{\boldsymbol{k}} = 0 = \boldsymbol{k}\cdot\boldsymbol{v_k}$. Using (5.17) we calculate the average of a quantity F according to

$$\langle F\rangle = \int \prod_{\boldsymbol{k}} d\boldsymbol{v_k} d\overline{\boldsymbol{v}}_{\boldsymbol{k}} d\boldsymbol{b}^*_{\boldsymbol{k}} d\overline{\boldsymbol{b}^*}_{\boldsymbol{k}}\; F\,\mathscr{P}\,, \tag{5.18}$$

which will be used for all averages in the present section. Because all invariants are quadratic in $\boldsymbol{u}$ the integrations of (5.18) are all Gaussian, allowing us to achieve our goal of finding correlations of the form $\langle u_i u_j\rangle = A^{-1}_{i,j}$; however, this requires the inversion of the 8 by 8 matrix

$$A = \begin{pmatrix} a & 0 & 0 & f & c & 0 & 0 & 0\\ 0 & a & -f & 0 & 0 & c & 0 & 0\\ 0 & -f & a & 0 & 0 & 0 & c & 0\\ f & 0 & 0 & a & 0 & 0 & 0 & c\\ c & 0 & 0 & 0 & d & 0 & 0 & b\\ 0 & c & 0 & 0 & 0 & d & -b & 0\\ 0 & 0 & c & 0 & 0 & -b & d & 0\\ 0 & 0 & 0 & c & b & 0 & 0 & d \end{pmatrix}, \tag{5.19}$$

where $a := \alpha$, $b = \beta/k$, $c = \gamma$, $f := k(\beta d_e^2 + \gamma d_i)$ and $d := \alpha/(1 + k^2 d_e^2)$. The inverse matrix fortunately has the same form as the simpler MHD case, and

is given by

$$A^{-1} = \frac{1}{\Delta}\begin{pmatrix} P & 0 & 0 & X & Q & 0 & 0 & Y \\ 0 & P & -X & 0 & 0 & Q & -Y & 0 \\ 0 & -X & P & 0 & 0 & -Y & Q & 0 \\ X & 0 & 0 & P & Y & 0 & 0 & Q \\ Q & 0 & 0 & Y & R & 0 & 0 & W \\ 0 & Q & -Y & 0 & 0 & R & -W & 0 \\ 0 & -Y & Q & 0 & 0 & -W & R & 0 \\ Y & 0 & 0 & Q & W & 0 & 0 & R \end{pmatrix}, \tag{5.20}$$

where the new coefficients are

$$P := a(d^2 - b^2) - c^2 d \quad \text{and} \quad X := f(b^2 - d^2) - c^2 b, \tag{5.21}$$

$$Q := c(c^2 - ad - bf) \quad \text{and} \quad Y := c(ab + df), \tag{5.22}$$

$$R := d(a^2 - f^2) - c^2 a \quad \text{and} \quad W := b(f^2 - a^2) - c^2 f, \tag{5.23}$$

$$\sqrt{\det A} =: \Delta = (fb + ad - c^2)^2 - (ab + fd)^2. \tag{5.24}$$

The matrix A has to be positive definite for the procedure to work, i.e. all of the eigenvalues must be positive [92]. The corresponding identities can be rearranged after a fair amount of algebra to arrive at the final set of positivity conditions

$$a > |f|, \quad d > |b| \quad \text{and} \quad c^2 < (a - |f|)(d - |b|). \tag{5.25}$$

A less strict, albeit useful, set of conditions can be derived as well:

$$ad + bf > c^2 \quad \text{and} \quad |af + db| < (ad + bf - c^2) \quad \text{and} \quad |c| < \frac{a + d}{2}. \tag{5.26}$$

From these inequalities, we see that $\Delta > 0, P > 0$ and $R > 0$ as expected, ensuring that the autocorrelations are positive. Because of the normalized

Alfvén scaling, it is clear that $k > 1$ must be valid, as otherwise we are concerning ourselves with length scales greater than the size of the system. Finally, the spectral quantities can be duly evaluated.

We write the Hamiltonian as the sum of kinetic and magnetic energies, $H = H_K + H_B$, with the spectra of each given, respectively, by

$$E_K = 2\pi k^2 \sum_l \left\langle v_{l\boldsymbol{k}}\, \overline{v}_{l\boldsymbol{k}} \right\rangle = \frac{8\pi k^2 P}{\Delta}, \tag{5.27}$$

$$E_B = \frac{2\pi k^2}{1+k^2 d_e^2} \sum_l \left\langle b^*_{l\boldsymbol{k}}\, \overline{b^*}_{l\boldsymbol{k}} \right\rangle = \frac{8\pi k^2}{1+k^2 d_e^2} \frac{R}{\Delta}. \tag{5.28}$$

Similarly, the spectra of the generalized magnetic and cross helicities, respectively, are

$$E_M = 2\pi k^2 \sum_{l,m,n} \epsilon_{lmn} k_l \left(d_e^2 \left\langle v_{m\boldsymbol{k}}\, \overline{v}_{n\boldsymbol{k}} \right\rangle + \frac{\left\langle b^*_{m\boldsymbol{k}}\, \overline{b^*}_{n\boldsymbol{k}} \right\rangle}{k^2} \right) = 8\pi k\, \frac{d_e^2 k^2 X + W}{\Delta} \tag{5.29}$$

$$E_C = 2\pi k^2 \sum_l \left(2\left\langle v_{l\boldsymbol{k}}\, \overline{b^*}_{l\boldsymbol{k}} \right\rangle + \sum_{m,n} d_i\, \epsilon_{lmn} k_l \left\langle v_{m\boldsymbol{k}}\, \overline{v}_{n\boldsymbol{k}} \right\rangle \right) = 8\pi k^2\, \frac{2Q + d_i k X}{\Delta} \tag{5.30}$$

It is easy to obtain the spectra of the original generalized helicities via the relation $\mathcal{K}_\pm = 2(\kappa_\pm H_C + H_M)$, i.e. by

$$K_\pm := 2\big(\kappa_\pm E_C + E_M\big)\,. \tag{5.31}$$

.

5.2.4 Hall MHD Cascades

If we consider the Hall MHD limit as $1 < k \ll d_e^{-1}$, i.e. the range where Hall effects are important, we obtain the following conditions

$$\alpha > k|\gamma| d_i \quad \text{and} \quad \alpha > \frac{|\beta|}{k} \quad \text{and} \quad \gamma^2 < (\alpha - k|\gamma| d_i)\Big(\alpha - \frac{|\beta|}{k}\Big). \tag{5.32}$$

In addition, we also have

$$\alpha^2 + \beta\gamma d_i > \gamma^2 \quad \text{and} \quad \alpha > |\gamma| \quad \text{and} \quad \alpha^2 > |\beta\gamma| d_i. \tag{5.33}$$

During the process of computing the last inequality in (5.32) for k, we also computed the discriminant

$$\mathcal{D} := (\alpha^2 + |\gamma\beta| d_i - \gamma^2)^2 - 4\alpha^2 |\gamma\beta| d_i. \tag{5.34}$$

Requiring the existence of a k-spectrum ($\mathcal{D} > 0$) leads us to a stricter version of the first inequality in (5.33):

$$\alpha > |\gamma| + \sqrt{|\gamma\beta| d_i}. \tag{5.35}$$

To see how this inequality is obtained, let us rewrite (5.34) as

$$0 < \mathcal{D} = \big((\alpha - \sqrt{|\gamma\beta| d_i})^2 - \gamma^2\big)(\alpha^2 + |\gamma\beta| d_i - \gamma^2 + 2\alpha\sqrt{|\gamma\beta| d_i}). \tag{5.36}$$

The second term in the product is clearly positive according to (5.33). Thus, one requires the first term to be positive which leads us to (5.35). In turn, this leads us to stricter requirements on k than the ones of the first two inequalities in (5.32). Our bounds are thus given by

$$\frac{|\beta|}{\alpha} < \frac{\alpha^2 + |\beta\gamma| d_i - \gamma^2 - \sqrt{\mathcal{D}}}{2\alpha|\gamma| d_i} < k < \frac{\alpha^2 + |\beta\gamma| d_i - \gamma^2 + \sqrt{\mathcal{D}}}{2\alpha|\gamma| d_i} < \frac{\alpha}{|\gamma| d_i}. \tag{5.37}$$

The lower bound on k is also present in ideal MHD, but the upper limit appears to be solely due to the inclusion of the Hall term. Notice that if we wish to extend the range of k much further beyond d_i^{-1} it is reasonable to

impose $\alpha \gg |\gamma|$. Therefore, since $d_i \ll 1$ is typically valid, the assumption $\alpha^2 - \gamma^2 \gg |\gamma\beta| d_i$ is also justified. If we use this, along with an expansion in d_i, the limits can be approximated as

$$\frac{\alpha|\beta|}{\alpha^2 - \gamma^2} \lesssim k \lesssim \frac{\alpha^2 - \gamma^2}{\alpha|\gamma| d_i} \tag{5.38}$$

so that the parameters can be adjusted to allow for $1 < k \ll d_e^{-1}$.

In the Hall limit the different spectral densities are given by

$$E_K = 8\pi\alpha \frac{k^2(\alpha^2 - \gamma^2) - \beta^2}{(\alpha^2 + \beta\gamma d_i - \gamma^2)^2 - \alpha^2(k\gamma d_i + \beta/k)^2}, \tag{5.39}$$

$$E_B = 8\pi\alpha k^2 \frac{\alpha^2 - \gamma^2 - \gamma^2 k^2 d_i^2}{(\alpha^2 + \beta\gamma d_i - \gamma^2)^2 - \alpha^2(k\gamma d_i + \beta/k)^2}, \tag{5.40}$$

$$E_M = 8\pi \frac{\gamma^2 d_i(\beta d_i - \gamma)k^2 - \beta\alpha^2}{(\alpha^2 + \beta\gamma d_i - \gamma^2)^2 - \alpha^2(k\gamma d_i + \beta/k)^2}, \tag{5.41}$$

$$E_C = 8\pi\gamma k^2 \frac{d_i^2(\beta^2 - \alpha^2 k^2) - \gamma\beta d_i - 2(\alpha^2 + \beta\gamma d_i - \gamma^2)}{(\alpha^2 + \beta\gamma d_i - \gamma^2)^2 - \alpha^2(k\gamma d_i + \beta/k)^2}. \tag{5.42}$$

We note that each of these spectra are identical to the previous expressions obtained by [226] (see their Eqs. (26)-(29)), after undertaking a minor change of variables. This is not surprising as the authors had derived them using the same approach, viz. by constructing the absolute equilibrium states. We also wish to point out an important result that has also been predicted by many others before - the absence of equipartition between the kinetic and magnetic spectra in Hall MHD [103, 144, 97, 98, 226, 228, 152, 153]. This trait is unique to Hall MHD, as it is absent both in ideal MHD and inertial MHD; we shall demonstrate the latter in Sec. 5.2.5.

Notice that the average total energy spectrum $E = E_K + E_B$ can be computed from (5.39) and (5.40), and has the form

$$E = 8\pi\alpha k^2 \frac{2(\alpha^2 + \beta\gamma d_i - \gamma^2) - (k\gamma d_i + \beta/k)^2}{(\alpha^2 + \beta\gamma d_i - \gamma^2)^2 - \alpha^2(k\gamma d_i + \beta/k)^2}, \tag{5.43}$$

which is also equal to the formula provided in [226]. The parameters α, β, and γ are found by matching the integrated spectral quantities with their actual spatial values, e.g., by using $\int_{k_{min}}^{k_{max}} E_K \, dk$, where we imagine a continuum limit. Thus, it is obvious that one cannot provide simple expressions for these parameters, since they will be complicated transcendental equations in general.

As noted earlier, the dependence of the spectral quantities on k will reveal the directionality of the cascades. The direct cascade of some invariant can be expected if the spectral density is peaked at high wavenumbers and vice-versa. Based on the complexity of the above formulae even for Hall MHD, it appears as though any definitive statements are not possible. It is reasonable to expect that the same quantity may undergo both cascades depending on the length scale at which the energy is supplied to the system.

The simplest case one can investigate is to consider cases where the cross-helicity vanishes, viz. $E_C = 0 \Rightarrow \gamma = 0$. For this case we have verified that the standard MHD results presented in [92] are obtained, i.e. the direct cascade of energy and the inverse cascade of magnetic helicity. This result is not at all surprising because the magnetic helicity is an invariant of both ideal and Hall MHD. Our analysis confirms that, in the absence of global cross-

helicity, when magnetic helicity is injected at length scales much larger than the electron skin depth, it undergoes an inverse cascade within the framework of Hall MHD.

Let us consider another simple limit, where $\beta = 0$. At first glimpse, it doesn't have such a simple interpretation. We can make the picture more transparent by introducing the definitions

$$\frac{\gamma}{\alpha} =: \sin\phi \quad \text{and} \quad \frac{\cos^2\phi}{|\sin\phi|\, d_i} =: k_* > k, \tag{5.44}$$

where the second equality follows from the second relation in (5.38). The corresponding spectral quantities in these new variables are thus given by

$$E_K = \frac{8\pi}{\alpha\cos^2\phi}\frac{k^2}{1-\dfrac{k^2}{k_*^2}} \quad \text{and} \quad E_B = E_K\Big(1-\frac{k^2}{k_*^2}\cos^2\phi\Big), \tag{5.45}$$

together with

$$E_M = -d_i E_K \sin\phi\tan^2\phi \quad \text{and} \quad E_C = -E_K\sin\phi\Big(2+\frac{k^2}{k_*^2}\cot^2\phi\Big). \tag{5.46}$$

After a careful inspection and evaluation, one can verify that these expressions yield direct cascades of energy and cross-helicity.

In order to visualize these relations, we have plotted the different spectra in Fig. 5.3. It is particularly noteworthy that the magnetic helicity cascade becomes increasingly complex in the presence of strong cross-helicity. This is purely due to the additional perturbation coming from the Hall term, as the ideal MHD range remains completely in the inverse cascade mode.

Hence, we sum up this preliminary analysis by observing that $\mathcal{K}_+$ can undergo both forward and inverse cascades as predicted by [27]. We have also verified that our XMHD spectra, in the Hall MHD limit, are equal to the ones obtained earlier by [226].

5.2.5 Inertial MHD Cascades

We begin by recalling that inertial MHD is a model which lacks the Hall drift, but is endowed with electron inertia effects [130, 159]. Thus, the existence of the second condition implies that the model may become relevant in the range $k \gg d_e^{-1}$, i.e. at scales smaller than electron skin depth. Although this quantity is small in many fusion plasmas, recall that it is highly relevant in astrophysical and space plasmas, such as the Earth's magnetosphere and the solar wind. With this choice of k, observe that $d \approx \alpha/k^2 d_e^2$ holds true.

Following the same procedure as in Hall MHD, we analyze the necessary inequalities, and find that

$$\alpha > k|\beta|d_e^2 \quad \text{and} \quad \alpha \gtrsim |\gamma|. \tag{5.47}$$

Although $d_e \ll 1$, we also have $kd_e \gg 1$ in this case, and hence the condition $\alpha \gtrsim |\beta|$ appears to be quite reasonable. We also must inspect a counterpart of the third inequality in (5.25), which according to the constraints listed above collapses to

$$|\gamma| < \frac{\alpha}{kd_e} - |\beta|d_e. \tag{5.48}$$

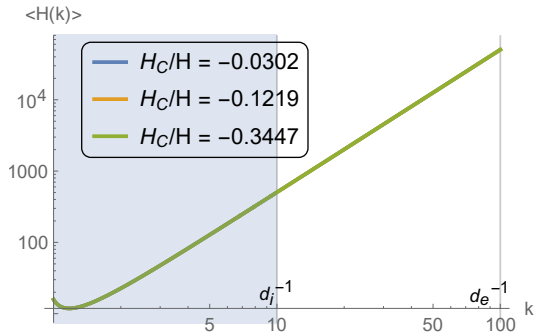

(a) Total Energy H

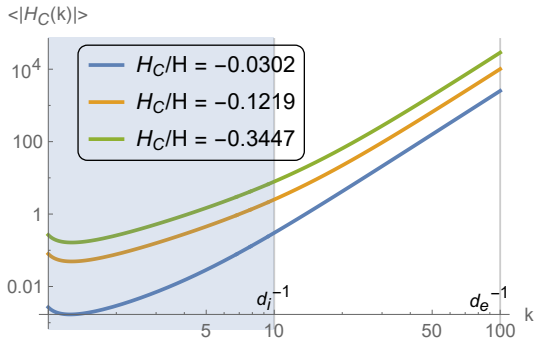

(b) Magnetic helicity H_M

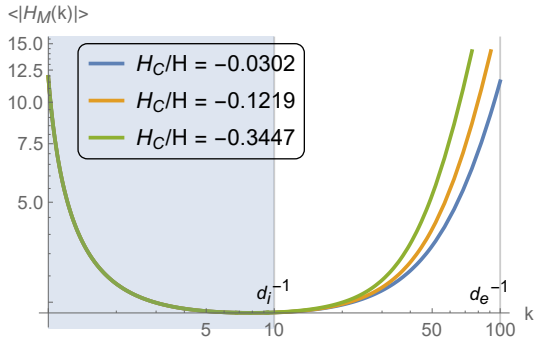

(c) Cross helicity H_C

Figure 5.3: Log-Log Plots for total energy, magnetic and cross-helicity. The parameters used here are $\alpha = 10$, $\beta = 9$ and $\gamma = \{0.001, 0.03, 0.1\}$ is varied so that different values of H_C are obtained (color-coded, see the legend for the description). The microscales were chosen to be $d_i = 0.1$ and $d_e = 0.01$.

Upon computation, the spectra become

$$E_K = E_B = \frac{8\pi\alpha}{d_e^2} \frac{\frac{\alpha^2}{k^2 d_e^2} - \beta^2 d_e^2 - \gamma^2}{\left(\beta^2 + \frac{\alpha^2}{k^2 d_e^2} - \gamma^2\right)^2 - \frac{4\alpha^2}{\beta^2 k^2}}, \tag{5.49}$$

$$E_M = -16\pi\beta k^2 d_e^2 \frac{\frac{\alpha^2}{k^2 d_e^2} + \gamma^2 - \beta^2 d_e^2}{\left(\beta^2 + \frac{\alpha^2}{k^2 d_e^2} - \gamma^2\right)^2 - \frac{4\alpha^2}{\beta^2 k^2}}, \tag{5.50}$$

$$E_C = -16\pi\gamma k^2 \frac{\beta^2 d_e^2 + \frac{\alpha^2}{k^2 d_e^2} - \gamma^2}{\left(\beta^2 + \frac{\alpha^2}{k^2 d_e^2} - \gamma^2\right)^2 - \frac{4\alpha^2}{\beta^2 k^2}}. \tag{5.51}$$

An important and pleasing feature is immediately apparent. We see that inertial MHD restores the energy equipartition feature of ideal MHD [231]. This is along expected lines, since inertial MHD and ideal MHD are very akin to each other. In fact, it was shown by [159] in 2D that the Hamiltonian (Poisson bracket) structure of these two models is identical under the transformation $\mathbf{B} \to \mathbf{B}^*$.

We also see that the generalized magnetic and cross helicities vanish when β and γ are set to zero respectively. Hence, it is instructive to take these two limits and inspect the resultant expressions. When $\beta = 0$, the total energy is

$$E = \frac{16\pi\alpha}{\frac{\alpha^2}{k^2} - \gamma^2 d_e^2}, \tag{5.52}$$

and the cross-helicity is

$$E_C = -E\frac{\gamma}{\alpha} k^2 d_e^2. \tag{5.53}$$

The other case, with $\gamma = 0$, corresponds to the state with zero cross-helicity. In this instance, we find that the spectra are

$$E = \frac{16\pi\alpha}{\dfrac{\alpha^2}{k^2} - \beta^2 d_e^4} \quad \text{and} \quad E_M = -E\frac{\beta}{\alpha}k^2 d_e^4. \tag{5.54}$$

In each of these two limiting cases, we find that all spectral quantities undergo direct cascades [171] in contrast to the MHD and Hall MHD limits. This appears to be consistent, to an extent, with previous results in the literature although most previous studies relied on 2D simulations as opposed to our 3D analysis [43, 44, 71]. We have plotted the spectra in Fig. 5.3, which confirms our analytical estimates. Although the wavenumber range from k to $1/d_e^2$, for inertial MHD is not applicable everywhere - instead, its presence is likely to be felt only when $k > 1/d_e$. In reality, there is a finite Hall MHD range before this limit is attained.

We note in passing, that the inclusion of a strong guide field can induce anisotropic turbulence, and the existence of both inverse and direct cascades, but this falls outside the scope of our present work

5.3 Electron skin depth and ion sound Larmor radius effects

Besides Hall MHD and XMHD a number of reduced fluid models exist that account for additional two-fluid plasma effects, models that are amenable to simpler analytical and numerical treatments. Such reduced models (see, e.g., Ref. [241]) typically rely on the assumption of a magnetic field with a strong

constant component along one direction (strong guide field assumption) and are valid at frequencies much lower than the ion cyclotron frequency based on such a guide field. This situation is relevant for some laboratory plasmas as well as for a number of astrophysical situations (see, e.g., Ref. [220]). These models are also characterized by the property of possessing only quadratic nonlinearities and by a spatial anisotropy induced by the presence of the guide field.

The purpose of the following parts of the chapter is to investigate the direction of turbulent cascades in one such reduced fluid model[57] that accounts for the electron skin depth scale and an additional scale, the ion sound Larmor radius $\hat{\rho}_s = \sqrt{T_e/m_i}/\omega_{ci}$, with T_e the equilibrium electron temperature, m_i the ion mass and ω_{ci} the ion cyclotron frequency based on the guide field. This additional scale, which accounts for finite electron temperature, proved, for instance, to be crucial for the nonlinear evolution of the current density and plasma vorticity during a magnetic reconnection process.[106, 75]

In our analysis we consider the two-dimensional (2D) case, assuming translational invariance along the direction of the guide field. This assumption could be justified by the presence of a strong guide field. We remark that, in its original and more general formulation,[221] the model assumes only weak variations along the guide field and, in particular, nonlinear terms only involve derivatives along directions perpendicular to the direction of the guide field. Moreover, the appearance of coherent structures in two-dimensional turbulence and the possible occurrence of reconnection events induced by electron

inertia, as suggested by recent observations of the fast solar wind,[202] make the 2D version of the model of interest in its own right. Some comparison with cascade properties of 3D XMHD will nevertheless be made. In 2D the model is known to possess two infinite families of integral invariants [221] (Casimir invariants) associated with the noncanonical Hamiltonian structure of the model. A qualitative change in the form of these families of invariants occurs when the normalized ion sound Larmor radius $\rho_s = \hat{\rho}_s/L$ (with L a characteristic length of the system) is set equal to zero.

One of the main objectives of the present analysis is to see if the cascade reversal of magnetic helicity at the electron skin depth predicted in Ref. [171] has a counterpart in the 2D reduced model considered in this paper. (We anticipate that, when neglecting toroidal velocity and magnetic field components, the 2D incompressible limit of XMHD,[108] which we will refer to as to '2D planar incompressible XMHD', formally reduces to the 2D reduced model studied here in the limit $\rho_s = 0$). As is well known, the directions of cascades change when going from 3D to 2D in hydrodynamics and in MHD, although in the latter case regimes exist where AES predict the same direction for energy cascade in 2D and 3D (see, e.g., Ref. [40]).

5.3.1 The model and its invariants

As stated in Sec. 5.3, we consider the model of Ref. [57], which was used earlier in Hamiltonian reconnection studies. [107, 106] This model is applicable to low-β plasmas, with β indicating the ratio of the kinetic and magnetic

pressures, and it can be seen as an extension of the previously investigated reduced MHD model of Ref. [96], accounting also for the effects of electron inertia and finite, constant electron temperature. As such, it describes plasmas with a strong magnetic guide field and it can be used to locally model phenomena such as collisionless reconnection and turbulence, in situations where a detailed description of the temperature and heat flux evolution is not required. Because the processes occur on time scales shorter than dissipation time scales, a collisionless Hamiltonian treatment is appropriate. However, in a realistic turbulence scenario dissipation cannot be ignored, even if the resistivity and viscosity appear negligible. The model can be obtained from a more general three-field model [221] in the cold ion limit and assuming an ion response with ion density fluctuations proportional to vorticity fluctuations. Alternatively, the model can be obtained from a two-moment closure of drift-kinetic equations.[74, 270, 240]

The model equations, in dimensionless form, are given by

$$\begin{aligned} \frac{\partial \psi^\star}{\partial t} &= \{\psi^\star, \mathcal{H}\} = [\psi^\star, \phi] + \rho_s^2[\omega, \psi], \\ \frac{\partial \omega}{\partial t} &= \{\omega, \mathcal{H}\} = [\omega, \phi] + [\psi^\star, \nabla^2\psi], \end{aligned} \tag{5.55}$$

where $\omega = \nabla^2\phi$ indicates the vorticity associated with a stream function ϕ (normalized electrostatic potential), whereas $\psi^\star = \psi - d_e^2\nabla^2\psi$, with ψ the poloidal magnetic flux function of a magnetic field $\mathbf{B} = \nabla\psi \times \hat{z} + \hat{z}$. The parameter d_e denotes the constant electron skin depth and the second constant parameter ρ_s corresponds to the ion sound Larmor radius. The bracket $[\,,\,]$ is

defined as usual by $[f, g] := \nabla f \times \nabla g \cdot \hat{z}$ for two functions f and g and the noncanonical Poisson bracket $\{\,,\,\}$ is defined below.

Using a caret to denote dimensional quantities, we have adopted the normalizations, $d_e = \hat{d}_e/L$, $\rho_s = \hat{\rho}_s/L$, $t = \hat{t}/\tau_A, \phi = c\hat{\phi}/(B_0 v_A L)$, and $\psi = \hat{\psi}/(B_0 L)$, where as noted above L is a characteristic length and $\tau_A = L/v_A$ with v_A being the Alfvén speed based on the amplitude B_0 of the guide field. The latter is assumed directed along the $\hat{z}$ axis of a Cartesian coordinate system (x, y, z). Due to the 2D assumption, the z coordinate is taken as ignorable. Note that, when two-fluid effects are suppressed (i.e. $d_e = \rho_s = 0$), the model reduces to the 2D reduced MHD model of Ref. [238].

The first equalities of Eqs. (5.55) indicate that the system possesses a Hamiltonian formulation characterized by a Hamiltonian functional

$$\mathcal{H} := \frac{1}{2}\int d^2x\,(-\phi\,\omega - \psi^\star\nabla^2\psi + \rho_s^2\omega^2), \tag{5.56}$$

and a noncanonical Poisson bracket (see Ref. [182] for review)

$$\begin{aligned}\{P, Q\} &= \int d^2x \left\{\omega\left(\left[\frac{\delta P}{\delta\omega}, \frac{\delta Q}{\delta\omega}\right] + d_e^2\rho_s^2\left[\frac{\delta P}{\delta\psi^\star}, \frac{\delta Q}{\delta\psi^\star}\right]\right)\right. \\ &+ \left.\psi^\star\left(\left[\frac{\delta P}{\delta\psi^\star}, \frac{\delta Q}{\delta\omega}\right] + \left[\frac{\delta P}{\delta\omega}, \frac{\delta Q}{\delta\psi^\star}\right]\right)\right\}. \end{aligned} \tag{5.57}$$

We remark that when electron temperature effects are neglected, i.e., when $\rho_s = 0$, Eqs. (5.55) reduce to the 2D inertial MHD (IMHD) system of Ref. [159] or, equivalently, as stated above, to 2D planar incompressible XMHD.

The complexity of the Poisson Bracket of (5.57) can be reduced by the coordinate transformation $\psi_\pm := \psi^\star \pm d_e\rho_s\omega$ to normal coordinates, in which the Poisson bracket has the following form:

$$\{P,Q\} = 2d_e\rho_s \int d^2x \left(\psi_- \left[\frac{\delta P}{\delta \psi_-}, \frac{\delta Q}{\delta \psi_-} \right] - \psi_+ \left[\frac{\delta P}{\delta \psi_+}, \frac{\delta Q}{\delta \psi_+} \right] \right). \tag{5.58}$$

With the bracket in the form of (5.58), it is easily seen that the systems possesses two infinite families of Casimir invariants:

$$C_\pm = \int d^2x \, \mathcal{F}_\pm(\psi_\pm) \,, \tag{5.59}$$

for arbitrary functions $\mathcal{F}_\pm$. Casimir invariants are functionals C that satisfy $\{C,Q\} = 0$ for all functionals Q. They are thus preserved for dynamics generated by any Hamiltonian.

5.3.2 Spectral Analysis

Equilibrium states of XMHD have been studied (see, e.g., Ref. [121]) leading to a generalization of the Grad-Shafranov equation. In contrast, here we are interested in statistical equilibrium in Fourier space, and the analysis of the associated direction of cascades.

Using a standard Fourier representation $\psi(\mathbf{x}) = \sum_{\mathbf{k}} \psi_{\mathbf{k}} \, e^{i\,\mathbf{k}\cdot\mathbf{x}}$, so that $\psi^\star_{\mathbf{k}} = (1 + k^2 d_e^2)\psi_{\mathbf{k}}$, Eqs. (5.55) become

$$\dot{\psi}^\star_{\mathbf{k}} = \hat{z} \cdot \sum_{\mathbf{k}',\mathbf{k}''} \delta_{\mathbf{k},\,\mathbf{k}'+\mathbf{k}''} \, \mathbf{k}'' \times \mathbf{k}' \left(\frac{\omega_{\mathbf{k}'} \, \psi^\star_{\mathbf{k}''}}{k'^2} + \rho_s^2 \, \omega_{k'} \psi_{k''} \right) \tag{5.60}$$

and

$$\dot{\omega}_{\mathbf{k}} = \hat{z} \cdot \sum_{\mathbf{k}',\mathbf{k}''} \delta_{\mathbf{k},\,\mathbf{k}'+\mathbf{k}''} \, \mathbf{k}'' \times \mathbf{k}' \left(\frac{\omega_{\mathbf{k}'} \, \omega_{\mathbf{k}''}}{k'^2} + k'^2 \psi_{\mathbf{k}'} \, \psi^\star_{\mathbf{k}''} \right) . \tag{5.61}$$

These equations can be generated by the Hamiltonian of (5.56) and Poisson bracket of (5.57) written in terms of Fourier series. Consequently, they preserve the energy and all Casimir invariants written in terms of their Fourier series.

Of particular interest to us are the quadratic invariants preserved by (5.60) and (5.61), the so-called rugged invariants. These are the Hamiltonian and the quadratic Casimirs. The main reason for this is that such invariants survive wave-number truncations, $k_{min} < k < k_{max}$, which is common for spectral Galerkin codes. Another motivation for using these invariants is the ease of handling Gaussian statistics.

Of course, in general there may be other criteria, possibly motivated by experimental results, to ignore or select certain invariants in an analysis of our type, based on the effects of viscosity/resistivity or other aspects ignored in ideal models. For instance in order to determine the relevant invariants, the authors of Ref. [119] have resorted to experiments. In our case, this possibility is excluded by the difficulty of obtaining experimental measures on the invariants for our system. Therefore we stick with the quadratic invariants and introduce linear combinations of the Casimirs of (5.59), viz. the following:

$$F := \frac{1}{2}\int d^2x \, \left[(\psi^\star)^2 + d_e^2\rho_s^2\,\omega^2\right] \tag{5.62}$$

$$G := \int d^2x\,\omega\,\psi^\star\,. \tag{5.63}$$

The Hamiltonian (5.56) and the constants of (5.62) and (5.63) expressed in

terms of Fourier series are

$$\mathcal{H} = \frac{1}{2}\sum_{\mathbf{k}}\left((\rho_s^2+k^{-2})|\omega_{\mathbf{k}}|^2+\frac{k^2|\psi^\star_{\mathbf{k}}|^2}{1+k^2d_e^2}\right), \tag{5.64}$$

$$F = \frac{1}{2}\sum_{\mathbf{k}}(|\psi^\star_{\mathbf{k}}|^2+d_e^2\rho_s^2|\omega_{\mathbf{k}}|^2), \tag{5.65}$$

$$G = \frac{1}{2}\sum_{\mathbf{k}}\left(\omega_{\mathbf{k}}\psi^\star_{-\mathbf{k}}+\omega_{-\mathbf{k}}\psi^\star_{\mathbf{k}}\right). \tag{5.66}$$

Equations (5.65) and (5.66) can be thought of as 2D remnants of the magnetic and cross helicities[156] if we set $\rho_s = 0$, although since there is no third dimension they lose their topological meaning associated with linking. It can be shown via direct calculation that these helicity remnants are indeed rugged. For instance, using (5.60) and (5.61) and the reality condition $\overline{\omega}_{\mathbf{k}} = \omega_{-\mathbf{k}}$ with overbar being complex conjugate, we find

$$\dot{G} = \sum_{\mathbf{k},\mathbf{k}''}\hat{z}\cdot\mathbf{k}''\times\mathbf{k}\,\left((\mathbf{k}+\mathbf{k}'')^2\,\psi^\star_{\mathbf{k}}\psi^\star_{\mathbf{k}''}+\rho_s^2\omega_{\mathbf{k}}\omega_{\mathbf{k}''}\right)\psi_{\mathbf{k}'} = 0\,. \tag{5.67}$$

Tt is not hard to show (similar to Sec. 5.2.2) that a Liouville theorem is satisfied, i.e.,

$$\frac{\partial\dot{\omega}_{\mathbf{k}}}{\partial\omega_{\mathbf{k}}} = 0 \quad \text{and} \quad \frac{\partial\dot{\psi}^\star_{\mathbf{k}}}{\partial\psi^\star_{\mathbf{k}}} = 0\,. \tag{5.68}$$

5.3.3 Absolute Equilibrium States

For more detailed discussion on how AES apply see Sec. 5.2.3.

We seek AES given by the phase space probability density of the form

$$\mathcal{P} = Z^{-1}e^{-\alpha\mathcal{H}-\beta F-\gamma G} =: Z^{-1}e^{-A^{ij}u_iu_j/2}\,, \tag{5.69}$$

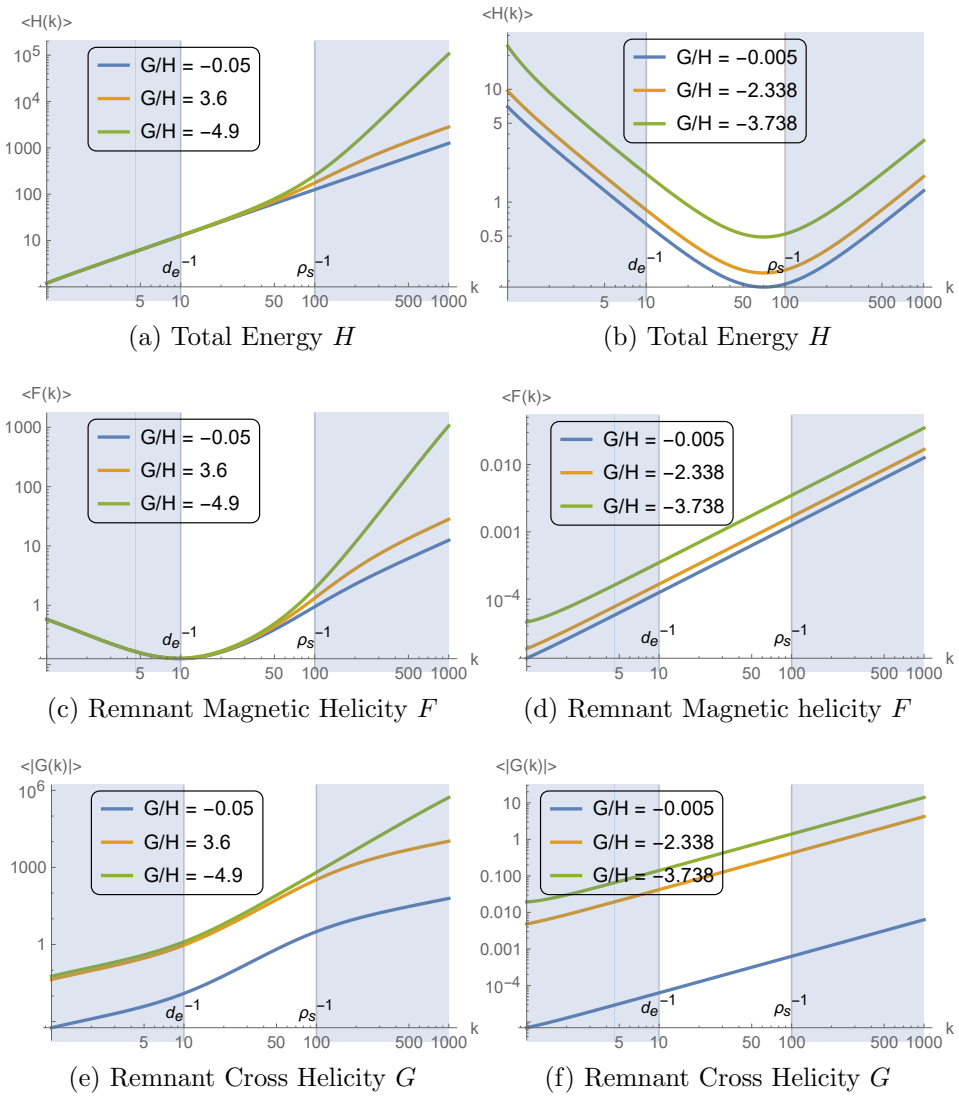

(a) Total Energy H (b) Total Energy H

(c) Remnant Magnetic Helicity F (d) Remnant Magnetic helicity F

(e) Remnant Cross Helicity G (f) Remnant Cross Helicity G

Figure 5.4: Log-Log Plots for total energy, remnant magnetic helicity and cross-helicity. The parameters used in Figures (a,c,e) are $\alpha = 10$, $\beta = 1$ and $\gamma = \{0, -.75, 1\}$ is varied so that different values of G are obtained (color-coded, see the legend for the description). The microscales were chosen to be $d_e = 0.1$ and $\rho_s = 0.01$. Notice that plots are obtained under the assumption that $k_{\min} = 1$ and not 2π for the simplicity. The parameters used in Figures (b,d,f) are $\alpha = -0.1$, $\beta = 10^6$ and $\gamma = \{0, 500, 800\}$ is varied. Helicity F seems to only have direct cascade, when $\alpha < 0$. This can also be seen from able 5.1 since β is so large.

where $u_i := \{\omega^{\Re}_{\mathbf{k}}, \omega^{\Im}_{\mathbf{k}}, \psi^{\star\Re}_{\mathbf{k}}, \psi^{\star\Im}_{\mathbf{k}}\}$ and according to (5.64), (5.65), and (5.66) the matrix (A^{ij}) is given by

$$A := \begin{pmatrix} \delta & 0 & \gamma & 0 \\ 0 & \delta & 0 & \gamma \\ \gamma & 0 & \eta & 0 \\ 0 & \gamma & 0 & \eta \end{pmatrix},$$

where

$$\delta := (\alpha + \beta d_e^2)\rho_s^2 + \frac{\alpha}{k^2} \quad \text{and} \quad \eta := \frac{\alpha k^2}{1 + k^2 d_e^2} + \beta\,. \tag{5.70}$$

The parameters α, β and γ present in Eq. (5.69) are Lagrange multipliers. Their values in terms of the parameters d_e and ρ_s are determined by a normalization condition and by imposing that the expectation values of the invariants $\mathcal{H}$, F and G match their initial values (see Eqs. (5.79), (5.80) and (5.81)). This will be carried out in Sec. 5.3.4. These Lagrange multipliers are akin to the inverse temperatures found in statistical mechanics.

Using (5.69) the partition function Z follows from the normalization condition

$$\int \mathcal{P}(k)\, d\Gamma(k) = \int \mathcal{P}(k)\; d\psi^{\star\Re}_{\mathbf{k}}\, d\psi^{\star\Im}_{\mathbf{k}}\, d\omega^{\Re}_{\mathbf{k}}\, d\omega^{\Im}_{\mathbf{k}} = 1, \tag{5.71}$$

where $\psi^{\star}_{\mathbf{k}} =: \psi^{\star\Re}_{\mathbf{k}} + i\,\psi^{\star\Im}_{\mathbf{k}}$. Because the statistics are Gaussian, integration is straightforward and the partition function is found to be

$$Z = \frac{(2\pi)^2}{\sqrt{\det A}}\,. \tag{5.72}$$

One can also invert the matrix A to obtain various expectation values, such as $\langle u_i u_j \rangle = A^{-1}_{ij}$.[122] In addition, it is necessary to investigate the realizability condition that the matrix A needs to be positive-definite. Thus we

impose the condition of positivity of its eigenvaules, otherwise the probability distribution would not be integrable. After some algebra we arrive at the following inequalities

$$(\alpha + \beta d_e^2)\rho_s^2 k^2 + \alpha > 0\,, \tag{5.73}$$

$$(\alpha + \beta d_e^2)k^2 + \beta > 0 \tag{5.74}$$

$$\Big[(\alpha + \beta d_e^2)\rho_s^2 k^2 + \alpha\Big]\Big[(\alpha + \beta d_e^2)k^2 + \beta\Big] > k^2(1 + k^2 d_e^2)\gamma^2\,. \tag{5.75}$$

At this point it is important to observe that $\alpha > 0$ when we set $\rho_s = 0$. Thus 2D planar incompressible XMHD cannot have the so-called "negative temperature states" (NTS) that correspond to $\alpha < 0$. It appears that NTS are in principle possible if ρ_s is not ignorable, i.e., when thermal electron effects are taken into account. This is interesting since it is known that in 2D fluid turbulence they are associated with the inverse cascade of energy.[195] Actually NTS have been analytically predicted in gyrokinetics [268] in the 2+1D case as well as in some earlier works on drift-wave turbulence.[99, 137] The latter works consider fluid models formed by an incompressible Euler equation together with an equation for an advected scalar. Therefore they differ qualitatively from the model (5.55) that we are using .

It is evident from (5.73) that if $\alpha < 0$ then $\tilde{\alpha} := \alpha + \beta d_e^2 > 0$. Alternatively, we can have $\alpha > 0$, which if $\beta > 0$ obviously implies $\tilde{\alpha} > 0$ and on the other hand if $\beta < 0$ then (5.74) implies that $\tilde{\alpha}$ is again positive. Thus we

have the useful inequality independent of k

$$\tilde{\alpha} := \alpha + \beta d_e^2 > 0\,. \tag{5.76}$$

We proceed with evaluating various expectations of correlations. The quantities of interest are the average squared generalized flux function per wave-mode

$$\frac{1}{2}\langle|\psi_{\mathbf{k}}^*|^2\rangle = \Big[\frac{\tilde{\alpha}k^2+\beta}{1+k^2d_e^2} - \gamma^2\frac{1}{\tilde{\alpha}\rho_s^2+\alpha k^{-2}}\Big]^{-1} \tag{5.77}$$

and the average squared vorticity

$$\frac{1}{2}\langle|\omega_{\mathbf{k}}|^2\rangle = \Big[\tilde{\alpha}\rho_s^2 + \frac{\alpha}{k^2} - \gamma^2\frac{1+k^2d_e^2}{\tilde{\alpha}k^2+\beta}\Big]^{-1}. \tag{5.78}$$

To calculate the remnant cross-helicity we need to add cross-correlation terms

$$\langle G(k)\rangle = -\frac{\gamma}{\Big(\tilde{\alpha}\rho_s^2+\dfrac{\alpha}{k^2}\Big)\dfrac{\tilde{\alpha}k^2+\beta}{1+k^2d_e^2} - \gamma^2}\,. \tag{5.79}$$

To simplify the analysis we assume that the remnant cross-helicity G is zero and therefore $\gamma = 0$. Thus, per wave mode, we obtain the expressions

$$\langle F(k)\rangle = \frac{d_e^2\rho_s^2k^2}{\alpha+\tilde{\alpha}\rho_s^2k^2} + \frac{1+k^2d_e^2}{\tilde{\alpha}k^2+\beta}\,, \tag{5.80}$$

$$\langle H(k)\rangle = \frac{1+\rho_s^2k^2}{\alpha+\tilde{\alpha}\rho_s^2k^2} + \frac{k^2}{\tilde{\alpha}k^2+\beta}. \tag{5.81}$$

This is consistent with the MHD results of Ref. [96] (if we relabel appropriately $\alpha \to 2\alpha, \beta \to 2\gamma, \gamma \to 2\beta$) and apply $\rho_s \to 0$ limit.

We observe that, for large k, the remnant helicity and energy spectra behave as follows:

$$2\pi k\langle F(k)\rangle \approx \mathcal{O}\Big(1/k\Big), \quad 2\pi k\langle \mathcal{H}(k)\rangle \approx \mathcal{O}(k)\,, \tag{5.82}$$

similarly to MHD. On the other hand, at large scales, the presence of finite electron temperature can yield a different behavior, depending on the value of parameters. Relevant limits of the remnant helicity and energy spectra will be discussed in Sec. 5.4.

5.3.4 Qualitative analysis

In this section we will discuss different regimes that the system exhibits. The parameters α and β can be found from the total energy and the remnant helicity, which are obtained as $H = \int 2\pi k \langle H(k) \rangle \, dk$ and $F = \int 2\pi k \langle F(k) \rangle \, dk$. It also turns out to be convenient to introduce the variable $\tilde{F} := F - d_e^2 H$ and the ratio

$$K := \frac{H}{\tilde{F}} = 2 \frac{k_{\max}^2 - k_{\min}^2}{\ln \dfrac{(\beta + \tilde{\alpha} k_{\max}^2)(\alpha + \tilde{\alpha} \rho_s^2 k_{\min}^2)^{d_e^2/\rho_s^2}}{(\beta + \tilde{\alpha} k_{\min}^2)(\alpha + \tilde{\alpha} \rho_s^2 k_{\max}^2)^{d_e^2/\rho_s^2}}} - \frac{\beta}{\tilde{\alpha}} \,. \tag{5.83}$$

Notice that $\alpha H + \beta F = \tilde{\alpha} H + \beta \tilde{F}$; however, since $\tilde{F}$ is not a Casimir, in the following we will focus on the invariant F. In addition we observe the well-known identity

$$\alpha H + \beta F = 2\pi \left(k_{\max}^2 - k_{\min}^2 \right) . \tag{5.84}$$

For simplicity we first consider the 2D planar incompressible XMHD limit $\rho_s \to 0$. Then (5.83) becomes

$$K \to \frac{2}{(k_{\max}^2 - k_{\min}^2)^{-1} \ln \dfrac{\beta + \tilde{\alpha} k_{\max}^2}{\beta + \tilde{\alpha} k_{\min}^2} - d_e^2 \dfrac{\tilde{\alpha}}{\alpha}} - \frac{\beta}{\tilde{\alpha}} \,. \tag{5.85}$$

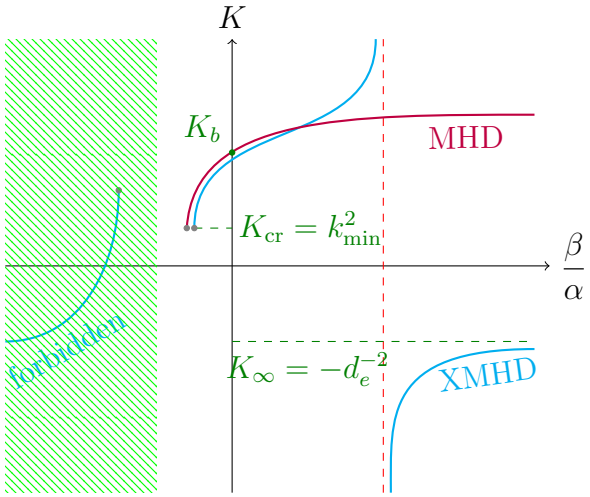

Figure 5.5: Description of the K vs β/α dependence (not to scale) according to (5.85) when $\rho_s = 0$.

The parameter β switches sign at

$$K_b := K(\beta = 0) = \frac{2}{(k_{\rm max}^2 - k_{\rm min}^2)^{-1} \ln \dfrac{k_{\rm max}^2}{k_{\rm min}^2} - d_e^2}\,, \tag{5.86}$$

signaling the emergence of negative temperature states. Notice that $K_b > 0$ provided d_e is small enough. The local minimum is reached when

$$K_{\rm cr} := K\left(\frac{\beta}{\alpha} = -\frac{k_{\rm min}^2}{1 + k_{\rm min}^2 d_e^2}\right) = k_{\rm min}^2\,. \tag{5.87}$$

A depiction of the behavior is shown in Fig. 5.5. Notice that at $K_{\rm cr}$ the remnant helicity condenses to the lowest wavenumber $k_{\rm min}$. This can be seen from the second term in (5.80) and is a direct analogy of the energy condensation in HD proposed by Kraichnan [140] and others.

In addition, it can be shown that the logarithm found in the denominator of (5.85) is a monotonically decreasing function of β/α because $k_{\rm max} > k_{\rm min}$,

while the magnitude of the second term is linearly increasing and thus there exists a pole. This pole is absent in MHD, where therefore $K > 0$. This will be important below. The analysis is concluded by observing that as $\beta/\alpha \to \infty$, K approaches $K_\infty = -d_e^{-2}$ and thus curiously there seems to be a gap in the admissible values of K.

Now let us step back to MHD by letting $d_e \to 0$ and explicitly follow an argument found in Refs. [96, 95]. In this case the following identity can be found from (5.85) in the limit $k_{\max} \to \infty$:

$$\frac{\beta}{\alpha} + k_{\min}^2 = k_{\max}^2 \exp\left[-\frac{2k_{\max}^2}{K}\right] \to 0\,. \tag{5.88}$$

Thus, the authors conclude that physically one can expect condensation to the lowest wavenumber since β becomes negative. If β is negative we can have a low-lying pole as will be described below. And when K reaches it local minimal value (associated with a specific negative value of β, see Fig. 5.5 and Eq. (5.87)) then this pole coincides with $k_{\min}$. Existence of a pole naturally implies that most of the spectral quantity is going to condense there.

If we redo these arguments for the XMHD case, we obtain

$$K \to -d_e^{-2}\left(\frac{\alpha}{\tilde{\alpha}} + 1\right) \Rightarrow \frac{\beta}{\alpha} \to -d_e^{-2}\left(1 + d_e^2 K\right) \tag{5.89}$$

and therefore β/α may remain positive, thus avoiding condensation for some values of K even if $k_{\max} \to \infty$.

When the electron temperature is not ignorable ($\rho_s > 0$) we recover the $\alpha < 0$ regime and the situation becomes more complicated according to

(5.83). From (5.80) and (5.81) we can see that there are two poles. In the vicinity of one pole the other term can be ignored. When β is negative the remnant helicity condenses to $k_{\mathrm{cr},1} \sim \sqrt{-\beta/\tilde{\alpha}}$ as described above in the XMHD case. However in the $\alpha < 0$ case the pole $k_{\mathrm{cr},2} \sim \sqrt{-\alpha\rho_s^{-2}/\tilde{\alpha}}$ dominates and the roles of H and F are interchanged. Notice that both poles cannot occur simultaneously since that would clearly violate (5.76). When ρ_s is small enough one expects a diagram similar to that of Fig. 5.5. It is not hard to show that β changes sign at

$$K_b = 2\frac{k_{\mathrm{max}}^2 - k_{\mathrm{min}}^2}{\ln\dfrac{k_{\mathrm{max}}^2}{k_{\mathrm{min}}^2} - \dfrac{d_e^2}{\rho_s^2}\ln\dfrac{1+\rho_s^2 k_{\mathrm{max}}^2}{1+\rho_s^2 k_{\mathrm{min}}^2}}\,, \tag{5.90}$$

which generalizes (5.86). In fact, because the second term in the denominator is monotonic, it turns out that as a function of ρ_s the quantity K_b is bounded from below by (5.86), which is positive provided that d_e is sufficiently small, so we can assume $K_b > 0$. Similarly, α changes sign at

$$K_a = -d_e^{-2} - \frac{2\rho_s^2}{d_e^2}\frac{k_{\mathrm{max}}^2 - k_{\mathrm{min}}^2}{\ln\dfrac{k_{\mathrm{max}}^2}{k_{\mathrm{min}}^2} - \dfrac{\rho_s^2}{d_e^2}\ln\dfrac{1+d_e^2 k_{\mathrm{max}}^2}{1+d_e^2 k_{\mathrm{min}}^2}} \tag{5.91}$$

and by the same argument $K_a < 0$, provided that ρ_s is sufficiently small.

5.4 Comparisons and summary

Our new results concern the limit $kd_e \gg 1$, where

$$2\pi k\langle F(k)\rangle \approx \mathcal{O}(k), \quad 2\pi k\langle \mathcal{H}(k)\rangle \approx \mathcal{O}(k)\,. \tag{5.92}$$

Length Scale Choices	$\langle H(k) \rangle$	$\langle F(k) \rangle$
$1 < k \ll (d_e^{-1}, \rho_s^{-1})$	$\frac{1}{\alpha} + \frac{1}{\alpha + \beta k^{-2}}$	$\frac{1}{\alpha k^2 + \beta}$
$1 \ll d_e^{-1} \ll k \ll \rho_s^{-1}$	$\frac{1}{\alpha} + \frac{1}{\alpha + \beta d_e^2}$	$\frac{1}{\alpha d_e^{-2} + \beta}$
$1 \ll \rho_s^{-1} \ll k \ll d_e^{-1}$	$\frac{1}{\alpha + \beta d_e^2} + \frac{1}{\alpha + \beta k^{-2}}$	$\frac{1}{\alpha k^2 + \beta} + \frac{1}{\alpha d_e^{-2} + \beta}$
$1 \ll (d_e^{-1}, \rho_s^{-1}) \ll k$	$\frac{2}{\alpha + \beta d_e^2}$	$\frac{2}{\alpha d_e^{-2} + \beta}$

Table 5.1: Various limits of spectral densities when $\alpha > 0$ and β not too large. The first row corresponds to the large scale MHD limit; it was assumed that β is not orders of magnitude larger than α to avoid singular perturbation and most likely this situtation is not realizable if one solves for the parameters via integrals of motion. The second row pertains to the 2D planar incompressible XMHD high k limit, where gyroeffects have been ignored. The third row displays an opposite situation, where gyrophysics is relevant but the electron skin depth ignorable. The last row demonstrates the microscopic k limit, and may be unphysical depending on how the model ordering works. Notice that terms were simply ignored based on the ordering, a more precise description would involve Taylor series.

Thus we see that the scaling changes from the inverse to direct, which suggests cascade reversal for the remnant magnetic helicity F. Table 5.1 contains our analyses for behavior across scales when $\rho_s > 0$. The cascade reversal behavior indicated by (5.82) and (5.92) is seen in this more general analysis. Thus there is cascade reversal behavior at the electron skin depth in 2D planar incompressible XMHD as was predicted for 3D XMHD in Ref. [171], although the details may vary. In Figure. 5.4 we plot spectral quantities for non-zero γ.

As pointed out in Ref. [96], when $kd_e \ll 1$ the inverse cascade implies the presence of large scale structures in $\psi^\star$. In our model due to the presence of ρ_s this can be achieved in the $\alpha > 0$ regime; on the other hand when $\rho_s = 0$ states $\alpha < 0$ are forbidden. In 3D MHD, the large scale presence of magnetic helicity is often associated with the generation of large scale magnetic fields.[7, 26] In Sec. 5.2 [171] we have explored the influence the electron inertia can have on the development of the turbulent cascade of the magnetic helicity in 3D. As stated earlier, in absence of ρ_s the present paper can be seen as a natural continuation of the earlier work, where geometry is simplified to two dimensions. In 2D MHD we see that instead of inverse cascade of magnetic helicity one has inverse cascade of the square vector potential and so we reach similar conclusions. The fact that magnetic helicity would condense to large scales is often cited as evidence of the dynamo action in MHD.[95, 45] The antidynamo theorem applies in the absense of the external magnetic field or a magnetic source. [227] For comparison see spectral quantities in 3D XMHD in Fig. 5.3 (see Ref. [171] and Table 5.2 for more details).

We are led to conclude that there may be barriers for finer-scale fluctuation amplifications (such as $kd_e \gg 1$). Also a natural conclusion could be that fluctuations of magnetic helicity F are suppressed on the d_e^{-1} scale. Often times in this regime the electron MHD (EMHD) model is applied [43, 169, 168] and so it is worthwhile comparing these models. For the analysis, what matters are integrals of motion, thus we compare EMHD and inertial MHD (which corresponds to Eqs. (5.55) with $\rho_s = 0$) in Table 5.2. It appears that the similarity is greater in 2D than in 3D. Direct cascade of energy is also found in Ref. [44]. However the model we use can also have non-zero electron temperatures ($\rho_s \neq 0$) that for some choice of parameters can lead to the inverse cascade of energy.

Models	Energy	Magnetic-Helicity
2D EMHD	$-\int d^2x\, \frac{1}{2}(\psi^\star \nabla^2 \psi + \phi^\star \omega)$	$\int d^2x\, \frac{1}{2}(\psi^\star)^2$
2D IMHD	$-\int d^2x\, \frac{1}{2}(\psi^\star \nabla^2 \psi + \phi\, \omega)$	$\int d^2x\, \frac{1}{2}(\psi^\star)^2$
3D EMHD	$\int d^3x\, \frac{1}{2}\mathbf{B}^\star \cdot \mathbf{B}$	$\int d^3x\, \frac{1}{2}\mathbf{A}^\star \cdot \mathbf{B}^\star$
3D IMHD	$\int d^3x\, \frac{1}{2}(V^2 + \mathbf{B}^\star \cdot \mathbf{B})$	$\int d^3x\, \frac{1}{2}(\mathbf{A}^\star \cdot \mathbf{B}^\star + \mathbf{d_e^2 V} \cdot \nabla \times \mathbf{V})$
3D XMHD	$\int d^3x\, \frac{1}{2}(V^2 + \mathbf{B}^\star \cdot \mathbf{B})$	$\int d^3x\, \frac{1}{2}(\mathbf{A}^\star \cdot \mathbf{B}^\star + \mathbf{d_e^2 V} \cdot \nabla \times \mathbf{V})$

Table 5.2: Comparison of the integrands for invariants in various extended MHD models. Notice that IMHD is normalized to the Alfven time-scale, while EMHD to a whistler time-scale $\tau_H = L^2\omega_{pe}^2/(c^2\Omega_e)$. In all cases the operator $* := 1 - d_e^2\nabla^2$.

2D IMHD and 2D EMHD can both be derived from 2D XMHD in specific limits. The former, as already mentioned, is obtained after setting

to zero the out-of-plane components of the velocity and magnetic field. The latter is obtained by rescaling the time with respect to the whistler time and by retaining the leading order terms in the limit $d_i \gg 1$, where d_i is the normalized ion skin depth. This comparison puts us in a position to discuss recent comments [267] regarding 2-fluid absolute equilibrium states.[171, 269] We agree with Ref. [267] that the qualitative picture of a direct cascade of the magnetic helicity is achieved in both 3D EMHD[269] and 3D IMHD;[171] however, the details of spectral dependence are different, for instance in our model [171] we recover energy equipartition for MHD.

When the effects of ion sound Larmor radius are included the eigenvalue analysis demonstrates that NTS ($\alpha < 0$) are possible and we observe that in the low k limit the total energy per wave-number $2\pi k\langle\mathcal{H}(k)\rangle$ scales inversely with k for the portion of inertial range, suggesting inverse cascade of energy (see Fig. 5.4b), as was first predicted by Onsager[195] for two-dimensional hydrodynamics. The inverse cascade of energy can also be inferred from the expression (5.81) because β is so large. Observed dependence of the invariants in this regime qualitatively agrees with the picture of the dual cascade obtained in drift wave two-field fluid models [99, 137] and a gyrokinetic model [268] investigated later.

Naturally, prior to proceeding to the more general reduced extended MHD case like that of Ref. [108], these predictions have to be confirmed by direct numerical simulations. For instance, there is evidence of broken ergodicity and coherent structures[229, 230] in MHD. Broken ergodicity is observed in

many other physical systems including classical dipolar spin systems.[170] It is most suitable to consider a pseudo-spectral code [107] to investigate whether the relaxation of the Fourier modes in MHD can occur. The advantages of using Galerkin methods in general involve accuracy and "semiconservation" of the integrals of motion.[196] Although for us it has an additional advantage since we are interested in the k-space behavior. Alternatively, since relaxation to equilibria subject to constraints is sought, it could be beneficial to apply recently developed symplectic/Poisson integration algorithms like the ones of Refs. [143, 257]. This would also further justify the Hamiltonian treatment the problem has received.

In closing we note that there are many plasma models where similar analysis can be performed. One of the candidates we intend to work with in the future is a special relativistic two-fluid model that was recently shown to possess Hamiltonian form.[125] This model can be applied in relativistic jets and laser fusion.

Chapter 6

Cascade reversal seen in numerics

6.1 Pseudospectral code

In this chapter we will discuss our latest work where we take the model found in Sec. 5.3.1 and simulate it via a parallel pseudospectral MHD code [105] modified for our purposes. This is necessary primarily because the analysis in Sec. 5.3.3 ignores dissipation and is based on the assumption that the ideal system relax to the most likely state given by the Gibbs distribution. We have only proved the Liouville's theorem that shows the conservation of the phase-space volume but not the H-theorem for this system that would justify the principle of maximum entropy, which is not expected since turbulence is quite far from equilibrium.

The equations we simulate are a straightforward generalization of (5.55),

$$\frac{\partial \psi^\star}{\partial t} + \mathbf{u}\cdot\nabla\psi^\star = \eta^+\Delta^n\psi^\star + \eta^-\Delta^{-m}\psi^\star + \phi_\psi, \tag{6.1}$$

$$\frac{\partial \omega}{\partial t} + \mathbf{u}\cdot\nabla\omega = \mathbf{b}^\star\cdot\nabla j + \nu^+\Delta^n\omega + \nu^-\Delta^{-m}\omega + \phi_\omega, \tag{6.2}$$

where η^+ and ν^+ are hyper-dissipation (higher order improves the inertial range), while η^- and ν^- are hypodissipation. The latter, while having no physical counterpart, operates at low wave-numbers and is used to limit the

condensation of appropriate spectral quantities. Finally, ϕ_ψ and ϕ_ω represent random forcing.

The details of the procedures used can be found in Refs. [105, 63]; however, it suffices to say that the fields are asssumed to be defined on a periodic domain from 0 to 2π using Fourier expansion. As a result PDEs are replaced by a set of coupled ODEs. They are advanced in time using the second order Runge-Kutta scheme.

The main goal is to add stirring at a certain wavenumber (injection scale) k_f. This wavenumber is chosen in such a way that there is enough inertial range on both sides so that the inverse cascade can be observed. The choice of k_f also depends on the resolution. The rule of thumb is to use $k_f = 8$ for 512×512, $k_f = 16$ for 1024×1024 etc.

The fluxes may be calculated in the following manner: from Eqs. (5.60), (5.61) and (5.64) we see that

$$\dot{H}_k + \langle \phi[\omega, \phi] + d_e^2 J[\phi, J] + \phi[J, \psi] + J[\phi, \psi] \rangle_k = 0, \tag{6.3}$$

where, the k subscript indicates we take only a summand, i.e. the corresponding harmonics of (5.64). The Poisson bracket here can be inferred from the R.H.S. of Eqs. (5.60), (5.61). The second term is denoted π_k and represents the flux through a wavenumber. Of course we have ignored the dissipation and forcing on the R.H.S. Likewise, from Eqs.. (5.60), (5.61) and (5.65) we see

$$\dot{F}_k + \langle \psi^\star [\phi, \psi^\star] \rangle_k = 0. \tag{6.4}$$

6.2 Results

We are happy to report that the cascade reversal of F, predicted in Sec. 5.4, is indeed observed around $kd_e \sim 1$. This can be seen invariably in multiple trials where we changed the parameter d_e. In particular, we see in Fig. 6.1a how the direction of the F is reversed as the parameter $k_f d_e$ is varied. Regimes below $k_f d_e < 0.5$ can be associated with MHD (inverse cascade of the magnetic square potential). On the other hand, regimes above $d_e k_f \sim 1.3$ can be associated with the forward cascade of F, as was predicted in Chapter 5.

However, when we look at Fig. 6.1b the picture is less promising (or more depending on what one is after). In particular, simultaneously with the reversal of F one observes the transition to the incomplete inverse cascade of energy above $d_e k_f \sim 1.3$. This is at odds with what was predicted from the AES theory.

It is even more interesting when one looks at the actual real space distribution of the fields (see Figs. 6.3 and 6.2) in the MHD regime and compares it to the IMHD regime (see Figs. 6.5 and 6.4). In the MHD regime we see fine structure in the stream-function (Fig. 6.3b) and consequently velocity flow, and island chains in the magnetic vector potential (Fig. 6.2b) that can be identified with the in-plane magnetic field lines. On the other hand, after inspecting the IMHD regime one finds that the roles of ϕ and ψ are reversed, along with the appearance of isolated vortices (Fig. 6.5a).

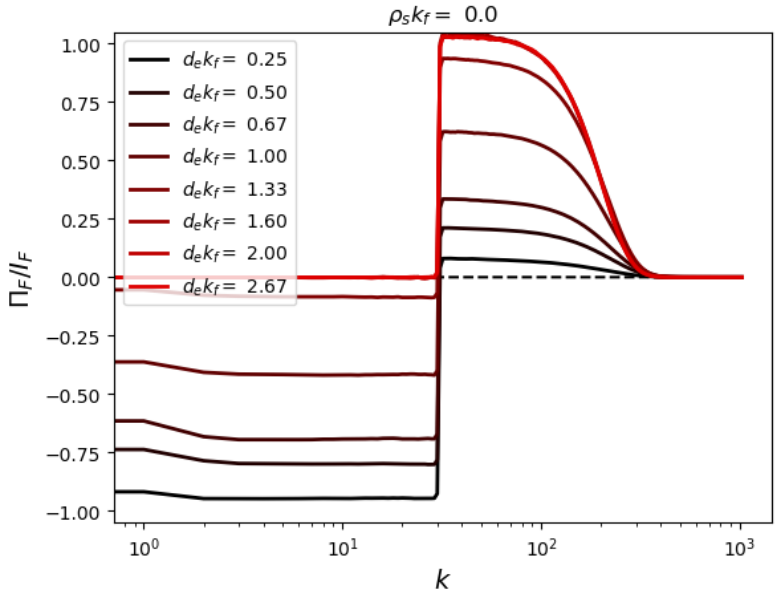

(a) Helicity F

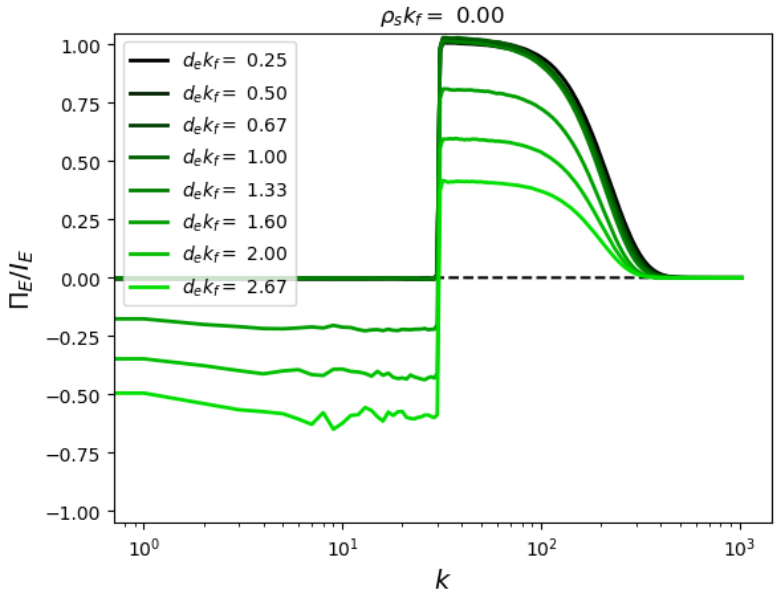

(b) Total Energy E

Figure 6.1: Plot of the mean fluxes (averaged after the stationary regime is reached) as a function of wavenumber (see Eqs. (6.4) and (6.3)).

It is not clear why the energy reverses numerically in the $\rho_s = 0$ regime. In addition we observe that the transition is critical in the sense that there exists a critical value of $k_f d_e$ when we start getting an inverse cascade of the energy and a direct cascade of F. We will defer the demonstration of this as well as many other intersting features for the future publication.

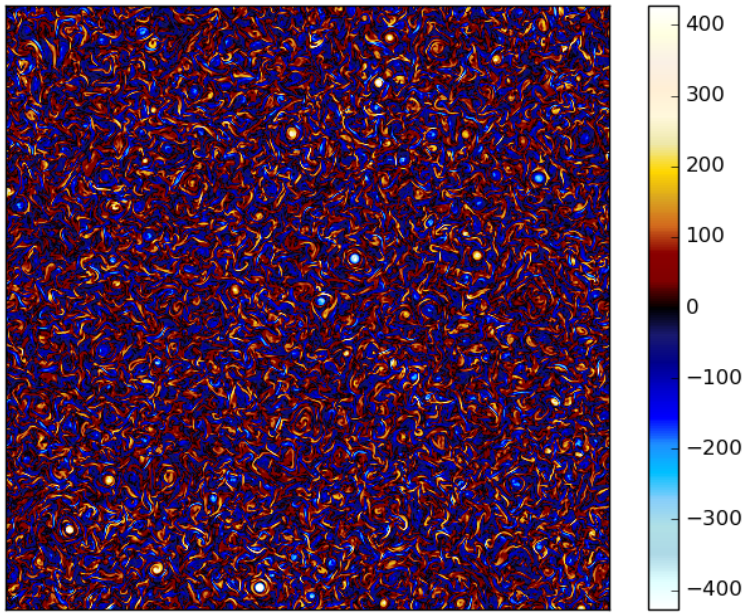

(a) j

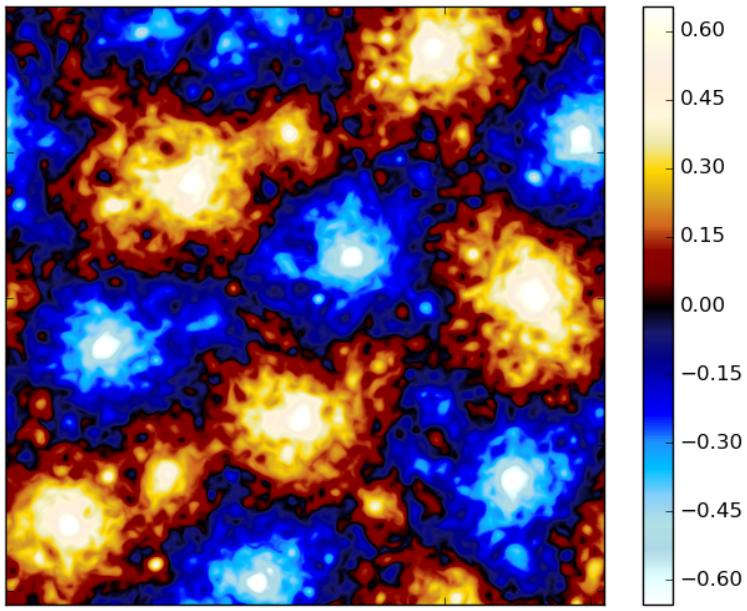

(b) ψ

Figure 6.2: The final stages of evolution for $d_e k_f = 0.25$ (MHD regime) and $\rho_s = 0$.

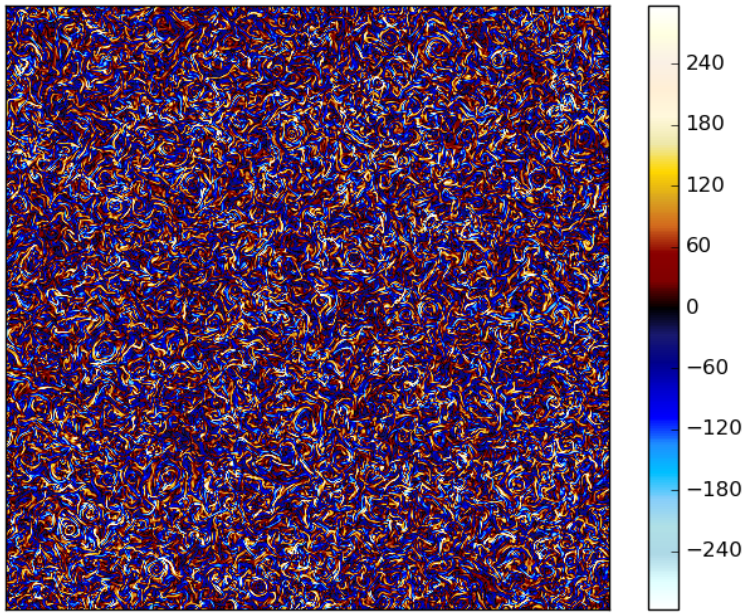

(a) ω

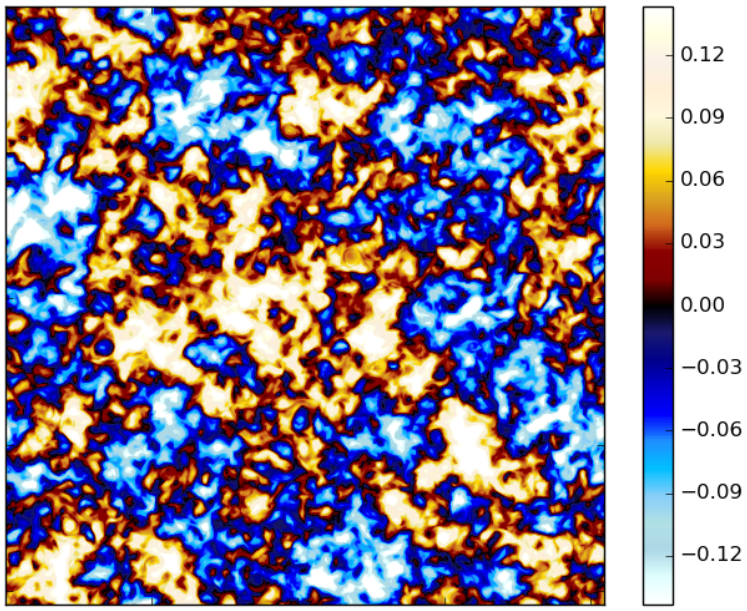

(b) ϕ

Figure 6.3: The final stages of evolution for $d_e k_f = 0.25$ (MHD regime) and $\rho_s = 0$.

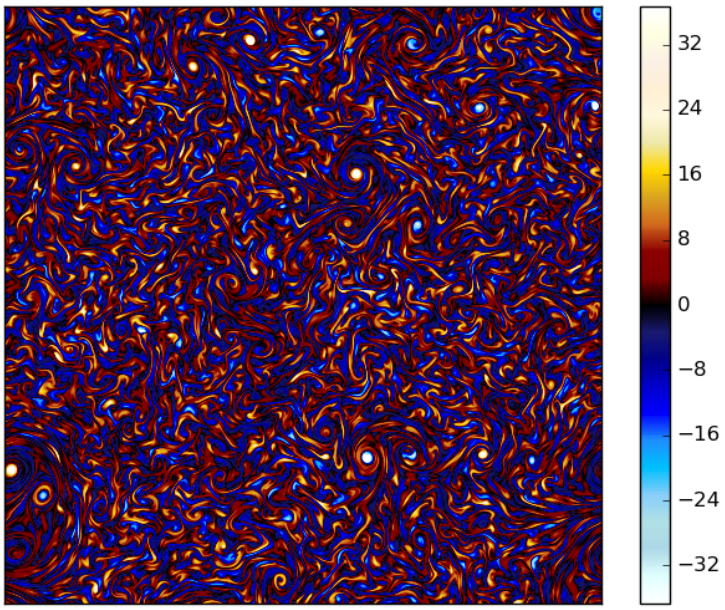

(a) j

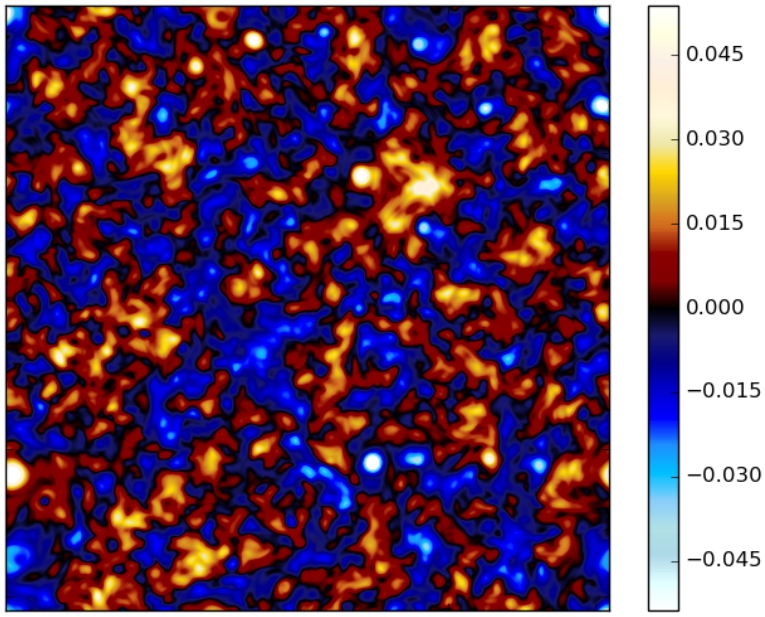

(b) ψ

Figure 6.4: The final stages of evolution for $d_e k_f = 2.67$ (IMHD regime) and $\rho_s = 0$.

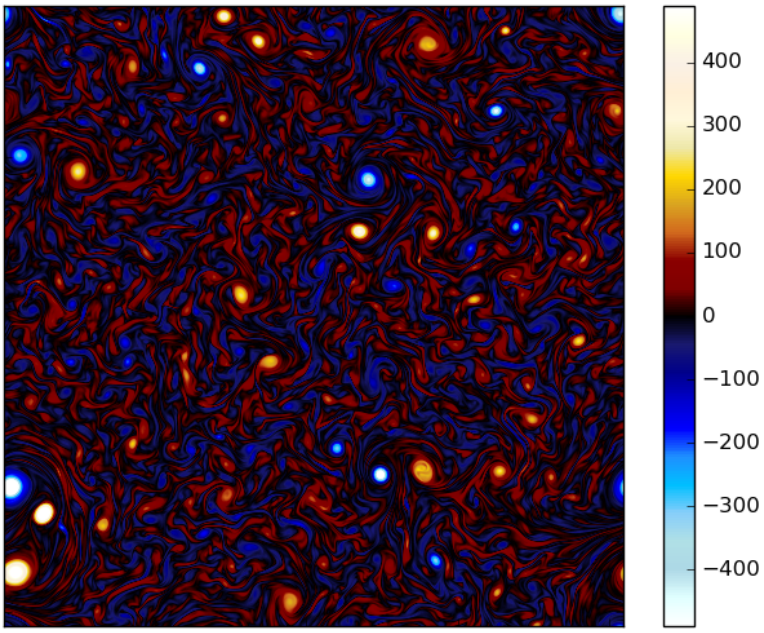

(a) ω

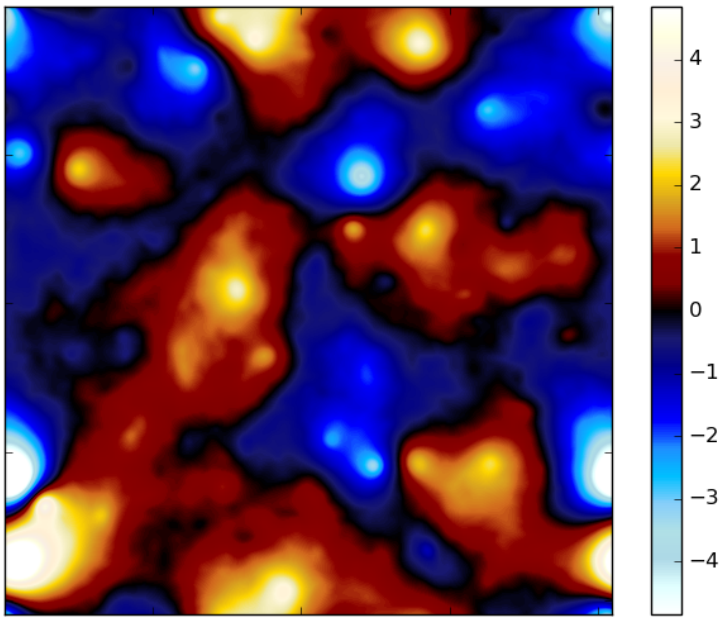

(b) ϕ

Figure 6.5: The final stages of evolution for $d_e k_f = 2.67$ (IMHD regime) and $\rho_s = 0$.

Chapter 7

Special relativistic extended magnetohydrodynamics

7.1 Introduction

In this chapter, we obtain APs for relativistic magnetofluid models. The material here is heavily based on Ref [125][1]. The key ingredient for constructing APs for a fluid-like systems is a means for implementing constraints, because direct extremization yields trivial equations of motion. There are various formalisms available, depending on how the constraints are implemented. One is to follow Lagrange [147] and incorporate constraints into the definition of the variables. This procedure is invoked when using Lagrangian coordinates with the time evolution of variables (fluid element attributes) (e.g., density and entropy) described a priori by conservation of differential forms along stream lines. APs in the Lagrangian coordinates have been obtained for the nonrelativistic neutral fluid, magnetohydrodynamics (MHD),[192] and various generalized magnetofluid models (e.g. extended MHD (XMHD), inertial MHD (IMHD), and Hall MHD (HMHD)),[120, 159, 72] as well as for the relativistic

[1] Y. Kawazurea, G. Miloshevich, P. J. Morrison , "Action principles for relativistic extended magnetohydrodynamics: A unified theory of magnetofluid models" Phys. Plasmas, 24(2):022103 February 2017. George Miloshevich is a secondary author. His contribution was significant and it involved some analytical calculations.

neutral fluid [244, 78, 217] and MHD.[3, 126] In obtaining such formulations several complications arise, e.g., the inference of the appropriate Lagrangian variables, the map between the Lagrangian and Eulerian coordinates in the relativistic case,[126] and the existence of multiple flow characteristics for generalized magnetofluid models.[120, 72]

A second type of AP, one that is formulated in terms Eulerian variables, implements the constraints via Lagrange multipliers, and in this way extremization of the action can lead to correct equations of motion.[225, 151] Upon enforcing the constraints of conservation of density, entropy, and a Lagrangian label,[151] this procedure was recently used to obtain nonrelativistic HMHD.[258] Then, this formulation for HMHD was used to regularize the singular limit to MHD by a renormalization of variables, thereby obtaining an AP for MHD.[258] For the relativistic neutral fluid, the velocity norm (light-cone) condition ($u^\mu u_\mu = 1$ with fluid four velocity u^μ) is required as another constraint.[223, 206, 224, 128, 84] Instead of taking limit from HMHD with renormalization, there are alternative formulations for nonrelativistic [253] and relativistic [29, 30] MHD, in which the Ohm's law or the induction equation *per se* is employed as a constraint.

A third type of AP, one of general utility that incorporates a covariant Poisson bracket in terms of Eulerian variables, was introduced in Ref. [166]. Instead of including the constraints in the action with Lagrange multipliers, the constraints are implemented via the degeneracy of a Poisson bracket that effects constrained variations. In addition to the neutral fluid, such Poisson

bracket APs have been described for particle mechanics, electromagnetism, the Vlasov-Maxwell system, and the gravitational field.[166] Most recently, this kind of action was obtained for relativistic MHD.[73]

From Table 7.1, which summarizes the aforementioned APs, we see there are missing pieces: the APs for fluid-dynamical systems are (i) the Lagrangian AP, (ii) Eulerian constrained least AP, and (iii) the Eulerian bracket AP, for relativistic generalized magnetofluid models. In this chapter, we formulate the latter two APs: (ii) and (iii), and show that they are related by variable transformation. Then we derive APs for HMHD and MHD by taking limits of the XMHD AP. Relativistic HMHD is derived for the first time in the present study by this method. Also, we show that the nonrelativistic limit of the bracket AP gives nonrelativistic XMHD as a Hamiltonian system.

This chapter is organized as follows. In Sec. 7.2 we formulate a constrained least AP for relativistic XMHD. In Sec. 7.3 the bracket AP is derived by a transformation of phase space variables in the constrained least AP. In Sec. 7.4 we derive relativistic HMHD and MHD by taking limits of the bracket AP for XMHD. These results are used in Sec. 7.5 where remarkable features of relativistic HMHD pertaining to collisionless reconnection are considered. In Sec. 7.6, the nonrelativistic limit of the bracket AP is shown. Finally in Sec. 7.7 we conclude.

	Constrained least AP
Nonrelativistic fluid	Lin (1963) [151]
Nonrelativistic MHD	Yoshida & Hameiri (2013) [259] (limit from HMHD) Webb et al. (2014) [253] (Ohm's law constraint)
Nonrelativistic XMHD	Yoshida & Hameiri (2013) [259] (HMHD)
Relativistic fluid	Schutz (1970)[223]
Relativistic MHD	**Present study [125] (limit from HMHD)** Bekenstein & Oron (2000) (Ohm's law constraint) [29]
Relativistic XMHD	**Present study**[125]
	Lagrangian description AP
Nonrelativistic fluid	Lagrange (1788) [147]
Nonrelativistic MHD	Newcomb (1962) [192]
Nonrelativistic XMHD	Keramidas Charidakos et al. (2014) [65]
Rel. fluid	Salmon (1988) [216]
Relativistic MHD	Achterberg (1983) [3] Kawazura et al. (2014) [126]
	Covariant bracket AP
Nonrelativistic fluid	**Present study**[125]
Nonrelativistic MHD	**Present study**[125]
Nonrelativistic XMHD	**Present study**[125]
Relativistic fluid	Marsden et al. (1986) [166]
Relativistic MHD	D'Avignon et al. (2015) [73]
Relativistic XMHD	**Present study**[125]

Table 7.1: Summary of APs for fluid-dynamical systems.

7.2 Constrained least action principle

Consider a relativistic plasma consisting of positively and negatively charged particles with masses m_+ and m_-, where subscript signs denote species labels, and assume the Minkowski spacetime with the metric tensor diag$(1, -1, -1, -1)$. In addition, a proper charge neutrality condition is imposed so that rest frame particle number densities of each species satisfy $n_+ = n_- = n$.[134] The four velocities of each species are denoted by ${u_\pm}^\mu$, which obey the velocity norm conditions

$$ {u_\pm}^\mu u_{\pm\mu} = 1 \,. \tag{7.1} $$

Using the four velocities ${u_\pm}^\mu$, the four center of mass velocity and the four current density can be written as

$$ u^\mu = (m_+/m){u_+}^\mu + (m_-/m){u_-}^\mu \,, \tag{7.2} $$

$$ J^\mu = e({u_+}^\mu - {u_-}^\mu) \,, \tag{7.3} $$

respectively, with $m = m_+ + m_-$ and the electric charge e. The time and space components of these fields are written as $u^\mu = (\gamma,\, \gamma\mathbf{v}/\mathbf{c})$ and $J^\mu = (\rho_q,\, \mathbf{J})$ with speed of light c, Lorentz factor $\gamma = 1/\sqrt{1 - (|\mathbf{v}|/\mathbf{c})^\mathbf{2}}$, and charge density ρ_q. The thermodynamic variables needed are the energy density $\rho_\pm$, the enthalpy density $h_\pm$, the entropy density $\sigma_\pm$, and the isotropic pressure $p_\pm$. These are related by $nh_\pm = p_\pm + \rho_\pm = n(\partial\rho_\pm/\partial n) + \sigma_\pm(\partial\rho_\pm/\partial\sigma_\pm)$.[166] We also define total energy density $\rho = \rho_+ + \rho_-$ and total pressure $p = p_+ + p_-$.

Adding the continuity equations for each species together leads an equation for n,

$$\partial_\nu (n u^\nu) = 0\,, \tag{7.4}$$

while the adiabatic equations of each species can be written as

$$\partial_\nu \left(\sigma_\pm {u_\pm}^\nu\right) = 0. \tag{7.5}$$

In addition to the above constraint equations we include conservations of the Lagrangian labels $\varphi_\pm$,

$$u_{\pm_\nu} \partial^\nu \varphi_\pm = 0. \tag{7.6}$$

The full set of independent variables of our action are chosen to be (u^μ, J^μ, n, $\sigma_\pm$, $\varphi_\pm$, A^μ), where A^μ is a four vector potential that defines a Faraday tensor $\mathcal{F}^{\mu\nu} = \partial^\mu A^\nu - \partial^\nu A^\mu$. Here we consider CGS unit getting rid of a factor $c/4\pi$ in the Faraday tensor by renormalization (i.e., $c\mathcal{F}^{\mu\nu}/4\pi \to \mathcal{F}^{\mu\nu}$). In a manner similar to that of Lin's formalism [151] for the nonrelativistic neutral fluid, we bring (7.4), (7.5), and (7.6) into an action as constraints as follows:

$$\begin{aligned} S[u,\, J,\, n,\, \sigma_\pm,\, A,\, \varphi_\pm] = & \\ \int \Bigg\{ & \sum_\pm \left[-\frac{1}{2} n h_\pm u_{\pm_\nu} {u_\pm}^\nu + \frac{1}{2}(p_\pm - \rho_\pm) \right] - J^\nu A_\nu \\ & -\frac{1}{4}(\partial^\mu A^\nu - \partial^\nu A^\mu)(\partial_\mu A_\nu - \partial_\nu A_\mu) - \phi \partial^\nu (n u_\nu) \\ & - \sum_\pm \left[\eta_\pm \partial^\nu (\sigma_\pm u_{\pm_\nu}) - \lambda_\pm u_{\pm_\nu} \partial^\nu \varphi_\pm \right] \Bigg\} \mathrm{d}^4 x, \end{aligned} \tag{7.7}$$

where $\sum_\pm$ is summation over species, and ϕ, $\eta_\pm$, and $\lambda_\pm$ are Lagrange multipliers. The first and second terms of (7.7) are the fluid part for each species, the

third term is an interaction between the fluid and the electromagnetic (EM) field, the fourth term is the pure EM part, and the other terms represent the constraints. The velocity norm conditions (7.1) will be imposed after taking a variation of the action.[2]

Variation of the action, i.e., setting $\delta S = 0$, gives

$$\delta u_\nu \quad : \quad nhu^\nu + \frac{\Delta h}{e} J^\nu = n\partial^\nu \phi + \sum_\pm (\sigma_\pm \partial^\nu \eta_\pm + \lambda_\pm \partial^\nu \varphi_\pm) \tag{7.8}$$

$$\delta J_\nu \quad : \quad A^\nu + \frac{\Delta h}{e} u^\nu + \frac{h^\dagger}{ne^2} J^\nu = \sum_\pm \left[\pm \frac{m_\mp}{men} (\sigma_\pm \partial^\nu \eta_\pm + \lambda_\pm \partial^\nu \varphi_\pm) \right] \tag{7.9}$$

$$\delta \sigma_\pm \quad : \quad u_{\pm\nu} \partial^\nu \eta_+ = \frac{\partial \rho_\pm}{\partial \sigma_\pm} \tag{7.10}$$

$$\delta \varphi_+ \quad : \quad \partial^\nu (\lambda_+ u_{\pm\nu}) = 0 \tag{7.11}$$

$$\delta A^\nu \quad : \quad J_\nu = \partial^\mu \mathcal{F}_{\mu\nu} \tag{7.12}$$

$$\delta n \quad : \quad n u_\nu \partial^\nu \phi = A^\nu J_\nu + n \sum_\pm \frac{\partial \rho_\pm}{\partial n}, \tag{7.13}$$

with $h := h_+ + h_-$, $\Delta h := (m_-/m)h_+ - (m_+/m)h_-$, and $h^\dagger = (m_-^2/m^2)h_+ + (m_+^2/m^2)h_-$. Using (7.4), (7.5), (7.6), and (7.8)-(7.13), the momentum equa-

[2]We remark the difference of the treatment of the velocity norm condition between preceding works of relativistic single fluid AP [206, 128, 84]. In their actions, the velocity norm condition is included in the action with Lagrange multiplier. However this method cannot be applied for generalized magnetohydrodynamic models since there are multiple velocity norm conditions for each species and the multipliers cannot be determined.

tion and generalized Ohm's law are obtained:

$$\partial_\nu \left[nhu^\mu u^\nu + \frac{\Delta h}{e}(u^\mu J^\nu + J^\mu u^\nu) + \frac{h^\dagger}{ne^2} J^\mu J^\nu \right] \tag{7.14}$$
$$= \partial^\mu p + J^\nu \mathcal{F}^\mu{}_\nu,$$
$$\partial_\nu \left[n(\Delta h) u^\mu u^\nu + \frac{h^\dagger}{e}(u^\mu J^\nu + J^\mu u^\nu) + \frac{\Delta h^\sharp}{ne^2} J^\mu J^\nu \right] \tag{7.15}$$
$$= \frac{m_-}{m}\partial^\mu p_+ - \frac{m_+}{m}\partial^\mu p_- + enu^\nu \mathcal{F}^\mu{}_\nu - \frac{m_+ - m_-}{m} J^\nu \mathcal{F}^\mu{}_\nu,$$

with $\Delta h^\sharp = (m_-^3/m^3)h_+ - (m_+^3/m^3)h_-$. These are equivalent to the relativistic XMHD equations previously formulated by Koide.[134, 135] The generalized Ohm's law of (7.14) can be rewritten as

$$eu_\nu \mathcal{F}^{\star\mu\nu} - \frac{J_\nu}{n} F^{\dagger\mu\nu} = \frac{m_-}{m}\left(T_+ \partial^\mu \frac{\sigma_+}{n}\right) - \frac{m_+}{m}\left(T_- \partial^\mu \frac{\sigma_-}{n}\right), \tag{7.16}$$

with

$$\begin{aligned} A^{\dagger\nu} &= \frac{m_+ - m_-}{m} A^\nu - \frac{h^\dagger}{e} u^\nu - \frac{\Delta h^\sharp}{ne^2} J^\nu, \\ \mathcal{F}^{\star\mu\nu} &= \partial^\mu A^{\star\nu} - \partial^\nu A^{\star\mu} \quad \text{and} \quad \mathcal{F}^{\dagger\mu\nu} = \partial^\mu A^{\dagger\nu} - \partial^\nu A^{\dagger\mu}, \end{aligned}$$

where a generalized vector potential $A^\star$ is defined by

$$A^{\star\nu} = A^\nu + \frac{\Delta h}{e} u^\nu + \frac{h^\dagger}{ne^2} J^\nu. \tag{7.17}$$

Note, the following must hold as an identity:

$$\partial^\mu \left(\epsilon_{\mu\nu\rho\sigma} \mathcal{F}^{\star\rho\sigma}\right) = 0, \tag{7.18}$$

where $\epsilon_{\mu\nu\rho\sigma}$ is the four dimensional Levi-Civita symbol. Upon taking the four

dimensional curl of (7.16), we obtain the generalized induction equation

$$e\left[\partial^\mu\left(u_\lambda \mathcal{F}^{\star\nu\lambda}\right)-\partial^\nu\left(u_\lambda \mathcal{F}^{\star\mu\lambda}\right)\right]-\left[\partial^\mu\left(\frac{J_\lambda}{n}\mathcal{F}^{\dagger\nu\lambda}\right)\right.$$
$$\left.-\partial^\nu\left(\frac{J_\lambda}{n}\mathcal{F}^{\dagger\mu\lambda}\right)\right]-\frac{m_-}{m}\left[\partial^\mu T_+\partial^\nu\left(\frac{\sigma_+}{n}\right)-\partial^\nu T_+\partial^\mu\left(\frac{\sigma_+}{n}\right)\right]$$
$$+\frac{m_+}{m}\left[\partial^\mu T_-\partial^\nu\left(\frac{\sigma_-}{n}\right)-\partial^\nu T_-\partial^\mu\left(\frac{\sigma_-}{n}\right)\right]=0. \tag{7.19}$$

Next, upon combining (7.14) and (7.15) we obtain equations for the canonical momenta [165] of each species

$$u_{\pm_\nu}\left(\partial^\mu \wp_\pm{}^\nu-\partial^\nu \wp_\pm{}^\mu\right)+T_\pm\partial^\mu\left(\frac{\sigma_\pm}{n}\right)=0,$$

where $\wp_\pm{}^\nu = h_\pm u_\pm{}^\nu \pm eA^\nu$. Several simplifications have been proposed to make these equations tractable;[134, 135] e.g., the assumption of $\Delta h = 0$ (i.e., $h_+ = (m_+/m)h$ and $h_- = (m_-/m)h$) and/or the usage of the velocity norm condition $u_\mu u^\mu = 1$ with (7.2) instead of (7.1). The latter condition requires $J_\mu J^\mu = 0$ to be consistent with (7.1) (referred to as the "break down condition" in Ref. [134]). Such a simplified model has recently come into usage.[67, 17, 19] Imposing $\Delta h = 0$ on the action (7.7) and/or replacing (7.1) by $u_\mu u^\mu = 1$ and $J_\mu J^\mu = 0$, this simplified model is directly obtained from the AP.

7.3 Covariant bracket action principle

Now we construct our covariant action principle. To this end we define a kinetic momentum $\mathfrak{m}^\nu = nhu^\nu$ and a generalized momentum $\mathfrak{m}^{\star\nu} = \mathfrak{m}^\nu + (\Delta h/e)J^\nu$. Then (7.8) and (7.9) can then be viewed as the Clebsch

representations for $\mathfrak{m}^{\star\nu}$ and $A^{\star\nu}$. The reason for introducing these new field variables is that the action (7.7) takes a beautiful form in terms of them:

$$S = \int \left[\frac{\mathfrak{m}^{\star\nu}\mathfrak{m}_\nu}{2nh} + \sum_{\pm} \frac{1}{2}(p_\pm - \rho_\pm) \right. \\ \left. -\frac{1}{4}(\partial^\mu A^{\star\nu} - \partial^\nu A^{\star\mu})(\partial_\mu A_\nu - \partial_\nu A_\mu) \right] \mathrm{d}^4x. \tag{7.20}$$

Interestingly, upon letting $\mathfrak{m}^{\star\nu} \to \mathfrak{m}^\nu$ and $A^{\star\nu} \to A^\nu$, the action (7.20) becomes identical to the recently proposed relativistic MHD action of Ref. [73]. When the simplification $\Delta h \to 0$ is imposed, $\mathfrak{m}^{\star\nu}$ becomes the kinetic momentum and $A^{\star\nu}$ is decoupled from the kinetic momentum (the nonrelativistic version of such a vector potential was previously proposed for nonrelativistic IMHD [159] and XMHD [1, 158]). In other words, the difference of the thermal inertiae between species (i.e. Δh) intertwines the kinetic momentum field and the EM field. Since the nonrelativistic limit ($h_+ \to m_+c^2$ and $h_- \to m_-c^2$) results in $\Delta h \to 0$, such a coupling is distinctive of the relativistic two-fluid plasma.

For our covariant action it is convenient to use the Clebsch variables

$$z = (n,\, \phi,\, \sigma_\pm,\, \eta_\pm,\, \lambda_\pm,\, \varphi_\pm)$$

as the independent variables of the action (7.20). With these variables all of the dynamical equations (7.4), (7.5), (7.6), (7.10), (7.11), and (7.13) are derived from the least AP (i.e. $\delta S = 0$). In terms of z we can simply restate the AP of Sec. 7.2 as a canonical covariant bracket version of the formalism of Refs. [166, 73]. A canonical Poisson bracket is defined for functionals F and

G as

$$\{F,\, G\}_{\text{canonical}} = \int \frac{\delta F}{\delta z} \mathcal{J}_{\text{c}} \frac{\delta G}{\delta z}\, \mathrm{d}^4x = \int \left[\frac{\delta F}{\delta \phi}\frac{\delta G}{\delta n} - \frac{\delta G}{\delta \phi}\frac{\delta F}{\delta n} \right. \tag{7.21}$$
$$\left. + \sum_{\pm} \left(\frac{\delta F}{\delta \eta_\pm}\frac{\delta G}{\delta \sigma_\pm} - \frac{\delta G}{\delta \eta_\pm}\frac{\delta F}{\delta \sigma_\pm} + \frac{\delta F}{\delta \varphi_\pm}\frac{\delta G}{\delta \lambda_\pm} - \frac{\delta G}{\delta \varphi_\pm}\frac{\delta F}{\delta \lambda_\pm} \right) \right] \mathrm{d}^4x,$$

where $\mathcal{J}_{\text{c}}$ is the symplectic matrix and $\delta F/\delta z$ denotes the functional derivative obtained by linearizing a functional, e.g.

$$\delta F = \int \delta n\, \frac{\delta F}{\delta n}\, \mathrm{d}^4x\,. \tag{7.22}$$

(See Ref. [182] for review.) Since $\mathcal{J}_{\text{c}}$ is non-degenerate, with (n, ϕ), $(\sigma_\pm, \eta_\pm)$, and $(\lambda_\pm, \varphi_\pm)$ being canonically conjugate pairs, the least AP is equivalent to a bracket AP, i.e., $\{F[z],\, S\}_{\text{canonical}} = 0$ where $F[z]$ is an arbitrary functional of z, is equivalent to $\delta S = 0$.

Transformation to new "physical" independent variables defined by

$$\bar{z} = (n, \sigma_\pm, \mathfrak{m}^{\star\nu}, \mathcal{F}^{\star\mu\nu})$$

yields a noncanonical covariant bracket because the $\bar{z}$ are not canonical variables. To transform the bracket of (7.21) we consider functionals that satisfy

$\bar{F}[\bar{z}] = F[z]$, and calculate functional derivatives by the chain rules:

$$\begin{aligned}
\frac{\delta F}{\delta n} &= \frac{\delta \bar{F}}{\delta n} + \frac{\delta \bar{F}}{\delta \mathfrak{m}^{\star\nu}} \partial^\nu \phi \\
&\quad + \frac{2m_- \sigma_+}{men^2} \partial^\mu \left(\frac{\delta \bar{F}}{\delta \mathcal{F}^{\star\mu\nu}} \partial^\nu \eta_+ \right) + \frac{2m_- \lambda_+}{men^2} \partial^\mu \left(\frac{\delta \bar{F}}{\delta \mathcal{F}^{\star\mu\nu}} \partial^\nu \varphi_+ \right) \\
&\quad - \frac{2m_+ \sigma_-}{men^2} \partial^\mu \left(\frac{\delta \bar{F}}{\delta \mathcal{F}^{\star\mu\nu}} \partial^\nu \eta_- \right) - \frac{2m_+ \lambda_-}{men^2} \partial^\mu \left(\frac{\delta \bar{F}}{\delta \mathcal{F}^{\star\mu\nu}} \partial^\nu \varphi_- \right)
\end{aligned}$$

$$\begin{aligned}
\frac{\delta F}{\delta \phi} &= -\partial^\nu \left(n \frac{\delta \bar{F}}{\delta \mathfrak{m}^{\star\nu}} \right), \\
\frac{\delta F}{\delta \sigma_\pm} &= \frac{\delta \bar{F}}{\delta \sigma_\pm} + \frac{\delta \bar{F}}{\delta \mathfrak{m}^{\star\nu}} \partial^\nu \eta_\pm \mp \frac{2m_\mp}{men} \partial^\mu \left(\frac{\delta \bar{F}}{\delta \mathcal{F}^{\star\mu\nu}} \partial^\nu \eta_\pm \right), \\
\frac{\delta F}{\delta \eta_\pm} &= -\partial^\nu \left(\sigma_\pm \frac{\delta \bar{F}}{\delta \mathfrak{m}^{\star\nu}} \right) \pm \frac{2m_\mp}{me} \partial^\mu \left(\frac{\delta \bar{F}}{\delta \mathcal{F}^{\star\mu\nu}} \partial^\nu \frac{\sigma_\pm}{n} \right), \\
\frac{\delta F}{\delta \lambda_\pm} &= \frac{\delta \bar{F}}{\delta \mathfrak{m}^{\star\nu}} \partial^\nu \varphi_\pm \mp \frac{2m_\mp}{men} \partial^\mu \left(\frac{\delta \bar{F}}{\delta \mathcal{F}^{\star\mu\nu}} \partial^\nu \varphi_\pm \right), \\
\frac{\delta F}{\delta \varphi_\pm} &= -\partial^\nu \left(\lambda_\pm \frac{\delta \bar{F}}{\delta \mathfrak{m}^{\star\nu}} \right) \pm \frac{2m_\mp}{me} \partial^\mu \left(\frac{\delta \bar{F}}{\delta \mathcal{F}^{\star\mu\nu}} \partial^\nu \frac{\lambda_\pm}{n} \right)
\end{aligned}$$

Substituting these into (7.21) gives the following noncanonical Poisson bracket:

$$\begin{aligned}
\{\bar{F},\,\bar{G}\}_{\mathrm{XMHD}} &= -\int\Bigg\{ n\left(\frac{\delta\bar{G}}{\delta\mathfrak{m}^{\star\nu}}\partial^{\nu}\frac{\delta\bar{F}}{\delta n}-\frac{\delta\bar{F}}{\delta\mathfrak{m}^{\star\nu}}\partial^{\nu}\frac{\delta\bar{G}}{\delta n}\right)\\
&+ \mathfrak{m}^{\star\nu}\left(\frac{\delta\bar{G}}{\delta\mathfrak{m}^{\star\mu}}\partial^{\mu}\frac{\delta\bar{F}}{\delta\mathfrak{m}^{\star\nu}}-\frac{\delta\bar{F}}{\delta\mathfrak{m}^{\star\mu}}\partial^{\mu}\frac{\delta\bar{G}}{\delta\mathfrak{m}^{\star\nu}}\right)\\
&+ \sum_{\pm}\Bigg[\sigma_{\pm}\left(\frac{\delta\bar{G}}{\delta\mathfrak{m}^{\star\nu}}\partial^{\nu}\frac{\delta\bar{F}}{\delta\sigma_{\pm}}-\frac{\delta\bar{F}}{\delta\mathfrak{m}^{\star\nu}}\partial^{\nu}\frac{\delta\bar{G}}{\delta\sigma_{\pm}}\right)\\
&\quad \pm\frac{2m_{\mp}}{me}\left(\frac{\delta\bar{F}}{\delta\sigma_{\pm}}\partial^{\mu}\frac{\delta\bar{G}}{\delta\mathcal{F}^{\star\mu\nu}}-\frac{\delta\bar{G}}{\delta\sigma_{\pm}}\partial^{\mu}\frac{\delta\bar{F}}{\delta\mathcal{F}^{\star\mu\nu}}\right)\partial^{\nu}\frac{\sigma_{\pm}}{n}\Bigg]\\
&+ 2\left(\frac{\delta\bar{F}}{\delta\mathfrak{m}^{\star\lambda}}\partial^{\mu}\frac{\delta\bar{G}}{\delta\mathcal{F}^{\star\mu\nu}}-\frac{\delta\bar{G}}{\delta\mathfrak{m}^{\star\lambda}}\partial^{\mu}\frac{\delta\bar{F}}{\delta\mathcal{F}^{\star\mu\nu}}\right)\mathcal{F}^{\star\nu\lambda}\\
&+ \frac{4}{ne}\left(\partial^{\mu}\frac{\delta\bar{F}}{\delta\mathcal{F}^{\star\mu\nu}}\right)\left(\partial^{\lambda}\frac{\delta\bar{G}}{\delta\mathcal{F}^{\star\lambda\kappa}}\right)\mathcal{F}^{\dagger\kappa\nu}\Bigg\}\,\mathrm{d}^4x\,. \qquad (7.23)
\end{aligned}$$

The fluid parts (the first three terms) of (7.23) correspond to the covariant Poisson bracket for the neutral fluid given in Ref. [166]. Next, in order to use this bracket in a variational sense, the action (7.20) is considered to be the functional of $(n,\sigma_{\pm},\mathfrak{m}^{\star\nu},\mathcal{F}^{\star\mu\nu})$, i.e. $\bar{S}[\bar{z}]$, and its functional derivatives are calculated as

$$\frac{\delta\bar{S}}{\delta\mathfrak{m}^{\star\nu}}=u_{\nu},\quad \frac{\delta\bar{S}}{\delta\mathcal{F}^{\star\mu\nu}}=-\frac{1}{2}\mathcal{F}_{\mu\nu},\quad \frac{\delta\bar{S}}{\delta\sigma_{\pm}}=-\frac{\partial\rho_{\pm}}{\partial\sigma_{\pm}}$$

$$\begin{aligned}
\frac{\delta\bar{S}}{\delta n} &= h_{+}\frac{m_{-}}{men}J_{\nu}\left(u^{\nu}+\frac{m_{-}}{men}J^{\nu}\right)-h_{-}\frac{m_{+}}{men}J_{\nu}\left(u^{\nu}-\frac{m_{+}}{men}J^{\nu}\right)\\
&\quad -\frac{\partial\rho_{+}}{\partial n}-\frac{\partial\rho_{-}}{\partial n}+\frac{\Delta h}{ne}J_{\nu}u^{\nu}+\frac{h^{\dagger}}{n^2e^2}J_{\nu}J^{\nu}.
\end{aligned}$$

Then equations (7.4), (7.5), (7.14), and (7.19) follow from $\{\bar{F}[\bar{z}],\,\bar{S}\}=0$ for all $\bar{F}$.

Here we must remark that the equations obtained from the bracket action principle are not closed unless (7.18) is imposed. Although (7.18) is automatically satisfied by the Clebsch variable definition of $\mathcal{F}^{\star\mu\nu}$, it does not emerge from the bracket AP. Therefore, the bracket AP, only by itself, does not give the closed set of equations. This is a marked difference between a Hamiltonian formalism of nonrelativistic MHD;[181] although $\nabla \cdot \mathbf{B} = \mathbf{0}$ is not derived from the Hamiltonian equation, the obtained equations are closed even if $\nabla \cdot \mathbf{B} \neq \mathbf{0}$. On the other hand, in the relativistic case, if (7.18) is abandoned, we lose $\partial_t \mathbf{B} = -\mathbf{c}\nabla \times \mathbf{E}$ as well.

There may be two remedies for this problem. One is to define a Faraday tensor that builds-in the Ohm's law (7.16) and consider (7.18) as a dynamical equation of the new Faraday tensor [14, 73]. This strategy, however, is difficult because the Ohm's law (7.16) is more complicated than that of relativistic MHD, and then it is hard to formulate the appropriate Faraday tensor. A second approach is to transform $\mathcal{F}^{\star\mu\nu}$ to $A^{\star\mu}$ so as to make the bracket action principle yield Ohm's law instead of the induction equation. To write the bracket of (7.23) in terms of $A^{\star\mu}$ we consider the functional chain rule to relate functional derivatives with respect to $\mathcal{F}^{\star\mu\nu}$ with those with respect to $A^{\star\mu}$, i.e.

$$2\partial_\nu \frac{\delta \bar{G}}{\delta \mathcal{F}^{\star\mu\nu}} = \frac{\delta \bar{G}}{\delta A^{\star\mu}}. \tag{7.24}$$

Using (7.24), one can eliminate $\mathcal{F}^{\star\mu\nu}$ from the Poisson bracket (7.23) while introducing the variable $A^{\star\mu}$. This will give a bracket where the Ohm's law

(7.16) is obtained direct. The transformation (7.24) yields

$$\begin{aligned}
\{\bar{F},\,\bar{G}\}_{\text{XMHD}} &= -\int\Bigg\{ n\left(\frac{\delta\bar{G}}{\delta\mathfrak{m}^{\star\nu}}\partial^{\nu}\frac{\delta\bar{F}}{\delta n}-\frac{\delta\bar{F}}{\delta\mathfrak{m}^{\star\nu}}\partial^{\nu}\frac{\delta\bar{G}}{\delta n}\right)\\
&+ \mathfrak{m}^{\star\nu}\left(\frac{\delta\bar{G}}{\delta\mathfrak{m}^{\star\mu}}\partial^{\mu}\frac{\delta\bar{F}}{\delta\mathfrak{m}^{\star\nu}}-\frac{\delta\bar{F}}{\delta\mathfrak{m}^{\star\mu}}\partial^{\mu}\frac{\delta\bar{G}}{\delta\mathfrak{m}^{\star\nu}}\right)\\
&+ \sum_{\pm}\Bigg[\sigma_{\pm}\left(\frac{\delta\bar{G}}{\delta\mathfrak{m}^{\star\nu}}\partial^{\nu}\frac{\delta\bar{F}}{\delta\sigma_{\pm}}-\frac{\delta\bar{F}}{\delta\mathfrak{m}^{\star\nu}}\partial^{\nu}\frac{\delta\bar{G}}{\delta\sigma_{\pm}}\right)\\
&\quad \mp\frac{m_{\mp}}{me}\left(\frac{\delta\bar{F}}{\delta\sigma_{\pm}}\frac{\delta\bar{G}}{\delta A^{\star\nu}}-\frac{\delta\bar{G}}{\delta\sigma_{\pm}}\frac{\delta\bar{F}}{\delta A^{\star\nu}}\right)\partial^{\nu}\frac{\sigma_{\pm}}{n}\Bigg]\\
&+ \left(\frac{\delta\bar{G}}{\delta\mathfrak{m}^{\star\nu}}\frac{\delta\bar{F}}{\delta A^{\star\mu}}-\frac{\delta\bar{F}}{\delta\mathfrak{m}^{\star\nu}}\frac{\delta\bar{G}}{\delta A^{\star\mu}}\right)\mathcal{F}^{\star\mu\nu}\\
&- \frac{1}{ne}\frac{\delta\bar{F}}{\delta A^{\star\mu}}\frac{\delta\bar{G}}{\delta A^{\star\nu}}\mathcal{F}^{\dagger\mu\nu}\Bigg\}\mathrm{d}^4x. \qquad (7.25)
\end{aligned}$$

Ohm's law follows from $\{A^{\star\alpha},\,\bar{S}\}_{\text{XMHD}}=0$ with $\delta\bar{S}/\delta A^{\star\mu}=J_{\mu}$; the other equations are unaltered so the system is closed.

The noncanonical bracket of (7.25) has the form

$$\{\bar{F},\,\bar{G}\}_{\text{XMHD}}=\int\frac{\delta\bar{F}}{\delta\bar{z}}\,\mathcal{J}\,\frac{\delta\bar{G}}{\delta\bar{z}}\mathrm{d}^4x\,,$$

with a new Poisson operator $\mathcal{J}$. However, because the transformation $z\mapsto\bar{z}$ is not invertible, the Poisson operator $\mathcal{J}$ is degenerate. Since the bracket AP, $\{\bar{F}[\bar{z}],\,\bar{S}\}=0$, is equivalent to $\mathcal{J}\delta\bar{S}/\delta\bar{z}=0$, because of this degeneracy it is no longer true that $\mathcal{J}\,\delta\bar{S}/\delta\bar{z}=0$ is identical to $\delta S=0$. In this way the constraints of the action (7.7) are transferred to the degeneracy of the Poisson bracket.[166, 73]

Before closing this section, let us make a remark about the alternative expression of EM field. The Faraday tensor may be decomposed as $\mathcal{F}^{\mu\nu} = \epsilon^{\mu\nu\lambda\sigma} b_\lambda u_\sigma + u^\mu e^\nu - u^\nu e^\mu$ with a magnetic field like four vector $b^\nu = u_\mu \epsilon^{\mu\nu\lambda\sigma} \mathcal{F}_{\lambda\sigma}$ and a electric field like four vector $e^\nu = u_\mu \mathcal{F}^{\mu\nu}$. [150, 14, 201] This decomposition is especially useful in the relativistic MHD because the standard Ohm's law is equivalent to $e^\nu = 0$, and thus EM field is concisely expressed only by b^ν. In the context of action principle, D'Avignon *et al.* formulated the bracket AP for the relativistic MHD using b^ν. [73] It may be possible to reformulate the relativistic XMHD action principle in terms of b^ν instead of $\mathcal{F}^{\mu\nu}$. The key is how we define a generalized four vector (let us call $b^{\star\nu}$) that incorporates inertia effect in the similar way as $\mathcal{F}^{\mu\nu} \to \mathcal{F}^{\star\mu\nu}$. Recently, such a generalization of b^ν has been proposed by Pegoraro. [201] Formulation of the action principle with $b^{\star\nu}$ and the unification with the MHD action principle [73] will be a future work.

7.4 Limits to reduced models

In this section we show how to reduce the bracket AP to obtain APs for unknown relativistic models, with known relativistic counterparts.

First consider the electron-ion plasma, where now the species labels $+$ and $-$ are replaced by i and e, respectively. Defining electron to ion mass ratio $\mu := m_\mathrm{e}/m_\mathrm{i} \ll 1$, we approximate $m_\mathrm{e}/m \sim \mu$, $m_\mathrm{i}/m \sim 1$. The ion and

electron four-velocities become

$$u_{\rm i}^\nu = u^\nu + \frac{\mu J^\nu}{ne}, \quad u_{\rm e}^\nu = u^\nu - \frac{J^\nu}{ne}\,,$$

while the enthalpy variables reduce to $\Delta h \sim \mu h_{\rm i} - h_{\rm e}$, $h^\dagger \sim \mu^2 h_{\rm i} + h_{\rm e}$, and $\Delta h^\sharp \sim \mu^3 h_{\rm i} - h_{\rm e}$, and the generalized vectors become

$$\mathfrak{m}^{\star\nu} = nhu^\nu + \frac{1}{e}(\mu h_{\rm i} - h_{\rm e})J^\nu \tag{7.26}$$

$$A^{\star\nu} = A^\nu + \frac{1}{e}(\mu h_{\rm i} - h_{\rm e})u^\nu + \frac{1}{ne^2}(\mu^2 h_{\rm i} + h_{\rm e})J^\nu \tag{7.27}$$

$$A^{\dagger\nu} = A^\nu - \frac{1}{e}(\mu^2 h_{\rm i} + h_{\rm e})u^\nu - \frac{1}{ne^2}(\mu^3 h_{\rm i} - h_{\rm e})J^\nu. \tag{7.28}$$

Next, in this approximation the noncanonical Poisson bracket (7.25) becomes

$$\begin{aligned}
\left\{\bar{F},\,\bar{G}\right\}_{\rm XMHD} \;=\; & -\int\Bigg\{ n\left(\frac{\delta\bar{G}}{\delta\mathfrak{m}^{\star\nu}}\partial^\nu\frac{\delta\bar{F}}{\delta n} - \frac{\delta\bar{F}}{\delta\mathfrak{m}^{\star\nu}}\partial^\nu\frac{\delta\bar{G}}{\delta n}\right) \\
& + \;\mathfrak{m}^{\star\nu}\left(\frac{\delta\bar{G}}{\delta\mathfrak{m}^{\star\mu}}\partial^\mu\frac{\delta\bar{F}}{\delta\mathfrak{m}^{\star\nu}} - \frac{\delta\bar{F}}{\delta\mathfrak{m}^{\star\mu}}\partial^\mu\frac{\delta\bar{G}}{\delta\mathfrak{m}^{\star\nu}}\right) \\
& + \;\sigma_{\rm i}\left(\frac{\delta\bar{G}}{\delta\mathfrak{m}^{\star\nu}}\partial^\nu\frac{\delta\bar{F}}{\delta\sigma_{\rm i}} - \frac{\delta\bar{F}}{\delta\mathfrak{m}^{\star\nu}}\partial^\nu\frac{\delta\bar{G}}{\delta\sigma_{\rm i}}\right) \\
& - \;\frac{\mu}{e}\left(\frac{\delta\bar{F}}{\delta\sigma_{\rm i}}\frac{\delta\bar{G}}{\delta A^{\star\nu}} - \frac{\delta\bar{G}}{\delta\sigma_{\rm i}}\frac{\delta\bar{F}}{\delta A^{\star\nu}}\right)\partial^\nu\left(\frac{\sigma_{\rm i}}{n}\right) \\
& + \;\sigma_{\rm e}\left(\frac{\delta\bar{G}}{\delta\mathfrak{m}^{\star\nu}}\partial^\nu\frac{\delta\bar{F}}{\delta\sigma_{\rm e}} - \frac{\delta\bar{F}}{\delta\mathfrak{m}^{\star\nu}}\partial^\nu\frac{\delta\bar{G}}{\delta\sigma_{\rm e}}\right) \\
& + \;\frac{1}{e}\left(\frac{\delta\bar{F}}{\delta\sigma_{\rm e}}\frac{\delta\bar{G}}{\delta A^{\star\nu}} - \frac{\delta\bar{G}}{\delta\sigma_{\rm e}}\frac{\delta\bar{F}}{\delta A^{\star\nu}}\right)\partial^\nu\left(\frac{\sigma_{\rm e}}{n}\right) \\
& + \;\left(\frac{\delta\bar{G}}{\delta\mathfrak{m}^{\star\nu}}\frac{\delta\bar{F}}{\delta A^{\star\mu}} - \frac{\delta\bar{F}}{\delta\mathfrak{m}^{\star\nu}}\frac{\delta\bar{G}}{\delta A^{\star\mu}}\right)\mathcal{F}^{\star\mu\nu} \\
& - \;\frac{1}{ne}\frac{\delta\bar{F}}{\delta A^{\star\mu}}\frac{\delta\bar{G}}{\delta A^{\star\nu}}\mathcal{F}^{\dagger\mu\nu}\Bigg\}\mathrm{d}^4x.
\end{aligned} \tag{7.29}$$

Using the approximate bracket of (7.29) with a reduced action $\bar{S}$, the covariant AP produces the continuity equation (7.4) along with the following system of equations:

$$\partial_\nu \Bigg[nhu^\mu u^\nu + \frac{1}{e}(\mu h_\mathrm{i} - h_\mathrm{e})(u^\mu J^\nu + J^\mu u^\nu) + \frac{1}{ne^2}(\mu^2 h_\mathrm{i} + h_\mathrm{e}) J^\mu J^\nu \Bigg] = \partial^\mu p + J_\nu \mathcal{F}^{\mu\nu}, \tag{7.30}$$

$$e u_\nu \mathcal{F}^{\star\mu\nu} - \frac{J_\nu}{n} \mathcal{F}^{\dagger\mu\nu} - \mu T_\mathrm{i} \partial^\mu \left(\frac{\sigma_\mathrm{i}}{n} \right) + T_\mathrm{e} \partial^\mu \left(\frac{\sigma_\mathrm{e}}{n} \right) = 0, \tag{7.31}$$

$$\partial_\nu \left[\sigma_\mathrm{i} \left(u^\nu + \frac{\mu J^\nu}{ne} \right) \right] = 0, \tag{7.32}$$

$$\partial_\nu \left[\sigma_\mathrm{e} \left(u^\nu - \frac{J^\nu}{ne} \right) \right] = 0. \tag{7.33}$$

Next consider a further reduction using $\mu \to 0$, meaning the electron rest mass inertia is discarded. This limit gives HMHD, which is well known in the nonrelativistic case but has not been proposed in the relativistic case. The terms including h_e must not be ignored when the electron thermal inertia is greater than the rest mass inertia (i.e., $h_\mathrm{e} \gg m_\mathrm{e} c^2$). For example, the temperature of electrons in an accretion disk near a black hole can be more than $10^{11}\,\mathrm{K}$.[263] Then, the thermal inertia h_e is on the order of $100\, m_\mathrm{e} c^2$, estimated by an equation of state for an ideal gas $h_\mathrm{e} = m_\mathrm{e} c^2 + [\Gamma/(\Gamma - 1)] T_\mathrm{e}$ with a specific heat ratio $\Gamma = 4/3$.[243] In such a case, the h_e terms are not negligible.

Let us employ the following normalizations:

$$\partial^\nu \to L^{-1}\partial^\nu, \quad n \to n_0 n, \quad T_{\rm i,e} \to mc^2 T_{\rm i,e},$$
$$\sigma_{\rm i,e} \to n_0 \sigma_{\rm i,e}, \quad \mathcal{F}^{\mu\nu} \to \sqrt{n_0 mc^2}\,\mathcal{F}^{\mu\nu},$$

using a typical scale length L and density scale n_0. Then the generalized momentum density and vector potential are normalized as

$$\mathfrak{m}^{\star\nu} \to n_0 mc^2 \left[nhu^\nu - d_{\rm i} h_{\rm e} J^\nu \right]$$
$$A^{\star\nu} \to L\sqrt{n_0 mc^2} \left[A^\nu - d_{\rm i} h_{\rm e} u^\nu + {d_{\rm i}}^2 h_{\rm e} \frac{J^\nu}{n} \right],$$

where $\sqrt{(mc^2)/(e^2 n_0 L^2)} \sim \sqrt{(m_{\rm i} c^2)/(e^2 n_0 L^2)} = c/(\omega_{\rm i} L) = d_{\rm i}$ is the normalized ion skin depth, and the normalized Poisson bracket becomes

$$\begin{aligned}
\left\{ \bar{F},\, \bar{G} \right\}_{\rm HMHD} &= -\int \left\{ n \left(\frac{\delta \bar{G}}{\delta \mathfrak{m}^{\star\nu}} \partial^\nu \frac{\delta \bar{F}}{\delta n} - \frac{\delta \bar{F}}{\delta \mathfrak{m}^{\star\nu}} \partial^\nu \frac{\delta \bar{G}}{\delta n} \right) \right. \\
&+ \mathfrak{m}^{\star\nu} \left(\frac{\delta \bar{G}}{\delta \mathfrak{m}^{\star\mu}} \partial^\mu \frac{\delta \bar{F}}{\delta \mathfrak{m}^{\star\nu}} - \frac{\delta \bar{F}}{\delta \mathfrak{m}^{\star\mu}} \partial^\mu \frac{\delta \bar{G}}{\delta \mathfrak{m}^{\star\nu}} \right) \\
&+ \sigma_{\rm i} \left(\frac{\delta \bar{G}}{\delta \mathfrak{m}^{\star\nu}} \partial^\nu \frac{\delta \bar{F}}{\delta \sigma_{\rm i}} - \frac{\delta \bar{F}}{\delta \mathfrak{m}^{\star\nu}} \partial^\nu \frac{\delta \bar{G}}{\delta \sigma_{\rm i}} \right) \\
&+ \sigma_{\rm e} \left(\frac{\delta \bar{G}}{\delta \mathfrak{m}^{\star\nu}} \partial^\nu \frac{\delta \bar{F}}{\delta \sigma_{\rm e}} - \frac{\delta \bar{F}}{\delta \mathfrak{m}^{\star\nu}} \partial^\nu \frac{\delta \bar{G}}{\delta \sigma_{\rm e}} \right) \\
&- 2d_{\rm i} \left(\frac{\delta \bar{F}}{\delta \sigma_{\rm e}} \partial^\mu \frac{\delta \bar{G}}{\delta \mathcal{F}^{\star\mu\nu}} - \frac{\delta \bar{G}}{\delta \sigma_{\rm e}} \partial^\mu \frac{\delta \bar{F}}{\delta F^{\star\mu\nu}} \right) \partial^\nu \frac{\sigma_{\rm e}}{n} \\
&+ 2 \left(\frac{\delta \bar{F}}{\delta \mathfrak{m}^{\star\lambda}} \partial^\mu \frac{\delta \bar{G}}{\delta \mathcal{F}^{\star\mu\nu}} - \frac{\delta \bar{G}}{\delta \mathfrak{m}^{\star\lambda}} \partial^\mu \frac{\delta \bar{F}}{\delta \mathcal{F}^{\star\mu\nu}} \right) \mathcal{F}^{\star\nu\lambda} \\
&+ \left. \frac{4d_{\rm i}}{n} \left(\partial^\mu \frac{\delta \bar{F}}{\delta \mathcal{F}^{\star\mu\nu}} \right) \left(\partial^\lambda \frac{\delta \bar{G}}{\delta \mathcal{F}^{\star\lambda\kappa}} \right) \mathcal{F}^{\star\kappa\nu} \right\} {\rm d}^4 x. \qquad (7.34)
\end{aligned}$$

The bracket AP with this scaling gives the following equations:

$$\partial_\nu \left[nhu^\mu u^\nu - d_\mathrm{i} h_\mathrm{e} (u^\mu J^\nu + J^\mu u^\nu) + d_\mathrm{i}^2 \frac{h_\mathrm{e}}{n} J^\mu J^\nu \right] = \partial^\mu p + J^\nu \mathcal{F}^\mu{}_\nu, \tag{7.35}$$

$$\left(u_\nu - d_\mathrm{i} \frac{J_\nu}{n} \right) \mathcal{F}^{\star\mu\nu} = -d_\mathrm{i} T_\mathrm{e} \partial^\mu \left(\frac{\sigma_\mathrm{e}}{n} \right) \tag{7.36}$$

$$\partial_\nu \left(\sigma_\mathrm{i} u^\nu \right) = 0, \tag{7.37}$$

$$\partial_\nu \left[\sigma_\mathrm{e} \left(u^\nu - d_\mathrm{i} \frac{J^\nu}{n} \right) \right] = 0. \tag{7.38}$$

Note, this relativistic HMHD is different from usual nonrelativistic HMHD. In Sec. 7.5 we explore some consequences of this.

Next, upon taking the limit $d_\mathrm{i} \to 0$, we obtain relativistic MHD.[150, 80, 14] The Poisson bracket for the relativistic MHD obtained by this reduction is different from the one proposed by D'Avignon *et al.* in Ref. [73] because a magnetic field like four vector b^ν was used there instead of A^μ. The relation between the two brackets has yet to be clarified.

The same reduction procedure (from XMHD to MHD) is applicable for the constrained least AP of Sec. 7.2. For example, if we ignore the electron rest mass, the velocities of each species are reduced as ${u_+}^\mu \to u^\mu$ and ${u_-}^\mu \to u^\mu - J^\mu/ne$. Similarly, the entropy and Lagrangian label constraints are reduced accordingly. With these reductions the constrained least AP gives the relativistic HMHD equations. We note, the renormalization method used in Ref. [259] to derive AP for MHD is also applicable for relativistic HMHD.

There are formalisms alternative to the one we presented that employ either Ohm's law or the induction equation *per se* as a constraint for non-

relativistic [253] and relativistic [29, 30] MHD. However, these formulations cannot be reduced from the constrained action (7.7). Whereas the physical meaning of the constraints in (7.7) is obvious, embedding the Ohm's law as a constraint is unnatural and arbitrary. Furthermore, the EM field cannot be expressed by Clebsch potentials from the AP with the Ohm's law constraint, unlike the case for our formulation where this emerges naturally in (7.9).

7.5 Relativistic Collisionless Reconnection

In nonrelativistic MHD with the inclusion of electron (rest mass) inertia (i.e., IMHD), a consequence of electron inertia is the violation of the frozen-in magnetic flux condition (see Sec. 4.3), and instead, a flux determined by a generalized field is conserved.[159] Such an electron inertia effect was suggested as a mechanism for a collisionless magnetic reconnection[198] and has now been widely studied. However, nonrelativistic HMHD does satisfy the frozen-in magnetic flux condition because the electron inertia is discarded by the $\mu \to 0$ limit. Hence, there is no direct mechanism causing collisionless reconnection in nonrelativistic HMHD.

On the other hand, in relativistic XMHD, there are two kinds of electron inertiae: one from the electron rest mass $m_{\rm e}$ and the other from the electron temperature $h_{\rm e}$. The $\mu \to 0$ limit corresponds to neglecting the former and keeping the latter. Even though the former is small, the latter may not be ignorable when electron temperature is large enough. The latter effect still allows for the violation of the frozen-in magnetic flux con-

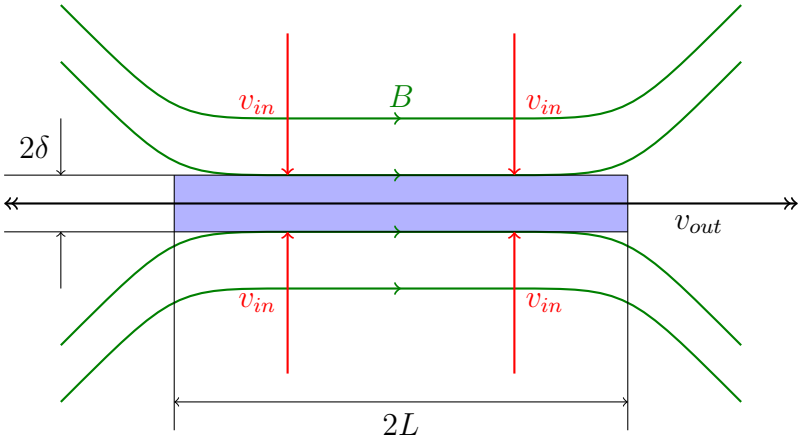

Figure 7.1: Geometry of Sweet-Parker model.

dition. Such a collisionless reconnection mechanism was previously proposed by Comisso *et al.* using a Sweet–Parker model in the context of relativistic XMHD.[67] Here we find an alternative flux given by the generalized vector potential $A^{\star\nu} \to A^\nu - d_\mathrm{i} h_\mathrm{e} u^\nu + d_\mathrm{i}^2 (h_\mathrm{e}/n) J^\nu$ to be frozen-in.

Let us stress the difference between our present study and the pair plasma study by Comisso *et al.*[67] In the latter, the relativistic electron–positron plasma with the assumption $\Delta h = 0$ was considered. For HMHD, however, this $\Delta h = 0$ assumption removes the aforementioned collisionless reconnection mechanism. From (7.27) and (7.28), we find $A^{\star\mu} \to A^\mu$ and $A^{\dagger\mu} \to A^\mu$ when we take both $\Delta h = 0$ and $\mu = 0$, so there is no longer the alternative frozen-in flux in HMHD.

To make this statement more explicit, we write the relativistic HMHD induction equation in a reference frame moving with the center-of-mass (ion)

velocity. When the electron fluid is homentropic, the right-hand side of (7.36) vanishes. Taking a curl of a spatial component of (7.36), we obtain the induction equation in the reference frame,

$$\partial_t \mathbf{B}^\star + \nabla \times (\mathbf{B}^\star \times \widetilde{\mathbf{v}}_\mathrm{e}) = \mathbf{0}, \tag{7.39}$$

where

$$\mathbf{B}^\star = \mathbf{B} + \nabla \times \left(-\mathbf{d}_\mathrm{i}\mathbf{h}_\mathrm{e}\gamma\mathbf{v} + \mathbf{d}_\mathrm{i}^\mathbf{2}\mathbf{h}_\mathrm{e}\frac{\mathbf{J}}{\mathbf{n}} \right) \tag{7.40}$$

and

$$\widetilde{\mathbf{v}}_\mathrm{e} = \left(\mathbf{v} - \mathbf{d}_\mathrm{i}\frac{\mathbf{J}}{\gamma\mathbf{n}} \right) \left(1 - d_\mathrm{i}\frac{\rho_q}{\gamma n} \right)^{-1}. \tag{7.41}$$

Here, $\widetilde{\mathbf{v}}_\mathrm{e}$ is a modified electron velocity that becomes the electron velocity $\mathbf{v}_\mathrm{e}$ in the nonrelativistic limit $\gamma \to 1$ and $\rho_q \to 0$. Evidently from (7.39) and (7.40), the magnetic field $\mathbf{B}$ is no longer frozen-in.

Let us compare (7.40) with the induction equations for other magnetohydrodynamic models, summarized in Table 7.2. The frozen-in condition for $\mathbf{B}$ is satisfied in nonrelativistic MHD, HMHD, and relativistic MHD. The frozen-in condition is violated in nonrelativistic two dimensional IMHD, while the alternative field $\mathbf{B}+\nabla\times(\mathbf{d}_\mathrm{e}^\mathbf{2}\mathbf{J}/\mathbf{n})$, with the electron skin depth d_e as characteristic length,[198] is frozen-in. Therefore, the scale length of the collisionless reconnection caused by the electron inertia is d_e. On the other hand, the alternative frozen-in field in relativistic HMHD is $\mathbf{B} + \nabla \times (-\mathbf{d}_\mathrm{i}\mathbf{h}_\mathrm{e}\gamma\mathbf{v} + \mathbf{d}_\mathrm{i}^\mathbf{2}\mathbf{h}_\mathrm{e}\mathbf{J}/\mathbf{n})$, which has a characteristic scale length with $\sqrt{h_\mathrm{e}}d_\mathrm{i}$. Since the scale length d_e in nonrelativistic IMHD is replaced to $\sqrt{h_\mathrm{e}}d_\mathrm{i}$ in relativistic HMHD, the reconnection scale is expected to be $\sqrt{h_\mathrm{e}}d_\mathrm{i}$. This estimate is the same as that for

the Sweet–Parker model for relativistic electron–positron XMHD [67] (recall that $h_{\rm e}$ is normalized by mc^2 in this study). Here we have inferred the reconnection scale just by comparing non-relativistic and relativistic Ohm's law. However, in non-relativistic case, it was shown that the reconnection scale is not determined by the generalized Ohm's law alone when there is a strong magnetic guide field. The analysis of gyrofluid model revealed that the relevant scale becomes the ion sound Larmor radius in this case. [69] Hence, the above discussion on the collisionless reconnection is applicable when there is no guide field.

	Barotropic induction eq.	frozen-in field
Nonrelativistic MHD	$\partial_t \mathbf{B} + \nabla \times (\mathbf{B} \times \mathbf{v}) = \mathbf{0}$	$\mathbf{B}$
Nonrelativistic Hall MHD	$\partial_t \mathbf{B} + \nabla \times (\mathbf{B} \times \mathbf{v}_{\rm e}) = \mathbf{0}$	$\mathbf{B}$
Nonrelativistic 2D Inertial MHD	$\partial_t \mathbf{B}^\star + \nabla \times (\mathbf{B}^\star \times \mathbf{v}) = \mathbf{0}$	$\mathbf{B}^\star = \mathbf{B} + \nabla \times \left(\mathbf{d}_{\rm e}^{\mathbf{2}} \mathbf{J}/\mathbf{n}\right)$
Relativistic MHD	$\partial_t \mathbf{B} + \nabla \times (\mathbf{B} \times \mathbf{v}) = \mathbf{0}$	$\mathbf{B}$
Relativistic Hall MHD	$\partial_t \mathbf{B}^\star + \nabla \times (\mathbf{B}^\star \times \widetilde{\mathbf{v}}_{\rm e}) = \mathbf{0}$	$\mathbf{B}^\star = \mathbf{B} +$ $\nabla \times (-d_{\rm i} h_{\rm e} \gamma \mathbf{v} + \mathbf{d}_{\rm i}^{\mathbf{2}} \mathbf{h}_{\rm e} \mathbf{J}/\mathbf{n})$

Table 7.2: Induction equations for nonrelativistic MHD, HMHD and IMHD, and relativistic MHD and HMHD.

7.6 Nonrelativistic XMHD – 3+1 decomposition

The covariant Poisson bracket AP formalism also encompasses nonrelativistic theories. We will show this in the context of XMHD, then infer that this is the case for nonrelativistic MHD and the nonrelativistic ideal fluid. Because nonrelativistic theories contain space and time separately, it is natural to pursue this end by beginning from the 3+1 decomposition for relativistic theories described in Ref. [166]. To this end we state some general tools before proceeding to the task at hand.

The functional derivative of (7.22) is defined relative to the space-time pairing, while functional derivatives in conventional Hamiltonian theories are defined relative to only the spatial pairing, i.e.

$$\delta\mathscr{F} = \int \delta n \, \frac{\delta\mathscr{F}}{\delta n} \, \mathrm{d}^3x \, . \tag{7.42}$$

For functionals of the form $F = \int \mathscr{F} \mathrm{d}x^0$ where $\mathscr{F}$ contains no time derivatives of a field, it follows e.g. that

$$\frac{\delta F}{\delta n(x^0, \mathbf{x})} = \frac{\delta\mathscr{F}}{\delta n(\mathbf{x})} \, , \tag{7.43}$$

where we explicitly display the arguments to distinguish space-time from space functional derivatives. For nonrelativistic theories, we need to consider functionals that are localized in time, i.e., have the form

$$F = \int \delta(x^0 - x^{0\prime}) \, \mathscr{F} \, \mathrm{d}x^0 \, . \tag{7.44}$$

Observe, in this case, if $\mathscr{F}$ contains no time derivatives of the field n, then

$$\frac{\delta F}{\delta n(x^0, \mathbf{x})} = \delta(x^0 - x^{0\prime}) \, \frac{\delta\mathscr{F}}{\delta n(\mathbf{x})} \, , \tag{7.45}$$

and similarly for other fields. Next, let us suppose that a functional G is separable in the following sense

$$G = G^0 + \int \mathscr{G}\, \mathrm{d}x^0\,, \tag{7.46}$$

where all of the time-like components of fields are contained in the functionals G^0 and $\mathscr{G}$ contains no time derivatives of fields. For functionals G for the form of (7.46) and F for the form of (7.44), it will be shown that

$$0 = \{F, G\} = -\frac{\mathrm{d}\mathscr{F}}{\mathrm{d}t} + \{\mathscr{F}, \mathscr{G}\}^{(3)} \tag{7.47}$$

where $\{F, G\}$ is the canonical bracket (7.21) or the noncanonical bracket (7.23), and $\{\mathscr{F}, \mathscr{G}\}^{(3)}$ is the appropriate nonrelativistic Poisson bracket. In this way one can establish the connection between Poisson bracket APs and usual noncanonical Poisson bracket Hamiltonian formulations.

For the case at hand, let us return to the arbitrary mass plasma (m_+ and m_-) and consider a nonrelativistic limit with

$$h \to mc^2,\ \ \Delta h \to 0,\ \ h^\dagger \to (m_+ m_-)c^2/m,\ \ \gamma_\pm \to 1,\ \partial_t \mathbf{E} = \mathbf{0}.$$

These result in $J^0 = en(\gamma_+ - \gamma_-) \to 0$ and $\mathbf{J} = \nabla \times \mathbf{B}$, and the generalized fields become

$$\begin{aligned} \mathfrak{m}^{\star\nu} &\to nmc^2 u^\nu = \mathfrak{m}^\nu\,, \\ A^{\star\nu} &\to A^\nu + \frac{1}{ne^2}\left(\frac{m_+ m_-}{m} c^2\right) J^\nu\,, \end{aligned}$$

and

$$A^{\dagger\nu} = \frac{m_+ - m_-}{m} A^{\star\nu} - \frac{m_- m_+ c}{me} u^\nu\,,$$

with the four velocity becoming $u^\nu = (1, \mathbf{v}/\mathbf{c})$. Using the thermodynamic relations $\rho = n(mc^2 + \mathcal{E})$ and $p = nh - \rho$, with internal energy $\mathcal{E}$, the following limit is calculated

$$\frac{1}{2}(\rho - p) = n(mc^2 + \mathcal{E}) - \frac{1}{2}nh \;\rightarrow\; n\left(\frac{1}{2}mc^2 + \mathcal{E}\right).$$

We first show a nonrelativistic Hamilton's equation for the Clebsch variables. The action (7.7) is separated as

$$S[z] = \int \left[n\partial^0\phi + \sum_{\pm} \left(\sigma_\pm \partial^0 \eta_\pm + \varphi_\pm \partial^0 \lambda_\pm\right)\right] \mathrm{d}^4x - \int \mathscr{H} \mathrm{d}^0x,$$

with a Hamiltonian

$$\mathscr{H}[z] = \int \left[n(mc^2 + \mathcal{E}_+ + \mathcal{E}_-) + \frac{1}{2}nmv^2 + \frac{1}{2}\mathbf{J}\cdot\mathbf{A}^\star \right] \mathrm{d}^3x. \tag{7.48}$$

Here $\mathbf{v} = \mathfrak{m}/\mathbf{nmc}$, $\mathbf{A}^\star$. Substituting, this action and the localized functional (7.44) to the covariant canonical bracket (7.21), we get

$$\{F,\, S\}_{\text{canonical}} = \int \left(\frac{\mathrm{d}\mathscr{F}}{\mathrm{d}t} - \{\mathscr{F},\, \mathscr{H}\}^{(3)}_{\text{canonical}} \right) \delta(x^0 - x^{0\prime})\, \mathrm{d}x^0$$

where $\{\mathscr{F},\, \mathscr{H}\}^{(3)}_{\text{canonical}}$ is a canonical Poisson bracket defined in the three dimensional space. Thus, we get the nonrelativistic canonical Hamilton's equation as

$$\frac{\mathrm{d}\mathscr{F}}{\mathrm{d}t} = \{\mathscr{F},\, \mathscr{H}\}^{(3)}_{\text{canonical}},$$

which describes the time evolution of the Clebsch variables z. Transforming the Clebsch variables to $\mathbf{v}$ and $\mathbf{B}^\star$, we obtain the non-relativistic XMHD equations, which will be explicitly shown below.

Now we are set to apply this 3+1 procedure to the noncanonical bracket (7.23). Upon rearranging the action of (7.20) we obtain

$$\bar{S} = \int \frac{\mathfrak{m}_0 \mathfrak{m}^0}{2nmc^2} \mathrm{d}^4x - \int \mathscr{H} \mathrm{d}x^0, \tag{7.49}$$

with the Hamiltonian

$$\mathscr{H}\left[n,\, \sigma,\, \mathfrak{m}^i,\, A^{\star i}\right] = \tag{7.50}$$

$$\int \left[-\frac{\mathfrak{m}_i \mathfrak{m}^i}{2nmc^2} + n\left(\frac{1}{2}mc^2 + \mathcal{E}_+ + \mathcal{E}_-\right) - \frac{A^{\star i} J_i}{2} \right] \mathrm{d}^3x,$$

where we used $J^0 = 0$ to get the last term.

Then we calculate $\{\bar{F},\, \bar{S}\}_{\mathrm{XMHD}} = 0$ to get the nonrelativistic XMHD equations. The phase space variables must be $(n,\, \sigma_\pm,\, \mathfrak{m}^i, A^{\star i})$. Hence we put $\bar{F} = \bar{F}[n,\, \sigma_\pm,\, \mathfrak{m}^i, A^{\star i}]$. Since the action (7.49) does not depends on $A^{\star 0}$, we may write $\bar{S} = \bar{S}[n,\, \sigma_\pm,\, \mathfrak{m}^0,\, \mathfrak{m}^i, A^{\star i}]$. Therefore all the terms including $\delta\bar{F}/\delta\mathfrak{m}^0$, $\delta\bar{F}/\delta A^{\star 0}$, and $\delta\bar{S}/\delta A^{\star 0}$ are dropped. Upon writing

$$\bar{F} = \int \delta(x^0 - x^{0\prime})\, \mathscr{F}[n,\, \sigma_\pm,\, \mathfrak{m}^i, A^{\star i}]\, \mathrm{d}x^0\,,$$

the covariant bracket AP can be written as

$$
\begin{aligned}
0 \;=\; & \left\{\bar{F},\,\bar{S}\right\}_{\mathrm{XMHD}} = -\int\left\{ n\frac{\mathfrak{m}_0}{nmc^2}\partial^0\left[\delta(x^0-x^{0\prime})\,\frac{\delta\mathscr{F}}{\delta n}\right]\right.\\
+\; & \delta(x^0-x^{0\prime})\,n\left[-\frac{\delta\mathscr{H}}{\delta\mathfrak{m}^i}\partial^i\frac{\delta\mathscr{F}}{\delta n}+\frac{\delta\mathscr{F}}{\delta\mathfrak{m}^i}\partial^i\left(\frac{\mathfrak{m}_0\mathfrak{m}^0}{2n^2mc^2}+\frac{\delta\mathscr{H}}{\delta n}\right)\right]\\
+\; & \sum_{\pm}\left(\sigma_{\pm}\frac{\mathfrak{m}_0}{nmc^2}\partial^0\left[\delta(x^0-x^{0\prime})\,\frac{\delta\mathscr{F}}{\delta\sigma_{\pm}}\right]\right.\\
& \quad +\delta(x^0-x^{0\prime})\,\sigma_{\pm}\left[-\frac{\delta\mathscr{H}}{\delta\mathfrak{m}^i}\partial^i\delta\mathscr{F}\sigma_{\pm}+\frac{\delta\mathscr{F}}{\delta\mathfrak{m}^i}\partial^i\left(\frac{\delta\mathscr{H}}{\delta\sigma_{\pm}}\right)\right]\\
& \quad \left.\pm\delta(x^0-x^{0\prime})\,\frac{m_{\mp}}{me}\left(\frac{\delta\mathscr{F}}{\delta\sigma_{\pm}}\frac{\delta\mathscr{H}}{\delta A^{\star i}}-\frac{\delta\mathscr{H}}{\delta\sigma_{\pm}}\frac{\delta\mathscr{F}}{\delta A^{\star i}}\right)\partial^i\left(\frac{\sigma_{\pm}}{n}\right)\right)\\
+\; & \mathfrak{m}^i\left(\frac{\mathfrak{m}^0}{nmc^2}\partial^0\left[\delta(x^0-x^{0\prime})\,\frac{\delta\mathscr{F}}{\delta\mathfrak{m}^i}\right]\right)+\delta(x^0-x^{0\prime})\,\mathfrak{m}^0\left(-\frac{\delta\mathscr{F}}{\delta\mathfrak{m}^i}\partial^i\frac{\mathfrak{m}^0}{nmc^2}\right)\\
-\; & \delta(x^0-x^{0\prime})\,\mathfrak{m}^j\left(\frac{\delta\mathscr{H}}{\delta\mathfrak{m}^i}\partial^i\frac{\delta\mathscr{F}}{\delta\mathfrak{m}^j}-\frac{\delta\mathscr{F}}{\delta\mathfrak{m}^i}\partial^i\frac{\delta\mathscr{H}}{\delta\mathfrak{m}^j}\right)\\
+\; & \delta(x^0-x^{0\prime})\,\left(\frac{\mathfrak{m}_0}{nmc^2}\frac{\delta\mathscr{F}}{\delta A^{\star i}}\right)\left(\partial^i A^{\star 0}-\partial^0 A^{\star i}\right)\\
+\; & \delta(x^0-x^{0\prime})\,\left(\frac{\delta\mathscr{H}}{\delta\mathfrak{m}^i}\frac{\delta\mathscr{F}}{\delta A^{\star j}}-\frac{\delta\mathscr{F}}{\delta\mathfrak{m}^i}\frac{\delta\mathscr{H}}{\delta A^{\star j}}\right)F^{\star ji}\\
-\; & \left.\delta(x^0-x^{0\prime})\,\frac{1}{ne}\frac{\delta\mathscr{F}}{\delta A^{\star i}}\frac{\delta\mathscr{F}}{\delta A^{\star j}}F^{\dagger ij}\right\}\mathrm{d}^4x.
\end{aligned}
$$

Next we substitute $\mathfrak{m}^0=\mathfrak{m}_0=nmc^2$ and manipulate some of the terms to obtain

$$
\int\left(\frac{\delta\mathscr{F}}{\delta n}\partial^0 n+\frac{\delta\mathscr{F}}{\delta\sigma_+}\partial^0\sigma_++\frac{\delta\mathscr{F}}{\delta\sigma_-}\partial^0\sigma_-+\frac{\delta\mathscr{F}}{\delta\mathfrak{m}^i}\partial^0\mathfrak{m}^i+\frac{\delta\mathscr{F}}{\delta A^{\star i}}\partial^0 A^{\star i}\right)\mathrm{d}^3x=\frac{1}{c}\frac{\mathrm{d}\mathscr{F}}{\mathrm{d}t}\,,
$$

yielding

$$
\begin{aligned}
\left\{\bar{F},\,\bar{S}\right\}_{\mathrm{XMHD}} = & \frac{1}{c}\int\left(\frac{\mathrm{d}\mathscr{F}}{\mathrm{d}t}-\left\{\mathscr{F},\,\mathscr{H}\right\}^{(3)}\right)\delta(x^0-x^{0\prime})\,\mathrm{d}x^0\\
& +\int A^{\star 0}\partial^i\left(\frac{\delta\mathscr{F}}{\delta A^{\star i}}\right)\delta(x^0-x^{0\prime})\,\mathrm{d}^4x\,,
\end{aligned}
$$

with a three dimensional Poisson bracket $\{\mathscr{F}, \mathscr{G}\}^{(3)}$ that will be explicitly shown below. Evaluating the δ-function shows $\left\{\bar{F}, \bar{S}\right\}_{\text{XMHD}} = 0$ is equivalent to Hamilton's equation along with a gauge-like condition:

$$\frac{\mathrm{d}\mathscr{F}}{\mathrm{d}t} = \{\mathscr{F}, \mathscr{H}\}^{(3)} \quad \text{and} \quad \nabla \cdot \left(\frac{\delta \mathscr{F}}{\delta \mathbf{A}^\star}\right) = 0. \tag{7.51}$$

The second equation of (7.51), the gauge condition, is handled manifestly by transforming from the phase space variable $\mathbf{A}^\star$ to $\mathbf{B}^\star$; since $\delta\mathscr{F}/\delta\mathbf{A}^\star = \nabla \times (\delta\mathscr{F}/\delta\mathbf{B}^\star)$, with this transformation the second condition is automatically satisfied. Finally, we transform $\mathfrak{m}$ to $\mathbf{v}$ and find that the Poisson bracket $\{\mathscr{F}, \mathscr{G}\}^{(3)}$ becomes

$$\begin{aligned}
\{\mathscr{F}, \mathscr{G}\}^{(3)} \;=\; & \int \Bigg\{ \left(\frac{\delta \mathscr{G}}{\delta \mathbf{v}} \cdot \nabla \frac{\delta \mathscr{F}}{\delta \varrho} - \frac{\delta \mathscr{F}}{\delta \mathbf{v}} \cdot \nabla \frac{\delta \mathscr{G}}{\delta \varrho}\right) \\
& + \frac{\nabla \times \mathbf{v}}{\varrho} \cdot \left(\frac{\delta \mathscr{F}}{\delta \mathbf{v}} \times \frac{\delta \mathscr{G}}{\delta \mathbf{v}}\right) \\
& + \sum_{\pm} \Bigg[\frac{\sigma_\pm}{\varrho} \left(\frac{\delta \mathscr{G}}{\delta \mathbf{v}} \cdot \nabla \frac{\delta \mathscr{F}}{\delta \sigma_\pm} - \frac{\delta \mathscr{F}}{\delta \mathbf{v}} \cdot \nabla \frac{\delta \mathscr{G}}{\delta \sigma_\pm}\right) \\
& \quad \mp \frac{c m_\mp}{e} \Bigg(\frac{\delta \mathscr{F}}{\delta \sigma_\pm} \left(\nabla \times \frac{\delta \mathscr{G}}{\delta \mathbf{B}^\star}\right) \\
& \qquad - \frac{\delta \mathscr{G}}{\delta \sigma_\pm} \left(\nabla \times \frac{\delta \mathscr{F}}{\delta \mathbf{B}^\star}\right) \Bigg) \cdot \nabla \left(\frac{\sigma_\pm}{\varrho}\right) \Bigg] \\
& - \left[\frac{\delta \mathscr{G}}{\delta \mathbf{v}} \times \left(\nabla \times \frac{\delta \mathscr{F}}{\delta \mathbf{B}^\star}\right) - \frac{\delta \mathscr{F}}{\delta \mathbf{v}} \times \left(\nabla \times \frac{\delta \mathscr{G}}{\delta \mathbf{B}^\star}\right)\right] \cdot \frac{\mathbf{B}^\star}{\varrho} \\
& - \frac{mc}{\varrho e} \left[\left(\nabla \times \frac{\delta \mathscr{F}}{\delta \mathbf{B}^\star}\right) \times \left(\nabla \times \frac{\delta \mathscr{G}}{\delta \mathbf{B}^\star}\right)\right] \cdot \mathbf{B}^\dagger \Bigg\} \mathrm{d}^3 x,
\end{aligned} \tag{7.52}$$

where $\varrho = mn$ and $\nabla = -\partial^i$. This Poisson bracket is a generalization of the nonrelativistic electron-ion XMHD bracket proposed before [1, 156]. The

bracket of (7.52) differs from the previous results (See Eq. (3.22)) by the choice of scaling and, more importantly, the assumption $m_- \ll m_+$ is not made.

Now consider the Hamiltonian of (7.50); it becomes

$$\mathscr{H}\left[n,\, \sigma,\, \mathbf{v},\, \mathbf{B}^\star\right] = \int \left[\frac{\varrho|\mathbf{v}|^{\mathbf{2}}}{2} + \varrho\left(\frac{1}{2}mc^2 + \mathcal{E}_+ + \mathcal{E}_-\right) + \frac{\mathbf{B}^\star \cdot \mathbf{B}}{2}\right] \mathrm{d}^3x, \tag{7.53}$$

where $\mathcal{E}_\pm/m$ is rewritten as $\mathcal{E}_\pm$. The functional derivatives of $\mathscr{H}$ are

$$\frac{\delta\mathscr{H}}{\delta\varrho} = \frac{1}{m}\frac{\delta\mathscr{H}}{\delta n} = \frac{v^2}{2} + \frac{c^2}{2} + \sum_\pm \left(\mathcal{E}_\pm + \varrho\frac{\partial\mathcal{E}_\pm}{\partial\varrho}\right) + \frac{m_+m_-c^2}{2\varrho^2e^2}J^2,$$
$$\frac{\delta\mathscr{H}}{\delta\sigma_\pm} = \varrho\frac{\partial\mathcal{E}_\pm}{\partial\sigma_\pm}, \quad \frac{\delta\mathscr{H}}{\delta\mathbf{v}} = \varrho\mathbf{v}, \quad \frac{\delta\mathscr{H}}{\delta\mathbf{B}^\star} = \mathbf{B}\,.$$

Finally, using the above Hamilton's equations of (7.51) give

$$\frac{\partial\varrho}{\partial t} = \{\varrho,\, \mathscr{H}\}^{(3)} = -\nabla\cdot(\varrho\mathbf{v})$$

$$\frac{\partial\sigma_\pm}{\partial t} = \{\sigma_\pm,\, \mathscr{H}\}^{(3)} = -\nabla\cdot\left[\left(\mathbf{v} \pm \frac{\mathbf{cm}_\mp}{\varrho\mathbf{e}}\mathbf{J}\right)\sigma_\pm\right]$$

$$\frac{\partial\mathbf{B}^\star}{\partial t} = \{\mathbf{B}^\star,\, \mathscr{H}\}^{(3)} = \sum \pm\nabla\times\left[\frac{cm_\mp}{e}T_\pm\nabla\left(\frac{\sigma_\mp}{\varrho}\right)\right] + \nabla\times(\mathbf{v}\times\mathbf{B}^\star) - \nabla\times\left(\frac{mc}{\varrho e}\mathbf{J}\times\mathbf{B}^\dagger\right)$$

$$\frac{\partial\mathbf{v}}{\partial t} = \{\mathbf{v},\, \mathscr{H}\}^{(3)} = -(\nabla\times\mathbf{v})\times\mathbf{v} - \nabla\left(\frac{\mathbf{v^2}}{\mathbf{2}} + \frac{\mathbf{m_+m_-c^2}}{\mathbf{2}\varrho^\mathbf{2}\mathbf{e^2}}\mathbf{J^2}\right) - \frac{\nabla p}{\varrho} + \frac{\mathbf{J}\times\mathbf{B}^\star}{\varrho}\,,$$

the nonrelativistic Lüst equations [163]. Note, here we used the thermodynamic relations

$$\mathrm{d}\mathcal{E} = T\mathrm{d}\left(\frac{\sigma}{\varrho}\right) + \frac{p}{\varrho^2}\mathrm{d}\varrho = \frac{T}{\varrho}\mathrm{d}\sigma + \frac{1}{\varrho^2}(p - T\sigma)\mathrm{d}\varrho$$

and

$$\varrho\mathrm{d}\left(\mathcal{E} + \varrho\frac{\partial\mathcal{E}}{\partial\varrho}\right) + \sigma\mathrm{d}\left(\varrho\frac{\partial\mathcal{E}}{\partial\sigma}\right) = \mathrm{d}p.$$

In closing this section, we seek the Casimirs of (7.52) for the barotropic case. They must satisfy $\forall F:\ 0 = \{F, C\}$ leading to a system

$$\nabla \times \left(\frac{\mathbf{B}^\star}{\varrho} \times C_{\mathbf{v}} + C_{\mathbf{A}^\star} \times \frac{\mathbf{B}^\star}{\varrho}\right) = 0 \tag{7.54}$$

$$\nabla \cdot C_{\mathbf{v}} = 0 \quad \text{and} \quad C_{\mathbf{v}} \times \frac{\nabla \times \mathbf{v}}{\varrho} + C_{\mathbf{A}^\star} \times \frac{\mathbf{B}^\star}{\varrho} - \nabla C_\varrho = 0, \tag{7.55}$$

where we use the abbreviated notation $C_\varrho := \delta C/\delta\varrho$. Seeking a helicity Casimir we assume a linear combination

$$C^{(\lambda)} = \frac{1}{2}\int d^3x \left(\mathbf{A}^\star + \lambda\,\mathbf{v}\right) \cdot \left(\mathbf{B}^\star + \lambda\,\nabla \times \mathbf{v}\right), \tag{7.56}$$

which is substituted into (7.54) and (7.55) leading to a quadratic equation for λ with roots $\lambda_\pm = \pm m_\pm c/e$. These new Casimirs constitute topological constraints for a plasma with m_+, m_- species masses. In the limit $m_- \ll m_+$ these Casimirs become those of Refs. [1, 158]. For a discussion of topological properties of XMHD see Ref. [156]. Notice that the $C^\pm$ coincide exactly with the known 2-fluid canonical helicities $\int P \wedge dP$ for each species of Refs. [165, 260]. However we emphasize here the importance of the variables $\mathbf{v}$ and $\mathbf{A}^\star$.

In addition the helicity Casimirs, when barotropic condition is violated we obtain the family

$$C^{(\sigma)} = \int d^3x \; \varrho \, f\left(\frac{\sigma_+}{\varrho}, \frac{\sigma_-}{\varrho}\right), \tag{7.57}$$

albeit with the condition σ_+/ϱ being a function of σ_-/ϱ or $f_{,+-} = 0$, where $f_{,+}$ denotes differentiation with respect to the first argument.

7.7 Conclusion

We have formulated APs for relativistic XMHD.[125] For the constrained least action principle, the constraints, namely, conservation of number density, entropy, and Lagrangian labels for each species, were employed in the manner of Lin. Extremization of the constrained action led to Clebsch potential expressions for the generalized momentum and the generalized vector potential. Then, variable transformation from the Clebsch potentials to the physical variables led to the covariant Poisson bracket for XMHD. In the Poisson bracket AP the constraints are hidden in the degeneracy of the Poisson bracket. Through these APs we have unified the Eulerian APs for all magnetofluid models. Indeed, returning to Table 7.1 we see that all slots for Eulerian APs have been completed. Now, the only remaining work is the formulation of the AP for relativistic XMHD in the Lagrangian description. Examination of the results of Ref. [72] for nonrelativistic XMHD suggests this may not be an easy task.

Another important result was our formulation of relativistic HMHD,

obtained by taking a limit of the AP for XMHD. We observed that while nonrelativistic HMHD does not have a direct mechanism for collisionless reconnection, relativistic HMHD does allow the violation of the frozen-in magnetic flux condition via the electron thermal inertia effect. We also found an alternative frozen-in flux, in a manner similar to that for nonrelativistic IMHD. The scale length of the collisionless reconnection was shown to correspond to the reconnection layer width estimated by Sweet–Parker model.[67] Further study of relativistic HMHD, such as a numerical simulation of (7.39), will be the subject of future work.

Lastly in this chapter, we passed to a nonrelativistic limit within the covariant bracket formalism, thus arriving at a "covariant" bracket for nonrelativistic XMHD. [125] Then we derived the usual 3+1 noncanonical Poisson bracket. However, beyond the results of Refs. [1, 156], the result of (7.52) does not assume smallness of electron mass and thus is also applicable to electron–positron plasmas.

Chapter 8

General relativistic fluids

8.1 Introduction

In the previous chapter we discussed how a covariant Poisson bracket can be obtained for relativistic XMHD [125]. This should in principle open relativistic XMHD to analyses that use Hamiltonian form, such as energy-Casimir stability, etc. However it is not easy to find such Casimirs and let alone interpret them as integrals of motion in the covariant language. For instance in the 3+1 case we have $\forall F : \{C, F\} = 0$ implies foliation of phase space by Casimirs as well as $\dot{C} = \{C, H\} = 0$. However in the covariant case the Poisson bracket is essentially a derivative of an action principle with constraints hidden in the degeneracy of the Poisson operator. Equations of motion are obtained by commuting arbitrary functionals with the action as opposed to the Hamiltonian, i.e. requiring $\{S, F\} = 0$. In addition, the covariant approach may suffer from a problem stated in private communications by Eric D'Avignon, namely that if we add gravity to the fluid Poisson bracket [166] then it is not clear how the Jacobi identity is satisfied.

Therefore we propose a step towards purely Hamiltonian description, i.e. to find a 3+1 Hamiltonian formulation for relativistic XMHD. This can be

done systematically using the Arnowitt, Deser, Misner approach [16]. Originally it was devised to quantize gravity although now it is more often used to numerically simulate general relativity. The details of the procedure are outlined in section 8.3. Thus once the ADM Poisson bracket for the matter model is obtained, adding gravity is automatic. Some may wonder where one would apply general relativistic extended magnetohydrodynamics. For this we direct the audience to [135, 18]. One could object that near black holes quantum effects may become important. However, we are confident that there are regions where a classical treatment is sufficient (for instance in the black hole accretion discs and magnetosphere[134]). For example, in test-relativistic hydrodynamics[1], the density of the fluid is low and thus its effect on gravity can be neglected. This can be done if the energy density of the fluid is low enough and so in this limit one can ignore quantum field theory effects. In addition, using ADM treatment allows one to cast special relativistic XMHD in general coordinate systems even if the space is flat. Also, special-relativistic XMHD has applications to laser accelerated plasmas.

The outline of this chapter is as follows. In Sec. 8.2 we consider a simplified fluid case that lacks electro-magnetic contribution. The purpose of that section will be to re-derive covariant noncanonical Poisson bracket for the ideal fluid. In Sec. 8.3 we will discuss how a space-time foliation can be done in a rigorous controlled way. In Sec. 8.4 the 3+1 fluid bracket will

[1]Test relativistic hydrodynamics refers to a model where the fluid is subject to the background curvature of space-time however the energy of the fluid is sufficiently small that it does not alter the gravitational field

be re-derived using the standard Legendre transform. Next, in Sec. 8.5 the covariant noncanonical Poisson bracket will be derived for test-relativistic Hall MHD (when gravity is decoupled from the fluid the Jacobi identity is satisfied). Sec. 8.6 will involve exposition of the new canonical ADM Poisson bracket for general relativistic Hall MHD using Clebsch variables. In Sec. 8.7 we repeat the derivation of the invariants for GR MHD. Finally, Sec. 8.8 deals with GR XMHD invariants along with some discussion on quasineutrality.

8.2 Coviariant fluid action principle

We start by describing the well known covariant action principle [166, 125]. Although it evaluates to pressure on-shell $u^\alpha u_\alpha = -1$[2] like the one used by [222, 49] it differs from both and is more closely related to the dust action described in [50, 46].

$$S = \int \sqrt{-g}\, d^4x \left(-\frac{hn\, u^\alpha u^\beta g_{\alpha\beta}}{2} + \frac{p-\rho}{2} \right). \tag{8.1}$$

Here h is enthalpy, n is the rest mass density and u is the four-velocity. Barotropic quantities such as therest mass density $\rho = \rho(n)$ and pressure $p = p(n)$ are related as

$$h = \frac{\mathrm{d}\rho}{\mathrm{d}n} = \frac{p+\rho}{n} \tag{8.2}$$

The action principle (AP) is one in terms of Clebsch potentials,

$$m_\alpha := hnu_\alpha = n\partial_\alpha\phi + \lambda_I \partial_\alpha \phi^I \tag{8.3}$$

[2]We choose metric signature opposite to the one used in Chapter 7 in accordance with the ADM literature. Another important change in what follows is that we will resort to $c = 1$ units.

In the covariant theory, variational derivatives are defined in the intrinsic sense,

$$\delta F = \int \sqrt{-g}\, d^4x\, \frac{\widetilde{\delta} F}{\delta \chi^k} \delta \chi^k. \tag{8.4}$$

If S is varied with respect to these fields $\chi = (n, \phi, \lambda_I, \phi^I)$ one obtains

$$0 = \frac{\widetilde{\delta} S}{\delta \phi} = \frac{1}{\sqrt{-g}} \partial_\alpha \left(\frac{m^\alpha}{hn} n \sqrt{-g} \right) = (n u^\alpha)_{;\alpha}, \tag{8.5}$$

$$0 = \frac{\widetilde{\delta} S}{\delta \phi^I} = (\lambda_I u^\alpha)_{;\alpha} \quad \text{and} \quad 0 = \frac{\widetilde{\delta} S}{\delta \lambda^I} = -u^\alpha \partial_\alpha \phi^I, \tag{8.6}$$

$$0 = \frac{\widetilde{\delta} S}{\delta n} = \frac{u^\alpha u_\alpha}{2} \frac{\mathrm{d}}{\mathrm{d}n}(hn) + \frac{h}{2} + \frac{n}{2} \frac{\mathrm{d}h}{\mathrm{d}n} - h - u^\alpha \partial_\alpha \phi \tag{8.7}$$

which can be reduced to

$$u^\alpha \partial_\alpha \phi = (u^\alpha u_\alpha + 1) \frac{n}{2} \frac{\mathrm{d}h}{\mathrm{d}n} + (u^\alpha u_\alpha - 1) \frac{h}{2}. \tag{8.8}$$

There is a hidden constraint here that is seen by applying the Clebsch decomposition of (8.3) to (8.8) and using (8.6)

$$m^\alpha m_\alpha = m^\alpha n\, \partial_\alpha \phi + n m^\alpha \lambda_i \partial_\alpha \phi^i = n^2 h u^\alpha \partial_\alpha \phi \Rightarrow \left(n \frac{\mathrm{d}h}{\mathrm{d}n} - h \right) (u^\alpha u_\alpha + 1) = 0.$$

Thus $u^\alpha u_\alpha = -1$ follows. Moreover, the equation of motion for the fluid in terms of the physical fields can be obtained from (8.5) - (8.8) as follows:

$$(m_\beta u^\alpha)_{;\alpha} = n u^\alpha \phi_{;\beta\alpha} + \lambda_I u^\alpha \phi^I{}_{;\beta\alpha} = n (u^\alpha \phi_{,\alpha})_{,\beta} - n\, h u_\alpha u^\alpha{}_{;\beta}, \tag{8.9}$$

and thus

$$(n h u_\beta u^\alpha)_{;\alpha} = p_{,\beta} \frac{u_\alpha u^\alpha - 1}{2} + n \left(\frac{u^\alpha u_\alpha + 1}{2} n \frac{\mathrm{d}h}{\mathrm{d}n} \right)_{,\beta}, \tag{8.10}$$

which is consistent with the known equations of motion since $u^\alpha u_\alpha = -1$. As a consistency check we observe that the energy-momentum tensor evaluates to

$$T^{\alpha\beta} = -2\frac{\widetilde{\delta} S}{\delta g_{\alpha\beta}} = (\rho + p)u^\alpha u^\beta + p g^{\alpha\beta}. \tag{8.11}$$

We can also establish the covariant Poisson bracket in the spirit of [166]. Because the Legendre transform is not a covariant process, we choose to assign fields as coordinates or momenta depending on a form that can later be successfully reduced to noncanonical bracket based on the n, m^α fields. The canonical bracket is thus defined

$$\{F, G\}^{\text{cc}}_{\text{fluid}} = \int \sqrt{-g} d^4\, x \left(\frac{\widetilde{\delta} F}{\delta \phi}\frac{\widetilde{\delta} G}{\delta n} + \frac{\widetilde{\delta} F}{\delta \phi^I}\frac{\widetilde{\delta} G}{\delta \lambda_I} - F \leftrightarrow G \right), \tag{8.12}$$

such that the AP: $0 = \{F, S\}$ for arbitrary functional $F = F[\phi, n, \phi^I, \lambda_I]$ and the action S (8.1) yields equations of motion (8.5) - (8.8). Next we perform a coordinate change from canonical to noncanonical variables $(\phi, n, \phi^I, \lambda_I) \to (n, m_\alpha)$ by applying the chain rule to (8.3):

$$\frac{\widetilde{\delta} G}{\delta n} \to \frac{\widetilde{\delta} G}{\delta n} + \phi_{,\beta}\frac{\widetilde{\delta} G}{\delta m_\beta} \quad \text{and} \quad \frac{\widetilde{\delta} F}{\delta \phi} \to -\left(n\frac{\widetilde{\delta} F}{\delta m_\alpha} \right)_{;\alpha} \tag{8.13}$$

$$\frac{\widetilde{\delta} G}{\delta \lambda_i} \to \phi^I{}_{,\beta}\frac{\widetilde{\delta} G}{\delta m_\beta} \quad \text{and} \quad \frac{\widetilde{\delta} F}{\delta \phi^I} \to -\left(\lambda_I\frac{\widetilde{\delta} F}{\delta m_\alpha} \right)_{;\alpha}. \tag{8.14}$$

This transforms (8.12) to the following covariant bracket[166, 125]

$$\{F, G\}^{\text{cl}}_{\text{fluid}} = -\int d^4x\sqrt{-g}\left(n\frac{\widetilde{\delta} G}{\delta m_\alpha}\partial_\alpha\frac{\widetilde{\delta} F}{\delta n} + m_\beta\frac{\widetilde{\delta} G}{\delta m_\alpha}\partial_\alpha\frac{\widetilde{\delta} F}{\delta m_\beta} - F \leftrightarrow G \right) \tag{8.15}$$

It appears that $m_\alpha m^\alpha = -h^2 n^2$ is no longer a a dynamical constraint and must be imposed on top of the AP. The latter can be rewritten as

$$\begin{aligned} 0 &= \{F,S\}^{\rm cl}_{\rm fluid} = \int d^4x\sqrt{-g}\Bigg[\left(n\frac{\widetilde{\delta}S}{\delta m_\alpha}\right)_{;\alpha}\frac{\widetilde{\delta}F}{\delta n} + n\frac{\widetilde{\delta}F}{\delta m_\alpha}\partial_\alpha\frac{\widetilde{\delta}S}{\delta n} \\ &+ \frac{\widetilde{\delta}F}{\delta m_\alpha}\frac{1}{\sqrt{-g}}\left(\sqrt{-g}\,m_\alpha\frac{\widetilde{\delta}S}{\delta m_\beta}\right)_{,\beta} + m_\beta\frac{\widetilde{\delta}F}{\delta m_\alpha}\partial_\alpha\frac{\widetilde{\delta}S}{\delta m_\beta}\Bigg], \end{aligned} \tag{8.16}$$

where we have used $(\sqrt{-g}V^\alpha)_{,\alpha}/\sqrt{-g} = (V^\alpha)_{;\alpha}$. The variational derivatives of the action are

$$\frac{\widetilde{\delta}S}{\delta m_\alpha} = -u^\alpha \quad \text{and} \quad \frac{\widetilde{\delta}S}{\delta n} = -h. \tag{8.17}$$

Since $\tilde{\delta}F/\delta n$ and $\tilde{\delta}F/m_\alpha$ are arbitrary we must have $(nu^\alpha)_{;\alpha} = 0$ and

$$0 = n\partial_\alpha(-h) - \frac{1}{\sqrt{-g}}\partial_\beta(nhu_\alpha u^\beta\sqrt{-g}) - nh\,u_\beta\partial_\alpha u^\beta = \tag{8.18}$$

$$-\partial_\alpha p + (nhu_\alpha u^\beta)_{;\beta} + \Gamma_{\nu\beta\alpha}\,u^\nu u^\beta hn - nh\,u_\beta u^\beta{}_{;\alpha} - nh\,u^\beta\Gamma_{\nu\beta\alpha}\,u^\nu \tag{8.19}$$

consistent with (8.10). One problem of the covariant Poisson bracket as described above is that we are unable to find any Casimirs and even if some were found interpret them as some structure on the phase space; thus, so far, the advantages of covariant Hamiltonian approach are not explicit.

Sometimes it is useful to work with Taub's current $V^\alpha := hu^\alpha$. For instance the bracket (8.15) then is rewritten as

$$\{F,G\}^{\rm nc}_{\rm fluid} = -\int d^4x\sqrt{-g}\left(\frac{\widetilde{\delta}G}{\delta V_\alpha}\partial_\alpha\frac{\widetilde{\delta}F}{\delta n} - \frac{\widetilde{\delta}F}{\delta V_\alpha}\partial_\alpha\frac{\widetilde{\delta}G}{\delta n} - \frac{\partial_\alpha V_\beta - \partial_\beta V_\alpha}{n}\frac{\widetilde{\delta}G}{\delta V_\alpha}\frac{\widetilde{\delta}F}{\delta V_\beta}\right), \tag{8.20}$$

while variations of the action are now

$$\frac{\widetilde{\delta}S}{\delta V_\alpha} = -n\frac{V^\alpha}{h} \quad \text{and} \quad \frac{\widetilde{\delta}S}{\delta n} = 0. \tag{8.21}$$

The expression $\{V_\alpha, S\}^{\rm nc}_{\rm fluid} = 0$ leads to compact equations

$$0 = V^\alpha(\partial_\alpha V_\beta - \partial_\beta V_\alpha) = V^\alpha(V_{\beta;\alpha} - V_{\alpha;\beta}), \tag{8.22}$$

because of the antisymmetry.

8.3 Space-Time Foliation

Here we review the formalism necessary for developing our ideas in general relativity. There are two major ways to construct Hamiltonian formalisms there: using the multi-symplectic formalism [250] and the ADM approach [16], which involves splitting the space-time into a foliated family of the space-like hypersurfaces. We choose this second approach because it appears to be an easier and more straightforward generalization of non-relativistic results. One purpose of constructing a Hamiltonian theory for General Relativistic Extended MHD is to analyze the stability of astrophysical objects. It is also possible to pass to the special relativistic context, which applies to laboratory plasmas (notice that this retains the freedom of using some general coordinate system). The price to pay is the loss of manifest covariance. This makes the theory less elegant, however much easier to apply to numerical calculations. Another advantage for adopting the ADM is that it should be relatively easy to couple the plasma to gravity since Hamiltonian gravity in this context has already been developed.

Following the standard prescription we introduce (For background see [176, 28, 46]) the scalar field t that foliates the space-time manifold into hyper-

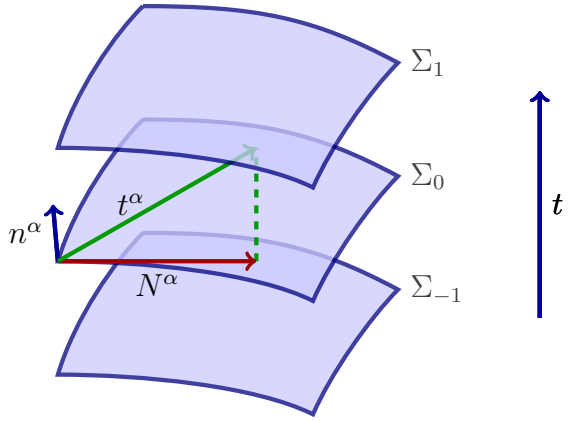

Figure 8.1: Foliation of space-time $\mathcal{M}$ by hypersurfaces Σ.

surfaces (See Fig. 8.1). In what follows Greek indicies will label components of 4-vectors $(0, 1, 2, 3)$. The normal unit vector n^α has covariant components $n_\alpha = -N t_{,\alpha}$, where N is a lapse function that measures the difference in the rate at which the time flows between "Eulerian" and "coordinate" observers. An eulerian observer is defined to follow the n^α congruence, while a coordinate observer is one that follows the t^α congruence. By definition $N = (-t_{,\alpha}\, g_{\alpha\beta}\, t_{,\beta})^{1/2}$. The four-vector t^α is chosen so that t corresponds to a time-like coordinate of the coordinate observer: $t_{,\alpha} t^\alpha := 1$. This has the consequence $n_\alpha t^\alpha = -N$. It is convenient to work with the metric on a hypersurface $\gamma_{\alpha\beta}$ (also a projection operator) defined as $\gamma_{\alpha\beta} := g_{\alpha\beta} + n_\alpha n_\beta$. With this it is natural to define shift vectors that measure how 3-coordinates connect to each other as we move accross hypersurfaces $N^\alpha := \gamma^\alpha{}_\beta\, t^\beta$, i.e. project t^α onto a hypersurface. We see that $t^\alpha - N^\alpha = N n^\alpha$. It is important to distinguish between the special vectors, say $\vec{\mathbf{N}}$ obtained by projecting and 4-vectors, like

n^α. Clearly, in this case, $\overline{\mathbf{n}} \cdot \vec{\mathbf{N}} := n_\alpha N^\alpha = 0$.

In the coordinate basis, where $i = (1, 2, 3)$ latin indices label component of 3-vectors like $N^\alpha = (0, N^i)$, while $n_\alpha = (-N, 0, 0, 0)$ and $n^\alpha = (1/N, -N^i/N)$. So long as we are concerned with the time evolution of scalars, the Lie derivative is $t^\alpha \partial_\alpha = \partial/\partial t$. The metric itself can be represented in this basis as

$$\begin{pmatrix} g_{00} & g_{0j} \\ g_{i0} & g_{ij} \end{pmatrix} = \begin{pmatrix} N_k N^k - N^2 & N_j \\ N_i & \gamma_{ij} \end{pmatrix}, \tag{8.23}$$

with the inverse

$$\begin{pmatrix} g^{00} & g^{0j} \\ g^{i0} & g^{ij} \end{pmatrix} = \begin{pmatrix} -1/N^2 & N^j/N^2 \\ N^i/N^2 & \gamma^{ij} - N^i N^j/N^2 \end{pmatrix}. \tag{8.24}$$

It can be shown that $g := \det g_{h\nu} = -N^2 \det \gamma_{h\nu} =: -N^2\gamma$. It is useful to know that the contravariant time-like components of spatial tensors including γ^{0i} and $\gamma^0{}_i$ vanish.

8.4 ADM fluid bracket

Now we apply the space-time split described in the previous section. The Lagrangian in this splitting is

$$L = \int N\sqrt{\gamma}\, d^3x \left(-\frac{m_\alpha m_\beta}{2hn} \left[\gamma^{\alpha\beta} - \frac{(t^\alpha - N^\alpha)(t^\beta - N^\beta)}{N^2} \right] + \frac{p-\rho}{2} \right), \tag{8.25}$$

which using (8.3) we can rewrite this as

$$L = \int d^3x \left(\frac{\sqrt{\gamma}}{2Nhn} (n\dot{\phi} + \lambda_I \dot{\phi}^I - m_\alpha N^\alpha)^2 + N\sqrt{\gamma}\, \frac{p-\rho}{2} - \frac{m_\alpha m_\beta \gamma^{\alpha\beta}}{2hn} \sqrt{\gamma} N \right).$$

The ADM variations are performed in the 3+1 sense in contrast to (8.4),

$$\delta F = \int d^3x \, \frac{\delta F}{\delta \chi^k} \delta \chi^k \tag{8.26}$$

Now, following the approach outlined in [50] we define the canonical momenta as

$$\pi := \frac{\delta L}{\delta \dot{\phi}} = \frac{\sqrt{\gamma}}{N} \frac{n\dot{\phi} + \lambda_J \dot{\phi}^J - m_\alpha N^\alpha}{h} = \sqrt{\gamma} n u^\alpha n_\alpha \tag{8.27}$$

$$\pi_I := \frac{\delta L}{\delta \dot{\phi}^i} = \frac{\sqrt{\gamma}\lambda_I}{N} \frac{n\dot{\phi} + \lambda_J \dot{\phi}^J - m_\alpha N^\alpha}{h} = \frac{\lambda_i \pi}{n}. \tag{8.28}$$

Thus $\pi \, \partial_\alpha \phi + \pi_I \, \partial_\alpha \phi^I = \pi m_\alpha / n$ and the Legendre transform yields

$$H = \int d^3x (\pi \dot{\phi} + \pi_i \dot{\phi}^i) - L = \int d^3x (\pi \, \partial_\alpha \phi + \pi_i \, \partial_\alpha \phi^i)(N^\alpha + n^\alpha N) - L. \tag{8.29}$$

After some transformations we obtain

$$H = \int d^3x \left(N\mathcal{H} + N^\alpha \mathcal{H}_\alpha \right), \tag{8.30}$$

where

$$\mathcal{H}_\alpha := h\pi u_\alpha = \pi \partial_\alpha \phi + \pi_I \partial_\alpha \phi^I, \tag{8.31}$$

$$\mathcal{H} := \frac{h\pi^2}{2\sqrt{\gamma} n} - \sqrt{\gamma} \frac{p - \rho}{2} + \frac{m_\alpha m_\beta \gamma^{\alpha\beta} \sqrt{\gamma}}{2hn}. \tag{8.32}$$

Now there is no momentum conjugate to n, which imposes a Dirac constraint

$$0 = \frac{\delta H}{\delta n} = N \frac{\delta \mathcal{H}}{\delta n} = \frac{N\sqrt{\gamma}}{2} \left(n \frac{\mathrm{d}h}{\mathrm{d}n} + h \right) \left(\frac{\pi^2}{\gamma n^2} - 1 - \frac{m_i \gamma^{ij} m_j}{h^2 n^2} \right). \tag{8.33}$$

This leads to $\pi^2 = n^2 \gamma (1 + u_i \gamma^{ij} u_j)$. From (8.27) we see that

$$\pi = -n \sqrt{\gamma (1 + u_i \gamma^{ij} u_j)}. \tag{8.34}$$

If we set $-1 = u_\alpha u^\alpha = u_\alpha u_\beta \gamma^{\alpha\beta} - u_\alpha u_\beta n^\alpha n^\beta \Rightarrow (n_\alpha u^\alpha)^2 = 1 + u_i \gamma^{ij} u_j \Rightarrow N u^0 = -n_\alpha u^\alpha = \sqrt{1 + u_i \gamma^{ij} u_j}$ consistent with (8.34); thus, $-1 = u_\alpha u^\alpha$ follows from (8.33). This is similar to how (8.7) works. Using (8.34) one can simplify (8.32)

$$\mathcal{H} = \frac{h\pi^2}{\sqrt{\gamma} n} - \sqrt{\gamma} p = \sqrt{\gamma} \left[\rho(1 + u_i \gamma^{ij} u_j) + p u_i \gamma^{ij} u_j \right] = \sqrt{\gamma}\, n_\alpha T^{\alpha\beta} n_\beta. \quad (8.35)$$

In addition we observe that $\mathcal{H}_i = \sqrt{\gamma} \gamma_{i\mu} T^{\mu\nu} n_\nu$. At this point the formalism becomes equivalent to the one described in [49]. The difficulty with (8.34) is that its dependence on n is implicit in $h(n)$. Since in general we are unable to invert this expression, we need to apply it as a constraint when taking variations of Hamiltonian. More specifically, using $\delta\sqrt{\gamma} = \sqrt{\gamma} \gamma^{ij} \delta\gamma_{ij}/2$[3] we obtain the constraint

$$\begin{aligned} h\sqrt{1 + u_i u^i}\delta\pi &+ \frac{\sqrt{\gamma} n h}{2} \left[\gamma^{ij}(1 + u_i \gamma^{ik} u_k) - \gamma^{il} u_l \gamma^{jk} u_k \right] \delta\gamma_{ij} + \sqrt{\gamma} n \gamma^{ij} u_j \delta(h u_i) \\ &+ \sqrt{\gamma} \left[-n u_i \gamma^{ij} u_j \frac{\mathrm{d}h}{\mathrm{d}n} + (1 + u_i \gamma^{ij} u_j) h \right] \delta n = 0. \end{aligned} \quad (8.36)$$

This can be applied directly to the variation of the Hamiltonian

$$\begin{aligned} \delta\mathcal{H} &= -2h\sqrt{1 + u_i \gamma^{ij} u_j}\delta\pi - \left[h(1 + u_i \gamma^{ij} u_j) - n \frac{\mathrm{d}h}{\mathrm{d}n} u_i \gamma^{ij} u_j \right] \delta n \\ &- \frac{\sqrt{\gamma} \gamma^{ij} \delta\gamma_{ij}}{2} \left[nh(1 + u_i \gamma^{ij} u_j) + p \right], \end{aligned} \quad (8.37)$$

leading to

$$\delta\mathcal{H} = \frac{\sqrt{\gamma}}{2} \left[p\gamma^{ij} + (\rho + p) u^i u^j \right] \delta\gamma_{ij} - \frac{h\delta\pi + u^i \delta\mathcal{H}_i}{\sqrt{1 + u_k \gamma^{kj} u_j}}. \quad (8.38)$$

[3] Whether the following operations can be performed without specifying coordinate observer should be addressed later

This allows calculation of Hamilton's equations of motion using the canonical ADM-Poisson bracket

$$\{F,G\}^{\rm ac}_{\rm fluid} = \int d^3x \left(\frac{\delta F}{\delta \phi}\frac{\delta G}{\delta \pi} + \frac{\delta F}{\delta \phi^I}\frac{\delta G}{\delta \pi_I} - F \leftrightarrow G \right), \tag{8.39}$$

obtaining

$$\dot{\phi} = \{\phi, H\}^{\rm ac}_{\rm fluid} = \frac{\delta H}{\delta \pi} = -N\frac{h + u^i \phi_{,i}}{\sqrt{1 + u_k \gamma^{kj} u_j}} + N^i \phi_{,i}\,, \tag{8.40}$$

which can be rewritten as

$$-h = \frac{\sqrt{1 + u_i \gamma^{ij} u_j}}{N}(\dot{\phi} - N^\alpha \phi_{,\alpha}) + \gamma^{ij} u_i \phi_{,j} = -n^\beta n^\alpha u_\beta \phi_{,\alpha} + \gamma^{\alpha\beta} u_\beta \phi_{,\alpha} = g^{\alpha\beta} u_\alpha \phi_{,\beta}$$

equivalent to (8.8). Similarly,

$$\dot{\pi} = -\frac{\delta H}{\delta \phi} = \left(N^i \pi - \frac{N \gamma^{ij} u_j \pi}{\sqrt{1 + u_k \gamma^{kl} u_l}} \right)_{,i} \quad \text{or} \tag{8.41}$$

since π must be a tensor density of weight 1 [46] and $\dot{\pi} = \mathcal{L}_t \pi$ is a Lie-derivative

$$0 = (t^\alpha \pi - N^\alpha \pi)_{,\alpha} - (N\sqrt{\gamma} u_i \gamma^{ij} n)_{,j} = (\sqrt{-g} n^\alpha n n^\beta u_\beta)_{,\alpha} - (\sqrt{-g} u_\beta \gamma^{\beta\alpha} n)_{,\alpha}\,,$$

also consistent with (8.5). The same procedure can be repeated for the other two phase space variables

$$\dot{\phi}^I = \{\phi^I, H\}^{\rm ac}_{\rm fluid} = \frac{\delta H}{\delta \pi_I} = -N\frac{\phi^I{}_{,j} \gamma^{ji} u_i}{\sqrt{1 + u_k \gamma^{kl} u_l}} + N^j \phi^I{}_{,j} \tag{8.42}$$

$$\dot{\pi}_I = -\frac{\delta H}{\delta \pi_I} = \left(N^j \pi_I - \frac{N \gamma^{ji} u_i \pi_I}{\sqrt{1 + u^k \gamma^{kl} u_l}} \right)_{,j}. \tag{8.43}$$

Now that we have recovered the correct equations of motion we may choose to transform to noncanonical coordinates again. Using (8.31) and the chain rule we see

$$\frac{\delta G}{\delta \pi} \to \frac{\delta G}{\delta \pi} + \phi_{,i} \frac{\delta G}{\delta \mathcal{H}_i} \quad \text{and} \quad \frac{\delta F}{\delta \phi} \to -\left(\pi \frac{\delta F}{\delta \mathcal{H}_i} \right)_{,i} \tag{8.44}$$

$$\frac{\delta G}{\delta \pi_I} \to \phi^I{}_{,j} \frac{\delta G}{\delta \mathcal{H}_j} \quad \text{and} \quad \frac{\delta F}{\delta \phi^I} \to -\left(\pi_I \frac{\delta F}{\delta \mathcal{H}_j} \right)_{,j}, \tag{8.45}$$

and (8.39) becomes

$$\{F, G\}^{\text{lc}}_{\text{fluid}} = -\int d^3x \left(\pi \frac{\delta G}{\delta \mathcal{H}_i} \partial_i \frac{\delta F}{\delta \pi} + \mathcal{H}_j \frac{\delta G}{\delta \mathcal{H}_i} \partial_i \frac{\delta F}{\delta \mathcal{H}_j} - F \leftrightarrow G \right). \tag{8.46}$$

Recall that because of the negative sign in π this actually matches the form of the non-relativistic fluid bracket. Thus the same Casimirs (with renormalized density and velocity) trivially follow. The equations of motion for π, equivalent to (8.41), trivially lead to baryon conservation. The momentum equation from (8.46) and (8.38),

$$\dot{\mathcal{H}}_k = \{\mathcal{H}_k, H\}^{\text{lc}}_{\text{fluid}} = -\pi \partial_k \frac{h}{u^0} + \partial_i \left[\mathcal{H}_k \left(N^i - \frac{\gamma^{ij} u_j}{u^0} \right) \right] + \mathcal{H}_i \, \partial_k \left(N^i - \frac{\gamma^{ij} u_j}{u^0} \right), \tag{8.47}$$

is a little more involved and to see that it is equivalent to (8.10) it is useful to define a dummy variable,

$$j^\alpha := \sqrt{-g} n u^\alpha = N \sqrt{\gamma} \, n (\gamma^{\alpha\beta} - n^\alpha n^\beta) u_\beta = -\pi \left(\frac{\gamma^{\alpha\beta} u_\beta}{u^0} + t^\alpha - N^\alpha \right). \tag{8.48}$$

Thus in addition to $\partial_\alpha j^\alpha = 0$ we have

$$j^0 = -\pi, \quad j^i = \left(N^i - \frac{\gamma^{ij} u_j}{u^0} \right) \pi \quad \text{and} \quad \mathcal{H}_\alpha j^\alpha = \frac{h \pi^2}{u^0}, \tag{8.49}$$

which using (8.41) allows rewriting (8.47) as

$$j^\alpha \partial_\alpha \frac{\mathcal{H}_k}{\pi} + \mathcal{H}_\alpha \partial_k \frac{j^\alpha}{\pi} = \pi \partial_k \frac{h}{u^0} = -\partial_k \pi \frac{\mathcal{H}_\alpha j^\alpha}{\pi^2} + \partial_k \frac{\mathcal{H}_\alpha j^\alpha}{\pi}. \tag{8.50}$$

This can be compactly represented as

$$j^\alpha \left(\partial_\alpha \frac{\mathcal{H}_k}{\pi} - \partial_k \frac{\mathcal{H}_\alpha}{\pi} \right) = 0, \tag{8.51}$$

consistent with (8.22). Alternatively it is possible to rewrite (8.47) in the form

$$\partial_\alpha \left(\mathcal{H}_k v^\alpha \right) = N\sqrt{\gamma}\, \partial_k p + \mathcal{H}_\alpha \partial_k t^\alpha - \frac{\pi h u_\beta u^\beta{}_{;k}}{u^0} + \frac{\mathcal{H}_\alpha u^\beta \Gamma^\alpha{}_{\beta k}}{u^0}, \tag{8.52}$$

where $v^\alpha := u^\alpha / u^0$ and we have introduced the $\Gamma^\alpha{}_{\beta k}$ Christoffel symbols. If we define $S_i := -\mathcal{H}_i / \sqrt{\gamma}$ in the coordinates ($t^\alpha = (1,0,0,0)$), the last expression becomes.

$$\partial_0 \left(\sqrt{\gamma} S_i \right) + \partial_j \left(\sqrt{\gamma} S_i v^j \right) = -N\sqrt{\gamma} \left(\partial_i p + \frac{S_\alpha S_\beta}{2NS^0}\, \partial_i g^{\alpha\beta} \right), \tag{8.53}$$

which can be found in [28] (eq. 5.14).

Sometimes it is more convenient to work with Taub's current $V_i := h u_i$, like in the covariant case of Eq. (8.20). Clearly from the covariant example it is clear that the ADM version will take the form

$$\{F, G\}^{\rm nc}_{\rm fluid} = -\int d^3x \left(\frac{\delta G}{\delta V_i} \partial_i \frac{\delta F}{\delta \pi} - \frac{\delta F}{\delta V_i} \partial_i \frac{\delta G}{\delta \pi} - \frac{(\partial_i V_j - \partial_j V_i)}{\pi} \frac{\delta G}{\delta V_i} \frac{\delta F}{\delta V_j} \right). \tag{8.54}$$

It is not hard to show from (8.38) that

$$\frac{\delta H}{\delta V_i} = j^i \quad \text{and} \quad \frac{\delta H}{\delta \pi} = V_0. \tag{8.55}$$

What follows are Hamilton's equations of motion:

$$\dot{\pi} = \{\pi, H\}^{\text{nc}}_{\text{fluid}} = \partial_i j^i \Rightarrow \partial_\alpha j^\alpha = 0 \quad \text{and} \tag{8.56}$$

$$\dot{v}_k = \partial_k V_0 - \frac{\partial_k V_j - \partial_j V_k}{\pi} j^j \Rightarrow \frac{j^0 \partial_0 V_k + j^j \partial_j V_k}{\pi} = \frac{j^0 \partial_k V_0 + j^j \partial_k V_j}{\pi} \tag{8.57}$$

equivalent to (8.51).

8.5 Covariant Bracket for GR Hall MHD

Here for simplicity we consider the electron inertia-less and non-relativistic temperature limit of the AP described in [125, 124] and in Chapter 7. The action is

$$S[\phi, \phi_\pm, n, \zeta_\pm] = \int \sqrt{-g}\, d^4x \left(-\frac{m^\nu m_\nu}{2nh} - \frac{F^{\mu\nu} F_{\mu\nu}}{4} + \frac{p-\rho}{2} \right), \tag{8.58}$$

where

$$m_\nu = nhu_\nu = nV_\nu = n\partial_\nu \phi + n\zeta_+ \partial_\nu \phi_+ + n\zeta_- \partial_\nu \phi_- \quad \text{and} \quad A_\nu = -\frac{\zeta_- \partial_\nu \phi_-}{e}. \tag{8.59}$$

Denoting $J^\mu := F^{\mu\nu}{}_{;\nu}$, equations of motion are obtained as follows

$$0 = \frac{\widetilde{\delta} S}{\delta n} = \left(n \frac{\mathrm{d}h}{\mathrm{d}n} - h \right) \frac{u_\nu u^\nu + 1}{2} \tag{8.60}$$

$$0 = \frac{\widetilde{\delta} S}{\delta \phi} = (n u^\nu)_{;\nu} \qquad 0 = \frac{\widetilde{\delta} S}{\delta \zeta_+} = -n u^\nu \phi_{+,\nu} \qquad 0 = \frac{\widetilde{\delta} S}{\delta \phi_+} = (n \zeta_+ u^\nu)_{;\nu} \tag{8.61}$$

$$0 = \frac{\widetilde{\delta} S}{\delta \zeta_-} = -n \left(u^\nu - \frac{J^\nu}{en} \right) \phi_{-,\nu} \qquad 0 = \frac{\widetilde{\delta} S}{\delta \phi_-} = \left[n\, \zeta_- \left(u^\nu - \frac{J^\nu}{en} \right) \right]_{;\nu}, \tag{8.62}$$

It is not hard to see using (8.59) that (8.60) implies

$$u^\nu \phi_{,\nu} = e A_\nu u^\nu - h. \tag{8.63}$$

It is not clear whether the other constraint for the electron four-velocity is also obtained in the similar fashion

$$\left(u_\nu - \frac{J_\nu}{en}\right)\left(u^\nu - \frac{J^\nu}{en}\right) = -1. \tag{8.64}$$

It is possible that the reason we are unable to produce this constraint is that quasineutrality has been imposed a priori, i.e. otherwise we would have separate bulk and electron densities and potential ϕ-s. Be that as it may, this constraint is not necessary to produce the right equations of motion from the AP. The extension of (nonrelativistic) Hall MHD without the assumption of quasineutrality is considered in [52].

Next, we construct the covariant canonical bracket

$$\{F,G\}^{\rm ac}_{\rm Hall} = \int \sqrt{-g}\, d^4\, x \left(\frac{\widetilde{\delta} F}{\delta \phi}\frac{\widetilde{\delta} G}{\delta n} + \sum_{\pm}\frac{\widetilde{\delta} F}{\delta \phi_\pm}\frac{\widetilde{\delta} G}{\delta \lambda_\pm} - F \leftrightarrow G\right), \tag{8.65}$$

and effect the coordinate change to (n, V^α, A_β) resulting in the bracket

$$\begin{aligned}\{F,G\}^{\rm ac}_{\rm Hall} &= \int d^4x\sqrt{-g}\left(\frac{\widetilde{\delta} F}{\delta V_\alpha}\partial_\alpha\frac{\widetilde{\delta} G}{\delta n} - \frac{\partial_\alpha V_\beta}{n}\frac{\widetilde{\delta} F}{\delta V_\alpha}\frac{\widetilde{\delta} G}{\delta V_\beta} - \frac{\partial_\alpha A_\beta}{n}\frac{\widetilde{\delta} F}{\delta A_\alpha}\frac{\widetilde{\delta} G}{\delta V_\beta}\right.\\ &+ \left.\frac{\partial_\alpha A_\beta}{en}\frac{\widetilde{\delta} F}{\delta A_\alpha}\frac{\widetilde{\delta} G}{\delta A_\beta} + \frac{A_\beta}{en}\left[\frac{\widetilde{\delta} F}{\delta A_\alpha}\right]^{;\alpha}\frac{\widetilde{\delta} G}{\delta A_\beta} - F \leftrightarrow G\right).\end{aligned} \tag{8.66}$$

To achieve full gauge invariance, however, one realizes that $F^{\mu\nu}$ constitute the true physical fields and not A^μ. Using

$$\frac{\widetilde{\delta} G}{\delta A^\mu} = \left(\frac{\widetilde{\delta} G}{\delta F^{\mu\nu}} - \frac{\widetilde{\delta} G}{\delta F^{\nu\mu}}\right)^{;\nu} = 2\left(\frac{\widetilde{\delta} G}{\delta F^{\mu\nu}}\right)^{;\nu}, \tag{8.67}$$

where the last equality is possible if the functional involves $F^{\mu\nu}$ quadratically. So the last term in (8.68) vanishes[4] and we arrive at

$$\begin{aligned}\{F,G\}^{\rm an}_{\rm Hall} &= \int d^4x\sqrt{-g}\left(\frac{\widetilde{\delta}F}{\delta V_\alpha}\partial_\alpha\frac{\widetilde{\delta}G}{\delta n}-\frac{\widetilde{\delta}G}{\delta V_\alpha}\partial_\alpha\frac{\widetilde{\delta}F}{\delta n}-\frac{\partial_\alpha V_\beta-\partial_\beta V_\alpha}{n}\frac{\widetilde{\delta}F}{\delta V_\alpha}\frac{\widetilde{\delta}G}{\delta V_\beta}\right.\\ &- \left.\frac{F_{\alpha\beta}}{n}\frac{\widetilde{\delta}F}{\delta A_\alpha}\frac{\widetilde{\delta}G}{\delta V_\beta}+\frac{F_{\alpha\beta}}{n}\frac{\widetilde{\delta}G}{\delta A_\alpha}\frac{\widetilde{\delta}F}{\delta V_\beta}+\frac{F_{\alpha\beta}}{en}\frac{\widetilde{\delta}F}{\delta A_\alpha}\frac{\widetilde{\delta}G}{\delta A_\beta}\right). \qquad (8.68)\end{aligned}$$

With the help of

$$\frac{\widetilde{\delta}S}{\delta V_\alpha}=-nu^\alpha \qquad \frac{\widetilde{\delta}S}{\delta A_\nu}=-J^\nu \qquad V^\alpha V_\alpha=-h^2 \qquad (8.69)$$

and

$$\frac{\widetilde{\delta}S}{\delta n}=\left(\frac{n}{h}\frac{\mathrm{d}h}{\mathrm{d}n}-1\right)(V^\alpha V_\alpha+h^2)=0, \qquad (8.70)$$

one obtains

$$0=\{V_\mu,S\}^{\rm an}_{\rm Hall}=u^\nu(V_{\nu;\mu}-V_{\mu;\nu})=-\frac{F_{\mu\nu}J^\nu}{n}, \qquad (8.71)$$

while $\{A_\mu,S\}^{\rm an}_{\rm Hall}=0$ reproduces Ohm's law

$$F_{\mu\nu}\left(u^\nu-\frac{J^\nu}{en}\right)=0 \qquad (8.72)$$

and $0=\{n,S\}^{\rm an}_{\rm Hall}=-(nu^\alpha)_{;\alpha}$ is trivial.

[4] One must be careful about the Jacobi identity when dropping terms from the Poisson Bracket

8.6 ADM Hall MHD

From (8.58) proceeding analogously to (8.25) we see that space-time split yields

$$\begin{aligned} L &= \int d^3x \left(\frac{n\sqrt{\gamma}}{2Nh}(\dot{\phi} + \zeta_+\dot{\phi}_+ + \zeta_-\dot{\phi}_- - V_\alpha N^\alpha)^2 + N\sqrt{\gamma}\,\frac{p-\rho}{2} \right. \qquad (8.73) \\ &- \left. \frac{\sqrt{\gamma}Nm_\alpha m_\beta \gamma^{\alpha\beta}}{2hn} + \frac{N\sqrt{\gamma}}{2}\gamma^{\beta\nu}n^\alpha n^\mu F_{\alpha\beta}F_{\mu\nu} - \frac{N\sqrt{\gamma}}{4}\gamma^{\beta\nu}\gamma^{\alpha\mu}F_{\alpha\beta}F_{\mu\nu} \right). \end{aligned}$$

Fortunately the bulk of the fluid behaves as before,

$$\pi := \sqrt{\gamma} n u^\alpha n_\alpha \quad \text{and} \quad \pi_+ := \frac{\delta L}{\delta \dot{\phi}_+} = \zeta_+ \pi. \qquad (8.74)$$

However, the electron-EM part yields

$$\pi_- := \frac{\delta L}{\delta \dot{\phi}_-} = \zeta_-\pi + \frac{\sqrt{\gamma}}{e} n^\alpha F_{\alpha\beta} D^\beta \zeta_- = \zeta_-\pi + \frac{\sqrt{\gamma}}{e} n^\alpha F_{\alpha\beta}\partial^\beta \zeta_-, \qquad (8.75)$$

where we have introduced typical notation for spatial covariant derivatives: $D_\alpha f := \gamma_{\alpha\beta}\partial^\beta f$. Also notice that the second equality holds because $n^\alpha n^\beta F_{\alpha\beta} = 0$. But this expression involves time derivatives of ζ_-. This is because of the form $n^\alpha F_{\alpha\beta}$. Therefore, in order to be able to invert for time derivatives we must introduce a new canonical momentum not considered earlier.

$$\theta_- := \frac{\delta L}{\delta \dot{\zeta}_-} = -\frac{\sqrt{\gamma}}{e} n^\alpha F_{\alpha\beta} D^\beta \phi_-. \qquad (8.76)$$

Next, Legendre transform is performed as usual, giving

$$\begin{aligned} H &= \int d^3x (\pi\dot{\phi} + \pi_+\dot{\phi}_+ + \pi_-\dot{\phi}_- + \theta\,\dot{\zeta_-}) - L \qquad (8.77) \\ &= \int d^3x \left(\frac{h\pi^2 N}{2n\sqrt{\gamma}} + \pi V_\nu N^\nu - N\sqrt{\gamma}\frac{p-\rho}{2} + \frac{N\sqrt{\gamma}nV_\alpha\gamma^{\alpha\beta}V_\beta}{2h} \right. \\ &+ \left. \frac{N\sqrt{\gamma}\gamma^{\alpha\mu}\gamma^{\beta\nu}F_{\alpha\beta}F_{\mu\nu}}{4} + \frac{N\sqrt{\gamma}n^\alpha n^\mu \gamma^{\beta\nu}F_{\alpha\beta}F_{\mu\nu}}{2} + \sqrt{\gamma}n^\alpha F_{\alpha\beta}\gamma^{\beta\nu}N^\mu F_{\mu\nu} \right). \end{aligned}$$

The last term corresponds to electromagnetic flux and can be re-written using the identity

$$\sqrt{\gamma}n^{\alpha}F_{\alpha\beta}\gamma^{\beta\nu}F_{\mu\nu}\gamma^{\mu\delta} = (\pi_- - \zeta_-\pi)D^{\delta}\phi_- + \theta D^{\delta}\zeta_-. \tag{8.78}$$

Equations (8.75) and (8.76) can be inverted to give

$$n^{\alpha}\partial_{\alpha}\phi_- = \mathcal{L}_n\phi_- = 2\frac{e^2\vec{D}\phi_-}{\sqrt{\gamma}}\cdot\frac{(\pi_- - \zeta_-\pi)\vec{D}\phi_- + \theta\vec{D}\zeta_-}{J^{ij}_{\phi\zeta}J^{ij}_{\phi\zeta}} \tag{8.79}$$

and

$$n^{\alpha}\partial_{\alpha}\zeta_- = \mathcal{L}_n\zeta_- = 2\frac{e^2\vec{D}\zeta_-}{\sqrt{\gamma}}\cdot\frac{(\pi_- - \zeta_-\pi)\vec{D}\phi_- + \theta\vec{D}\zeta_-}{J^{ij}_{\phi\zeta}J^{ij}_{\phi\zeta}}. \tag{8.80}$$

Here we defined $J^{ij}_{\phi\zeta} := D^i\phi_- D^j\zeta_- - D^j\phi_- D^i\zeta_-$. The expressions above allow writing

$$\frac{\sqrt{\gamma}n^{\alpha}n^{\mu}\gamma^{\beta\nu}F_{\alpha\beta}F_{\mu\nu}}{2} = \frac{e^2}{\sqrt{\gamma}}\frac{\left[(\pi_- - \zeta_-\pi)\vec{D}\phi_- + \theta\vec{D}\zeta_-\right]^2}{J^{ij}_{\phi\zeta}J^{ij}_{\phi\zeta}}. \tag{8.81}$$

Finally, the fully space-like components of the electromagnetic action are

$$\frac{N\sqrt{\gamma}\gamma^{\alpha\mu}\gamma^{\beta\nu}F_{\alpha\beta}F_{\mu\nu}}{4} = N\sqrt{\gamma}\,\frac{J^{ij}_{\phi\zeta}J^{ij}_{\phi\zeta}}{4e^2}. \tag{8.82}$$

Notice that now we can rewrite the Taub-current as

$$v_i = \partial_i\phi + \zeta_-\partial_i\phi_- + \frac{\pi_+}{\pi}\partial_i\phi_+. \tag{8.83}$$

Thus Hamiltonian reduces to

$$\begin{aligned} H &= \int d^3x\left[N\left(\frac{h\pi^2}{n\sqrt{\gamma}} - p\sqrt{\gamma} + \frac{e^2}{2\sqrt{\gamma}}\frac{\left[(\pi_- - \zeta_-\pi)\vec{D}\phi_- + \theta\vec{D}\zeta_-\right]^2}{J^{ij}_{\phi\zeta}J^{ij}_{\phi\zeta}} + \sqrt{\gamma}\frac{J^{ij}_{\phi\zeta}J^{ij}_{\phi\zeta}}{2e^2}\right)\right. \\ &+ \left.\vec{N}\cdot\left(\pi\vec{D}\phi + \pi_+\vec{D}\phi_+ + \pi_-\vec{D}\phi_- + \theta\vec{D}\zeta_-\right)\right], \end{aligned} \tag{8.84}$$

where like in the fluid case

$$\delta \int d^3x N \left(\frac{h\pi^2}{n\sqrt{\gamma}} - p\sqrt{\gamma} \right) = -\frac{h\delta\pi + \gamma^{ij} u_j \delta \left(\pi \partial_i \phi + \pi_+ \partial_i \phi_+ + \pi \zeta_- \partial_i \phi_- \right)}{u^0}. \tag{8.85}$$

Hamilton's equations of motion for π, ϕ_+ and π_+ are equivalent to the fluid case. The first non-trivial one is as follows:

$$\dot{\phi}_- = \frac{\delta H}{\delta \pi_-} = \frac{N e^2 \vec{D}\phi_-}{\sqrt{\gamma}} \cdot \frac{(\pi_- - \zeta_- \pi)\vec{D}\phi_- + \theta \vec{D}\zeta_-}{J^{ij}_{\phi\zeta} J^{ij}_{\phi\zeta}} + N^i \partial_i \phi_-, \tag{8.86}$$

and is actually equivalent to (8.79). The equation for $\dot{\zeta}_-$ is very similar and reproduces, unsurprisingly, (8.80).

Using (8.79) we see that

$$t^\alpha \phi_{,\alpha} = \frac{\delta H}{\delta \pi} = -\frac{h}{u^0} - \frac{\gamma^{ij} u_i \partial_j \phi + \gamma^{ij} u_i \zeta_- \partial_j \phi_-}{u^0} - \zeta_- \mathcal{L}_n \phi_- + N^i \phi_{,i}, \tag{8.87}$$

which is consistent with (8.63). After more tedious manipulations one also obtains

$$\dot{\pi}_- = -\frac{\delta H}{\delta \phi_-} = -\partial_i \left(\frac{\pi \zeta_- \gamma^{ij} u_j}{u^0} - N\sqrt{\gamma} \frac{J^{ij}_{\phi\zeta} D^j \zeta_-}{e^2} - N^i \pi_- + \right.$$
$$\left. e^2 N \sqrt{\gamma} \frac{\vec{D}\zeta_- \cdot \left(\theta \vec{D}\zeta_- + (\pi_- - \pi\zeta_-)\vec{D}\phi_- \right) \left(\theta D^k \zeta_- + (\pi_- - \pi\zeta_-) D^k \phi_- \right) J^{ki}_{\phi\zeta}}{J^{ij}_{\phi\zeta} J^{ij}_{\phi\zeta}} \right).$$

Using (8.75), (8.79) and (8.80) this can then be rewritten as

$$\partial_\alpha \left(N\sqrt{\gamma} n^\alpha n^\mu u_\mu n \zeta_- - N\sqrt{\gamma} \gamma^{\alpha\mu} u_\mu n \zeta_- \right)$$
$$-\partial_\alpha \left(\frac{N\sqrt{\gamma}}{e} F^{\alpha\nu} \gamma_{\nu\beta} \partial^\beta \zeta_- \right) = -\partial_\alpha \left(\frac{N\sqrt{\gamma}}{e} F^{\alpha\nu} n_\nu n_\beta \partial^\beta \zeta_- \right), \tag{8.88}$$

which reduces to the second equation in (8.62). The derivation of the θ equation is similar and is thus omitted; it reproduces the first equation in (8.62). Therefore we have constructed a canonical Poisson bracket that successfully describes relativistic Hall MHD in 3+1 decomposition. Now adding gravity is trivial.

In summary the Hamiltonian (8.84) is quite complex but the Poisson bracket for general relativistic Hall MHD is relatively simple because it constitutes a canonical 3+1 bracket:

$$\{F,G\} = \int d^3x \left(\frac{\delta F}{\delta \phi}\frac{\delta G}{\delta \pi} + \frac{\delta F}{\delta \phi_+}\frac{\delta G}{\delta \pi_+} + \frac{\delta F}{\delta \phi_-}\frac{\delta G}{\delta \pi_-} + \frac{\delta F}{\delta \zeta_-}\frac{\delta G}{\delta \theta} - F \leftrightarrow G \right). \tag{8.89}$$

This Poisson bracket works, however Clebsch is known to have gauge freedom. So one may wish to re-write the Poisson bracket in terms of observables, such as electric and magnetic fields measured by the Eulerian observer. Such fields may be obtained from the Faraday tensor decomposition,

$$F^{\alpha\beta} = n^\alpha E^\beta - E^\alpha n^\beta + \epsilon^{\alpha\beta\gamma} B_\gamma, \tag{8.90}$$

which corresponds to $E_\alpha = F_{\alpha\beta} n^\beta$ and $B^\gamma = \epsilon^{\alpha\beta\gamma} F_{\alpha\beta}/2$, while $\epsilon^{\alpha\beta\mu} := n_\nu \epsilon^{\nu\alpha\beta\mu}$. With this decomposition the Hamiltonian (8.84) takes a simple form

$$\begin{aligned} H &= \int d^3x \left[N \left(\frac{h\pi^2}{n\sqrt{\gamma}} - p\sqrt{\gamma} + \sqrt{\gamma}\,\frac{E^\alpha E_\alpha + B^\alpha B_\alpha}{2} \right) \right. \\ &+ \left. N^\alpha (\pi V_\alpha + \sqrt{\gamma}\epsilon_{\alpha\mu\nu} E^\mu B^\nu) \right]. \end{aligned} \tag{8.91}$$

Notice that in relativistic case the Hamiltonian explicitly depends on the electric field. The expression further motivates finding a Poisson bracket in terms

of (π, v_i, E^i, B^i). However trying to directly perform coordinate change appears formidable, since the expression for E^i depends on (8.79) and (8.80). With the covariant approach this is not the problem. In the 3+1 fluid case, one can get rid of such terms, but in the Hall or even the MHD case the time derivatives persist. This is probably due to the fact that, expressed in terms of observables, equations of motion are time dependent both in velocity and the EM fields in the same equation (see (8.71)), which is caused by the displacement current in relativity. Perhaps this should motivate one to look for some other variable, a combination of V and E that would serve as a momentum.

In fact this approach exists in relativistic MHD numerical simulations [28], where a 3+1 decomposition without a Poisson bracket has been obtained. However the approach is not well suitable for analytics. If one introduces generalized magnetic field derived from the four-vector $b^\alpha := \epsilon^{\alpha\beta\mu\nu} u_\beta F_{\nu\mu}$,

$$\mathcal{B}^\alpha := \sqrt{\gamma} N u^0 (b^\alpha + v^\alpha b^0), \tag{8.92}$$

one is pleased to learn that Faraday induction takes a form akin to the non-relativistic case,

$$\partial_t \mathcal{B}^i = \partial_j \left(v^i \mathcal{B}^j - v^j \mathcal{B}^i \right) \tag{8.93}$$

Momentum conservation does looks appear formidable at first glance,

$$\partial_t (\sqrt{\gamma} S_i) + \partial_j \left(N \sqrt{\gamma}\, T_i^j \right) = \frac{1}{2} N \sqrt{\gamma} T^{\alpha\beta} g_{\alpha\beta,i}\,, \tag{8.94}$$

where T_j^i is a stress tensor and $S_i = (nh + b^2)\, N u^0 u_i - N b_i b^0$ is a sought for expression of the total momentum. However, complexity is hidden in the

expressions relating $\mathcal{B}_i$ and b_α (see [28], section 5.2.4) if one insists on making $(\pi, \mathcal{H}_i, \mathcal{B}_i)$ phase space variables, then the Hamiltonian takes a cumbersome form

$$H = \int d^3x \left[N \left(\frac{h\pi^2}{n\sqrt{\gamma}} - p\sqrt{\gamma} + \sqrt{\gamma}\, b^2 \left(u_i \gamma^{ij} u_j + \frac{1}{2} \right) - \left(N b^0 \right)^2 \sqrt{\gamma} \right) + N^i \mathcal{H}_i \right].$$

So, calculating variational expressions such as (8.38) seems difficult, let alone guessing the correct Poisson bracket.

8.7 Geometry in Relativistic MHD

Here we sum up the invariants for Relativistic MHD that are easier to obtain. This work is based on [260] and a presentation by Eric Gourgoulhon on a geometrical approaches to relativistic magnetohydrodynamics. Notice that the equations of motion can be cast into the very simple form

$$dF = 0, \quad u \cdot F = 0, \quad \text{and} \quad i_u \cdot dV = \frac{j}{n} \cdot dA, \tag{8.95}$$

where the letters are forms and vectors identified with the coordinate representations described above. Using Cartan's identity we see that the Lie derivative

$$\mathcal{L}_u A = i_u dA + d(i_u A) = d(i_u A) \Rightarrow \mathcal{L}_u F = 0 \tag{8.96}$$

Thus in accordance with [260] using the Leibniz rule of the Lie derivative acting on the wedge product [88] we obtain

$$\frac{\mathrm{d}}{\mathrm{d}\tau} \int A \wedge dA = \int \mathcal{L}_u A \wedge dA + A \wedge L_u F = \int d(i_u A\, F) = 0. \tag{8.97}$$

Similarly

$$\mathcal{L}_u V = i_u dV + d(i_u V) = \frac{1}{n} i_j dA + d(i_u V) = \frac{1}{n} i_j F - dh. \tag{8.98}$$

In Ref [126] relativistic cross-helicity was derived using relabeling symmetry. However the derivation is quite cryptic and thus we present a straightforward geometric version, which is systematically given by

$$\frac{\mathrm{d}}{\mathrm{d}\tau} \int V \wedge F = \int \mathcal{L}_u V \wedge F + V \wedge \mathcal{L}_u F = \int \frac{1}{n} i_j F \wedge F - dh \wedge dA = 0. \tag{8.99}$$

To show this we shall incorporate a property of the interior product, namely that it acts as an antiderivation [88],

$$i_j(F \wedge F) = i_j F \wedge F + (-1)^2 F \wedge i_j F \Rightarrow i_j F \wedge F = \frac{1}{2} i_j (F \wedge F), \tag{8.100}$$

and it can be shown that

$$F \wedge F = -E \cdot B \, dt \wedge dx \wedge dy \wedge dz = 0, \tag{8.101}$$

which is true in MHD due to Ohm's law. There is one more conserved quantity, namely the energy, which can be obtained from the action (8.58) directly using (8.11)

$$T^{\alpha\beta} = nhu^\alpha u^\beta + pg^{\alpha\beta} + F^{\alpha\mu} F^{\beta}{}_{\mu} - \frac{g^{\alpha\beta}}{4} F^{\mu\nu} F_{\mu\nu}. \tag{8.102}$$

This then leads to the so called Hamiltonian constraint (a term multiplying $N\sqrt{\gamma}$ in (8.91))

$$n_\alpha T^{\alpha\beta} n_\beta = (1 + u_i \gamma^{ij} u_j) nh - p + \frac{E^2 + B^2}{2}. \tag{8.103}$$

The other term in the Hamiltonian (8.91) (the so-called diffeomorphic constraint) can be obtained in the similar fashion by considering space-time components of the energy-momentum tensor. We can further simplify the Hamiltonian constraint by solving for the electric field using Ohm's law. This calculation is an exercise in Ref. [28] and we also leave it for the reader:

$$NE_i + \epsilon_{ijk}\left(v^j + N^j\right)B^k = 0. \tag{8.104}$$

In flat space this expression becomes familiar Ohm's law. The three collected invariants should allow one to carry out an analysis similar to [171] and [2] for relativistic turbulence.

To calculate turbulent spectra, all three invariants must be written in a specific frame. In flat space this is particularly simple. For the helicity this leads to a flat foliation of space-time (shift and lapse functions are zero and lapse is unity) and thus if we choose the right observer the expression for the magnetic helicity just reproduces the three-dimensional version

$$H_M = \int d^3x A \cdot B, \tag{8.105}$$

even though we are considering the relativistic scenario: and so too with cross-helicity.

8.8 Relativistic XMHD and quasineutrality

First of all, let us point out a difficulty in extending the action in [125] to general relativity. The action can be written as

$$S = \int \sqrt{-g}\, d^4x \left(-\frac{m^{\star\nu} m_\nu}{2nh} - \frac{F^{\star\mu\nu} F_{\mu\nu}}{4} + \frac{p-\rho}{2} \right), \tag{8.106}$$

where,

$$m^{\star\nu} := m^\nu + \frac{\Delta h}{e} J^\nu \quad \text{and} \quad A^{\star\nu} := A^\nu + \frac{\Delta h}{e} u^\nu + \frac{h^\dagger}{ne^2} J^\nu. \tag{8.107}$$

If we just repeat the calculation done in the previous section we obtain

$$T^{\alpha\beta} = m^{\star\alpha} u^\beta + F^{\star\alpha\mu} F^\beta{}_\mu + g^{\alpha\beta} \left(-\frac{m^{\star\mu} u_\mu}{2} + \frac{p-\rho}{2} - \frac{F^{\star\mu\nu} F_{\mu\nu}}{4} \right), \tag{8.108}$$

which manifestly not symmetric, in principle it can be symmetrized. We are supposed to make use of the normalization for u and J [125], which can be reduced to

$$nh(u^\mu u_\mu + 1) + 2\frac{\Delta h}{e} u_\mu J^\mu + \frac{h^\dagger}{ne^2} J_\mu J^\mu = 0 \quad \text{and} \quad 2u_\mu J^\mu + \frac{J_\mu J^\mu}{en} = 0. \tag{8.109}$$

The problem is we need to obtain [135] the sum of 2 fluid tensors for the electrons and ions respectively and the E-M tensor, which evaluates as

$$T^{\alpha\beta} = nhu^\alpha u^\beta + g^{\alpha\beta} p + \frac{\Delta h}{e} \left(u^\beta J^\alpha + J^\alpha u^\beta \right) + \frac{h^\dagger}{n^2 e^2} J^\alpha J^\beta + F^{\alpha\mu} F^\beta{}_\mu - \frac{g^{\alpha\beta}}{4} F^{\mu\nu} F_{\mu\nu}. \tag{8.110}$$

If the energy-momentum tensor is symmetrized every term except the 5th with $J^\alpha J^\beta$ is obtained, but also many other unexpected terms appear. This is at odds with the equations of motion. Is something wrong with the action? At

any rate this is an interesting question that can be answered in future work. Here we can simply adopt the Koide's energy-momentum tensor as the correct one. To see this we construct a straightforward two-fluid action

$$S = \int \sqrt{-g} d^4x \left(-\frac{1}{2} \sum_{\pm} n h_{\pm} u_{\pm\nu} u_{\pm}{}^{\nu} + \frac{p-\rho}{2} - \frac{1}{4} F^{\mu\nu} F_{\mu\nu} \right) \tag{8.111}$$

which can be rewritten as

$$S = \int \sqrt{-g} d^4x \left(-\frac{1}{2} n h u_\nu u^\nu + \frac{\Delta h}{e} J^\mu u_\mu - \frac{\Delta h}{2e^2 n} J^\nu J_\nu + \frac{p-\rho}{2} - \frac{1}{4} F^{\mu\nu} F_{\mu\nu} \right). \tag{8.112}$$

From herem (8.110) can be obtained readily, as well as (8.106) after remembering $J^\mu = F^{\mu\nu}{}_{;\nu}$ and some integration by parts. So it appears that this is where our problem lies, in identifying J^μ through $F^{\mu\nu}$ since that introduces a four-divergence and hence another metric coefficient that will be varied when obtaining the energy-momentum tensor.

However in all of this a more sinister problem is lurking. Suppose one wishes to obtain energy from (8.110) and look for a non-relativistic limit. Recall that in the non-relativistic limit energy is [130]

$$H = \int d^3x \left(\frac{m\pi v^2}{2} + m\pi U + \frac{B^2}{2} + \frac{1}{2} \frac{m_+ m_-}{m\pi e^2} J^2 \right), \tag{8.113}$$

where π is the positive non-relativistic Eulerian density. Notice that in the non-relativstic case this works out as

$$\frac{m_+ \pi v_+^2}{2} + \frac{m_- \pi v_-^2}{2} = \frac{m\pi v^2}{2} + \frac{1}{2} \frac{m_+ m_-}{m\pi e^2} J^2 \tag{8.114}$$

Now suppose we look at the non-relativistic limit of (8.110) for T^{00} and we notice that all the J^0 terms that relate to XMHD effects disappear! This

appears to be due the implicit choice of the covariant proper charge neutrality $n_+ = n_- = n$ employed as opposed to the frame-dependent regular charge neutrality $\pi_+ = \pi_-$. Suppose we choose the latter. In this case the fluid-part of the energy density evaluates as

$$n_+ h_+ (v_+^0)^2 + n_- h_- (v_-^0)^2 = \pi_+ h_+ \gamma_+ + \pi_- h_- \gamma_- \approx \pi m_+ + \pi m_- + \pi \frac{m_+ v_+^2 + m_- v_-^2}{2},$$

from where one just has to continue following (8.114). So the question of what constitutes the right quasineutrality condition seems to be still open. There is even a possibility that quasineutrality must be avoided all together and instead electromagnetism with separate two fluid equations has to be integrated. On the other hand, if we were to choose properly symmetrized (8.108) as the correct energy-momentum tensor (that was just deemed to be incorrect in the disscussion above), with the application of proper charge neutrality then at first inspection it looks like the non-relativistic energy does follow. The reason we care about the non-relativistic limit is two-fold: first, it has been established more precisely through observation, simulations, etc and second, it is believed that the non-relativistic limit must be somehow a part of a greater relativistic theory. The problem with second approach (in this paragraph) is that while proper charge neutrality has a nice feature of being frame-independent, it appears to be ad hoc (it is not clear why it must be true). The problem with the first approach is that while quasineutrality makes sense, because it's violation would redistribute charge in such a way as to cancel the charges, unless both fluids have the same velocity, imposing quasineutrality in one frame, violates

it in the other frame, and thus it is frame dependent. This raises a question of what is so special about the frame in which quasineutrality is imposed?

Now let us direct the discussion towards helicities. We know[260] that for each species [165, 125] we have the canonical momenta $\mathcal{P}_\pm = h_\pm u_\pm \pm eA = \pm e(A^\star \pm (m_\pm m^\star)/(men)) =: \pm eA_\pm$ satisfying

$$u_\pm \cdot d\mathcal{P}_\pm = 0 \Rightarrow \mathcal{L}_{u_\pm}\mathcal{P}_\pm = \text{exact} \Rightarrow \frac{\mathrm{d}}{\mathrm{d}\tau}\int \mathcal{P}_\pm \wedge d\mathcal{P}_\pm = 0 \tag{8.115}$$

Alternatively one may wish to work with $A_\pm \wedge dA_\pm$ and make the integrals of motion more MHD-like. In any event, these helicities hopefully could serve as a template to start guesswork for the general-relativistic 3+1 bracket, which one expects would look similar to its non-relativistic daughter.

Chapter 9

Conclusions and future work

In this thesis we have explored different Hamiltonian and topological ramifications of XMHD. Connections between various XMHD models such as HMHD and IMHD were duly established through a coordinate change in the Poisson bracket. Helicities, that are Casimir invariants of the Poisson bracket, have been scrutinized. This lead us to investigate the directionality of the associated turbulent cascades. We have confirmed existence of a cascade transition of the square magnetic potential through the use of pseudospectral numerical simulations. In particular, in MHD regime we observed its inverse cascade, which then reverses its direction in the IMHD regime. This is associated with the development of the partial inverse cascade of energy (even when the ion sonic Larmor radius is ignorable), which in itself is interesting, yet unaccounted for effect. Our subsequent efforts will be concentrated on this topic, where we will further explore the criticality of the transition as well as perhaps a better theoretical description of the phenomenon. One may attempt to apply a weak turbulence theory approach. Moreover, we wish to perform simulations with non-zero ion sound Larmor radius ρ_s, which are currently not available due to some problems with the CFL condition.

In addition, the action principle for relativistic XMHD was established. However, in doing so we have encountered some problems with quasineutrality and thus we see a necessity in exploring this topic further. Of course one expects that turbulence plays a role in violent astrophysical phenomena such as gamma ray bursts, thus it could be interesting to repeat the work we did in 2D XMHD, in the relativistic setting. Moreover, motivated by the recent LIGO detection [21], there is increased interest in the description of neutron star mergers. This may involve understanding the relativistic behavior of a neutron spin-fluid coupled to a shallow layer of electron-iron ion plasma on the surface of neutron stars. In the future, we seek to better assess the evolution of global magnetic fields as the neutron stars merge via a relativistic XMHD model with the addition of neutron spin-fluid.

In Ref. [156] (Sec. 4.5) we have emphasized that the topological properties of extended MHD models can be viewed as a consequence of the Hamiltonian description, viz. helicities can also be seen as Lie-dragged three-forms. In addition, inspired by a similar work in single fluid theory we have outlined the possibility of using Jones polynomials as a more concrete way of describing various field configurations compared to the approach relying on simply linking numbers (twist + writhe). Recall that ideal MHD conserves the topology of the field. The approach described above may be employed in the analysis of the three-dimensional reconnection due to non-ideal two-fluid effects, for instance in Solar Corona. To this date three dimensional collisionless reconnection (due to two-fluid effects) is not understood well.

Appendices

Appendix A

Jacobi identity for Hall MHD

In this section, we shall present a detailed proof of the Jacobi identity for the noncanonical Hall MHD bracket. The discussion in the preceding sections ensures that the proof of the Jacobi identity for other versions of extended MHD can also be established in an analogous manner.

In the absence of the Hall term, we see that (3.8) reduces to the ideal MHD bracket, first derived in [185]

$$\{F,G\}^{MHD} := -\int_D d^3x \Bigg(F_\rho \nabla\cdot G_{\mathbf{v}} - G_\rho \nabla\cdot F_{\mathbf{v}} + \frac{\nabla\times\mathbf{v}}{\rho}\cdot G_{\mathbf{v}}\times F_{\mathbf{v}} + \mathbf{B}\cdot\Big[\frac{F_{\mathbf{v}}}{\rho}\cdot\nabla G_{\mathbf{B}} - \frac{G_{\mathbf{v}}}{\rho}\cdot\nabla F_{\mathbf{B}} + \nabla\frac{F_{\mathbf{v}}}{\rho}\cdot G_{\mathbf{v}} - \nabla\frac{G_{\mathbf{v}}}{\rho}\cdot F_{\mathbf{v}}\Big]\Bigg), \quad \text{(A.1)}$$

which is known to satisfy Jacobi identity on its own [185, 181]. The convention that we will be using throughout is that ∇ operator acts only on the variable following it, and dyadics can be written in the coordinate form

$$\mathbf{B}\cdot\nabla\frac{F_{\mathbf{v}}}{\rho}\cdot G_{\mathbf{v}} = B_i\partial_i\Big(\frac{F_v^j}{\rho}\Big)G_v^j. \quad \text{(A.2)}$$

A.1 Hall - Hall Jacobi identity

The introduction of the Hall current leads to additional Hall bracket, identified previously in (3.9). We recall that it is given by

$$\{F,G\}^{Hall} := -d_i \int_D d^3x \frac{\mathbf{B}}{\rho} \cdot \Big[(\nabla \times F_{\mathbf{B}}) \times (\nabla \times G_{\mathbf{B}}) \Big]. \tag{A.3}$$

Demonstrating that Hall MHD bracket satisfies Jacobi is important since it is closely connected to the rest of the extended MHD models, as discussed previously. The Jacobi identity involves proving that cyclical permutations of any functionals F, G, H vanish, i.e. we require

$$0 = \{\{F,G\},H\} + \{\{G,H\},F\} + \{\{H,F\},G\} \equiv \{\{F,G\},H\} + \underset{F,G,H}{\circlearrowleft} \tag{A.4}$$

Here $\{,\} := \{,\}^{MHD} + \{,\}^{Hall}$. Because we already know that (A.1) satisfies Jacobi and according to the bilinearity of Poisson brackets, the general proof splits into two pieces

$$\{\{F,G\}^{MHD},H\}^{Hall} + \{\{F,G\}^{Hall},H\}^{MHD} + \underset{F,G,H}{\circlearrowleft} = 0, \tag{A.5}$$

and

$$\{\{F,G\}^{Hall},H\}^{Hall} + \underset{F,G,H}{\circlearrowleft} = 0. \tag{A.6}$$

This split occurs since (A.5) involves terms that are linear in d_i, whilst (A.6) is quadratic in d_i. We introduce the cosymplectic operator J which depends on the field variables u in general. It is known that Poisson brackets can be formally written in the form

$$\{F,G\} := \Big\langle \frac{\delta F}{\delta u} \Big| J \frac{\delta G}{\delta u} \Big\rangle. \tag{A.7}$$

The outer brackets in both (A.5) and (A.6) require evaluation of the variational derivatives of the inner bracket with respect to the field variables:

$$\frac{d}{d\epsilon}\{F,G\}[u+\epsilon\delta u]\Big|_{\epsilon=0} := \Big\langle \frac{\delta}{\delta u}\{F,G\}\Big|\delta u\Big\rangle = \Big\langle \frac{\delta^2 F}{\delta u\delta u}\delta u\Big| J\frac{\delta G}{\delta u}\Big\rangle + \Big\langle \frac{\delta F}{\delta u}\Big| J\frac{\delta^2 G}{\delta u\delta u}\delta u\Big\rangle + \Big\langle \frac{\delta F}{\delta u}\Big|\frac{\delta J}{\delta u}(\delta u)\frac{\delta G}{\delta u}\Big\rangle. \tag{A.8}$$

Proving the Jacobi identity for noncanonical Poisson brackets is aided by a theorem proven in [181], which states that the first two terms of the above expression vanish when plugged in the outer bracket, together with the other cyclic permutations. Thus, we can neglect second variations that appear throughout the following calculations. Since the outer Hall bracket involves variations with respect to $\mathbf{B}$, it is enough to consider

$$\frac{\delta}{\delta\mathbf{B}}\{F,G\}^{Hall} = -d_i\,(\nabla\times F_{\mathbf{B}})\times(\nabla\times G_{\mathbf{B}})+\cdots \equiv -d_i\,F_{\mathbf{A}}\times G_{\mathbf{A}}+\ldots, \tag{A.9}$$

where the second variations that arise implicitly are suppressed because we have established that they will not contribute to the Jacobi identity. Hence, it suffices to compute the variations with respect to the field variables that enter the Poisson bracket explicitly. Note that the last relation in (A.9) arises due to $\mathbf{B} =: \nabla\times\mathbf{A}$. This is evident through

$$\begin{aligned}\delta F &= \int_D d^3x\,\frac{\delta F}{\delta\mathbf{B}}\cdot\delta\mathbf{B} = \int_D d^3x\,\frac{\delta F}{\delta\mathbf{B}}\cdot\nabla\times\delta\mathbf{A}\\ &= \int_D d^3x\,\nabla\times\frac{\delta F}{\delta\mathbf{B}}\cdot\delta\mathbf{A} = \int_D d^3x\,\frac{\delta F}{\delta\mathbf{A}}\cdot\delta\mathbf{A}.\end{aligned} \tag{A.10}$$

A corollary of the above relation is that $F_{\mathbf{A}} \equiv \frac{\delta F}{\delta\mathbf{A}}$ is divergence-free, i.e. $\nabla\cdot F_{\mathbf{A}} = 0$. Substituting (A.9) into the Hall-Hall part of the Jacobi relation (A.6),

we obtain

$$d_i^2 \int_D d^3x\, \mathbf{B} \cdot \left(\nabla\Big(\frac{1}{2\rho^2}\Big) \times \Big[F_{\mathbf{A}} \times G_{\mathbf{A}}\Big] + \frac{1}{\rho^2} \nabla \times \Big[F_{\mathbf{A}} \times G_{\mathbf{A}}\Big] \right) \times H_{\mathbf{A}}. \quad \text{(A.11)}$$

This expression can be expanded using vector identities such as $\mathbf{X} \times (\mathbf{Y} \times \mathbf{Z}) = \mathbf{Y}\ (\mathbf{X} \cdot \mathbf{Z}) - \mathbf{Z}\ (\mathbf{X} \cdot \mathbf{Y})$ and $\nabla \times (\mathbf{X} \times \mathbf{Y}) = \nabla \cdot \big(\mathbf{Y}\,\mathbf{X}^T - \mathbf{X}\,\mathbf{Y}^T\big)$, which enables us to collect certain terms together. Since the Jacobi identity involves two additional cyclic permutations, we are allowed to carry out cyclic permutations of the above expression and collect similar terms together. Through a suitable permutation of the variables, and integrating by parts, we arrive at

$$\begin{aligned} \{\{F,G\}^{Hall},H\}^{Hall} \quad + \quad & \overset{\circlearrowleft}{}_{F,G,H} = d_i^2 \int_D d^3x\, \frac{1}{\rho^2} F_{\mathbf{A}} \times G_{\mathbf{A}} \cdot (H_{\mathbf{A}} \cdot \nabla)\mathbf{B} + \overset{\circlearrowleft}{}_{F,G,H} \\ = \quad & d_i^2 \int_D d^3x\, \frac{1}{\rho^2} \epsilon_{ijk} F_A^j\, G_A^k H_A^l \partial_l B^i + \overset{\circlearrowleft}{}_{F,G,H} \\ = \quad & d_i^2 \int_D d^3x\, \frac{F_{\mathbf{A}} \cdot G_{\mathbf{A}} \times H_{\mathbf{A}}}{\rho^2} \delta_i^l \partial_l B^i + \overset{\circlearrowleft}{}_{F,G,H}, \end{aligned} \quad \text{(A.12)}$$

where the last step becomes apparent when we explicitly write down the other two permutations, and use the antisymmetry of Levi-Civita tensor ϵ_{ijk} in addition to the identity $\epsilon_{ijk}\epsilon^{ljk} = 2\delta_i^l$. Finally, upon invoking the identity $\nabla \cdot \mathbf{B} = 0$, we see that the Hall - Hall Jacobi identity is satisfied.

A.2 Hall - Ideal MHD Jacobi identity

We observe that this part is harder to tackle, owing to the greater complexity of the resultant expression. Let us first express the first term in (A.5). As described in the previous section, the outer Hall bracket (A.3)

necessitates only the explicit variational derivatives with respect to $\mathbf{B}$. Hence, we only need to consider such variations of the inner MHD bracket (A.1):

$$\frac{\delta}{\delta \mathbf{B}}\{F,G\}^{MHD} = -\frac{F_{\mathbf{v}}}{\rho}\cdot\nabla\, G_{\mathbf{B}} + \frac{G_{\mathbf{v}}}{\rho}\cdot\nabla\, F_{\mathbf{B}} - \nabla\frac{F_{\mathbf{v}}}{\rho}\cdot G_{\mathbf{B}} + \nabla\frac{G_{\mathbf{v}}}{\rho}\cdot F_{\mathbf{B}} + \ldots, \quad \text{(A.13)}$$

and we have suppressed the implicit second-order variations, as they do not contribute to the Jacobi identity. After substitution into the outer Hall bracket, we get

$$\begin{aligned}\{\{F,G\}^{MHD},H\}^{Hall} \;+\; \overset{\circlearrowleft}{}_{F,G,H} = -d_i\int_D \frac{\mathbf{B}}{\rho^2}\cdot\Bigg[\nabla\times\Big(\frac{F_{\mathbf{v}}}{\rho}\cdot\nabla\, G_{\mathbf{B}} - \frac{G_{\mathbf{v}}}{\rho}\cdot\nabla\, F_{\mathbf{B}} \\ +\; \nabla\frac{F_{\mathbf{v}}}{\rho}\cdot G_{\mathbf{B}} - \nabla\frac{G_{\mathbf{v}}}{\rho}\cdot F_{\mathbf{B}}\Big)\times\nabla\times H_{\mathbf{B}}\Bigg] + \overset{\circlearrowleft}{}_{F,G,H}. \quad \text{(A.14)}\end{aligned}$$

We proceed to use the vector calculus identities $\nabla\times\nabla f = 0$ and $\mathbf{X}\times\nabla\times\mathbf{Y} = \nabla\mathbf{Y}\cdot\mathbf{X} - \mathbf{X}\cdot\nabla\mathbf{Y}$, which allows us to simplify the expression as follows:

$$\{\{F,G\}^{MHD},H\}^{Hall} = -d_i\int_D d^3x\,\frac{\mathbf{B}}{\rho}\cdot\left(\nabla\times\frac{F_{\mathbf{v}}\times G_{\mathbf{A}} - G_{\mathbf{v}}\times F_{\mathbf{A}}}{\rho}\times H_{\mathbf{A}}\right). \quad \text{(A.15)}$$

In the second term of (A.5) the outer MHD bracket requires evaluation of variations with respect to both $\mathbf{B}$ and ρ. We already have the first one from (A.9), while the second yields

$$\frac{\delta}{\delta\rho}\{F,G\}^{Hall} = -d_i\frac{\mathbf{B}}{\rho^2}\cdot F_{\mathbf{A}}\times G_{\mathbf{A}}. \quad \text{(A.16)}$$

Upon substituting them into the second term of (A.5), we end up with

$$-d_i\int_D d^3x\,\frac{\mathbf{B}}{\rho^2}\cdot(F_{\mathbf{A}}\times G_{\mathbf{A}})\,(\nabla\cdot H_{\mathbf{v}}) + \frac{\mathbf{B}}{\rho}\cdot\left(\nabla\times\frac{F_{\mathbf{A}}\times G_{\mathbf{A}}}{\rho}\times H_{\mathbf{v}}\right) + \overset{\circlearrowleft}{}_{F,G,H}. \quad \text{(A.17)}$$

Upon combining (A.15) and (A.17), we have

$$\begin{aligned}\mathcal{J} &= -d_i \int d^3x \left(\frac{\mathbf{B}}{\rho^2} \cdot F_{\mathbf{A}} \times G_{\mathbf{A}} \nabla \cdot H_{\mathbf{v}} + \frac{\mathbf{B}}{\rho} \cdot \left[\nabla \times \frac{F_{\mathbf{A}} \times G_{\mathbf{A}}}{\rho} \times H_{\mathbf{v}} \right] \right. \\ &\qquad \left. + \frac{\mathbf{B}}{\rho} \cdot \left[\nabla \times \frac{F_{\mathbf{v}} \times G_{\mathbf{A}} - G_{\mathbf{v}} \times F_{\mathbf{A}}}{\rho} \times H_{\mathbf{A}} \right] \right) + \underset{F,G,H}{\circlearrowleft} \\ &= \mathcal{J}_1 + \mathcal{J}_2 + \mathcal{J}_3, \end{aligned} \tag{A.18}$$

where $\mathcal{J}_i$'s represent the three contributions arising from (A.17) and (A.15), respectively. Applying the vector identities mentioned previously, and recollecting that variations with respect to $\mathbf{A}$ are divergence-free, the third term can be manipulated to yield

$$\begin{aligned}\mathcal{J}_3 &= d_i \int_D d^3x \, \frac{\mathbf{B}}{\rho} \cdot H_{\mathbf{A}} \times \left(G_{\mathbf{A}} \cdot \nabla \frac{F_{\mathbf{v}}}{\rho} - \nabla \cdot F_{\mathbf{v}} \frac{G_{\mathbf{A}}}{\rho} - F_{\mathbf{v}} \cdot \nabla \frac{G_{\mathbf{A}}}{\rho} - F_{\mathbf{A}} \cdot \nabla \frac{G_{\mathbf{v}}}{\rho} \right. \\ &+ \left. \nabla \cdot G_{\mathbf{v}} \frac{F_{\mathbf{A}}}{\rho} + G_{\mathbf{v}} \cdot \nabla \frac{F_{\mathbf{A}}}{\rho} \right) = d_i \int_D d^3x \left(\frac{2\mathbf{B}}{\rho^2} \cdot (F_{\mathbf{A}} \times G_{\mathbf{A}}) (\nabla \cdot H_{\mathbf{v}}) \right. \\ &+ \mathbf{B} \cdot (F_{\mathbf{A}} \times G_{\mathbf{A}}) \left[\nabla \cdot \left(\frac{H_{\mathbf{v}}}{\rho^2} \right) \right] + \mathbf{B} \cdot \left(\frac{H_{\mathbf{v}}}{\rho^2} \cdot \nabla \right) \left(F_{\mathbf{A}} \times G_{\mathbf{A}} \right) \\ &\qquad \left. - \frac{\mathbf{B}}{\rho} \cdot \left[F_{\mathbf{A}} \times (G_{\mathbf{A}} \cdot \nabla) - G_{\mathbf{A}} \times (F_{\mathbf{A}} \cdot \nabla) \right] \frac{H_{\mathbf{v}}}{\rho} \right). \end{aligned} \tag{A.19}$$

Here, we have used the freedom to permute F, G, H in a consistent manner. When combined with the first term $\mathcal{J}_1$, this results in

$$\begin{aligned}\mathcal{J}_1 + \mathcal{J}_3 &= d_i \int_D d^3x \left[\nabla \cdot \left[\frac{H_{\mathbf{v}}}{\rho} \frac{F_{\mathbf{A}} \times G_{\mathbf{A}}}{\rho} \right] \cdot \mathbf{B} \right. \\ &\quad - \left. \frac{\mathbf{B}}{\rho} \cdot \left[F_{\mathbf{A}} \times (G_{\mathbf{A}} \cdot \nabla) - G_{\mathbf{A}} \times (F_{\mathbf{A}} \cdot \nabla) \right] \frac{H_{\mathbf{v}}}{\rho} \right]. \end{aligned} \tag{A.20}$$

The second term of (A.18) can be rewritten as

$$\mathcal{J}_2 = -d_i \int_D d^3x \left(\frac{H_{\mathbf{v}}}{\rho} \cdot \nabla \left(\frac{F_{\mathbf{A}} \times G_{\mathbf{A}}}{\rho} \right) \cdot \mathbf{B} - \mathbf{B} \cdot \nabla \left(\frac{F_{\mathbf{A}} \times G_{\mathbf{A}}}{\rho} \right) \cdot \frac{H_{\mathbf{v}}}{\rho} \right). \tag{A.21}$$

Upon using (A.20) and (A.21), we can condense (A.18) into

$$\begin{aligned}\mathcal{J} &= d_i \int_D d^3x \Bigg(\mathbf{B} \cdot \left(\frac{F_{\mathbf{A}} \times G_{\mathbf{A}}}{\rho} \right) \left[\nabla \cdot \left(\frac{H_{\mathbf{v}}}{\rho} \right) \right] - \mathbf{B} \cdot \nabla \left(\frac{H_{\mathbf{v}}}{\rho} \right) \cdot \frac{F_{\mathbf{A}} \times G_{\mathbf{A}}}{\rho} \\ &\qquad - \frac{\mathbf{B}}{\rho} \cdot \Big[F_{\mathbf{A}} \times (G_{\mathbf{A}} \cdot \nabla) - G_{\mathbf{A}} \times (F_{\mathbf{A}} \cdot \nabla) \Big] \frac{H_{\mathbf{v}}}{\rho} \Bigg). \end{aligned} \tag{A.22}$$

The second term has been integrated by parts, by applying $\nabla \cdot \mathbf{B} = 0$ to obtain this expression. We shall not use any further permutations of F, G and H, as one such permutation was used previously. It can be shown, in coordinates for instance, or using the vector identities introduced previously, that the first two and the last two terms collapse into

$$\begin{aligned}\mathcal{J} &= d_i \int_D d^3x \Bigg(\frac{\mathbf{B}}{\rho} \cdot \left[\Big((F_{\mathbf{A}} \times G_{\mathbf{A}}) \times \nabla \Big) \times \frac{H_{\mathbf{v}}}{\rho} \right] \\ &\quad - \frac{\mathbf{B}}{\rho} \cdot \left[\Big((F_{\mathbf{A}} \times G_{\mathbf{A}}) \times \nabla \Big) \times \frac{H_{\mathbf{v}}}{\rho} \right] \Bigg) \equiv 0. \end{aligned} \tag{A.23}$$

As a result, we see that the Hall - MHD Jacobi identity is satisfied.

Hence, from the results derived in Sections A.1 and A.2, we conclude that the Hall MHD bracket (3.8) satisfies the Jacobi identity, thereby rendering it a valid noncanonical Poisson bracket. In turn, this ensures the validity of the inertial MHD bracket, and by applying the same procedures, it is possible to show that the extended MHD bracket satisfies the Jacobi identity.

Bibliography

[1] H. M. Abdelhamid, Y. Kawazura, and Z. Yoshida. Hamiltonian formalism of extended magnetohydrodynamics. *J. Phys. A Math. Gen.*, 48(23):235502, June 2015.

[2] H. M. Abdelhamid, M. Lingam, and S. M. Mahajan. Extended MHD turbulence and its applications to the solar wind. *Astrophys. J.*, 829:87, September 2016.

[3] A. Achterberg. Variational principle for relativistic magnetohydrodynamics. *Phys. Rev. A*, 28(4):2449–2458, oct 1983.

[4] P. M. Akhmetiev. On a new integral formula for an invariant of 3-component oriented links. *Journal of Geometry and Physics*, 53(2):180 – 196, 2005.

[5] J. Aldinger, I. Klapper, and M. Tabor. Formulae for the calculation and estimation of writhe. *Journal of Knot Theory and its Ramifications*, 04, 1995.

[6] A. Alexakis. Two-dimensional behavior of three-dimensional magnetohydrodynamic flow with a strong guiding field. *Phys. Rev. E*, 84:056330, Nov 2011.

[7] A. Alexakis, P. D. Mininni, and A. Pouquet. On the inverse cascade of magnetic helicity. *The Astrophysical J.*, 640(1):335, 2006.

[8] O. Alexandrova, C. H. K. Chen, L. Sorriso-Valvo, T. S. Horbury, and S. D. Bale. Solar Wind Turbulence and the Role of Ion Instabilities. *Space Sci. Rev.*, 178:101–139, October 2013.

[9] O. Alexandrova, J. Saur, C. Lacombe, A. Mangeney, J. Mitchell, S. J. Schwartz, and P. Robert. Universality of solar-wind turbulent spectrum from mhd to electron scales. *Phys. Rev. Lett.*, 103:165003, Oct 2009.

[10] T. Andreussi, P. J. Morrison, and F. Pegoraro. MHD equilibrium variational principles with symmetry. *Plasma Phys. Controlled Fusion*, 52(5):055001, May 2010.

[11] T. Andreussi, P. J. Morrison, and F. Pegoraro. Hamiltonian magnetohydrodynamics: Helically symmetric formulation, Casimir invariants, and equilibrium variational principles. *Phys. Plasmas*, 19(5):052102, May 2012.

[12] T. Andreussi, P. J. Morrison, and F. Pegoraro. Hamiltonian magnetohydrodynamics: Lagrangian, Eulerian, and dynamically accessible stability–Theory. *Phys. Plasmas*, 20(9):092104, September 2013.

[13] T. Andreussi, P. J. Morrison, and F. Pegoraro. Hamiltonian magnetohydrodynamics: Lagrangian, eulerian, and dynamically accessible stabil-

ityexamples with translation symmetry. *Phys. Plasmas*, 23(10):102112, 2016.

[14] A. M. Anile. *Relativistic Fluids and Magneto-fluids: With Applications in Astrophysics and Plasma Physics*. Cambridge Monographs on Mathematical Physics. Cambridge University Press, 1990.

[15] V. I. Arnold and Khesin B. A. *Topological Methods in Hydrodynamics*, volume 125 of *Applied Mathematical Sciences*. Springer, August 1999.

[16] R. Arnowitt, S. Deser, and C. W. Misner. Republication of: The dynamics of general relativity. *Gen. Relativ. Gravit.*, 40:1997 – 2027, 2008.

[17] F. A. Asenjo and L. Comisso. Generalized magnetofluid connections in relativistic magnetohydrodynamics. *Phys. Rev. Lett.*, 114:115003, Mar 2015.

[18] F. A. Asenjo and L. Comisso. Relativistic Magnetic Reconnection in Kerr Spacetime. *Phys. Rev. Lett.*, 118(5):055101, February 2017.

[19] F. A. Asenjo, L. Comisso, and S. M. Mahajan. Generalized magnetofluid connections in pair plasmas. *Phys. Plasmas*, 22(12):122109, 2015.

[20] M. Asgari-Targhi and M. Berger. Writhe in the stretch-twist-fold dynamo. *Geophys. Astrophys. Fluid Dyn.*, 103:69–87, February 2009.

[21] B. P. Abbott at al. Gw170817: Observation of gravitational waves from a binary neutron star inspiral. *Phys. Rev. Lett.*, 119:161101, Oct 2017.

[22] M. F. Atiyah. The geometry and physics of knots. In *Miniconference on Geometry and Physics*, pages 1–17, Canberra AUS, 1989. Centre for Mathematics and its Applications, Mathematical Sciences Institute, The Australian National University.

[23] K. Aziz and J. D. Hellums. Numerical solution of the three-dimensional equations of motion for laminar natural convection. *Phys. Fluids.*, 10(2):314 – 325, 1967.

[24] J. Baez and J. P. Muniain. *Gauge Fields, Knots and Gravity.* Series on Knots and Everything. World Scientific Publishing Company, October 1994.

[25] B. A. Bambah, S. M. Mahajan, and Chandrasekher M. Yang-mills magnetofluid unification. *Phys. Rev. Lett.*, 97:072301, Aug 2006.

[26] D. Banerjee and R. Pandit. Statistics of the inverse-cascade regime in two-dimensional magnetohydrodynamic turbulence. *Phys. Rev. E*, 90:013018, Jul 2014.

[27] S. Banerjee and S. Galtier. Chiral exact relations for helicities in hall magnetohydrodynamic turbulence. *Phys. Rev. E*, 93(033120), 2016.

[28] T. W. Baumgarte and S. L. Shapiro. *Numerical Relativity.* Cambridge University Press, 2010.

[29] J. D. Bekenstein and A Oron. Conservation of circulation in magneto-hydrodynamics. *Phys. Rev. E*, 62(4):5594–5602, oct 2000.

[30] J. D. Bekenstein and A. Oron. Extended Kelvin theorem in relativistic magnetohydrodynamics. *Foundations of Physics*, 31(6):895–907, 2001.

[31] P. M. Bellan. *Fundamentals of plasma physics*. Cambridge University Press, 2008.

[32] S. J. Benavides and A. Alexakis. Critical transitions in thin layer turbulence. *J. of Fluid Mech.*, 822:364385, 2017.

[33] M. A. Berger. Third-order link integrals. *J. Phys. A Math. Gen.*, 23(13):2787, 1990.

[34] M. A. Berger. *Topological Magnetohydrodynamics and Astrophysics*. Springer, 1992.

[35] M. A. Berger. Energy-crossing number relations for braided magnetic fields. *Phys. Rev. Lett.*, 70:705–708, Feb 1993.

[36] M. A. Berger and G. B. Field. The topological properties of magnetic helicity. *J. Fluid Mech.*, 147:133–148, October 1984.

[37] M. A. Berger and C. Prior. The writhe of open and closed curves. *J. Phys. A*, 39:8321–8348, June 2006.

[38] M. A. Berger and C. Prior. The writhe of open and closed curves. *J. Phys. A: Math. Gen.*, 39:8321–8348, 2006.

[39] J. Birn and E. R. Priest. *Reconnection of magnetic fields : magnetohydrodynamics and collisionless theory and observations*. Cambridge Univ. Press, 2007.

[40] D. Biskamp. *Nonlinear Magnetohydrodynamics*. Cambridge University Press, 1993.

[41] D. Biskamp. *Magnetic Reconnection in Plasmas*, volume 3 of *Cambridge monographs on plasma physics*. Cambridge Univ. Press, September 2000.

[42] D. Biskamp. *Magnetohydrodynamic Turbulence*. Cambridge University Press, July 2003.

[43] D. Biskamp, E. Schwarz, and J. F. Drake. Two-Dimensional Electron Magnetohydrodynamic Turbulence. *Phys. Rev. Lett.*, 76:1264–1267, February 1996.

[44] D. Biskamp, E. Schwarz, A. Zeiler, A. Celani, and J. F. Drake. Electron magnetohydrodynamic turbulence. *Phys. Plasmas*, 6(3):751–758, 1999.

[45] D. Biskamp and H. Welter. Magnetic field amplification and saturation in two-dimensional magnetohydrodynamic turbulence. *Phys. Fluids B*, 2:1787–1793, August 1990.

[46] M. Bojowald. *Canonical Gravity and Applications*. Cambridge University Press, 2011.

[47] F. Bouchet and A. Venaille. Statistical mechanics of two-dimensional and geophysical flows. *Phys. Reports*, 515(5):227 – 295, 2012. Statistical mechanics of two-dimensional and geophysical flows.

[48] A. Brandenburg. The Inverse Cascade and Nonlinear Alpha-Effect in Simulations of Isotropic Helical Hydromagnetic Turbulence. *Astrophysical Journal*, 550:824–840, April 2001.

[49] J. D. Brown. Action functionals for relativistic perfect fluids. *Classical and Quantum Gravity*, 10:1579–1606, August 1993.

[50] J. D. Brown and K. V. Kuchař. Dust as a standard of space and time in canonical quantum gravity. *Phys. Rev. D*, 51:5600–5629, May 1995.

[51] R. Bruno and V. Carbone. The Solar Wind as a Turbulence Laboratory. *Living Rev. Sol. Phys.*, 10:2, May 2013.

[52] J. W. Burby. Magnetohydrodynamic motion of a two-fluid plasma. *Phys. Plasmas*, 24(8):082104, 2017.

[53] J. L. Burch, T. E. Moore, R. B. Torbert, and B. L. Giles. Magnetospheric Multiscale Overview and Science Objectives. *Space Sci. Rev.*, 199:5–21, March 2016.

[54] J. L. Burch, T. E. Moore, R. B. Torbert, and B. L. Giles. Magnetospheric multiscale overview and science objectives. *Space Sci. Rev.*, 199(1):5–21, Mar 2016.

[55] J. M. Burgers. On the application of statistical mechanics to the theory of turbulent fluid motion I. *Koninklijke Nederlandse Akad. Wetenschappen.*, 32:414, 1929.

[56] E. Cafaro, D. Grasso, F. Pegoraro, F. Porcelli, and A. Saluzzi. Invariants and Geometric Structures in Nonlinear Hamiltonian Magnetic Reconnection. *Phys. Rev. Lett.*, 80:4430–4433, May 1998.

[57] E. Cafaro, D. Grasso, F. Pegoraro, F. Porcelli, and A. Saluzzi. Invariants and geometric structures in nonlinear hamiltonian magnetic reconnection. *Phys. Rev. Lett.*, 80:4430–4433, May 1998.

[58] M. G. Calkin. An action principle for magnetohydrodynamics. *Canadian J. Phys.*, 41(12):2241–2251, 1963.

[59] G. Calugareanu. Sur les classes d'isotopie des noeuds tridimensionnels et leurs invariants. *Czechoslovak Math. J.*, 11(4):588 – 625, 1961.

[60] A. Campa, T. Dauxois, and S. Ruffo. Statistical mechanics and dynamics of solvable models with long-range interactions. *Physics Reports*, 480:57–159, September 2009.

[61] J. Candy and W. Rozmus. A Symplectic integration algorithm for separable Hamiltonian functions. *J. Comp. Phys.*, 92:230–256, January 1991.

[62] J. Cantarella, D. DeTurck, and H. Gluck. The Biot-Savart operator for application to knot theory, fluid dynamics, and plasma physics. *J. Math. Phys.*, 42:876–905, February 2001.

[63] C. Canuto, M. Y. Hussaini, A. Quarteroni, and T. A. Zang Jr. *Spectral Methods in Fluid Dynamics*. Springer Series in Computational Physics. Springer-Verlag Berlin Heidelberg, 1988.

[64] J. R. Cary and A. J. Brizard. Hamiltonian theory of guiding-center motion. *Rev. Mod. Phys.*, 81:693–738, 2009.

[65] I. Keramidas Charidakos, F. L. Waelbroeck, and P. J. Morrison. A hamiltonian five-field gyrofluid model. *Phys. Plasmas*, 22(11):112113, 2015.

[66] A. Y. K. Chui and H. K. Moffatt. The energy and helicity of knotted magnetic flux tubes. *Proceedings of the Royal Society A*, 451, 1995.

[67] L. Comisso and F. A. Asenjo. Thermal-Inertial effects on magnetic reconnection in relativistic pair plasmas. *Phys. Rev. Lett.*, 113(4):045001, July 2014.

[68] L. Comisso, D. Grasso, E. Tassi, and F. L. Waelbroeck. Numerical investigation of a compressible gyrofluid model for collisionless magnetic reconnection. *Phys. Plasmas*, 19(4):042103, 2012.

[69] L. Comisso, D. Grasso, F. L. Waelbroeck, and D. Borgogno. Gyro-induced acceleration of magnetic reconnection. *Phys. Plasmas*, 20(9):092118, 2013.

[70] R. Courant and D. Hilbert. *Methods of Mathematical Physics*, volume 1. New York: Interscience Publishers, Inc., 1 edition, 1953.

[71] S. Dastgeer, A. Das, and P. Kaw. Hydrodynamic regime of two-dimensional electron magnetohydrodynamics. *Phys. Plasmas*, 7(5):1366–1373, 2000.

[72] E. C. D'Avignon, P. J. Morrison, and M. Lingam. Derivation of the Hall and extended magnetohydrodynamics brackets. *Phys. Plasmas*, 23:062101, June 2016.

[73] E. C. D'Avignon, P. J. Morrison, and F. Pegoraro. Action principle for relativistic magnetohydrodynamics. *Phys. Rev. D*, 91(8):084050, April 2015.

[74] H. J. de Blank. Kinetic model of electrons in drift-alfvén current-vortices. *Phys. Plasmas*, 8:3927, 2001.

[75] D. Del Sarto, F. Califano, and F. Pegoraro. Electron parallel compressibility in the nonlinear development of two-dimensional collisionless magnetohydrodynamic reconnection. *Mod. Phys. Lett. B*, 20:931, 2006.

[76] M. R. Dennis and J. H. Hannay. Geometry of calugareanu's theorem. *Proceedings of the Royal Society A*, 461:3245 – 3254, 2005.

[77] E. Deusebio, G. Boffetta, E. Lindborg, and S. Musacchio. Dimensional transition in rotating turbulence. *Phys. Rev. E*, 90:023005, Aug 2014.

[78] R. L. Dewar. Energy - momentum tensors for dispersive electromagnetic waves. *Australian Journal of Physics*, 30(6):533, 1977.

[79] P. A. M. Dirac. Generalized hamiltonian dynamics. *Proceedings of the Royal Society of London A: Mathematical, Physical and Engineering Sciences*, 246(1246):326–332, 1958.

[80] W. G. Dixon. *Special Relativity: The Foundation of Macroscopic Physics*. Cambridge University Press; Reprint edition, 1982.

[81] J. W. Dungey. *Cosmic Electrodynamics*. Cambridge Univ. Press, 1958.

[82] G. V. Dunne. Aspects of chern-simons theory. In A. Comtet, T. Jolicœur, S. Ouvry, and F. David, editors, *Aspects topologiques de la physique en basse dimension. Topological aspects of low dimensional systems*, pages 177–263, Berlin, Heidelberg, 1999. Springer Berlin Heidelberg.

[83] C. L. Ellison, J. M. Finn, H. Qin, and W. M. Tang. Development of variational guiding center algorithms for parallel calculations in experimental magnetic equilibria. *Plasma Phys. Cont. Fusion*, 57(5):054007, May 2015.

[84] H.-T. Elze, Y. Hama, T. Kodama, M. Makler, and J. Rafelski. Variational principle for relativistic fluid dynamics. *Journal of Physics G: Nuclear and Particle Physics*, 25(9):1935, 1999.

[85] E. G. Evstatiev and B. A. Shadwick. Variational formulation of particle algorithms for kinetic plasma simulations. *J. Comp. Phys.*, 245:376–398, July 2013.

[86] J. M. Finn and T. M. Antonsen. Magnetic helicity: what is it and what is it good for. *Comments Plasma Phys. Cont. Fusion*, 9:111, 1985.

[87] C.B. Forest, K. Flanagan, M. Brookhart, M. Clark, C.M. Cooper, V. Dsangles, J. Egedal, D. Endrizzi, I.V. Khalzov, H. Li, and et al. The wisconsin plasma astrophysics laboratory. *J. Plasma Phys.*, 81(5), 2015.

[88] T. Frankel. *The Geometry of Physics: An Introduction*. Cambridge University Press, 3 edition, 2011.

[89] M. H. Freedman and Zheng-Xu H. Divergence-free fields: Energy and asymptotic crossing number. *Annals of Mathematics*, 134(1):189–229, 1991.

[90] J. P. Freidberg. *Ideal MHD*. Cambridge Univ. Press, June 2014.

[91] U. Frisch. *Turbulence: The Legacy of Kolmogorov*. Cambridge University Press, 1995.

[92] U. Frisch, A. Pouquet, J. Leorat, and A. Mazure. Possibility of an inverse cascade of magnetic helicity in magnetohydrodynamic turbulence. *J. of Fluid Mech.*, 68:769–778, April 1975.

[93] F. B. Fuller. The writhing number of a space curve. *Proc. Natl. Acad. Sci. USA*, 68(4):815 – 819, 1971.

[94] F. B. Fuller. Decomposition of the linking number of a closed ribbon: A problem from molecular biology. *Proc. Natl. Acad. Sci. USA*, 75(8):3557 – 3561, 1978.

[95] D. Fyfe, G. Joyce, and D. Montgomery. Magnetic dynamo action in two-dimensional turbulent magneto-hydrodynamics. *J. Plasma Phys.*, 17:317–335, April 1977.

[96] D. Fyfe and D. Montgomery. High-beta turbulence in two-dimensional magnetohydrodynamics. *J. Plasma Phys.*, 16:181–191, 1976.

[97] S. Galtier. Wave turbulence in incompressible Hall magnetohydrodynamics. *J. Plasma Phys.*, 72:721–769, 2006.

[98] S. Galtier and E. Buchlin. Multiscale Hall-magnetohydrodynamic turbulence in the solar wind. *Astrophys. J.*, 656:560–566, February 2007.

[99] F. Y. Gang, B. D. Scott, and P. H. Diamond. Statistical mechanics of a twofield model of drift wave turbulence. *Phys. Fluids B: Plasma Phys.*, 1(6):1331–1333, 1989.

[100] A. N. Ganshin, V. B. Efimov, G. V. Kolmakov, L. P. Mezhov-Deglin, and P. V. E. McClintock. Observation of an inverse energy cascade in developed acoustic turbulence in superfluid helium. *Phys. Rev. Lett.*, 101:065303, Aug 2008.

[101] C. Gauss. *Werke*, volume 5. Gottingen: Konigliche Gesellschaft der Wissenschaften, 1867.

[102] W. K. George. Lectures in turbulence for the 21st century. http://www.uio.no/studier/emner/matnat/math/MEK4300/v13/undervisningsmateriale/tb_16january2013.pdf, 2013.

[103] S. Ghosh, E. Siregar, D. A. Roberts, and M. L. Goldstein. Simulation of high-frequency solar wind power spectra using Hall magnetohydrodynamics. *J. Geophys. Res.*, 101:2493–2504, February 1996.

[104] J. P. H. Goedbloed and S. Poedts. *Principles of Magnetohydrodynamics*. Cambridge University Press, August 2004.

[105] D. O. Gomez, P. D Mininni, and P. Dmitruk. Parallel simulations in turbulent mhd. *Physica Scripta*, 2005(T116):123, 2005.

[106] D. Grasso, F. Califano, F. Pegoraro, and F. Porcelli. Phase mixing and island saturation in Hamiltonian reconnection. *Phys. Rev. Lett.*, 86:5051–5054, May 2001.

[107] D. Grasso, F. Pegoraro, F. Porcelli, and F. Califano. Hamiltonian magnetic reconnection. *Plasma Physics and Controlled Fusion*, 41(12):1497, 1999.

[108] D. Grasso, E. Tassi, H. M. Abdelhamid, and P. J. Morrison. Structure and computation of two-dimensional incompressible extended MHD. *Phys. Plasmas*, 24(1):012110, January 2017.

[109] R. J. Hastie. Sawtooth Instability in Tokamak Plasmas. *Astrophys. Space Sci.*, 256:177–204, 1997.

[110] R. D. Hazeltine, C. T. Hsu, and P. J. Morrison. Hamiltonian fourfield model for nonlinear tokamak dynamics. *Phys. Fluids*, 30(10):3204–3211, 1987.

[111] M. Hirota, Y. Hattori, and P. J. Morrison. Explosive magnetic reconnection caused by an x-shaped current-vortex layer in a collisionless plasma. *Phys. Plasmas*, 22(5):052114, 2015.

[112] D. D. Holm, J. E. Marsden, T. Ratiu, and A. Weinstein. Nonlinear stability of fluid and plasma equilibria. *Phys. Rep.*, 123:1–116, July 1985.

[113] G. Hornig and C. Mayer. Towards a third-order topological invariant for magnetic fields. *J. Phys. A: Math. Gen.*, 35(17):3945, 2002.

[114] M. B. Isichenko and A. V. Gruzinov. Isotopological relaxation, coherent structures, and Gaussian turbulence in two-dimensional (2-D) magnetohydrodynamics (MHD). *Phys. Plasmas*, 1:1802–1816, June 1994.

[115] C. R. J.-J. Moreau. *Acad. Sci. Paris*, 252, 1961.

[116] R Jackiw, V P Nair, S-Y Pi, and A P Polychronakos. Perfect fluid theory and its extensions. *J. Phys. A Math. Gen.*, 37(42):R327, 2004.

[117] H. Jeong and J. Chae. Magnetic helicity injection in active regions. *The Astrophysical Journal*, 671(1):1022, 2007.

[118] C. E. Seyler Jr., Y. Salu, D. Montgomery, and G. Knorr. Two dimensional turbulence in inviscid fluids or guiding center plasmas. *Phys. Fluids*, 18, 1975.

[119] S. Jung, P. J. Morrison, and H. L. Swinney. Statistical mechanics of two-dimensional turbulence. *J. Fluid Mech.*, 554:433–456, May 2006.

[120] I. K. C., M. Lingam, P. J. Morrison, R. L. White, and A. Wurm. Action Principles for Extended MHD Models. *Phys. Plasmas*, 21(9):092118, September 2014.

[121] D. A. Kaltsas, G. N. Throumoulopoulos, and P. J. Morrison. Translationally symmetric extended MHD via Hamiltonian reduction: Energy-casimir equilibria. *Phys. Plasmas*, 24(9):092504, 2017.

[122] M. Kardar. *Statistical physics of particles*. Cambridge University Press, New York, NY Cambridge, 2007.

[123] L. H. Kauffman. *Knots and Physics*. World Scientific Publishing Co. Pte. Ltd., 3 edition, 2001.

[124] Y. Kawazura. Modification of magnetohydrodynamic waves by the relativistic hall effect. *arXiv preprint arXiv:1706.07077*, 2017.

[125] Y. Kawazura, G. Miloshevich, and P. J. Morrison. Action principles for relativistic extended magnetohydrodynamics: A unified theory of magnetofluid models. *Phys. Plasmas*, 24(2):022103, February 2017.

[126] Y. Kawazura, Z. Yoshida, and Y. Fukumoto. Relabeling symmetry in relativistic fluids and plasmas. *J. Phys. A Math. Gen.*, 47:465501, November 2014.

[127] H. Kedia, D. Foster, M. R. Dennis, and W. T. M. Irvine. Weaving knotted vector fields with tunable helicity. *Phys. Rev. Lett.*, 117:274501, Dec 2016.

[128] G.W. Kentwell. General relativistic fluid dynamics as a noncanonical hamiltonian system. *Phys. Lett. A*, 108(5):248 – 251, 1985.

[129] A. Khinchin. *Mathematical Foundations of Statistical Mechanics*. Dover Pubs., Inc., 1949.

[130] K. Kimura and P. J. Morrison. On energy conservation in extended magnetohydrodynamics. *Phys. Plasmas*, 21(8):082101, August 2014.

[131] M. G. Kivelson and C. T. Russell. *Introduction to Space Physics*. Cambridge Univ. Press, April 1995.

[132] D. Kleckner and W. T. M. Irvine. Creation and dynamics of knotted vortices. *Nature Physics*, 9:253–258, April 2013.

[133] D. Kleckner, M. W. Scheeler, and W. T. M. Irvine. The life of a vortex knot. *Phys. Fluids*, 26(9):091105, 2014.

[134] S. Koide. Generalized Relativistic Magnetohydrodynamic equations for pair and electron-ion plasmas. *Astroph. J.*, 696:2220–2233, May 2009.

[135] S. Koide. Generalized general relativistic magnetohydrodynamic equations and distinctive plasma dynamics around rotating black holes. *Astroph. J.*, 708(2):1459, 2010.

[136] A. Kolmogorov. The Local Structure of Turbulence in Incompressible Viscous Fluid for Very Large Reynolds' Numbers. *Akademiia Nauk SSSR Doklady*, 30:301–305, 1941.

[137] A. E. Koniges, J. A. Crotinger, W. P. Dannevik, G. F. Carnevale, P. H. Diamond, and F. Y. Gang. Equilibrium spectra and implications for a twofield turbulence model. *Phys. Fluids B: Plasma Phys.*, 3(5):1297–1299, 1991.

[138] R. H. Kraichnan. Inertial Ranges in Two-Dimensional Turbulence. *Phys. Fluids*, 10:1417–1423, July 1967.

[139] R. H. Kraichnan. Inertial ranges in two-dimensional turbulence. *Phys. Fluids*, 10(7):1417–1423, 1967.

[140] R. H. Kraichnan. Statistical dynamics of two-dimensional flow. *J. of Fluid Mech.*, 67(1):155175, 1975.

[141] R. H. Kraichnan and D. Montgomery. Two-dimensional turbulence. *Rep. Prog. Phys.*, 43:547–619, 1980.

[142] N. A. Krall and A. W. Trivelpiece. *Principles of plasma physics*. McGraw Hill, New York, 1973.

[143] M. Krauss, K. Kormann, P. J. Morrison, and E. Sonnendrcker. Gempic: geometric electromagnetic particle-in-cell methods. *J. Plasma Phys.*, 83(4), 2017.

[144] V. Krishan and S. M. Mahajan. Magnetic fluctuations and Hall magnetohydrodynamic turbulence in the solar wind. *J. Geophys. Res.*, 109(A18):A11105, November 2004.

[145] J. A. Krommes. Fundamental statistical descriptions of plasma turbulence in magnetic fields. *Physics Reports*, 360(1):1 – 352, 2002.

[146] R. M. Kulsrud. *Plasma physics for astrophysics*. Princeton University Press, 2005.

[147] J. L. Lagrange. *Mécanique Analytique*. Dordrecht Kluwer Academic, Boston, MA, 1997.

[148] L. D. Landau and Lifshitz E. M. *Statistical physics*, volume 7. Pergamon Pressx, 3 edition, 1980.

[149] T. D. Lee. On some statistical properties of hydrodynamical and magneto-hydrodynamical fields. *Quart. Appl. Math.*, 10(1):69–74, 1952.

[150] A. Lichnerowicz. *Relativistic Hydrodynamics and Magnetohydrodynamics*. W. A. Benjamin, Inc., 1967.

[151] C. C. Lin. Academic Press, 1963.

[152] M. Lingam and A. Bhattacharjee. A heuristic model for MRI turbulent stresses in Hall MHD. *Mon. Not. R. Astron. Soc.*, 460:478–488, July 2016.

[153] M. Lingam and A. Bhattacharjee. Hall Current Effects in Mean-Field Dynamo Theory. *Astrophys. J.*, 829:51, September 2016.

[154] M. Lingam and S. M. Mahajan. Modeling astrophysical outflows via the unified dynamoreverse dynamo mechanism. *Monthly Notices of the Royal Astronomical Society: Letters*, 449(1):L36–L40, 2015.

[155] M. Lingam and S. M. Mahajan. Modelling astrophysical outflows via the unified dynamo-reverse dynamo mechanism. *Mon. Not. R. Astron. Soc.*, 449:L36–L40, April 2015.

[156] M. Lingam, G. Miloshevich, and P. J. Morrison. Concomitant Hamiltonian and topological structures of extended magnetohydrodynamics. *Phys. Lett. A*, 380:2400–2406, July 2016.

[157] M. Lingam and P. J. Morrison. The action principle for generalized fluid motion including gyroviscosity. *Phys. Lett. A*, 378:3526–3532, November 2014.

[158] M. Lingam, P. J. Morrison, and G. Miloshevich. Remarkable connections between extended magnetohydrodynamics models. *Phys. Plasmas*, 22(7):072111, July 2015.

[159] M. Lingam, P. J. Morrison, and E. Tassi. Inertial magnetohydrodynamics. *Phys. Lett. A*, 379:570–576, March 2015.

[160] X. Liu and R. L. Ricca. The jones polynomial for fluid knots from helicity. *J. Phys. A Math. and Theoret.*, 45(20):205501, 2012.

[161] X. Liu and R. L. Ricca. On the derivation of the homflypt polynomial invariant for fluid knots. *J. Fluid Mech.*, 773:3448, 2015.

[162] D. W. Longcope. Topological methods for the analysis of solar magnetic fields. *Living Reviews in Solar Physics*, 2(1):7, Nov 2005.

[163] R. Lüst. Über die Ausbreitung von Wellen in einem Plasma. *Fortschr. Phys.*, 7:503–558, 1959.

[164] F. Maggioni and R. L. Ricca. On the groundstate energy of tight knots. *Proceedings of the Royal Society A*, 465:2761 – 2783, 2009.

[165] S. M. Mahajan. Temperature-transformed "minimal coupling": Magnetofluid unification. *Phys. Rev. Lett.*, 90:035001, Jan 2003.

[166] J. E. Marsden, R. Montgomery, P. J. Morrison, and W. B. Thompson. Covariant poisson brackets for classical fields. *Annals of Physics*, 169:29–47, 1986.

[167] W. H. Matthaeus and M. L. Goldstein. Measurement of the rugged invariants of magnetohydrodynamic turbulence in the solar wind. J. Geophys. Res., 87:6011–6028, August 1982.

[168] R. Meyrand and S. Galtier. A new turbulence regime in the solar-wind at electron scales. In S. Boissier, M. Heydari-Malayeri, R. Samadi, and D. Valls-Gabaud, editors, *SF2A-2010: Proceedings of the Annual meeting of the French Society of Astronomy and Astrophysics*, page 303, December 2010.

[169] R. Meyrand and S. Galtier. A Universal Law for Solar-wind Turbulence at Electron Scales. *Astrophys. J.*, 721:1421–1424, October 2010.

[170] G. Miloshevich, T. Dauxois, R. Khomeriki, and S. Ruffo. Dipolar needles in the microcanonical ensemble: Evidence of spontaneous magnetization and ergodicity breaking. *EPL (Europhysics Letters)*, 104:17011, October 2013.

[171] G. Miloshevich, M. Lingam, and P. J. Morrison. On the structure and statistical theory of turbulence of extended magnetohydrodynamics. *New Journal of Physics*, 19(1):015007, January 2017.

[172] G. Miloshevich, P. J. Morrison, and E. Tassi. Direction of cascades in a magnetofluid model with electron skin depth and ion sound larmor radius scales. *Phys. Plasmas*, 25(7):072303, 2018.

[173] G. Miloshevich, J.-P. Nguenang, T. Dauxois, R. Khomeriki, and S. Ruffo. Instabilities and relaxation to equilibrium in long-range oscillator chains. *Phys. Rev. E*, 91(3):032927, March 2015.

[174] G. Miloshevich, J. P. Nguenang, T. Dauxois, R. Khomeriki, and S. Ruffo. Traveling solitons in long-range oscillator chains. *J. Phys. A Math. Gen.*, 50(12):12LT02, March 2017.

[175] P. D. Mininni, D. O. Gomez, and S. M. Mahajan. Dynamo action in magnetohydrodynamics and hall-magnetohydrodynamics. *Astroph. J.*, 587(1):472, 2003.

[176] C. W. Misner, K. S. Thorne, and J. A. Wheeler. *Gravitation*. W. H. Freeman, 1995.

[177] H. K. Moffatt. The degree of knottedness of tangled vortex lines. *J. Fluid Mech.*, 35:117–129, 1969.

[178] H. K. Moffatt. The energy spectrum of knots and links. *Nature*, 347(6291):367 – 369, 1990.

[179] H. K. Moffatt and R. L. Ricca. Helicity and the Calugareanu invariant. *Proc. Roy. Soc. A*, 439:411–429, November 1992.

[180] D. Montgomery, L. Turner, and G. Vahala. Most probable states in magnetohydrodynamics. *J. Plasma Phys.*, 21:239–251, 1979.

[181] P. J. Morrison. Poisson Brackets for Fluids and Plasmas. In M. Tabor and Y. Treve, editors, *Mathematical Methods in Hydrodynamics and Integrability in Dynamical Systems*, volume 88, pages 13–46. New York: Am. Inst. Phys., 1982.

[182] P. J. Morrison. Hamiltonian description of the ideal fluid. Rev. Mod. Phys., 70:467–521, April 1998.

[183] P. J. Morrison. Hamiltonian and action principle formulations of plasma physics. *Phys. Plasmas*, 12:058102–1–13, 2005.

[184] P. J. Morrison. On Hamiltonian and Action Principle Formulations of Plasma Dynamics. In B. Eliasson and P. K. Shukla, editors, *New Developments in Nonlinear Plasma Physics: Proceedings for the 2009 ICTP College on Plasma Physics*, volume 1188, pages 329–344. New York: Am. Inst. Phys., November 2009.

[185] P. J. Morrison and J. M. Greene. Noncanonical Hamiltonian density formulation of hydrodynamics and ideal magnetohydrodynamics. Phys. Rev. Lett., 45:790–794, September 1980.

[186] P. J. Morrison and R. D. Hazeltine. Hamiltonian formulation of reduced magnetohydrodynamics. *Phys. Fluids*, 27:886–897, April 1984.

[187] P. J. Morrison, M. Lingam, and R. Acevedo. Hamiltonian and action formalisms for two-dimensional gyroviscous magnetohydrodynamics. *Phys. Plasmas*, 21(8):082102, August 2014.

[188] P. J. Morrison, E. Tassi, and N. Tronko. Stability of compressible reduced magnetohydrodynamic equilibria analogy with magnetorotational instability. *Phys. Plasmas*, 20:042109, 2013.

[189] Y. Narita, R. Nakamura, W. Baumjohann, K.-H. Glassmeier, U. Motschmann, B. Giles, W. Magnes, D. Fischer, R. B. Torbert, C. T. Russell, R. J. Strangeway, J. L. Burch, Y. Nariyuki, S. Saito, and S. P. Gary. On Electron-scale Whistler Turbulence in the Solar Wind. *Astrophys. J.*, 827:L8, August 2016.

[190] Y. Narita, R. Nakamura, W. Baumjohann, K.-H. Glassmeier, U. Motschmann, B. Giles, W. Magnes, D. Fischer, R. B. Torbert, C. T. Russell, R. J. Strangeway, J. L. Burch, Y. Nariyuki, S. Saito, and S. P. Gary. On electron-scale whistler turbulence in the solar wind. *The Astrophysical Journal Letters*, 827(1):L8, 2016.

[191] S. Nazarenko. *Wave Turbulence*, volume 825 of *Lecture Notes in Physics*. Springer-Verlag, 2011.

[192] W. A. Newcomb. *Nucl. Fusion Suppl.*, pt 2:451, 1962.

[193] A. Nindos, J. Zhang, and H. Zhang. The magnetic helicity budget of solar active regions and coronal mass ejections. *The Astrophysical Journal*, 594(2):1033, 2003.

[194] E. Noether. Invariant Variation Problems. *Nachr. d. Konig. Gesellsch. d. Wiss. zu Gottingen, Math-phys. Klasse*, pages 235–237, 1918.

[195] L. Onsager. Statistical hydrodynamics. *Il Nuovo Cimento (1943-1954)*, 6(2):279–287, Mar 1949.

[196] S. A. Orszag. Numerical simulation of incompressible flows within simple boundaries. i. galerkin (spectral) representations. *Studies in Applied Mathematics*, 50(4):293–327, 1971.

[197] S. Ortolani and D. D. Schnack. *Magnetohydrodynamics of Plasma Relaxation*. World Scientific, 1993.

[198] M. Ottaviani and F. Porcelli. Nonlinear collisionless magnetic reconnection. Phys. Rev. Lett., 71:3802–3805, December 1993.

[199] N. Padhye and P. J. Morrison. Fluid element relabeling symmetry. *Physics Letters A*, 219(5):287 – 292, 1996.

[200] C. E. Parnell and I. De Moortel. A contemporary view of coronal heating. *Phil. Trans. Roy. Soc. A*, 370:3217–3240, July 2012.

[201] F. Pegoraro. Generalised relativistic ohm's laws, extended gauge transformations, and magnetic linking. *Phys. Plasmas*, 22(11):112106, 2015.

[202] D. Perrone, O. Alexandrova, O. W. Roberts, S. Lion, C. Lacombe, A. Walsh, M. Maksimovic, and I. Zouganelis. Coherent structures at ion scales in fast solar wind: Cluster observations. *The Astrophysical Journal*, 849:49, 2017.

[203] D. Pfirsch and P. J. Morrison. Local conservation laws for the Maxwell-Vlasov and collisionless guiding-center theories. *Phys. Rev. A*, 32:1714–1721, 1985.

[204] A. Pouquet and R. Marino. Geophysical turbulence and the duality of the energy flow across scales. *Phys. Rev. Lett.*, 111:234501, Dec 2013.

[205] H. Qin and X. Guan. Variational Symplectic Integrator for Long-Time Simulations of the Guiding-Center Motion of Charged Particles in General Magnetic Fields. *Phys. Rev. Lett.*, 100(3):035006, January 2008.

[206] J. R. Ray. Lagrangian density for perfect fluids in general relativity. *J. Math. Phys.*, 13(10):1451–1453, 1972.

[207] R. L. Ricca. Topology bounds energy of knots and links. *Proceedings of the Royal Society of London A: Mathematical, Physical and Engineering Sciences*, 464(2090):293–300, 2008.

[208] R. L. Ricca and H. K. Moffatt. *The Helicity of a Knotted Vortex Filament*. Kluwer Academic Publishers, 1992.

[209] A. Ruzmaikin and P. Akhmetiev. Topological invariants of magnetic fields, and the effect of reconnections. *Phys. Plasmas*, 1:331–336, February 1994.

[210] T. Sahihi and H. Eshraghi. Biot-savart helicity versus physical helicity: A topological description of ideal flows. *J. Math. Phys.*, 55(8):083101, 2014.

[211] G. Sahoo, A. Alexakis, and L. Biferale. Discontinuous transition from direct to inverse cascade in three-dimensional turbulence. *Phys. Rev. Lett.*, 118:164501, Apr 2017.

[212] F. Sahraoui, G. Belmont, and L. Rezeau. Hamiltonian canonical formulation of Hall-magnetohydrodynamics: Toward an application to weak turbulence theory. *Phys. Plasmas*, 10:1325–1337, May 2003.

[213] F. Sahraoui, M. L. Goldstein, K. Abdul-Kader, G. Belmont, L. Rezeau, P. Robert, and P. Canu. Observation and theoretical modeling of electron scale solar wind turbulence. *Comptes Rendus Physique*, 12(2):132 – 140, 2011. Propagation and plasmas: new challenges, new applications.

[214] F. Sahraoui, M. L. Goldstein, P. Robert, and Y. V. Khotyaintsev. Evidence of a Cascade and Dissipation of Solar-Wind Turbulence at the Electron Gyroscale. *Phys. Rev. Lett.*, 102(23):231102, June 2009.

[215] F. Sahraoui, S. Y. Huang, G. Belmont, M. L. Goldstein, A. Rétino, P. Robert, and J. De Patoul. Scaling of the Electron Dissipation Range of Solar Wind Turbulence. *Astrophys. J.*, 777:15, November 2013.

[216] R. Salmon. Hamiltonian fluid mechanics. *Ann. Rev. Fluid Mech.*, 20:225–256, 1988.

[217] R. Salmon. Hamilton's principle and the vorticity laws for a relativistic perfect fluid. *Geoph. Astroph. Fluid Dynamics*, 43(2):167–179, 1988.

[218] R. Salmon, G. Holloway, and M. C. Hendershott. The equilibrium statistical mechanics of simple quasi-geostrophic models. *J. of Fluid Mech.*, 75(4):691703, 1976.

[219] M. W. Scheeler, D. Kleckner, D. Proment, G. L. Kindlmann, and W. T. M. Irvine. Helicity conservatio by flow across scales in reconnecting vortex links and knots. *Proc. Natl. Acad. Sci. USA*, 111(43):15350 – 15355, 2014.

[220] A. A. Schekochihin, S. C. Cowley, W. Dorland, G. W. Hammett, G. G. Howes, E. Quataert, and T. Tatsuno. Astrophysical gyrokinetics: Kinetic and fluid turbulent cascades in magnetized weakly collisional plasmas. *The Astrophysical Journal Supplement Series*, 182(1):310, 2009.

[221] T. J. Schep, F. Pegoraro, and B. N. Kuvshinov. Generalized two-fluid theory of nonlinear magnetic structures. *Phys. Plasmas*, 1:2843–2852, September 1994.

[222] B. Schutz. *Geometrical Methods for Mathematical Physics*. Cambridge University Press, 1980.

[223] B. F. Schutz. Perfect Fluids in General Relativity: Velocity Potentials and a Variational Principle. *Phys. Rev. D*, 2(12):2762–2773, dec 1970.

[224] B. F. Schutz and R. Sorkin. Variational aspects of relativistic field theories, with application to perfect fluids. *Annals of Physics*, 107(1):1 – 43, 1977.

[225] J. Serrin. *Mathematical Principles of Classical Fluid Mechanics*, pages 125–263. Springer Berlin Heidelberg, Berlin, Heidelberg, 1959.

[226] S. Servidio, W. H. Matthaeus, and V. Carbone. Statistical properties of ideal three-dimensional Hall magnetohydrodynamics: The spectral structure of the equilibrium ensemble. *Phys. Plasmas*, 15(4):042314, April 2008.

[227] K. Seshasayanan, S. J. Benavides, and A. Alexakis. On the edge of an inverse cascade. *Phys. Rev. E*, 90:051003, Nov 2014.

[228] D. Shaikh and P. K. Shukla. 3D Simulations of Fluctuation Spectra in the Hall-MHD Plasma. *Phys. Rev. Lett.*, 102(4):045004, January 2009.

[229] J. V. Shebalin. Broken ergodicity and coherent structure in homogeneous turbulence. *Physica D Nonlinear Phenomena*, 37:173–191, July 1989.

[230] J. V. Shebalin. Broken ergodicity in magnetohydrodynamic turbulence. *Geophysical & Astrophysical Fluid Dynamics*, 107(4):411–466, 2013.

[231] B. K. Shivamoggi. Electron magnetohydrodynamic turbulence: universal features. *Eur. Phys. J. D*, 69:55, February 2015.

[232] L. M. Smith and F. Waleffe. Transfer of energy to two-dimensional large scales in forced, rotating three-dimensional turbulence. *Phys. Fluids*, 11(6):1608–1622, 1999.

[233] R. G. Spencer and A. N. Kaufman. Hamiltonian structure of two-fluid plasma dynamics. Phys. Rev. A, 25:2437–2439, April 1982.

[234] L. Spitzer. *Physics of Fully Ionized Gases.* Interscience, New York, 1956.

[235] K. R. Sreenivasan and R. A. Antonia. The phenomenology of small-scale turbulence. *Annual Review of Fluid Mechanics*, 29(1):435–472, 1997.

[236] K. R. Sreenivasan and R. A. Antonia. The phenomenology of small-scale turbulence. *Annual Review of Fluid Mechanics*, 29(1):435–472, 1997.

[237] L. C. Steinhauer and A. Ishida. Relaxation of a two-specie magnetofluid. *Phys. Rev. Lett.*, 79:3423–3426, Nov 1997.

[238] H. R. Strauss. Nonlinear, three-dimensional magnetohydrodynamics of noncircular tokamaks. *Phys. Fluids*, 19:134, 1976.

[239] N. E. Sujovolsky and P. D. Mininni. Tridimensional to bidimensional transition in magnetohydrodynamic turbulence with a guide field and kinetic helicity injection. *Phys. Rev. Fluids*, 1:054407, Sep 2016.

[240] E. Tassi. Hamiltonian fluid reductions of electromagnetic drift-kinetic equations for an arbitrary number of moments. *Annals of Physics*, 362:239, 2015.

[241] E. Tassi. Hamiltonian closures in fluid models for plasmas. *Eur. Phys. J. D*, 71:269, 2017.

[242] E. Tassi, P. J. Morrison, F. L. Waelbroeck, and D. Grasso. Hamiltonian formulation and analysis of a collisionless fluid reconnection model. *Plasma Phys. Cont. Fusion*, 50(8):085014, August 2008.

[243] A. H. Taub. Relativistic rankine-hugoniot equations. *Phys. Rev.*, 74:328–334, Aug 1948.

[244] A. H. Taub. General relativistic variational principle for perfect fluids. *Phys. Rev.*, 94:1468–1470, Jun 1954.

[245] J. B. Taylor. Relaxation of Toroidal Plasma and Generation of Reverse Magnetic Fields. Phys. Rev. Lett., 33:1139–1141, November 1974.

[246] N. Tronko, A. Bottino, and E. Sonnendrücker. Second order gyrokinetic theory for particle-in-cell codes. *Phys. Plasmas*, 23(8):082505, August 2016.

[247] A. V. Tur and V. V. Yanovsky. Invariants in dissipationless hydrodynamic media. *J. Fluid Mech.*, 248:67106, 1993.

[248] L. Turner. Hall effects on magnetic relaxation. *IEEE Transactions on Plasma Science*, 14(6):849–857, Dec 1986.

[249] H. v. Bodecker and G. Hornig. Link invariants of electromagnetic fields. *Phys. Rev. Lett.*, 92:030406, Jan 2004.

[250] D. Vey. n-plectic maxwell theory, arxiv: math-ph/1303.2192v3.

[251] T. F. Viscondi, I. L. Caldas, and P. J. Morrison. A method for Hamiltonian truncation: a four-wave example. *J. Phys. A: Math. and Theoretical*, 49(16):165501, 2016.

[252] G. M. Webb, B. Dasgupta, J. F. McKenzie, Q. Hu, and G. P. Zank. Local and nonlocal advected invariants and helicities in magnetohydrodynamics and gas dynamics i: Lie dragging approach. *J. Phys. A: Math. Theor.*, 47, 2014.

[253] G. M. Webb, J. F. McKenzie, and G. P. Zank. Multi-symplectic magnetohydrodynamics. *J. Plasma Phys.*, 80(5):707743, 2014.

[254] J. H. White. Self-linking and the gauss integral in higher dimensions. *American Journal of Mathematics*, 91(3):693 – 728, 1969.

[255] E. Witten. Quantum field theory and the jones polynomial. *Communications in Mathematical Physics*, 121(3):351–399, Sep 1989.

[256] L. Woltjer. A Theorem on Force-Free Magnetic Fields. *Proc. Natl. Acad. Sci.*, 44:489–491, June 1958.

[257] J. Xiao, H. Qin, P. J. Morrison, J. Liu, Z. Yu, R. Zhang, and Y. He. Explicit high-order noncanonical symplectic algorithms for ideal two-fluid systems. *Phys. Plasmas*, 23(11):112107, November 2016.

[258] Z. Yoshida and E. Hameiri. Canonical Hamiltonian mechanics of Hall magnetohydrodynamics and its limit to ideal magnetohydrodynamics. *J. Phys. A*, 46:G5502, August 2013.

[259] Z. Yoshida and E. Hameiri. Canonical Hamiltonian mechanics of Hall magnetohydrodynamics and its limit to ideal magnetohydrodynamics. *J. Phys. A: Math. and Theoretical*, 46(33):335502, 2013.

[260] Z. Yoshida, Y. Kawazura, and T. Yokoyama. Relativistic helicity and link in Minkowski space-time. *J. Math. Phys.*, 55(4):043101, April 2014.

[261] Z. Yoshida and P. J. Morrison. Epi-two-dimensional fluid flow: A new topological paradigm for dimensionality. *Phys. Rev. Lett.*, 119:244501, Dec 2017.

[262] Z. Yoshida, P. J. Morrison, and F. Dobarro. Singular casimir elements of the euler equation and equilibrium points. *Journal of Mathematical Fluid Mechanics*, 16(1):41–57, Mar 2014.

[263] F. Yuan, S. Markoff, and H. Falcke. A jet-adaf model for sgra*. *Astronomy and Astrophysics*, 383(3):854–863, 2002.

[264] V. E. Zakharov and E. A. Kuznetsov. Hamiltonian formalism for nonlinear waves. *Physics - Uspekhi*, 40(1):1087–1116, 1997.

[265] V. E. Zakharov, V. S. L'Vov, and G. Falkovich. *Kolmogorov spectra of turbulence 1. Wave turbulence.* Springer, Berlin, 1992.

[266] V. E. Zakharov, S. L. Musher, and A. M. Rubenchik. Hamiltonian approach to the description of non-linear plasma phenomena. *Phys. Rep.*, 129:285–366, December 1985.

[267] J.-Z. Zhu. Chirality, extended magnetohydrodynamics statistics and topological constraints for solar wind turbulence. *Monthly Notices of the Royal Astronomical Society: Letters*, 470:L87–L91, September 2017.

[268] J.-Z. Zhu and G. W. Hammett. Gyrokinetic statistical absolute equilibrium and turbulence. *Phys. Plasmas*, 17(12):122307–122307, December 2010.

[269] J.-Z. Zhu, W. Yang, and G.-Y. Zhu. Purely helical absolute equilibria and chirality of (magneto)fluid turbulence. *J. of Fluid Mech.*, 739:479–501, January 2014.

[270] A. Zocco and A.A. Schekochihin. Reduced fluid-kinetic equations for low-frequency dynamics, magnetic reconnection, and electron heating in low-beta plasmas. *Phys. Plasmas*, 18:102309, 2011.